SEISMIC STABILITY EVALUATIONS OF CHESBRO, LENIHAN, STEVENS CREEK, AND UVAS DAMS (SSE2)

PHASE A: STEVENS CREEK AND LENIHAN DAMS

STEVENS CREEK DAM

SITE CHARACTERIZATION, MATERIAL PROPERTIES, AND GROUND MOTIONS

(REPORT No. SC-2)

Prepared for

SANTA CLARA VALLEY WATER DISTRICT
5750 Almaden Expressway
San Jose, CA 95118

May 2012

TERRA / GeoPentech
a Joint Venture

TABLE OF CONTENTS

TABLE OF CONTENTS

Tables

Figures

TABLE OF CONTENTS

1.1 GENERAL

In May 2010, the Santa Clara Valley Water District (District) retained Terra / GeoPentech (TGP), a joint venture of Terra Engineers, Inc. and GeoPentech, Inc., to complete seismic stability evaluations of Chesbro, Lenihan, Stevens Creek and Uvas Dams. These evaluations were required by the Division of Safety of Dams (DSOD) in June 2008 as part of their Phase III screening process of the State's dams located in highly seismic environments. The evaluations are also a vital part of the District's Dam Safety Program (DSP). Phase A of the project includes work on Stevens Creek and Lenihan Dams and has a planned completion date of February 2012. Phase B of the project includes work on Chesbro and Uvas Dams and is scheduled to begin in 2012 and to finish by the end of 2013. The general scope of the project consists of the field, laboratory, and office studies required to evaluate the seismic stability of the four referenced dams.

This document contains the results of our site characterization at Stevens Creek Dam based on the data available from the dam construction records and the field investigations and laboratory tests completed by prior investigators, and the results of supplemental site investigations and laboratory testing completed in 2011 and documented in Report No. SC-1 (Terra / GeoPentech, 2012).

The purpose of the site characterization is to:

1. summarize the geology of the site;
2. characterize the conditions of the dam and foundation and the material properties to be used in the engineering analyses for the seismic evaluation of the dam; and
3. provide ground motions to be used in the seismic deformation analyses of the dam.

The scope of the site characterization includes the following activities:

1. Review of design and construction history including modifications and previous evaluations;
2. Review and evaluation of engineering geology data;
3. Review and evaluation of information on faulting;
4. Review and evaluation of construction data;
5. Review and evaluation of dam monitoring data;
6. Review and evaluation of ground motion data;
7. Preparation of an updated plan view of the areal extent and thickness of native overburden soils left in place beneath the footprint of the dam, based on previous work by the District (Nelson, 2010a), data available from previous field investigations, and new information provided by the supplemental field explorations;
8. Summary and interpretation of physical and index property data for the embankment and foundation soils left in place beneath it;
9. Evaluation of laboratory data and development of static and dynamic engineering properties for embankment, foundation soils, and rock; and
10. Selection of earthquake ground motions for use in the seismic deformation analyses of the dam.

1.2 ORGANIZATION OF REPORT

This report contains eight sections, including this introduction. Section 2.0 describes the site and the history of Stevens Creek Dam including its construction and the various investigations and studies that were conducted at the dam by a number of investigators. Section 3.0 discusses the site geology, including regional and local conditions, and Section 4.0 addresses the foundation conditions at the dam. The various zones incorporated into the dam embankment and the characterization of the embankment and foundation material properties are discussed in Section 5.0. Section 6.0 documents the development of ground motions for use in the dynamic analyses and Section 7.0 provides a summary of the key site characterization findings. Section 8.0 is a list of references.

2.1 GENERAL

Stevens Creek Dam is located in Santa Clara County, California, about 1 mile southwest of the City of Monta Vista, as shown on Figure 2-1. The dam is an earthfill structure that was constructed across Stevens Creek in 1935. Major modifications were made in 1986 to address seismic stability and spillway capacity issues, as discussed later in this section. The dam impounds Stevens Creek Reservoir that has a maximum capacity of 3,138 acre-feet at the nominal spillway elevation of 537.8 feet[1]. DSOD has classified Stevens Creek Dam as a "High Hazard" dam because of the "highly urbanized community of Monte Vista, which is less than 1 mile downstream from the dam" (DSOD, 1981).

Appurtenant structures include a broad-crested concrete-lined side channel spillway located in the right abutment and an outlet conduit beneath the dam embankment connected to an inlet structure in the reservoir, on the right side of the streambed, and to an outlet structure that allows reservoir water to discharge into Stevens Creek approximately 50 feet beyond the toe of the dam.

2.2 DAM AND APPURTENANT STRUCTURES

Figure 2-2 is an aerial photograph of Stevens Dam that shows the outline of the embankment, the locations of the outlet works, and the locations of previous explorations in the dam. The outline of the original embankment is shown as well as the limits of upstream and downstream buttresses that were completed in 1986. The upstream buttress is 100 feet wide and half the dam height; the downstream buttress is 50 feet wide and extends to elevation 556.8 feet, nominally 19 feet above the spillway elevation. The slopes of the upstream and downstream buttresses are 2.5 horizontal to 1 vertical (2.5H : 1V); i.e., the same as those of the original embankment. Stationing along the new crest of the dam is also shown on Figure 2-2.

Figure 2-3 contains transverse sections through the current configuration of the dam at the maximum section (Station 7+50) and at Station 9+70 on the left side the dam. The original dam embankment was designed as a two-zone earthfill dam, with an "impervious" upstream zone and a "pervious" downstream zone. Subsequent studies have indicated that the dam may in fact be more like a homogenous embankment. Therefore, hereinafter the embankment zones will be referred to as upstream embankment and downstream embankment. A cutoff trench was constructed at about the midpoint of the upstream "impervious" zone by excavating through the overburden soils and into the Santa Clara Formation. The Santa Clara Formation is a poorly indurated conglomerate with lesser interbeds of sandstone, siltstone and claystone - it is essentially a very dense clayey gravel. Seismic stability evaluations of the dam were performed in the late 1970s (Wahler, 1978) and concluded that a Maximum Credible Earthquake on the San Andreas Fault could cause the dam to fail due to excessive deformation. As a result, seismic upgrades in the form of stabilizing buttress sections were constructed in 1985-1986 on the upstream and downstream slopes, with an inclined filter and drain placed between the original downstream slope and the new buttress fill (Wahler, 1982; 1984; 1986a; 1986b).

[1] Unless otherwise noted in this document, all elevations are referenced to NAVD88 vertical datum.

The locations of piezometers installed during previous investigations are shown on Figure 2-3. Nine pneumatic piezometers were installed in 1986 following the construction of buttresses (Shannon & Wilson, 1976); two of these (B-3 and B-6) are set in the dam foundation. One seepage weir was also installed following the modifications at the downstream toe to measure flow from the inclined filter/drain and toe blanket drain; however, the drain is founded on alluvium, and thus some unknown amount of the total seepage through the embankment and, to a much lesser extent, through the bedrock beneath the dam may be passing through the alluvial soils beneath the weir.

The foundation beneath the dam downstream of the cutoff trench includes older alluvial terrace deposits (Qoa, Figure 4-1) – mostly sands and gravels with varying amounts of fines, with some colluvium (Qc) on the mid and upper abutments. Younger alluvial deposits (Qya) – mostly sandy and silty gravels and some sand layers – underlie the channel section of the foundation downstream of the cutoff. Santa Clara Formation bedrock (QTsc) underlies the outlet pipe. In addition, within the channel section, fill overlies the younger alluvium at the base of the downstream buttress, as shown on Figure 2-3. This fill appears to have been placed downstream of the toe of the original embankment when the dam was built.

Overburden soils were generally removed from beneath the upstream embankment zone to the top of the Santa Clara Formation bedrock and from the cutoff trench that was excavated into the Santa Clara Formation bedrock and is located beneath the center of the upstream embankment zone. In addition, a minimum 50-foot wide strip of the upstream buttress foundation is underlain by Santa Clara Formation bedrock. Some younger alluvium appears to underlie the upstream portion of the original embankment (upstream of the cutoff trench) and the downstream margin of the upstream buttress. Details of our recent analysis of the distribution of the various foundation materials underlying the dam are presented in Section 4.0.

The spillway is located outside the dam in the right abutment and is founded on Santa Clara Formation. The existing spillway weir was removed during the dam modifications in 1985-1986 (hereinafter referred to as the 1986 modifications) and the length of the spillway crest was extended at a right angle at the same elevation to increase the capacity of the spillway (Wahler, 1986a).

The outlet works consist of a 50-inch diameter steel pipe encased in 9-inch thick reinforced concrete, an intake structure in the reservoir, and a downstream outlet structure. During the 1986 modifications, the conduit was extended both upstream and downstream to accommodate the construction of the upstream and downstream buttresses. The original intake structure was demolished and a new intake structure was built further upstream at the right abutment. The new downstream outlet structure is similar to the original structure with some minor dimensional changes to improve its performance under seismic loading (Wahler, 1984).

2.3 DESIGN AND CONSTRUCTION HISTORY

2.3.1 Initial Design and Construction

A relatively complete summary of the initial design and construction history of the dam and spillway was presented in the Phase 1 Inspection Report prepared by DSOD for the US Army

Corps of Engineers (DSOD, 1981). The reader is referred to this document for construction details that are not repeated herein.

The following is a list of milestone dates associated with the original design and construction.

August 1934	District submits application for approval of the construction of Stevens Creek Dam to DSOD.
October 1934	District's geological consultant, C. F. Tolman submits report on the geologic conditions at the proposed dam site to DSOD.
March 1935	Construction begins.
January 1936	DSOD performs final inspection of completed dam.
February 1938	DSOD issues Certificate of Approval.

2.3.2 Modifications

As documented in the Phase 1 Inspection Report (DSOD, 1981), the following modifications were made to the dam and appurtenant structures after the facility was initially completed:

1. In 1939, additional fill was placed on the crest to restore it to its design elevation after it was discovered that the dam had settled 0.6 feet in the center of the crest by February 1938.
2. In 1945, the inlet structure was raised to compensate for silting in the reservoir.
3. In 1961, the intake structure was raised again because of silting.

These modifications were followed in 1985-1986 by additional modifications that were designed by Wahler Associates (Wahler, 1984): upstream and downstream buttresses were constructed; the outlet conduit was extended both upstream and downstream; and the intake and outlet structures were replaced. The existing spillway weir was also removed during these dam modifications and the length of the spillway crest was extended at a right angle at the same elevation to increase the capacity of the spillway.

2.3.3 Instrumentation

Instrumentation at Stevens Creek Dam includes the following:

1. Twelve survey monuments were originally installed at the dam: eleven along the crest and one on the right side of the spillway. In 2000, nineteen survey monuments were added along the new crest of the dam constructed in 1986;
2. Seven pneumatic piezometers and two observation wells were installed at the dam in 1976 by Shannon & Wilson in support of a seismic stability assessment of the dam by Woodward-Clyde Consultants (WCC, 1976b) as discussed in Section 2.4. These instruments have all

been abandoned. Nine pneumatic piezometers were installed in 1985 after the dam modifications; and

3. A seepage weir was installed in 1986 to monitor flow from the inclined and blanket drains.

Maximum piezometric levels (i.e. measured total head at full reservoir level) from the pneumatic piezometers are shown on Figure 2-3.

Most recently, five Casagrande piezometers, two standpipe piezometers, and four vibrating wire piezometers were installed by TGP in 2010 and 2011 (Terra/GeoPentech, 2012).

2.4 CHRONOLOGY AND SCOPE OF PREVIOUS INVESTIGATIONS

The first significant post-construction investigations at Stevens Creek Dam were conducted by Woodward-Clyde Consultants (WCC) who completed a Seismic Stability Assessment in 1976 as part of an investigation of four Santa Clara Valley Water District dams (WCC, 1976b). WCC drilled eight borings, six of which were logged and extended into Santa Clara Formation bedrock. They also performed cross-hole shear wave tests in three of the borings, installed two open-well piezometers in the embankment, and performed limited index properties testing. WCC concluded they could not make a meaningful seismic stability evaluation with their data because they were unable to obtain cyclic strength data.

Shannon & Wilson, Inc. (S&W) installed seven piezometers in 1976 (S&W, 1976); one of these (A-3) was apparently installed in the alluvial foundation under the downstream embankment zone. S&W also performed very limited laboratory testing that included three grain size analyses and 17 water content measurements.

More significant field and laboratory investigations commenced with the Seismic Safety Evaluation study in 1978 by Wahler Associates (Wahler) that was followed by their 1982 Preliminary Remedial Design Investigation, and then by their final Remedial Design Report in 1984 (Wahler, 1978, 1982, and 1984). In all, Wahler performed:

- logging of two large diameter borings with down-hole logging and 6-inch diameter Pitcher Barrel sampling; one of these extended into the Santa Clara Formation bedrock;
- logging of four trenches with in-place density testing of embankment, terrace and younger alluvium materials;
- logging of ten rotary borings in the dam, some with frequent Pitcher Barrel sampling; only two of these appear to have extended into bedrock;
- a large number of classification and engineering properties testing including permeability, UU, ICU, ICD and cyclic triaxial tests;
- two sets of cross-hole shear wave tests; and
- logging of many test pits and borings in the borrow area.

Wahler also functioned as resident engineer and provided observation and testing services during construction of the dam modifications in 1985-1986 (Wahler, 1986a and 1986b). A summary of their field density tests, which included in-situ density testing of the alluvial foundation underlying the new outlet structure, was located during our review of DSOD files. As-built sections of the upstream buttress were also located during our review of District files.

All of the above data has been consolidated and reviewed as part of our work. In addition, six sets of black and white stereo aerial photographs were reviewed at the District's office. These photo sets are dated 11/04/1969, 3/31/1983, 6/19/1985, 11/20/1985, 1/10/1986, and 11/05/2002 (SCVWD, 2010c), and are listed on Table 2-1. The three sets from 1985-1986 span the period of the buttress construction and show the dam in various stages of modification with the reservoir area mostly drained.

2.5 SUPPLEMENTAL SITE INVESTIGATIONS AND LABORATORY TESTING

TGP completed supplemental site investigations and laboratory testing to fill data gaps identified by our detailed review of available data and by the results of our preliminary analyses of the seismic stability of the dam (Terra / GeoPentech, 2010). The scope and the results of these supplemental investigations are documented in Report No. SC-1 (Terra /GeoPentech, 2012).

The supplemental site investigations included five sonic borings, six Cone Penetrometer Test (CPT) probes, four mud rotary borings, and eight Becker Penetration Test (BPT) borings. Casagrande piezometers were installed in each of the five sonic borings, a string of four vibrating wire piezometers was grouted in one of the BPT borings on the downstream slope, and standpipe piezometers were installed in two of the BPT borings at the toe of the dam. The plan locations of these supplemental investigations are shown on Figure 2-4. The new piezometers are also shown on the cross sections contained in Figure 2-5.

The supplemental laboratory testing included index property tests on embankment and foundation materials and engineering property tests on the embankment materials. The results of these tests as well as the data available from previous investigations were interpreted to develop the material properties discussed in Section 5.0. The insight into the groundwater conditions within the embankment and foundation provided by the existing and new piezometers are discussed in Section 4.5.

2.6 PREVIOUS SEISMIC PERFORMANCE

A major earthquake, the Loma Prieta earthquake, occurred on October 17, 1989 along a branch of the San Andreas Fault. The epicenter of this event was located about 21 miles (33 km) from Stevens Creek Dam. The dam experienced little to no deformation as a result of this earthquake. The maximum observed settlement was approximately 0.05 feet at the original crest monument located at the Station 8+00 (near the maximum section) and investigations of District Dams by R. L. Volpe & Associates (RLVA, 1990) indicated that Stevens Creek Dam was not damaged by the Loma Prieta earthquake.

3.1 GENERAL

This section describes the geologic and tectonic conditions that characterize the region and local site of Stevens Creek Dam. Section 3.2 describes the regional geology and tectonics and Section 3.3 discusses the local area geology, faulting and seismicity. Maps showing regional faulting and geology are presented as Figures 3-1 and 3-2, respectively.

3.2 REGIONAL GEOLOGIC AND TECTONIC SETTING

Stevens Creek Dam is located in the foothills along the northeast margin of the Santa Cruz Mountains that borders the west side of the Santa Clara Valley, within the northwest-trending California Coast Ranges geomorphic province. The Santa Cruz Mountains are divided into two major fault blocks that are composed of different basement rock and separated by the San Andreas Fault, which passes approximately 4 km southwest of the dam. The San Andreas Fault and associated sub-parallel San Gregorio, Calaveras, and Hayward faults comprise the principal faults of the San Andreas Fault system, and accommodate the majority of transverse tectonic motion between the Pacific and North American plates within the region of San Francisco Bay. Principal faults in the region of Stevens Creek Dam are shown on Figure 3-1, which is excerpted from AMEC (2009).

The fault block basement on the northeast side of the San Andreas Fault consists of an assemblage of rocks that originally formed along the convergent Mesozoic continental margin. These rocks include Jurassic and Cretaceous-age volcanic, sedimentary and meta-sedimentary rocks of the Franciscan Complex, Coast Range ophiolite and Great Valley Sequence. This basement and overlying younger rock comprise a subsidiary fault-bounded block referred to as the New Almaden block (McLaughlin et al., 2001) which, at the latitude of Stevens Creek Dam, extends from the San Andreas Fault on the west to perhaps as far as the east side of the Santa Clara Valley, where the Hayward Fault and a line of west-verging reverse faults form the west side of the Diablo Range (AMEC, 2009). Southeast of Lenihan Dam the basement is further broken into the Sierra Azul block, which separates the New Almaden block from the San Andreas along a complex line of locally merged reverse and oblique-slip faults including the Sargent, Berrocal, Sierra Azul and Aldercroft faults.

The principal fault movement in the region is dominantly right lateral but northeast-vergent (directed) thrusting along a number of reverse faults has resulted in crustal shortening and uplift of the Santa Cruz Mountains and foothills on the northeast side of the San Andreas Fault. This crustal shortening is due to a westward restraining bend in the San Andreas Fault where it passes through the Santa Cruz Mountains. Most of these faults are oriented sub-parallel to the San Andreas Fault and appear to merge with it at depth. These reverse and oblique slip faults include the aforementioned Sargent, Berrocal, Sierra Azul and Aldercroft faults, as well as the Stanford, Monte Vista and Shannon faults (a.k.a., the frontal thrust fault system) that define the range front along the lower foothills/Santa Clara Valley margin. As discussed further below, Stevens Creek Dam is situated on the New Almaden block within a subsidiary block that lies between the Berrocal fault to the southwest and the range-front Monte Vista fault to the northeast.

The Mesozoic basement of the New Almaden block is unconformably overlain by Eocene and Miocene marine deposits, and younger unconformably overlying strata of Pliocene and

Pleistocene fluvial deposits including the Santa Clara Formation. Since middle Pleistocene, these Miocene and younger rocks of the New Almaden block have been locally deformed and faulted along a number of these northeast-verging reverse and oblique slip faults (McLaughlin et al., 2001). Younger and typically less-deformed Pleistocene alluvial terrace deposits occur locally at elevated positions above the present base level of streams draining the mountains and foothills.

Holocene sediments derived from the Santa Cruz Mountains underlie the relatively flat floor of the Santa Clara Valley, and overlap the lowermost foothills along the west side of the valley. Within the mountains, the youngest Holocene deposits are usually limited to floors of the typically narrow stream valleys draining the range.

3.3 LOCAL GEOLOGY, FAULTING, AND SEISMICITY

3.3.1 Local Geology

Stevens Creek follows a sinuous north-northeastward course as it cuts across the foothills on the northeastern side of the Santa Cruz Mountains. These foothills extend from Monte Bello Ridge at the upstream end of the reservoir to the range front at the southwest margin of the Santa Clara Valley. Figure 3-2 is excerpted from Brabb et al (2000) and depicts the geology of the local region of Stevens Creek Reservoir. As shown on that figure, the dam site and entire reservoir area are underlain by the Plio-Pleistocene Santa Clara Formation, which in the local vicinity comprises the entire area of the foothills between the Berrocal and Monte Vista faults (these faults are indicated on Figure 3-2 and discussed in further detail below).

Upstream of the reservoir, Stevens Creek initially flows southeastward following the linear rift of the San Andreas Fault along Stevens Canyon. The creek diverges northeastward from the line of the fault and cuts across the Franciscan rocks that form Monte Bello Ridge, which lies between the San Andreas and Berrocal faults. Stevens Creek then bends north-northwest where it crosses the Berrocal Fault, and meanders across the foothills through the reservoir area and dam site downstream to where it emerges onto the floor of the Santa Clara Valley. Stevens Creek Dam was constructed across the relatively narrow valley of the creek one mile upstream from where it crosses the range front at the Monte Vista Fault. In the area of the dam axis, the channel floor was approximately 170 feet wide prior to construction.

The Santa Clara Formation (QTsc) consists mainly of coarse-grained fan and fluvial deposits including conglomerate and sandstone, with lesser fine grained lacustrine deposits including siltstone and claystone. The age of the Plio-Pleistocene formation has been approximately estimated at 0.3 – 4.8 million years (McLaughlin and Clark, 2004). It has been subdivided into a number of different lithofacies, including the Stevens Creek lithofacies that was derived from erosion of the Franciscan Complex upland to the south (ibid). Within the Santa Cruz Mountains, the Santa Clara Formation is exposed as erosional remnants outcropping mainly along the lower foothills, and more locally along the margins of major drainages, and as fault-bound slivers further within the mountains. Locally the Santa Clara Formation is faulted, deformed, and steeply and tightly folded where adjacent to the San Andreas and reverse faults of the range front system. The Santa Clara Formation strata in the immediate vicinity of Stevens Creek Dam dip uniformly to the east at approximately 30°. Where encountered during the supplemental field

explorations, the Santa Clara Formation is very dense and of very low permeability, with fine-grained material (typically clay) tightly infilling the interstitial space within coarser grained deposits (e.g., conglomerate and sandstone). The Santa Clara Formation underlies most of the upstream portion of Stevens Creek Dam and is described in further detail in Section 4.0.

Older alluvial stream and fan deposits (Qoa) occur mostly as variably well-defined terraces on the lower to upper valley flanks of Stevens Creek. As shown on Figure 3-2, these have been previously mapped at, and downstream of, the dam site as Pleistocene fluvial and alluvial fan deposits (Brabb et al, 2000). They can be distinguished from younger alluvium by "higher topographic position, stronger soil development" and "are less permeable than Holocene deposits" (ibid). A thin layer of terrace alluvium comprised of dense clayey sand with gravel was encountered in boring SC-105MR and its companion SC-105S that were drilled during the supplemental field explorations. Older alluvium deposits occur in the dam foundation on the mid and upper slopes of both abutments (see Figures 4-1 and 4-2), and are described in further detail in the following Section 4.0.

Younger alluvium (Qya) occurs along the floor of the Stevens Creek channel. Where investigated within the area of the dam site, the younger alluvium consists predominately of gravelly, coarse-grained deposits with some interbedded fine sand layers, and with typically minimal fines content. The younger alluvium was typically encountered during the supplemental explorations as a medium dense to dense material (see further discussion in Section 4.0). The younger alluvial deposits were completely removed from the dam foundation within the area of the cutoff and beneath most of the upstream embankment and upstream buttress and were largely left in-place beneath the downstream embankment. The younger alluvium is described in further detail Section 4.0.

Numerous landslides occur throughout the Santa Cruz Mountains region; in the vicinity of the dam site, they mostly occur along the west side of the reservoir. These slides include several large and dormant landslides that overlie the Berrocal Fault on the northeast flank of Monte Bello Ridge, on the west side of the reservoir and south of the Stevens Creek quarry (SCVWD, 1976). The closest slide to the dam consisted of a small translational wedge failure that slid above and presumably onto Stevens Canyon Road, on the upper left abutment above the crest of the dam. This slide occurred sometime prior to December 1955 (date of the earliest historic photo in District files that shows this slide), and possibly as early as during the late stages of construction in 1935, when excavation for the relocated road was underway. This slide clearly occurred as a result of undercutting and day lighting the Santa Clara Formation bedding that dips eastward and parallel to the slope on that side of the valley. Field examination during the supplemental explorations indicated no evidence for renewed movement in the area of this slide (the limits of this slide are depicted on Figure 4-1).

3.3.2 Local Faulting of Consequence to Stevens Creek Dam (San Andreas, Stanford-Monte Vista and Berrocal faults)

The Seismotectonic and Ground Motion Study for Seismic Stability Evaluation of DIP Phase 1 Dams, Technical Memorandum No. 3 (TM-3; AMEC, 2009) indicates that the San Andreas, Berrocal, and Stanford-Monte Vista faults are the controlling seismic sources at Stevens Creek Dam. As per TM-3, the Stanford-Monte Vista earthquake (M6.9) produces the highest

accelerations at short periods whereas the San Andreas earthquake (M7.9) dominates at longer periods. These faults are depicted on Figure 3-1.

The San Andreas Fault is a strike-slip fault with a very high slip rate (> 9mm/yr) and was the source of the M7.9 San Francisco earthquake in 1906. The closest mapped trace of the San Andreas Fault passes 3.8 km to the southwest of Stevens Creek Dam, through the upstream fault-controlled reach of Stevens Canyon. We noted that Table 2 in TM-3 (AMEC, 2009) shows the San Andreas Fault at a map distance of 4.2 km from the dam; however, the mapped trace is actually 3.8 km from the dam. A subsidiary oblique-slip fault that is part of the San Andreas system was the source of the M6.9 Loma Prieta earthquake in 1989, rupturing along a length of approximately 40 km through the region of the Santa Cruz Mountains southeast of Stevens Creek reservoir (Spudich, 1996). This southwest-dipping fault was previously unrecognized prior to the Loma Prieta event, and ruptured from the south side of, and northwards across, the main trace of the San Andreas Fault.

The conditionally active Berrocal and active Stanford-Monte Vista faults are both southwest-dipping reverse faults and are located to the southwest and northeast of the dam, respectively; the dam is therefore located on a block of rock that forms the footwall of the Berrocal Fault and the hanging wall of the Stanford-Monte Vista Fault. The surface trace of the Monte Vista Fault is located 1.6 km map distance to the northeast, along the range front, and it dips beneath the dam at a closest fault rupture distance (r_{rup}) of 1.3 km assuming a fault dip of 55° (average fault dip as per TM-3). We noted that Table 2 in TM-3 (AMEC, 2009) shows the Stanford-Monte Vista fault at a map distance of 2.4 km and r_{rup} distance of 2.0 km from the dam and then double checked to confirm that our distance estimates were indeed correct. The Berrocal Fault crosses Stevens Creek just south of the upstream end of the reservoir, and passes concealed beneath a landslide at a closest distance of 1.1 km southwest of the dam. We noted that Table 2 in TM-3 (AMEC, 2009) incorrectly shows the Berrocal Fault at a map distance of 0.3 km from the dam. Work by the USGS (McLaughlin et al., 2001; McLaughlin and Clark, 2004) notes that the locus of contractional deformation northeast of the San Andreas Fault has occurred primarily between the Berrocal Fault and the Monte Vista and Shannon faults, within the New Almaden block (AMEC, 2009). TM-3 (ibid) shows the Berrocal Fault as a conditionally active, low to moderate slip rate fault (< 0.1 to 1.0 mm/yr) whereas the Stanford-Monte Vista Fault is shown as an active, moderate slip rate fault (0.1 to 1.0 mm/yr).

DSOD has indicated in their comments on the SSE-1 Investigations DM-2 and Interim DM-4 for Guadalupe, Almaden, and Calero Dams (DSOD, 2010) that they have historically considered a combined rupture of the Shannon-Monte Vista faults, in contrast to the Stanford-Monte Vista Fault rupture scenario of AMEC. The combined Shannon-Monte Vista scenario is consistent with the interpretation of the fault as defined in Appendix A: California Fault Parameters for the National Seismic Hazard Maps and Working Group on California Earthquake Probabilities (Wills et al, 2008). However, TM-3 provides a basis for the segregation of the Shannon Fault from the Stanford-Monte Vista Fault in the vicinity of Blossom Hill, and we are herein utilizing the delineation of the Stanford-Monte Vista Fault as a single fault rupture source separate from the Shannon Fault as is described in TM-3. The maximum moment magnitude of M7 as assigned by DSOD to the Shannon - Monte Vista earthquake closely approximates the M6.9 estimate by AMEC for the Stanford - Monte Vista earthquake.

Our review of data related to the seismologic and tectonic conditions in the region of Stevens Creek Dam found no indications of tectonic deformation in the immediate vicinity of the dam. No faults are shown passing through, or in the immediate vicinity of, the dam site on the AMEC 2009 maps or on earlier USGS and California Division of Mines and Geology (CDMG) maps (Brabb et al, 2000; Sorg and McLaughlin, 1975). No faulting of the east-dipping Santa Clara Formation beds was noted at the dam site during construction (Marliave, 1936), and no linear features were noted crossing the dam site on the aerial photographs (SCVWD, 2010c) we reviewed.

3.3.3 Seismicity of Local Region

The 1906 M7.9 San Francisco and 1989 M6.9 Loma Prieta earthquakes dominate the historical seismicity in the region of Stevens Creek Dam. The 1906 earthquake produced ground rupture along the San Andreas Fault at various locations northwest to southeast of the dam, and the USGS has estimated that almost 15 feet of horizontal slip occurred at depth along the reach of the fault immediately to the southwest (USGS, 2011). Secondary triggered slip along the Stanford Fault may also have occurred as a result of the 1906 earthquake along the range front north-northwest of the dam (AMEC, 2009).

The 1989 earthquake occurred at an epicentral distance of 33 km southeast of the dam, along a southwest dipping rupture surface that is separate from the main trace of the San Andreas Fault. The earthquake produced right-oblique movement along the fault at depth, and uplift and shortening of the overlying crust that in the local epicentral region resulted in ridge-top spreading, extensional fissuring and other deformational surface features not directly related to faulting (Wells, 2004). The northernmost reach of fault rupture, as defined by the distribution of aftershocks, extended to a point about 8 km south-southeast of Stevens Creek Dam. The Loma Prieta earthquake triggered slip at several locations along the Monte Vista Fault, including an area of focused deformation that was noted along the Monte Vista Fault just northwest of Stevens Creek (McLaughlin and Clark, 2004).

4.1 GENERAL

This section documents our assessment of the foundation conditions at the dam based on our review of construction records and pre-construction as well as post-construction studies by others and the results of our 2010-2011 field explorations (Terra / GeoPentech, 2011b). The general characteristics of the foundation materials are also discussed in the following subsections.

4.2 GEOLOGY OF DAM SITE

Figure 4-1 shows the estimated distribution of the various geologic units underlying Stevens Creek Dam, as well as mapped locations of units and other geologic features in the areas immediately adjacent to the dam. The downstream portion of the original dam embankment was constructed on alluvial and colluvial deposits that overlie the Santa Clara Formation (hereinafter referred to as "bedrock"), whereas the majority of the upstream embankment was founded directly on the Santa Clara Formation after most of the alluvial deposits had been removed during construction. A foundation seepage cutoff beneath the upstream embankment was developed by excavating a trench into the Santa Clara Formation; this cutoff was excavated to an average depth of about 8 feet under the channel section, and to depths ranging from a minimum of about 5 feet on the right abutment to a maximum of about 40 feet on the left abutment.

The 1986 downstream buttress was founded on the younger and older alluvial deposits, whereas the majority of the upstream buttress was keyed into bedrock where, under the channel section, a minimum 50-foot wide strip of the buttress foundation is directly underlain by the Santa Clara Formation. As noted above, most of the alluvial and colluvial deposits were apparently removed from beneath the upstream zone of the original embankment, which extended upstream from the “downstream/upstream embankment” contact located a short distance downstream of the cutoff (as shown on DSOD, 1935-1936 and Marliave, 1936). However, some narrow areas of younger alluvium appear to remain under the upstream-most portion of the original embankment (upstream of the cutoff trench) and under the downstream and upstream margins of the upstream buttress. This observation is derived from a review of as-built cross sections prepared by Wahler (Wahler, 1986a). These cross sections depict both the configuration of the upstream buttress excavation and the buttress foundation conditions. This configuration was apparently necessary because complete removal of the alluvium beneath the entire buttress footprint would have required undercutting the original dam toe. In their records, DSOD noted that this approach was a change in the specified foundation design criteria that called for the entire upstream buttress to be founded on Santa Clara Formation bedrock (DSOD, 1985-1986). However, DSOD accepted founding the buttress on marginal areas of alluvium provided that a minimum 50-foot width of the buttress was founded on bedrock. This configuration is shown on the Wahler as-built sections and also indicated by the distribution of Santa Clara Formation bedrock in the upstream foundation area on Figure 4-1.

Most of the original outlet conduit was founded on Santa Clara Formation bedrock, set on a bench cut into the base of the steep lower right abutment slope that bordered the right side of the channel prior to construction. A short section of the conduit, across the cutoff, was deliberately undermined after its placement to allow for the subsequent excavation of the cutoff trench; this section was then re-supported with compacted “impervious” zone backfill placed within the

excavation beneath the pipe. The furthest downstream section of the 1986 outlet conduit extension was founded on alluvium, as was the downstream-relocated outlet structure. The details of the outlet structure foundation were revealed on construction field density test summary sheets (Wahler, 1986b). The position of the upstream outlet extension and intake on the right bank above the channel area, along with the top of rock elevations known in that area from the 1986 exploration and topography, suggest that the entire length of the upstream 1986 outlet extension and relocated intake were founded on excavations into the Santa Clara Formation.

The younger alluvial deposits remaining in the channel section of the foundation downstream of the upstream embankment are predominately coarse-grained, consisting mostly of sandy and silty-clayey gravels with some interbedded finer sand layers. The abutment foundations downstream of the cutoff include older alluvial terrace deposits and weathered Santa Clara Formation, most of which are clayey sands and gravels; localized more pervious gravel-filled channel deposits cut into the Santa Clara Formation on the upper left abutment. Some colluvium and/or residual soil also overlie the weathered Santa Clara Formation bedrock and underlie the embankment on portions of the abutments downstream of the cutoff. Details of the distribution and characteristics of these various foundation materials are presented in Sections 4.3 and 4.4.

Foundation conditions at Stevens Creek Dam have been evaluated via relatively limited investigations completed for geotechnical studies performed after the original construction. However, Wahler's initial 1978 investigation did include excavation of T-4, a deep trench into the younger alluvium located at the downstream toe of the dam (as shown of Figure 2-2), which provided a useful graphic geologic log and in-situ density test data on the gravelly and interbedded finer sandy alluvial deposits. These in-situ densities can be used to check that the seismic performance of the alluvium as indicated by the measured and inferred standard penetration test results [$(N_1)_{60}$ values] discussed later in Section 5.6 appear reasonable. Results from Wahler's trench T-3, excavated into the flat alluvial terrace at the downstream mid-right abutment toe of the original embankment (Figure 2-2), are also available but less useful because they were judged by Wahler to be in error, as further discussed in Section 4.4.2. Shear wave testing by Woodward Clyde Consultants (1976b) and Wahler (1982) penetrated a short distance into the younger alluvium beneath the embankment, but apparently did not extend across the entire alluvial section into the Santa Clara Formation. Other useful data on foundation properties from previous studies consist of piezometric level monitoring in the younger alluvial foundation, from Shannon & Wilson's piezometer A-3 (installed in the original embankment and later abandoned) and the District's piezometer B-3 (installed in 1986 following the embankment modifications).

Useful data on foundation materials were also produced during the initial design investigation and construction in the 1930s. The geologic studies for design of the original embankment included assessments of the Santa Clara Formation with permeability testing (Tolman, 1934), and as-built geologic conditions of the foundation were documented during and after construction (DSOD 1935-36 and Marliave, 1936, respectively). An as-built geologic section of the dam, along the axis of the cutoff trench, was prepared by Marliave and is reproduced on Figure 4-2.

4.3 FOUNDATION MODEL

The 2010-2011 field explorations included a variety of exploration and in-situ test methods, including sonic drilling, mud rotary drilling with Standard Penetration Tests (SPTs), down hole OYO P-S suspension logging, CPT soundings, Becker borings with BPTs, Pile Driving Analyzer (PDA) measurements for three of the Becker borings, piezometer installation and in-situ (falling head) permeability testing (Terra / GeoPentech, 2011b). The focus of this work was to more accurately define the following:

1. distribution and thickness of the younger and older alluvial deposits within the foundation; and
2. soil classification, grain size distribution, plasticity, permeability, strength, and shear wave velocity of the embankment and/or foundation materials; and
3. piezometric levels within the younger and older alluvial portions of the foundation and within the embankment.

The previous and current exploration data on foundation conditions were analyzed to assess material properties and to define the distribution (depth and thickness) of the alluvium and other soils within the foundation. The process used to consolidate these data and prepare a geologic model of the foundation is discussed in the following paragraphs.

Table 4-1 presents data on dam foundation surface elevations where encountered in the previous and current explorations. As noted above, foundation materials consist either of the younger channel alluvium (Qya), older terrace alluvium (Qoa), colluvium/residual soil (Qc) or Santa Clara Formation (QTsc) that underlie the embankment. The table also shows elevations of the top of the Santa Clara Formation bedrock where encountered either beneath alluvial or colluvial deposits remaining in the foundation, or directly underlying the embankment. Data on the inferred thickness of foundation soils (younger and older alluvium, and colluvium) that remain between the embankment and the underlying Santa Clara Formation bedrock are also indicated.

For our initial analysis of earlier data that was required to develop the work plan for the field explorations and laboratory testing (Terra / GeoPentech, 2010 and 2011a), we assumed that geologic interpretations presented on the previous consultants' exploration logs were correct. Upon completion of the current exploration program, some of these original interpretations were either changed or disregarded where our recent data or analysis indicated the original interpretations were in error (e.g., when the original logged contact depths were inconsistent with pre-construction or as-built elevation data and/or subsurface data from other nearby previous or current exploration). Those foundation elevation data that were re-interpreted from the original logs are indicated on Table 4-1. Note that special attention was paid to converting all the elevation data on previous maps and field explorations to the currently used NAVD 1988 vertical datum. The original design drawings, and the WCC and S&W studies, were based on a local vertical datum that was converted to NAVD 1988 vertical datum by adding 0.7 feet. The Wahler investigations data were based on the USGS 1929 vertical datum and were converted to NAVD 1988 vertical datum by adding 2.8 feet.

The foundation data on Table 4-1 were plotted on several geotechnical base maps that covered the area of the original and enlarged 1986 footprint. These maps included digitized as-built foundation topography (SCVWD, 2010d) showing the configuration of the excavated foundation

prior to placement of the embankment, and digitized original pre-construction (i.e., pre-excavation) topography of the dam site (SCVWD, 2010e). The as-built foundation surface contours were locally adjusted where required to accurately reflect the elevations of foundation contacts as encountered in the previous and current explorations. Comparison of this modified as-built topography with the pre-construction topography was useful for defining areas of minimal foundation excavation mostly downstream of the upstream embankment.

The pre-construction topographic map was also used to estimate the top of the Santa Clara Formation bedrock in the areas of the dam located downstream of the upstream embankment. This was done by making assumptions regarding the pre-construction thickness of surficial soils that were calibrated with known thicknesses from local explorations and as depicted on Marliave's as-built geologic profile along the cutoff trench (Figure 4-2).

New elevation contours were drawn for the upstream buttress foundation beyond the footprint of the original dam using the as-built sections showing the buttress configuration (Wahler, 1986a). Top of bedrock elevations between the original dam cutoff trench and the base of the approximately 50-foot wide cutoff trench through the alluvium that underlies the 1986 upstream buttress were estimated based on the Wahler as-built sections that show the level of the top of rock under the buttress.

The surfaces defined by the modified as-built foundation contours and estimated top of Santa Clara Formation contours were then combined to produce the isopach map presented in Figure 4-3 that shows the estimated distribution and thickness of the alluvial and colluvial soils that remain in-place within the foundation of the embankment. The local geology of the dam site area and foundation as depicted on Figure 4-1, which is a compilation of previous geologic mapping with our recent field mapping, was updated using data from Figure 4-3 to define the areas of the dam foundation estimated to be directly underlain by the Santa Clara Formation bedrock.

4.4 GENERAL CHARACTERISTICS OF FOUNDATION MATERIALS

4.4.1 Younger Alluvium

As shown on Figures 2-4 and 2-5, the younger alluvium that underlies the channel area of the foundation downstream of the upstream embankment was investigated in 2010-2011 by a number of field explorations along the maximum section through the embankment (Station 7+50). Figure 4-1 shows the extent of younger alluvium beneath the dam and also shows topographic contours for the dam and surrounding areas. Sonic boring SC-101S, mud rotary boring SC-101MR, and CPT-1 were drilled in a closely-spaced cluster at this station on the crest of the dam. SC-102S and Becker boring SC-102BPT were drilled on the downstream slope at approximate elevation 528 feet, and SC-103S and SC-103BPT and SC-104MR were drilled further downslope at approximate elevation 490 feet. Borings SC-104S, SC-104MR, and SC-104BPT; and CPT-3, CPT-5 and CPT-5a; were also drilled at Station 7+50, immediately downstream of the toe at approximate elevation 442 feet. The younger alluvium at the toe was also investigated across the width of the channel at SC-107BPT and SC-110BPT to the right/east of Station 7+50, and at SC-108BPT, 106BPT, 109BPT and CPT-4 to the left/west of Station

7+50. The younger alluvium had been investigated previously at various WCC, S&W and Wahler borings, and at one trench, as discussed further below.

The 2010-2011 field explorations indicate that the younger alluvium in the foundation is less than about 15 feet thick throughout most of the channel area. This thickness includes any thin overlying topsoil, colluvium or residual soils that may occur at the original uppermost surface of the alluvium. As shown on Table 4-1, the thicknesses of younger alluvium encountered during the recent and previous explorations range from 7 feet (along the left margin of the channel at the toe) to about 15 feet; thicknesses of 10 to 15 feet appear to be most common. Marliave's as-built geologic section along the cut-off trench (Figure 4-2) shows a uniform thickness of 15 feet across the alluvial channel, except for a locally thicker section of about 19 feet at the right margin of the channel.

The elevations of the dam foundation at the top of the younger alluvium as interpreted in the recent and previous borings are consistent with the pre-construction topographic contours, indicating that minimal foundation excavation was performed over the area of the channel downstream of the upstream embankment. Original dam construction inspection reports by State inspector G.F. Engle (DSOD 1935-1936) indicate that the contractor had initially requested approval for fill placement on portions of the downstream foundation that was denied because of inadequate stripping (organics, trees, etc. were reportedly left in-place); although Engle indicates that the prepared foundation surfaces were eventually accepted, this does suggest that excavation downstream of the upstream embankment was probably minimal.

Variations in the interpreted depth of the top of alluvium at the closely-spaced cluster of borings at SC-104, near the downstream toe of the dam, appear to correlate with the location of the original Stevens Creek channel thalweg where the depth of the channel surface/top of the alluvium would have been deeper.

Visual and laboratory classifications indicate that the majority of the younger alluvial deposits are coarser-grained, consisting of well- and poorly-graded gravels with varying amounts of silt, clay and sand (see photos 2, 4, and 6 on Figures 4-4A to 4-4C). Laboratory test data indicate that a predominance of the younger alluvium classifies as GP, GC, GW-GM, GP-GM, GW-GC, and GP-GC, as discussed in Section 5.0. Gradation analyses indicate a majority of the gravel fraction is less than 1.5 in. in diameter, although some coarse gravels and cobbles up to 4 in. in diameter were noted and apparently occur more concentrated in localized zones (see photos 4, 5, and 6 on Figures 4-4B and 4-4C). Occasional interbedded, finer silty sand (SM) layers, typically less than 2 feet thick, were encountered in most borings drilled into the younger alluvium (see photos 1, 3, and 5 on Figures 4-4A to 4-4C). The presence of finer sand layers at similar depths in adjacent crest borings SC-101S and SC-101MR (located about 10 feet right of SC-101S), along with the minimum 20-foot width of the fine SP-SM interbed noted in Wahler trench T-4 (discussed further below), indicates that at least some of these finer sand interbeds have considerable lateral continuity across the channel.

As shown on Figure 2-2, Trench T-4 (Wahler, 1978) was located at the downstream toe of the original embankment. The log for this test trench has been reproduced on Figure 4-5 and shows that approximately 13 feet of fill was encountered overlying the channel alluvium . The top of the alluvium was encountered at elevation 430.5 feet, which is consistent with the top of the alluvium as encountered in our recent borings at the toe. The alluvium in T-4 was classified as

predominately sandy gravel-gravelly sand with varying amounts of fines (GP-GM, SM-SC, and SW); in-situ testing of the coarser alluvium indicated dry densities of 109.6 and 114.0 pcf. The trench also exposed a 2-foot thick, interbedded fine sand layer (SP-SM) along a 20-foot long portion of the trench. In-situ testing of that sand resulted in an in-place dry density of 94.5 pcf. Wahler indicated that the in-place densities were approximately 91% of maximum density determined from compaction tests. Water was encountered in the lower part of the trench at elevation 423 feet, which is consistent with our recent piezometer readings near the toe.

4.4.2 Terrace Alluvium

The older alluvium (Qoa) that underlies portions of the embankment on the abutments downstream of the upstream embankment was investigated during the recent field explorations at approximately Station 4+00, on the right side of the dam. Sonic boring SC-105S, mud rotary boring SC-105MR, and CPT-2 were drilled in a closely-spaced cluster at this station, right of the angle point on the crest of the dam. This general area was also investigated further right with large-diameter Wahler boring SC-1, at approximate Station 2+20 on the crest of the original dam (Wahler, 1978).

As noted earlier, the older alluvial deposits have been previously mapped as alluvial Pleistocene channel and fan deposits (Brabb et al, 2000). A geomorphically pronounced terrace on the mid-right abutment underlies the downstream portion of the embankment, extending rightwards from about Station 5+70 to Station 4+00, and comprises the relatively flat areas immediately downstream of the dam and on the right side of the mid-section of the spillway. This terrace is underlain by relatively thin amounts of older alluvium, and little if any of this material was removed from the foundation downstream of the upstream embankment, as indicated by comparison of the pre-construction and as-built topography and subsurface data from the recent explorations and the Wahler studies.

Figure 4-2 shows that the thickest right side terrace alluvium is probably less than 8 feet thick, between approximate Stations 5+70 and 4+50 (Marliave, 1936). The recent work at SC-105 and Wahler's previous drilling further to the right at SC-1 suggest that, within the foundation at, and right of, approximate Station 4+00, the right side terrace alluvium together with any overlying topsoil, colluvium or residual soil is probably less than about 4 feet thick. These thin surficial soils are underlain by about 6 to 8 feet of weathered Santa Clara Formation, which in turn is underlain by harder, less weathered Santa Clara Formation. This sequence is consistent with Marliave's as-built geologic section along the cut-off trench presented on Figure 4-2.

Wahler trench T-3 was located on the west end of the right side terrace at the downstream toe of the original embankment (Figure 2-2), and encountered fine to coarse sandy gravel and cobbles to the trench bottom at a depth of 10 feet. This material was interpreted by Wahler as terrace alluvium, with in-place density tests indicating dry densities of 99.0 - 99.4 pcf. Wahler considered these tests to be erroneously low, and attributed the results to the use of an inappropriately-sized sand cone given the coarse-gravel and cobble fraction of the material. However, our comparison of the T-3 trench location with the pre-construction topography suggests that most of this trench was probably excavated within fill (possibly spoil placed outside the limits of embankment), given that the top 6 feet of the trench were above the preconstruction ground surface.

Original dam construction reports by Engle (DSOD 1935-1936) and Marliave (1936) indicate that deep older alluvial channels (described as "open gravel with little clay") crossed the upper left abutment, left (west) of approximate Station 10+15, to depths of up to about 30 feet below the original ground surface. The deepest channel is shown on Marliave's as-built geologic section (Figure 4-2) as extending down to about elevation 500 feet. These deposits required significant deepening of the cutoff trench across the upper left abutment. The presence of these older alluvial channel deposits on the upper left abutment is consistent with our recent reconnaissance geologic mapping and with earlier mapping of the area that was done as part of a landslide mapping investigation for the District (SCVWD, 1976). That mapping indicates the presence of older alluvial sands and gravels on the boat launch peninsula just upstream of the dam on the left (west) side of the reservoir, with the base of the deposit at about elevation 500 feet; i.e., approximately at the same elevation where Marliave's as-built geologic section depicts the lowest extent of alluvial channel deposits through the upper left abutment. The upper level older alluvium exposed in the area of the left side boat ramp consists of clean gravelly sand and sandy gravel that has more open inter-granular space as compared to the clayey sands of the older alluvium noted on the right abutment at SC-105, and probably represents the same open gravel channel deposits that were cut off by the deep excavation through the upper left abutment during construction (see Photo 7 on Figure 4-4D). The extent of the older alluvium on the upper left abutment is also depicted on Figures 4-1 and 4-3.

As shown in Figure 2-2, WCC borings WCC-1 and WCC-2 were located on the left side of the original embankment, along Station 9+70, and encountered about 10 feet of older alluvium remaining beneath the embankment and above the Santa Clara Formation bedrock downstream of the upstream embankment. These borings were located to the right (east) of the deep channel deposits noted above. Penetration resistance data on the WCC boring logs indicate that these older alluvial deposits are dense (WCC, 1976b).

4.4.3 Santa Clara Formation

The Santa Clara Formation (QTsc) bedrock that underlies the alluvial portions of the foundation and most of the upstream portion of the embankment was encountered in all borings drilled during the recent explorations, and refused penetration in all 6 CPT soundings that were advanced through the overlying embankment and alluvium. However, as shown on Table 4-1, the majority of borings drilled for previous studies did not penetrate into the Santa Clara Formation.

The Santa Clara Formation is a weakly indurated bedrock formation with generally low hardness (i.e., it can be readily gouged with the pick of a rock hammer). However, as a soil unit, it is very dense and of very low permeability, with fine-grained material (typically clay) tightly infilling the interstitial space within the coarser grained deposits of conglomerate and sandstone (see Photo 8 on Figure 4-4D).

At the dam site, the formation dips uniformly eastward at approximately 30° and consists predominately of thickly bedded to massive conglomerate and sandstone layers, interbedded with lesser beds of claystone. The recent laboratory testing indicates that, when broken down, the conglomerate units classify as clayey gravel with sand (GC) and gravel with silty clay and sand (GP-GC); the sandstone units classify as clayey sand with gravel (SC), and are generally

indistinct from the conglomerate except for a somewhat smaller gravel fraction; and the claystone classifies as lean clay (CL).

An upper veneer of more weathered Santa Clara Formation was encountered immediately underlying the alluvium, and was best defined in several borings on the basis of somewhat lower SPT penetration resistance and OYO shear wave velocity relative to the deeper Santa Clara Formation. At crest boring SC-101MR, approximately 4 feet of weathered Santa Clara Formation was encountered underlying the younger alluvium from 134 to 138 feet, with shear wave velocities ranging from 1,718 to 1,970 ft/sec; the underlying less weathered rock produced shear wave velocities ranging from 2,458 to 4,458 ft/sec. Right side crest boring SC-105MR encountered roughly 6 feet of weathered Santa Clara Formation under older alluvium from 52.5 to about 58.5 feet, with shear wave velocities ranging from 1,788 to 2,067 ft/sec; the underlying rock at SC-105MR produced SPT refusal and higher shear wave velocities ranging from 2,247 to 3,322 ft/sec. Laboratory testing of a large diameter sample obtained from Wahler boring SC-1 indicated a dry density of 133.7 pcf for what was probably weathered Santa Clara Formation (Wahler, 1978); this material was initially interpreted by Wahler as possible terrace alluvium.

4.5 GROUNDWATER CONDITIONS

Figures 2-3 and 2-5 show cross sections through the dam that illustrate the locations of previously installed piezometers and the locations of piezometers installed as part of the 2010-2011 field explorations by TGP, respectively. The maximum total heads measured in the previously installed piezometers are illustrated on Figure 2-3 and indicate that the alluvium left in place beneath the downstream embankment is functioning as a horizontal drain as evidenced by the downward gradient within the embankment piezometers and the very low piezometric levels in piezometer B-3. One of the primary purposes of the supplemental field investigation by TGP was to provide additional data on the piezometric levels within the alluvium and to further evaluate the presence of a downward gradient within the embankment materials above the alluvium. The locations of the piezometers installed by TGP in 2010-2011 are shown on Figure 2-5. Casagrande piezometers were installed at the base of the alluvium in all five sonic borings, a string of four vibrating wire piezometers were installed in Becker boring SC-102BPT, and standpipe piezometers were installed in Becker borings SC-106BPT and SC-107BPT to provide additional data on groundwater levels near the toe of the dam and allow field permeability testing.

Figure 4-6 summarizes the data collected on all new piezometers from the time they were installed in November 2010 or February 2011 to early June 2011. The reservoir level from November 2010 through early June 2011 is also plotted on this figure. As shown on Figure 2-5, piezometers SC-101S through SC-104S are located near the base of the alluvium at the maximum section of the dam. As shown on the enlarged scale plot on the lower right side of Figure 4-6, the total heads measured on these piezometers ranged from elevation 418 to 424 feet during this period. The total heads measured at piezometer SC-105S are approximately at elevation 495 feet and there is less variation of total head with time at that location. As shown on Figures 2-4 and 2-5, this piezometer is located beneath the crest of the dam at Station 4+00.

Figure 4-7 illustrates the variation with time and location of total heads within the alluvium at the maximum section of the dam. Each of the fifteen “thumbnail” plots on this figure illustrates the

groundwater levels within the alluvium on a particular date and compares the measured water level to the elevation of the top of the Santa Clara Formation as measured at each of the borings. On December 7, 10 and 16, 2010, we see that the groundwater levels vary from about elevation 421 feet at the crest of the dam to about elevation 418.5 feet near the toe of the dam and that the horizontal hydraulic gradient within the alluvium shows groundwater flowing from left to right, i.e. upstream to downstream. We can also see from the thumbnails for these dates that the saturated thickness of the alluvium varies from nearly zero at the crest to a maximum of about 10 feet near the toe.

The thumbnail plot on Figure 4-7 for December 30, 2010 provides data on piezometric levels following a period of heavy rain as indicated by the rise in reservoir level in the preceding 10-day period, as shown on Figure 4-6. Close inspection of the data on December 30 shows very little change in groundwater levels at the crest of the dam and a rise in groundwater level greater than 2 feet near the toe. The horizontal gradient within the alluvium on December 30 shows that water is flowing upstream from the downstream toe area and downstream from the crest area as the groundwater levels within the alluvium rise in response to higher groundwater levels downstream of the dam. The data for the thumbnails on January 15, January 24, and February 10, 2011 show the groundwater levels within the alluvium falling at a time when the reservoir level remained constant (because of little precipitation) and the groundwater again flowing from left to right (upstream to downstream). However, on February 18, 2011 we again see the groundwater levels near the toe of the dam rising in response to precipitation (as evidenced by the rise in reservoir level) with an even more pronounced rise in groundwater levels near the toe on February 21, following heavy rains between February 18 and February 21. The hydraulic gradient on February 21 clearly shows that the groundwater flow within the alluvium is from downstream to upstream as groundwater levels within the alluvium rise. The thumbnails for February 22, 23 and 24 show how the hydraulic gradient (indicating upstream flow) decreases as the water levels within the alluvium near the crest of the dam rise. On February 24, the groundwater levels are essentially flat and the saturated thickness of the alluvium has increased by about 3 feet at the crest of the dam and 5 feet near the toe of the dam relative to the levels observed on December 7, 2010. Data from readings taken on March 15, April 20, and May 24, 2011 are also shown on Figure 4-7 and are consistent with the previous observations. These data illustrate that the groundwater levels within the alluvium at the maximum dam section are low (within 2 to 10 feet of the bottom of the alluvium depending on location) and hydraulically controlled by the groundwater levels at the toe of the dam. The groundwater levels at the toe of the dam appear to be controlled by precipitation and recharge from Stevens Creek – not by reservoir level.

The measured total heads in the piezometers in the younger alluvium at the maximum section of the dam indicate that water is perched on the surface of the underlying comparatively impermeable Santa Clara Formation bedrock, and, within the area of the younger alluvium downstream of the upstream embankment, is strongly influenced by groundwater levels downstream of the dam which are in turn controlled by precipitation and recharge from Stevens Creek at the downstream outlet structure.

Some periodic recharge (probably limited to periods of intermittent higher runoff during the rainy season) is also apparently occurring from the poorly-drained tributary drainage that flows into Stevens Creek from the downstream left abutment, just downstream of the toe of the dam.

After a period of heavy rain in February 2011, water was observed ponding at this location within the tributary ravine at a level that is just a few feet lower than the ground surface at the toe; this level is considerably higher than the level of Stevens Creek. Drainage of this ravine across the left side toe area is apparently being impeded by vegetation and debris that clog the CMP culvert which passes this flow under the toe access road and into Stevens Creek. The groundwater levels near the toe of the dam are being measured by three piezometers, as shown in Figure 2-5. Table 4-2 summarizes the data from the piezometers at the toe. The groundwater levels in the standpipe piezometer at SC-106BPT are typically higher than the groundwater levels in the Casagrande piezometer at SC-104S by 0.4 feet or less, and the groundwater levels at SC-104 are typically 0.5 to 1.0 ft higher than the standpipe piezometer levels at SC-107BPT. These measurements indicate that groundwater is flowing from left to right at the toe of the dam and that the lower groundwater levels are in the vicinity of SC-107BPT that is located near the outlet structure at Stevens Creek.

Figure 4-6 summarized the data from the vibrating wire piezometers installed in Boring SC-102BPT and these data are tabulated in Table 4-3. Review of the data show that vibrating wire piezometers VW-1 through VW-3 reached stable values within one to two weeks of piezometer installation but that piezometer VW-4 did not reach an equilibrium value until about 10 weeks after installation. Figure 4-8 summarizes the total heads measured on June 2, 2011 at these piezometers. The total heads are plotted versus elevation and clearly show a strong downward vertical gradient (equal to 1 between VW-2 and VW-3). VW-4 is located approximately at the interface between the downstream embankment and the alluvium, and the total head at that piezometer is 6 feet above the elevation of the piezometers tip (i.e. the pressure head is 6 feet). Our best estimate of the distribution of total heads for steady state seepage is also shown on Figure 4-8. The downward gradients from the new piezometers shown on Figure 4-8 are consistent with the data from the existing piezometers shown on Figure 2-3.

The data from piezometer SC-105S located on the dam crest at Station 4+00 (see Figures 2-4 and 2-5 for location and Figure 4-6 for total head vs. time) indicate that some seepage probably occurs through the older terrace alluvium that remains in the foundation beneath both sides of the dam, and is likely fed by groundwater within the abutments. Note that the Casagrande piezometer installed in SC-105S appears to have been installed with its sensing zone within the upper, weathered Santa Clara Formation, rather than within the thin terrace alluvium that occurs at that particular location.

In summary, the new Casagrande, open standpipe, and vibrating wire piezometers clearly show that the alluvium beneath the embankment functions as a very effective horizontal drainage blanket.

5.1 GENERAL

This section summarizes the data on physical and index properties and engineering properties of the embankment and foundation materials from previous studies and from the field and laboratory data collected during the 2010-2011 supplemental investigations completed by TGP (Terra / GeoPentech, 2011b), and documents the selection of engineering properties that will be used for the seismic safety evaluation of Stevens Creek Dam. The following subsections address the zoning of the dam and the general sources of the embankment materials, the index properties and engineering properties of the embankment materials, and the index properties and engineering properties of the alluvium and Santa Clara Formation that are relevant to the engineering analyses.

5.2 DAM ZONING AND SOURCES OF MATERIALS

As noted in Section 2.2, Stevens Creek Dam was originally constructed as a two-zone earth embankment with an "impervious" upstream zone and a "pervious" downstream zone. Subsequent studies have indicated that the dam may in fact be more like an homogenous embankment. Therefore, in this report, the embankment zones are referred to as upstream embankment and downstream embankment. In 1986, upstream and downstream buttresses were added to the original embankment. An inclined filter/drain layer was placed between the original embankment and the downstream buttress and a horizontal drainage blanket was constructed on top of the foundation beneath the downstream buttress. As discussed in Section 4.0, alluvium was left in place under the downstream portion of the original dam and the downstream buttress but excavated under most of the upstream embankment material and upstream buttress.

Figure 5-1 shows the generalized configuration of the dam and its foundation at the maximum section (Station 7+50) and at a section through the right abutment (Station 4+00). The various material zones identified are: Upstream and Downstream of the original embankment; Upstream and Downstream Buttresses, Filter/Drain, and Rip Rap at Downstream Toe constructed in 1986; Alluvium; and Bedrock – Santa Clara Formation. The alluvium is further divided into two zones: Younger Alluvium (Qya) and Older Alluvium (Qoa).

Materials for the original dam and 1986 embankment modifications were obtained from the alluvial and colluvial deposits and Santa Clara Formation bedrock along the floor and lower flanks of the Stevens Creek channel in the area upstream of the dam. The original and 1986 construction photos clearly show the excavation terracing in borrow areas on both sides of the valley within the present reservoir area.

5.3 CLASSIFICATION AND INDEX PROPERTIES – EMBANKMENT MATERIALS

This section provides a summary and discussion of the embankment material classification and index properties data from previous investigations and construction testing performed by WCC (1976), S&W (1976), Wahler (1978, 1982, 1984, and 1986b) and from the supplemental investigations by TGP (2011b). Table 5-1 is a summary of the classification and index properties and includes soil classification based on the Unified Soil Classification System (USCS), in-situ conditions (i.e., dry unit weight, moisture content, and compaction), gradation characteristics (i.e., percent gravel, sand fines and clay fraction) and Atterberg limits (i.e., Liquid

limit and Plasticity Index). Average index properties are listed as well as minimum and maximum values, when available.

5.3.1 Classification, Gradation, Plasticity and Density

Based on the construction records reviewed, the Upstream portion of the original embankment is predominately founded on bedrock and has an upstream slope of approximately 2.5H:1V. Samples obtained from the upstream embankment zone have been classified as sandy clayey gravel (GC-SC) to sandy clays (CL). A total of 60 unit weight tests were performed on intact samples of upstream embankment material and show an average dry unit weight of 123 pcf. Similarly, a total of 62 moisture content tests have been performed on upstream embankment samples and show an average moisture content of 12.8%. Maximum density of one composite sample of upstream embankment material was determined to be 127.5 pcf based on ASTM D-1557 modified to 20,000 ft-lb/ft^3 of compactive energy (Wahler, 1982). This would correspond to an average relative compaction of 96% for the upstream embankment zone of the embankment.

The Downstream portion of the original embankment is predominately founded on alluvium and has a downstream slope of approximately 2.5H:1V. Samples obtained from the downstream embankment zone have been predominantly classified as clayey sand (SC) to clayey gravel (GC) with a few samples classified as silty gravel and silty sand (GM and SM, respectively). A total of 60 unit weight tests were performed on intact samples and 3 in-place sand cone density tests were performed on downstream embankment material showing an average dry unit weight of 123 pcf. Similarly, a total of 114 moisture content tests have been performed and showed an average moisture content of 12.1%. Maximum density of one sample of downstream embankment material was determined to be 127.7 pcf based on ASTM D-1557 modified to 20,000 ft-lb/ft^3 of compactive energy (Wahler, 1978). This would correspond to an average relative compaction of 96% for the downstream portion of the embankment, very similar to the relative compaction of the upstream portion of the embankment.

The Filter/Drain was an important element of the modification made to the dam in 1986. This filter/drain zone consists of a 12-foot wide inclined drain on the downstream face of the original embankment and an 8-foot thick blanket drain that underlies the new buttress beyond the original downstream toe and is founded on alluvium. The filter/drain was designed to prevent the downstream buttress from becoming saturated and was specified during design to consist of sandy gravel (GW) which met the appropriate filter criteria. A total of 8 in-place density tests were performed during installation of the filter/drain and show the drain has an average relative compaction of 96% based on ASTM D-1557 modified to 20,000 ft-lb/ft^3 of compactive energy (Wahler, 1986b).

The Upstream and Downstream Buttresses were also part of the 1986 dam modifications. According to construction records, these buttresses were constructed using similar source material as the original embankment. The upstream buttress is predominately founded on bedrock with a slope of approximately 2.5H:1V and the downstream buttress is predominately founded on filter/drain material underlain by alluvium, and also has a slope of approximately 2.5H:1V. Classification information for the source material of the embankments was documented by Wahler (1982, 1984) and has been supplemented with laboratory tests on

samples collected from the downstream buttress during the 2010-2011 investigation. Samples of buttress material have been predominantly classified as clayey sand (SC) with a few samples classified as silty sand and clayey gravel (SM and GC, respectively). In-situ conditions of the buttress materials have been determined by moisture content testing on intact samples as well as in-situ sand cone density tests performed during construction. A total of 103 in-place density tests were performed during construction showing average dry unit weight of 129 pcf. A total of 11 moisture content tests have been performed on samples from recent borings and show an average moisture content of 7.8%. Relative compaction results during construction indicate an average compaction of 97% based on based on ASTM D-1557 modified to 20,000 ft-lb/ft^3 of compactive energy. As discussed in Section 5.3.4, the relative compaction of 97% (per ASTM D-1557 modified to 20,000 ft-lb/ft^3) may be an underestimate when compared to the relative compaction of 96% (per ASTM D-1557 modified to 20,000 ft-lb/ft^3) observed for the downstream embankment and upstream embankment of the original dam.

5.3.2 Gradations

Figure 5-2 shows the ranges of gradations and average percent passing the #4 and #200 sieves for all embankment materials by zone. As shown on Figure 5-2, the range of gradations for the upstream embankment material and downstream embankment material are very similar. For the Upstream embankment a total of 36 gradation tests were performed with average gravel, sand, and fines contents of 27%, 44%, and 29%, respectively. Additionally, hydrometer tests were performed on 17 samples showing an average clay content of 12% on those samples determined to be suitable for hydrometer testing. It was noted in reviewing the gradation information that the gravel in the upstream embankment zone is generally finer than ¾-inch which distinguishes it from the downstream embankment material.

The cumulative frequency distribution of fines content is plotted on Figure 5-3 based on the results of sieve analysis on samples of the upstream embankment, downstream embankment, and buttress materials. We have found that cumulative frequency distribution plots provide a useful and well-established statistical method to summarize data on a variety of physical and engineering properties, and to compare the properties from different materials in a way that is easy to visualize. In this case, the data on fines content for each of the materials are ordered from lowest to highest value and a plot produced based on individual test results, with each test result depicted by a data point that represents the measured property (percent fines in this case) and the percentage of the test results that have a fines content that is equal to or less than that specific test result. The FREQUENCY statistical function in Microsoft Excel is used to perform the data analysis. If the parameter being plotted were to behave statistically as a normally distributed random variable, the median (or 50th percentile) value would be equal to the mean value and the 84th percentile and 16th percentile values would be equal to the mean plus and minus one standard deviation, respectively.

The range of fines in the upstream embankment is between 4% and 44% but most of the samples had between 20% and 35% fines by weight. For the downstream embankment, a total of 101 gradation tests were performed on samples with average gravel, sand, and fines contents of 31%, 43%, and 26%, respectively. Additionally, hydrometer tests were performed on 8 samples showing an average clay content of 16% on those samples determined to be suitable for

hydrometer testing. As stated above, with the exception of slightly higher gravel content and slightly lower fines content, the gradations of the downstream embankment material are very similar to those observed for the upstream embankment material. The cumulative distribution of fines content plotted on Figure 5-3 reinforces this. The range of fines in the downstream embankment is between 12% and 51% but that most of the samples had between 15% and 30% fines by weight.

The bottom portion of Figure 5-2 shows the gradation ranges of the Upstream and Downstream Buttresses and Filter/Drain materials that were part of the dam modifications in 1986. A total of 14 gradation tests were performed on filter/drain material during construction. The record tests show the filter/drain material was generally within the specified gradation and had an average fines content of 3%. The buttress material is observed to have a very similar range of gradations as the upstream and downstream portions of the original embankment. A total of 34 gradation tests were performed on samples with average gravel, sand, and fines contents of 31%, 43%, and 26%, respectively. It is noted that these averages are identical to the downstream embankment material and in strong agreement with the upstream embankment material. The cumulative distribution of fines content is plotted on Figure 5-3; the range of fines of the buttress material is between 5% and 56% but that most of the samples had between 12% and 40% fines by weight.

5.3.3 Plasticity and Liquidity Index

A total of 15 Atterberg limits tests were performed on upstream embankment samples, 49 Atterberg limits tests were performed on downstream embankment samples and 29 Atterberg limits tests were performed on buttress material samples. The results of these tests are grouped closely together as shown on the plasticity chart on Figure 5-4. Upstream embankment materials had a liquid limit (LL) range of 15 to 31 with an average value of 29, and a plasticity index (PI) range of 4 to 15 with an average value of 12. Downstream embankment materials had a LL range of 23 to 37 with an average value of 29, and a PI range of 4 to 19 with an average value of 12. It is noted that the average LL and PI for the downstream embankment material is identical to the average values for the upstream embankment material. Buttress materials had a LL range of 21 to 35 with an average value of 29, and a PI range of non-plastic (NP) to 18 with an average value of 12, again identical to the average values for the upstream and downstream embankment materials.

Moisture content and Atterberg limits information was combined to calculate liquidity index (LI) for 14 of the 15 upstream embankment samples, 41 of the 49 downstream embankment samples and 8 of the 29 buttress samples tested. The results are presented on the Liquidity Index Chart on Figure 5-5. It is observed that the LI values for the upstream embankment samples ranged from -2.0 to 0.2 with an average value of -0.6, the LI values for the downstream embankment samples ranged from -1.8 to 0.2 with an average value of -0.6 and the LI values for the buttress samples ranged from -2.6 to 0.7 with an average value of -0.8. These low values are as one would expect for soils compacted to 96% to 97% relative compaction (per ASTM D-1557 modified to 20,000 ft-lb/ft^3) and the scatter is probably associated with the relatively low plasticity index of the materials and the presence of varying amounts of sand- and gravel-sized particles.

5.4 ENGINEERING PROPERTIES – EMBANKMENT MATERIALS

The engineering analyses for the seismic evaluation of the dam require the following material properties for the various zones of the embankment shown on Figure 5-1: total unit weight, effective stress friction angle, undrained strength, and dynamic properties (i.e., shear-wave velocity, shear modulus reduction, and damping ratio curves). In addition, the permeability of the various materials is required as initial input to the seepage analyses that will support the engineering analyses of seismic deformations. The following sub-sections describe how material properties were derived from the existing and supplemental data for all zones of the embankment, except for the rip rap at the downstream toe that is incidental to the analyses. The material properties for the alluvium are discussed below in Section 5.5.

Table 5-2 provides a summary of the properties selected for each of the zones in terms of actual values and/or numbers of figures where the appropriate relationships are displayed. It should be noted that, in some cases, the same properties were chosen for more than one zone. This was supported by trends observed in the available data. Because of its relatively small cross section, the filter/drain zone will be considered equivalent to the buttress material in the engineering site response and deformation analyses. However, this zone will be included in the seepage analyses.

5.4.1 Unit Weight

The unit weight selected for each material corresponds to moist (or total) unit weight, γ_t, based on all test data discussed above. Figure 5-6 shows the cumulative distribution of unit weight for all three generalized zones: upstream embankment, downstream embankment, and buttress. Based on the results shown on this figure, the 50th percentile moist unit weight value was adopted for each material. Moist unit weights of 139 pcf and 137 pcf were selected for the upstream embankment and downstream embankment and buttress, respectively. The unit weight selected for the buttress was conservatively capped at 140 pcf.

5.4.2 Effective Stress Friction Angle

Based on the information presented in Section 5.3, the upstream embankment, downstream embankment, and buttress zones have the same source and are comprised of nearly equivalent materials. Additionally, it appears that both zones of the original dam were compacted to the same relative compaction and that the buttress material was compacted to a higher relative compaction. Recognizing that the effective stress strength of the buttress material is not a controlling factor, one effective stress friction angle corresponding to the original embankment materials was adopted for use in all three zones above the phreatic surface in the engineering analyses.

A total of fifteen (15) isotropically consolidated undrained triaxial compression (ICU'C) tests were performed on Pitcher samples and re-compacted samples of embankment materials. During previous studies, one Pitcher tube sample of upstream embankment material, 6 Pitcher tube samples of downstream embankment material, and 3 re-compacted samples of buttress material were tested. Based on these results, Wahler selected an effective friction angle of 37° for the embankment materials. Five additional tests were performed on downstream

embankment materials obtained using Pitcher tube samples during the 2010-2011 investigation. A secant effective stress friction angle was calculated at maximum obliquity for each test; i.e., the friction angle was determined as the angle of the line tangent to the failure envelope with zero cohesion intercept. The calculated values are plotted versus effective normal stress on potential failure surface on Figure 5-7. As shown on this figure, the new data suggest that the effective friction angle of 37° selected by Wahler is a reasonable value to be adopted for future analyses.

The 12 tests on Pitcher tube samples reported on Figure 5-7 were performed at various testing consolidation ratios defined as the ratio between the as-tested consolidation pressure to the estimated in-situ confining pressure of each sample. This testing consolidation ratio varies between 1.0 and 6.9 and no particular trend is apparent in the calculated effective stress friction angle.

5.4.3 Undrained Strength

Based on the similarities of the embankment zones with regard to classification and compaction, it is appropriate to group the data for the upstream embankment and downstream embankment.

The undrained shear strength at maximum obliquity for each of the 12 ICU'C tests on original embankment materials (7 by Wahler [Wahler, 1978] and 5 by TGP [Terra/GeoPentech, 2012]) are plotted versus laboratory effective confining pressure on Figure 5-8. As shown on this figure, the new data from TGP are in general agreement with the undrained strength data from Wahler. The undrained shear strength in kips/ft ^{2} (ksf) was found to vary with effective consolidation stress as follows:

$$S_u = 0.93\ ksf + 0.53\ \sigma'_c$$

5.4.4 Liquefaction Potential of Embankment Materials

The embankment materials are clayey and appear to be non-liquefiable. Nevertheless, based on discussions with DSOD, TGP made a thorough evaluation of the liquefaction potential of the embankment materials to verify that these materials were not liquefiable. This evaluation is presented below.

The upstream and downstream embankment zones have the following average gravel, sand and fines content based on the results of 137 gradation tests:

Material	% Gravel	% Sand	% Fines
Upstream Embankment	27	44	29
Downstream Embankment	31	43	26

Figure 5-4 contains the results of Atterberg limits plotted on the Plasticity Chart and shows that the fines are clays of low plasticity. Based on this, the classification of the soil in the Unified Soil Classification System (USCS) is clayey sand with gravel and the group symbol is SC.

The USCS classifies soils based on the percent by weight of the various size soil particles but, for soils with considerable amounts of fines (such as the embankment materials at Stevens Creek Dam), this classification system may not provide a clear indication of whether the soil will behave like a clay or a sand. One of the key issues is whether or not the fines fraction constitutes the stress-carrying matrix or skeleton for the soil mass, with the larger sand/gravel-sized particles essentially floating (isolated from each other) within the matrix.

The following subsection presents data from various sources that demonstrate that the embankment materials at Stevens Creek Dam do indeed behave as fine-grained soils. Given that finding, the work by Seed et al (2003) can be used to evaluate the liquefaction potential of the embankment materials. Zones A and B from Seed et al. (2003) are plotted on the PI Chart on Figure 5-9. Many of the tests fall into Zone A which would indicate the soils are potentially liquefiable if the in-situ water content is greater than 80% of the liquid limit. The rest of the tests fall into Zone B in which soils with water contents greater than 85% of the liquid limit should be tested to see if they are susceptible to liquefaction. In-situ water content was determined on 34 of the Atterberg limits test samples shown on Figure 5-9; water content tests from samples recovered from sonic cores have been excluded because sonic cores tend to result in slightly lower water content values. The ratios of water content to liquid limit for the 34 tests considered ranged from 31% to 72%, with an average of 45%, and are significantly lower than the thresholds for potentially liquefiable soils proposed by Seed et al. (2003) for Zones A and B. Consequently, the embankment materials are not susceptible to liquefaction based on Seed's recommended screening process.

5.4.4.1 Basis for Judging the Embankment Soils to Behave as Fine-Grained Soils

Mitchell (1976) provides an approach for estimating the clay content needed to fill the voids of a soil in Figure 9-3 of his book Fundamentals of Soil Behavior. The void ratio or dry density of the soil is a key parameter and Mitchell provides sample calculations. These calculations show that, for a granular soil in the loosest possible state, the amount of clay necessary to fill the voids is about 33%, i.e., 1/3 of the sample by weight.

We have updated Mitchell's calculations based on the following measured data on embankment materials at Stevens Creek Dam:

- dry density 123 lb/ft^3
- water content 12.5%
- % fines 27%

We have also estimated that the sand- and gravel-sized particles would be arranged such that, if they were in grain-to-grain contact, they would have a void ratio of about 0.50 which corresponds to a medium-dense packing. For this value of void ratio, the void space between the sand-and gravel- sized particles would be 0.27 ft^3 in a 1-ft^3 soil sample. For the embankment materials at Stevens Creek Dam the actual volume of soil fines and water that fills the space between the sand-and gravel-sized particles is 0.43 ft^3 in a 1-ft^3 soil sample, or 1.6 times the maximum amount of fines that would allow grain-to grain-contact of the sand- and gravel-sized particles. This strongly indicates that the sand- and gravel-sized particles within the

embankment materials are floating within the clay matrix, and that the embankment materials are expected to exhibit clay-like behavior.

As shown below, this indication that the embankment materials are expected to exhibit clay-like behavior is supported by the following test results on embankment materials:

1. K_o triaxial consolidation test;
2. permeability tests;
3. undrained triaxial compression tests;
4. post-cyclic triaxial compression tests; and
5. cone penetrometer tests.

K_o Triaxial Consolidation Test

A 4-inch diameter sample of embankment materials (Sample PB-7 from Boring SC-102 MR) was consolidated in a computer controlled K_o triaxial cell. This test showed that the maximum past pressure of the sample was approximately equal to the in-situ effective stress and that the virgin compression ratio (vertical strain per log cycle of stress) was approximately 0.08. This compression ratio corresponds to a value that would be expected for virgin compression of a CL soil and indicates that the clay matrix is continuous and that the granular particles within the sample are indeed floating in a clay matrix. Although we have only one consolidation test on embankment soils at Stevens Creek dam, the same behavior was also observed for embankment materials at Lenihan Dam where nine consolidation tests were completed on clayey sand embankment materials.

Permeability Tests

Wahler (1978) conducted triaxial permeability tests on four specimens obtained from a 48-inch diameter bucket auger borehole. Pairs of horizontal and vertical specimens from two depths were tested and the measured average values of vertical and horizontal permeability were $1x10^{-6}$ and $1x10^{-7}$ cm/sec, respectively. These permeability values are clearly consistent with a continuous clay matrix for the embankment materials.

Consolidated Undrained Triaxial Compression Tests

Figure 5-8 summarizes the measured undrained shear strengths at maximum obliquity for consolidated undrained triaxial compression tests on intact samples of embankment soils. The soils tested exhibited stress paths and stress-strain behavior that are typical of clay soils and the strong dependence of strength on effective consolidation stress in the laboratory is also consistent with the behavior of clay-like soils. The undrained strength of the embankment materials is higher than would be expected for normally consolidated clays. Professor Raymond Seed, a member of the District's Technical Review Board for this project, has indicated that the behavior of these broadly graded embankment materials are influenced by both the continuous clay matrix and the isolated granular soil particles floating in the clay matrix. The soil behavior is expected to be controlled by the continuous clay matrix during consolidation and shearing at small strains but the presence of significant amounts of sand and gravel would likely cause the soils to exhibit dilative behavior at larger strains that contribute to the higher undrained strength

of the material. As stated by Professor Seed, in many ways these are ideal materials for construction of an earth dam.

Post-Cyclic Undrained Triaxial Compression Tests on Intact Samples

Wahler (1984) conducted a large number of stress controlled cyclic triaxial compression tests. Wahler also conducted some tests on intact samples of embankment materials where the sample was allowed to consolidate under a certain confining stress, then subjected to undrained cyclic loading until nominally 10% axial strain was induced at which point the cyclic loading was stopped, pore pressures allowed to equilibrate under undrained conditions, and the sample was then slowly loaded at a constant rate of strain to 10% axial strain under undrained conditions with pore pressure measurements. The results of four post-cyclic undrained tests on intact samples are shown on Figure 5-10 and compared to the undrained strengths for the conventional undrained triaxial tests with monotonic loading that were shown on Figure 5-8. The measured stress-strain curves from these test results, in spite of severe cyclic loading, show that the soils exhibited dilative behavior during the post-cyclic shear test (the deviator stress was continuing to increase and pore pressures were continuing to decrease at the time the tests were stopped at 10% strain) and that the samples exhibited no reduction in undrained strength associated with the cyclic loading. This result is consistent with what would be expected from a compacted clay soil.

Cone Penetrometer Tests

Cone penetrometer tests were made at Stevens Creek Dam and were successfully advanced through the embankment materials and underlying alluvium without meeting refusal. The measured friction ratios in the embankment materials were generally greater than 3%, indicating clay-type soil behavior, and the fact that the CPTs did not refuse in the gravel-laden embankment soils indicates that the gravels are isolated particles that are floating in a clay matrix. Using the Soil Behavior Type Index, I_c, developed by Robertson and Wride (1998), the CPT data collected at the crest strongly indicate clay-like behavior of the original embankment materials. Over 90% of the original embankment data points obtained in three profiles at the crest had I_c values greater than 2.6 which is the approximate threshold between clay-like and sand-like behavior proposed by Robertson and Wride (1998).

5.4.4.2 Conclusion

The embankment materials behave as fine grained soils and are not susceptible to loss of strength due to cyclic loading. This finding is consistent with the results of the screening process for liquefaction of fine grained soils based on the procedure recommended by Seed et al (2003).

5.4.5 Dynamic Properties

Dynamic properties required for the engineering analyses consist of shear wave velocity, shear modulus reduction curves, and damping ratio curves. Undrained shear strength was discussed in Sections 5.4.3 and 5.4.4. Shear wave velocity data have been collected by several investigators using various methods during previous studies and the 2010-2011 investigation, including; cross-hole geophysics performed by WCC (1976), cross-hole geophysics and resonant column testing

performed by Wahler (1982) and OYO suspension logging in mud-rotary boreholes collected by TGP (2011b). The results of these tests are plotted on Figure 5-11 versus in-situ confining pressure showing an increase in shear wave velocity with an increase in confining pressure. A power function was used to develop a relationship between confining pressure and shear wave velocity by minimizing the sum of the residual squares. Because of the differences in degree of compaction between the original embankment and the buttresses added in 1986, and the difference in shear wave velocities between these materials, separate relationships were developed for the original embankment and the buttress materials as shown on Figure 5-11.

The small strain shear modulus for each material can be obtained from shear wave velocity and the known mass density of the material using the following relationship:

$$G_{max} = \rho \cdot V_S^2$$

In this relationship, G_{max} is the small strain shear modulus, ρ is the mass density of the material, and V_s is the shear wave velocity.

Based on the observed clayey nature of the material for all zones of the embankment, the shear modulus reduction and damping ratio curves were selected based on the work by Vucetic and Dobry (1991), corresponding to average PI values of 12 for the upstream embankment, downstream embankment and new buttress materials, as shown on Figure 5-12.

5.4.6 Permeability

The physical and index properties of the upstream embankment and the downstream embankment are very similar and Wahler (1978) concluded that there was no substantial difference in permeability. Wahler conducted triaxial permeability tests on four specimens from a 48-inch diameter bucket auger boring (DH-SC2) drilled at Station 8+26, about 30 feet upstream of the original dam crest. Pairs of specimens from nominal depths of 24 feet and 63 feet were tested: one specimen obtained from a vertically-oriented driven 5-inch diameter sample and one specimen from a horizontally-oriented pushed tube sample. The measured permeabilities were as follows:

Sample Depth, Feet	Vertical Permeability, cm/sec	Horizontal Permeability, cm/sec	Ratio of Horizontal to Vertical Permeability
24	3.5×10^{-8}	9.1×10^{-6}	260
63	6.6×10^{-7}	1.4×10^{-7}	0.21
Logarithmic Average	1.5×10^{-7}	1.1×10^{-6}	

The vertical permeability provides the better estimate of the permeability of the clay within the specimen and we believe that the vertical permeability of the embankment is approximately

$1x10^{-7}$ cm/sec (0.1 ft/year). The horizontal permeability of a compacted clayey fill is typically between 20 and 50. We will use a ratio of 20 as our initial estimate in the seepage analyses.

5.5 CLASSIFICATION AND INDEX PROPERTIES – ALLUVIUM

As discussed in detail in Sections 4.4.1 and 4.4.2, the alluvial soils that underlie the downstream embankment and downstream buttress consists of two units: younger alluvium deposits (Qya) and older alluvium terrace deposits (Qoa). Generally stated, the younger alluvium underlies the embankment in the central portion of the canyon coinciding with the maximum section of the dam, while the older alluvium underlies the smaller portions of the embankment at the left and right abutments. The foundation alluvium has been studied previously; however, the majority of classification information on these materials was collected during the recent investigation conducted by TGP (Terra/GeoPentech, 2012).

5.5.1 Classification, Gradation, Plasticity and Density

Samples of younger alluvium have been predominantly classified as poorly graded sandy gravel (GP) to silty sand (SM) with a few samples classified as clayey gravel and clayey sand (GC and SC, respectively). Samples of older alluvium (Terrace alluvium) have been predominantly classified as clayey gravel (GC) to clayey sand with gravel (SC) with a few samples classified as poorly graded gravel and silty sand (GP and SM, respectively). In-situ conditions of the alluvium has been determined by moisture content testing on intact samples as well as in-place sand cone density tests performed in test trenches. A total of 9 in-place density tests were performed during construction showing average dry unit weight of 112 pcf for the younger alluvium and 129 pcf for the older alluvium. A total of 30 moisture content tests have been performed on samples from recent borings and showed an average moisture content of 11.0% for the younger alluvium and 8.9% for the older alluvium.

5.5.2 Gradations

As shown on Figure 5-13, the ranges of gradation for the younger and older alluvium are similar. A total of 32 gradation tests were performed on younger alluvium with average gravel, sand, and fines contents of 35%, 48%, and 17%, respectively. A total of 7 gradation tests were performed on older alluvium samples with average gravel, sand, and fines contents of 32%, 45%, and 23%, respectively. It is noted that two samples of younger alluvium from the sonic core borings contained 4-in diameter cobbles which were not included in the grain-size analyses. Additionally, on average, 96% of the younger alluvium was finer than 1 ½-in diameter and 85% was finer than ¾-in diameter indicating that the majority of the gravel encountered was fine gravel. The cumulative distribution of fines content for the alluvium is plotted on Figure 5-14; it is noted that the older alluvium has slightly higher fines than the younger alluvium and 50% of the samples of younger alluvium had less than 13% fines by weight.

5.5.3 Plasticity

A total of 18 Atterberg limits tests were performed on alluvium samples. The results of these tests are shown on the plasticity chart on Figure 5-15 and generally indicate the low plasticity of

the CL and ML fines. Younger alluvium samples had a LL ranging from NP to 28 with an average value of 21, and a PI ranging from NP to 11 with an average value of 5. Older alluvium samples had a LL ranging from 20 to 33 with an average value of 27, and a PI ranging from 4 to 15 with an average value of 11. Moisture content and Atterberg limits information was combined to calculate LI for 15 of the 18 samples tested; the results are presented in the Liquidity Index Chart on Figure 5-16. It is observed that the LI values for the younger alluvium ranged from -5.1 to -0.2 with an average value of -2.0. LI values for older alluvium samples ranged from -1.3 to -0.4 with an average value of -0.7. These are very low values but they should be considered approximate because they are significantly influenced by the low PI values and the relatively small amount of fines.

5.6 ENGINEERING PROPERTIES – ALLUVIUM

Engineering properties were only developed for the younger alluvium (Qya), hereafter simply referred to as the alluvium, since the older alluvium (Qoa) exists only under the abutment areas of the dam which are less critical in terms of seismic performance. In addition to being less critical based on its location within the foundation, review of the limited information available shows that the older alluvium is Pleistocene in age, slightly higher in plasticity, slightly higher in fines content, and denser than the younger alluvium.

The following engineering properties were developed for the alluvium: unit weight, shear wave velocity, modulus reduction and damping curves. In addition, because the engineering analyses are targeted to estimate the seismic performance of the embankment during high shaking, the shear strength of the alluvium is a key material property and will depend upon the liquefaction potential of the alluvium. The key parameter for evaluation of liquefaction potential and residual shear strength is the corrected SPT blow count $(N_1)_{60}$. The data collected and methods used to estimate the $(N_1)_{60}$ values in the alluvium are discussed in detail in the following sub-sections. In addition, the permeability of the alluvium is required as initial input to the seepage analyses that will support the engineering analyses of seismic deformations.

A summary of the properties selected for the alluvium is contained in Table 5-2 in terms of actual values and/or numbers of figures where the appropriate relationships are displayed.

5.6.1 Unit Weight

The unit weight selected for the alluvium corresponds to moist (or total) unit weight, γ_t, based on the limited test data discussed above. Figure 5-17 shows the cumulative distribution of moist unit weight for the alluvium; based on the results shown on this figure, the 50th percentile moist unit weight value of 125 pcf was adopted for the alluvium. In selecting the moist unit weight, no attempt was made to correct for small potential differences in the degree of saturation of the materials.

5.6.2 Corrected SPT Blow Count $(N_1)_{60}$

Previous studies had investigated the alluvium with borings and trenches but prior to this investigation the liquefaction potential of the younger alluvium in the foundation had not been adequately evaluated. Further, due to the high shaking hazard from nearby faults as discussed in

Section 6.0, if the alluvium were liquefiable, the saturated portion of the layer would likely experience liquefaction or at least high excess pore water pressures as a result of the anticipated shaking. Thus, one of the key geotechnical issues addressed in the current site characterization effort is the liquefaction potential and residual shear strength of the materials left in place beneath the dam during seismic loading. As noted above, the key parameter used to evaluate liquefaction potential and residual shear strength is the corrected SPT blow count $(N_1)_{60}$.

As discussed in Sections 3.0 and 4.0, the younger alluvium in-place along the floor of the Stevens Creek channel is a Holocene, or pre-Holocene, deposit consisting predominately of gravelly, coarse-grained sandy material with some interbedded fine sand layers, and low fines content. This type of deposit is commonly studied for liquefaction potential in areas of high seismic activity, such as the Stevens Creek Dam site. The discussion of groundwater observations in Section 4.5 describes how the saturated thickness of the alluvium, although generally small, varies with groundwater levels downstream of the dam. Additionally, as noted in Section 5.5, the gradation tests results on alluvium samples showed that 50% of the samples had less than 12% fines by weight and the Atterberg limits tests on the same samples indicated the fines are clays or silts of low plasticity, signifying the relatively cohesionless nature of the deposit.

Several in-situ tests were employed to estimate values of $(N_1)_{60}$ for the alluvium, including: Standard Penetration Tests (SPTs), Becker Penetration Tests (BPTs), and Cone Penetrometer Tests (CPTs). The relatively high gravel content of the alluvium (35% on average) may influence measurements of $(N_1)_{60}$ using the SPT. As discussed below, the procedure for the SPT was modified to record the penetration of the SPT sampler for every blow and to convert this measurement of inches per blow to blows per inch. The data on blows per inch were then examined to evaluate the effects of gravel. BPTs were also used as a means of testing the soil to estimate $(N_1)_{60}$ values using methods proposed by Harder (1997) and Sy and Campanella (1994). CPT soundings were also performed and values of $(N_1)_{60}$ were estimated from correlations with cone tip resistance and friction ratio.

After several discussions with DSOD regarding the data for the alluvium obtained at the site, DSOD concluded that the effects of gravel on the penetration resistance within the alluvium may be significant and therefore it was agreed to use $(N_1)_{60}$ values estimated using the method proposed by Harder (1997). However, our evaluation of the data indicates that the mean $(N_1)_{60}$ values from BPT data interpreted using the Harder method may be extremely conservative and that $(N_1)_{60}$ values estimated from other field testing methods using 16th percentile values (corresponding to mean value minus one standard deviation) should also be used as a benchmark in our seismic safety evaluation.

Brief descriptions of the collection of data and of the methods for data reduction and evaluation are presented in the following sub-sections.

5.6.2.1 Standard Penetration Testing

The SPT is the most commonly used tool for evaluating liquefaction characteristics of sandy soils. The test measures the total number of blows (N-value) required to drive a standard split-spoon sampling tool 12-inches into the in-place material. Many studies have shown that SPT N-values correlate with density, compactness, liquefaction potential and many other

engineering properties of the soil in question. In the 2010-2011investigation, SPTs were performed on alluvium within mud-rotary borings at two locations along the maximum section of the dam. The SPTs were driven by an automatic 140-lb hammer with a 30-inch drop and the energy efficiency of the hammer was measured for all SPT samples taken at boring SC-105MR using a Pile Driving Analyzer (PDA) manufactured by Pile Dynamics, Inc. SPTs were performed as continuously as practical through the 8-ft of alluvium under the crest and the 11.5-ft of alluvium at the downstream toe for a total of 8 SPTs.

Each measured blow count, N_m, was corrected for energy ratio, borehole diameter, rod length and sampler type to result in a standardized value of N_{60}, corresponding to an energy ratio of 60%. Due to the high gravel content observed in the alluvium at the site, blows-per-inch were recorded at each location to assess the effects, if any, of gravel on the recorded blow count. Figure 5-18 presents the blow-per-inch data for each inch in the last 12-inches of the SPT run; Figure 5-19 presents the cumulative blow count by inch for each of the 8 SPTs. With only one exception (SC-101MR, SP-24) the data collected appear to be consistent, uniform blows-per-inch, over each 12-inch interval and the gravel particles appear to have little to no effect on the penetration resistance. Based on the variability of the younger alluvium with depth that was observed in both the sonic cores and the CPT signatures, the subtle changes in blows-per-inch are more likely due to the changes in the material rather than the influence of large gravel particles. This is reinforced by the fact that the SPT runs consistently achieved 1 foot or more of sample recovery, and the gradation results on the SPT samples had less than 10% coarse gravel content on average. As indicated above, the one exception is SP-24 in SC-101MR that hit refusal on what is assumed to be a large gravel particle or cobble; this blow count was excluded from consideration in our analysis.

The 7 remaining SPTs were corrected for overburden stress using the procedure developed by Idriss and Boulanger (2008). This procedure is an iterative process whereby the correction factor is calculated based on both the magnitude of the corrected blow count and the in-situ confining pressure. For the 2 samples under the crest of the dam, the overburden correction factor resulted in a reduction of approximately 50%, and for the 5 samples at the downstream toe, the correction factor resulted in a reduction of approximately 10%. The cumulative distribution of the resulting corrected standard penetration values, $(N_1)_{60}$, is plotted on Figure 5-20. In spite of the small number of data, the SPT blow counts appear to be very robust, and the relatively high values of $(N_1)_{60}$ suggest that the alluvium should have a high resistance to liquefaction and/or a high post-liquefaction residual shear strength ratio.

5.6.2.2 Becker Penetration Testing

BPTs are most often utilized to characterize soils with high gravel content and were employed at a number of locations at the site. The BPT characterizes soil resistance by measuring the blows required to drive a 168-mm diameter closed bit pipe one foot using a double-acting diesel pile hammer. Conducting BPTs in this standardized manner provides a continuous profile of blows-per-foot with no sample recovery.

BPT blow counts and measurements of bounce chamber pressure for the diesel hammer were recorded every foot of penetration within the younger alluvium at 8 locations: 2 locations on the downstream face of the embankment and 6 locations at the downstream toe of the dam. In

addition, dynamic measurements of force and acceleration at the top of the drill string were made for each blow of the Becker hammer using a PDA in boring SC-103BPT located on the downstream face of the dam and borings SC-104BPT and SC-108BPT that were located at the downstream toe.

The BPT data were interpreted to develop inferred values of N_{60} from the SPT using two methods: the method presented by Harder (1997) and the method developed by Sy and Campanella (1994). The Harder Method requires only the measured BPT blow count and the bounce chamber pressure and was applied for all the Becker borings. The Sy and Campanella Method requires dynamic measurements of hammer energy and estimates of static side friction based on field measurements or estimates developed from wave equation analyses of the dynamic pile measurements. Consequently, the Sy and Campanella method could only be applied for the three Becker borings where dynamic measurements were made using PDA equipment.

The Harder Method is relatively simple and uses the bounce chamber pressure to approximately correct the results to a standard hammer energy. However, the Harder Method does not explicitly consider the effect of side friction on the measured BPT blow count and implicitly includes an average but unknown allowance for side friction consistent with the data used to correlate the BPT blow counts at 30% hammer efficiency to the SPT N_{60} values. The Sy and Campanella Method is more complicated but explicitly considers corrections to the measured BPT blow counts for both hammer energy and the friction force on the side of the drill string, R_s. Figure 5-21 shows the relationship between measured BPT blow counts at 30% hammer energy and SPT blow counts for various values of shaft friction force that was developed by Sy and Campanella. As shown on this figure, the correction for side friction in the Sy and Campanella Method can be very significant. For example, a measured BPT blow count of 40 would have a corresponding $(N_1)_{60}$ value of 25 or 60 for values of side friction of 180 kilo Newtons (KN) or 90 KN, respectively. This indicates that not explicitly correcting for side friction based on the conditions at the site is a limitation on the use of the Harder Method.

Data Reduction Using Harder Method

As indicated above, the Harder Method has two fundamental steps:

1. the penetration data are corrected for hammer energy based on the bounce chamber pressure using the chart plotted on Figure 5-22; and
2. the corrected data are then correlated to N_{60} using the graphical relationship presented in the published work.

The measured BPT data are shown on Figure 5-22 and inspection of this figure shows that the penetration and bounce chamber pressures varied significantly between the data collected within the alluvium below the embankment and the data collected within the alluvium at the downstream toe. The data points collected at SC-102BPT were so high that many of them fell outside of the range of data used for the correlations and have a corrected BPT blow count greater than 100 at 27 psig. Conversely, the data points from tests performed at the downstream toe are substantially lower than those under the embankment. Review of the BPT data on Figure 5-22 (and noting that the BPT blow counts are plotted on a logarithmic scale) also shows that the average raw blow counts collected at the downstream toe and under the embankment at the lower

and upper access roads were 27, 80, and 272, respectively. Thus, the average raw blow counts recorded under the embankment were three to ten times higher than the raw blow counts collected at the downstream toe.

The data reduction by the Harder Method was completed by correcting the BPT-inferred N_{60} values for overburden stress using the procedure developed by Idriss and Boulanger (2008) and following the same process as for the SPT results.

Data Reduction Using the Sy and Campanella Method

The BPT data were also reduced using the techniques developed by Sy and Campanella (1994). As indicated above, the main difference between this approach and the procedure by Harder (1997) is that the Sy and Campanella Method explicitly considers the variability introduced by the energy transfer ratio and the shaft skin friction during testing. This approach requires the collection of PDA data during the BPT testing, which was completed at three locations: SC-103BPT, beneath the embankment, and SC-104BPT and SC-108BPTat the downstream toe. The first step in reducing the BPT data using the Sy and Campanella Method is to correct the observed blow counts to a normalized reference energy ratio of 30%. The energy transfer ratios measured at the three Becker borings ranged from 27% to 34% and the correction factor represented a relatively small change from the blow counts recorded. The second step in the Sy and Campanella Method accounts for the friction force acting on the driven shaft during the BPT testing. We discussed current approaches for estimating shaft friction with Alexander Sy, the principal developer of the Sy and Campanella Method, and he recommended that estimates of side friction be developed by wave equation analyses of the PDA data for particular hammer blows using CAPWAP analyses (Goble et al., 1980). The Case Pile Wave Analysis Program (CAPWAP) is a proprietary software package of Pile Dynamics, Inc. (2006), the manufacturer of the PDA used at the site. Alexander Sy cautioned against using estimates of side friction based on the Simplified Case Method (Goble et al., 1980) because he had found these results to be far less reliable than estimates of side friction developed using CAPWAP analyses. Consequently, eighteen CAPWAP analyses were made for hammer blows at approximately 2-foot intervals within the alluvium for all three Becker borings where PDA measurements had been made in order to estimate the side friction force for use in the Sy and Campanella Method.

Using the skin friction estimates from the CAPWAP analyses, the Sy and Campanella Method was carried through for the three Becker borings with PDA measurements. The measured BPT blow counts and shaft resistance values for each of the eighteen locations where CAPWAP analyses were made were then used to calculate inferred N_{60} values with the graphical correlation presented by Sy and Campanella (1994) and shown in Figure 5-21.

The BPT-inferred N_{60} values were then corrected for overburden stress using the procedure developed by Idriss and Boulanger (2008) following the same process as for the SPT and Harder BPT-inferred results.

Comparison of Results

Figure 5-23 shows the six profiles of BPT-inferred values of $(N_1)_{60}$ within the alluvium at the downstream toe of the dam. It is noted that the middle two profiles have two sets of data plotted: values inferred from the Harder Method are plotted as triangles and data inferred from the Sy and

Campanella Method are plotted as diamonds. The average values of $(N_1)_{60}$ at each of the borings at the toe are shown on Figure 5-23 and listed below. Also listed below for comparison purposes, are the average BPT-inferred $(N_1)_{60}$ values collected under the lower access road. These values are further discussed below.

Boring Number	Location	$(N_1)_{60}$		$(N_1)_{60}$ (Harder) / $(N_1)_{60}$ (S&C) %
		Harder Method	Sy and Campanella (S&C) Method	
SC-109BPT	DS Toe	15	Not Available	Not Available
SC-106BPT	DS Toe	14	Not Available	Not Available
SC-108BPT	DS Toe	17	38	45
SC-104BPT	DS Toe	17	43	40
SC-110BPT	DS Toe	20	Not Available	Not Available
SC-107BPT	DS Toe	26	Not Available	Not Available
SC-103BPT	Lower Access Road	27	80	34

It is apparent that the Harder Method calculates significantly lower values of $(N_1)_{60}$ at the downstream toe of the dam than are estimated using the Sy and Campanella Method. For the two borings at the downstream toe where PDA measurements were available, allowing the application of the Sy and Campanella Method, the $(N_1)_{60}$ values from the Harder Method were about 40% of those from the Sy and Campanella Method. This may be due in large part to the very low skin friction at these locations. It is also noted that the average $(N_1)_{60}$ value for each profile, as determined by the Harder Method, is higher on the right abutment side of the channel. This may be related to the increased construction activity in the area surrounding the outlet works near SC-107BPT.

Figure 5-24 shows the estimated values of $(N_1)_{60}$ calculated using the Harder Method and the Sy and Campanella Method for the three borings where PDA measurements were available. This figure also shows the values of $(N_1)_{60}$ measured using the SPT at boring SC-104MR. Inspection of this figure shows that the values of $(N_1)_{60}$ calculated using the Sy and Campanella Method are in close agreement to those measured using the SPT. This figure also shows the average values of $(N_1)_{60}$ from the Harder Method and the Sy and Campanella Method for all three boring locations. Referring to the list of average values tabulated above, we see that the ratio of the average values of $(N_1)_{60}$ from the Harder Method and the Sy and Campanella Method is 31% at boring location SC-103BPT located at the downstream access road and thus considerably less than the ratio of 40% observed at the downstream toe. However, it should be noted that four of the six values of $(N_1)_{60}$ for the Sy and Campanella Method at boring location SC-103BPT were extrapolated outside the range of values included in the charts and should be viewed as representing poorly defined but very high values of $(N_1)_{60}$. Unfortunately, we do not have

measurements of $(N_1)_{60}$ from SPTs at this location to compare with the inferred values of $(N_1)_{60}$ from either the Harder or Sy and Campanella Methods.

Figure 5-25 shows cumulative frequency diagrams of the values of $(N_1)_{60}$ from the Harder and Sy and Campanella Methods for the borings where we have PDA measurements that allowed the application of the Sy and Campanella Method. The significant differences between the values of $(N_1)_{60}$ from the two methods are evident. Also evident is the good agreement between the values of $(N_1)_{60}$ from the Sy and Campanella Method at boring locations SC-104 and SC-108, and the values of $(N_1)_{60}$ measured using the SPT at boring SC-104MR.

Figure 5-26 shows the same data in terms of frequency diagrams (histograms) with a class interval of 5 blows per foot. The increase in the values of $(N_1)_{60}$ from the Harder Method to the Sy and Campanella Method is evident from the shift in location of the frequency bars from the middle to the lower histogram. In addition, the agreement between the values of $(N_1)_{60}$ from the SPT data at the toe shown in the upper diagram and the inferred values of $(N_1)_{60}$ from the Sy and Campanella Method is evident from the similar distribution of the purple bars on the upper and lower histograms on Figure 5-26. This agreement is further illustrated in Figure 5-27 which provides a point by point comparison of the values of $(N_1)_{60}$ from the SPT and the inferred values of $(N_1)_{60}$ from the BPT data using the Harder Method and the Sy and Campanella Method. As shown on this figure, the values of $(N_1)_{60}$ measured using the SPT are slightly higher than the inferred values of $(N_1)_{60}$ from the Sy and Campanella Method but are over twice as high as the inferred values of $(N_1)_{60}$ from the Harder Method.

5.6.2.3 Cone Penetration Testing

CPTs in younger alluvium were performed at two locations, both along the maximum section, with data collected at 5-cm intervals. Screening was performed to identify any data points that appeared to be unduly influenced by the presence of gravel before using CPT results to develop inferred values of $(N_1)_{60}$. Significant spikes in the normalized tip resistance were identified at several locations and, in total, 24 of the 133 data points were excluded from use in this analysis. The remaining data, which included 39 data points beneath the crest and 70 data points at the downstream toe, were used to estimate SPT results following the procedure developed by Jeffries and Davies (1993) which uses the corrected tip resistance and the I_c for each data point to infer a SPT equivalent N_{60}. The CPT-inferred N_{60} values were then corrected for overburden stress using the procedure developed by Idriss and Boulanger (2008) following the same process as for the SPT and BPT results. The cumulative distribution of the resulting CPT-inferred values of $(N_1)_{60}$ are plotted on Figure 5-28. The data in this plot have been presented in three groups, CPT data below the crest, CPT data at the downstream toe, and the combined set of data. Review of this figure indicates that the data sets are very similar in terms of low values, high values and shape (i.e., the distribution of values); thus, these inferred values of $(N_1)_{60}$ appear to be well-behaved and appropriate for consideration when developing dynamic properties for the alluvium.

Figure 5-29 compares the measured values of $(N_1)_{60}$ at boring location SC-104 from the SPT to the inferred values of $(N_1)_{60}$ from the BPT interpreted using the Harder Method and the Sy and Campanella Method, and to the inferred values of $(N_1)_{60}$ from the CPT results at that location. As shown on this figure, the values of $(N_1)_{60}$ from the SPT, the BPT using the Sy and

Campanella Method and the CPT are all in reasonably good agreement and considerably higher than the values of $(N_1)_{60}$ from the BPT interpreted using the Harder Method.

Figure 5-30 is a cumulative frequency diagram showing the values of $(N_1)_{60}$ from the SPT, BPT interpreted using the Harder Method and the Sy and Campanella Method, and the values of $(N_1)_{60}$ inferred from the CPT data at the toe. The median $(N_1)_{60}$ value based on the BPT with the Harder Method is 19 when considering the borings made at the toe of the dam only. For the remaining data, the 50th percentile values of $(N_1)_{60}$ vary from 33 to 46 blows per foot and the 16th percentile values of $(N_1)_{60}$ (mean minus one standard deviation) vary from 25 to 31 blows per foot. Recommended values are discussed in Section 5.6.2.5 below.

5.6.2.4 Shear Wave Velocity Measurements

Shear wave velocity data has been collected using OYO suspension logging in mud rotary borings and using "seismic cone" in CPT soundings at the following three locations:

- below the dam crest;
- below the embankment 180 feet downstream of the crest (at the lower access road); and
- near the embankment toe 360 feet downstream of the crest.

Because of the large variability in confining pressure between these three locations, the shear wave velocity data should be normalized for overburden stress to provide a consistent evaluation. Effective overburden stress profiles were estimated at all three locations based on unit weights and piezometric conditions discussed earlier. These effective overburden stresses were then used to normalize the shear wave velocity data using the relationship recommended by Andrus and Stokoe (2000):

$$V_{S1} = V_S \left(\frac{P_a}{\sigma_v'}\right)^{0.25}$$

where V_{S1} = overburden stress-corrected shear wave velocity,

P_a = atmospheric pressure, and

σ_v' = estimated in-situ effective overburden stress.

All the data were normalized using this approach and the resulting profiles are plotted on the maximum dam cross section on Figure 5-31.

As shown on Figure 5-31, relatively high normalized shear wave velocities are observed for the full depth of the embankment and alluvium at all three locations. The normalized data generally fall between 300 and 400 meters per second (m/s) with no measurements less than 230 m/s. The threshold for triggering liquefaction of 205 m/s as proposed by Andrus and Stokoe (2000) is also shown on the three profiles on Figure 5-31 for reference purposes.

5.6.2.5 Recommended Values of $(N1)_{60}$

As indicated in the introduction to Section 5.6.2, after much discussion with DSOD regarding the data for the alluvium obtained at the site, DSOD concluded that the effects of gravel on the penetration resistance within the alluvium may be significant and therefore it was agreed to use

$(N_1)_{60}$ values estimated using the method proposed by Harder (1997). However, our evaluation of the data indicates that the mean $(N_1)_{60}$ values from BPT data interpreted using the Harder method may be extremely conservative and that $(N_1)_{60}$ values estimated from other field testing methods using 16th percentile values (corresponding to mean value minus one standard deviation) should be used as a benchmark in our seismic safety evaluation.

The mean $(N_1)_{60}$ values from BPT data interpreted using the Harder method based on test results from borings at the toe of the dam and one boring on the lower access road is 20 blows/foot. This will be used as the DSOD-approved mean $(N_1)_{60}$ value for the purposes of our seismic deformation analyses.

The $(N_1)_{60}$ values estimated from SPT data, BPT data interpreted using the Sy and Campanella method, and CPT measurements corresponding to mean value minus one standard deviation range from 25 to 31 blows/foot. We recommend using an $(N_1)_{60}$ value of 25 blows/ft as a benchmark in our seismic safety evaluation.

5.6.3 Dynamic Properties

Dynamic properties adopted for the engineering analyses consist of shear wave velocity, shear modulus reduction curves, and damping ratio curves. Shear wave velocity data considered for the alluvium are shown in Figure 5-31 and the average V_{S1} value observed from the OYO measurements was 332 m/s. As with the embankment materials, the small strain shear modulus can be obtained from the shear wave velocity and the known mass density of the material using the following relationship:

$$G_{max} = \rho \cdot V_S^2$$

In this relationship, G_{max} is the small strain shear modulus, ρ is the mass density of the material, and V_s is the shear wave velocity.

Based on the sandy nature of the alluvium, the shear modulus reduction and damping ratio curves were selected based on the work by Darendeli and Stoke (2001), who developed confining pressure dependent modulus reduction and damping ratio curves for three ranges of confining pressure, as shown on Figure 5-32.

5.6.4 Permeability

Borehole field permeability tests were made within the alluvium using the Casagrande and standpipe piezometers. The piezometer at SC-105S was screened in weathered Santa Clara Formation and terrace alluvium and the tests yielded a permeability of 3 x 10^{-6} cm/sec at that location. The standpipe piezometers at SC-106BPT and SC-107BPT yielded a permeability of 2 x 10^{-3}cm/sec in the saturated alluvium near the toe. The alluvium under the embankment was found to have a permeability of 2 x 10^{-5} cm/sec at piezometers at SC-102S and SC-103S and a permeability of 8 x 10^{-6} cm/sec at piezometer at SC-101S. The measured values at SC-101S through SC-103S are quite low for alluvium but the alluvium at these piezometers is not saturated and borehole permeability tests in unsaturated soils are of questionable reliability. We

believe the permeability of the partially saturated alluvium would be 10 to 100 times less than that of the saturated alluvium. Consequently, we recommend using a permeability of 2×10^{-3} cm/sec for saturated younger alluvium and a permeability of 2×10^{-5} cm/sec for unsaturated younger alluvium.

6.1 GENERAL

This section documents the earthquake ground motions from the controlling event on the Stanford-Monte Vista Fault and an additional ground motion associated with the San Andreas Fault developed for the Stevens Creek Dam site. These ground motions are developed in terms of response spectral values and candidate acceleration time histories to be used in developing time histories that are compatible with the specified response spectral values. The following subsections detail the seismic sources considered, the development of V_{S30}, the attenuation relationships used, the resulting response spectra for considered events, the candidate time histories and spectral matched time histories for the controlling event on the Stanford-Monte Vista Fault and the candidate time history selection process and spectral matched time histories for the San Andreas Fault. The selection of candidate time histories considered the previous work on site-specific ground motions for other District dams as described in Design Memorandum No. 4 (URS, 2010), and also the discussions between URS and DSOD on this design memorandum.

6.2 POTENTIAL SEISMIC SOURCES AND BACKGROUND INFORMATION

As discussed in detail in Section 3.0, the dam and entire reservoir area are underlain by the Plio-Pleistocene Santa Clara Formation, which in the local vicinity comprises the entire area of the foothills between the Berrocal and Monte Vista faults. Upstream of the reservoir, Stevens Creek initially flows southeastward following the linear rift of the San Andreas Fault along Stevens Canyon. The creek diverges northeastward from the line of the fault and cuts across the Franciscan rocks that form Monte Bello Ridge, which lies between the San Andreas and Berrocal faults. Stevens Creek then bends north-northwest where it crosses the Berrocal Fault, and meanders across the foothills through the reservoir area and dam site downstream to where it emerges onto the floor of Santa Clara Valley. Stevens Creek Dam was constructed across the relatively narrow valley of the creek one mile upstream from where it crosses the range front at the Monte Vista Fault.

The recent Seismotectonic and Ground Motion Study for Seismic Stability Evaluation of DIP Phase 1 Dams, Technical Memorandum No. 3 (TM-3; AMEC 2009) indicates that the San Andreas, Berrocal, and Stanford-Monte Vista faults are the controlling seismic sources at the dam site. These faults are depicted on Figure 3-1 and the key fault parameters are listed in Table 6-1. The San Andreas Fault is a strike-slip fault exhibiting a very high slip rate with the closest mapped trace passing 3.8 km to the southwest of Stevens Creek Dam. The conditionally active Berrocal and active Stanford-Monte Vista faults are both southwest-dipping reverse faults and are located to the southwest and northeast of the dam, respectively; the dam is therefore located on a block of rock that forms the footwall of the Berrocal Fault and the hanging wall of the Stanford-Monte Vista Fault. The surface trace of the Monte Vista Fault is located 1.6 km map distance to the northeast, along the range front, and it dips beneath the dam at a closest fault rupture distance (r_{rup}) of 1.3 km assuming a fault dip of 55° (average fault dip as per TM-3). The Berrocal Fault crosses Stevens Creek just south of the upstream end of the reservoir at a closest distance of 1.1 km southwest of the dam. TM-3 (ibid) shows the Berrocal Fault as a conditionally active, low to moderate slip rate fault (< 0.1 to 1.0 mm/yr) whereas the Stanford-

Monte Vista Fault is shown as an active, moderate slip rate fault (0.1 to 1.0 mm/yr). In TM-3 (ibid) maximum moment magnitudes of M6.8, M6.9 and M7.9 were assigned to the Berrocal, Stanford Monte-Vista and San Andreas faults, respectively.

As noted in Section 3.0, no tectonic deformation has been identified in the immediate vicinity of the dam.

6.3 DAM CONSEQUENCE CLASSIFICATION AND V_{S30}

Following the guidelines established in the work by Fraser and Howard (2002), the statistical level of the design earthquake ground motion was based on factors including dam consequence and slip rate for each fault. It is understood the DSOD classification for Stevens Creek Dam is high consequence due to the populated community of Cupertino downstream of the reservoir. Using the DSOD consequence-hazard matrix, the 84th percentile spectral accelerations were considered for all three faults studied.

The dam is founded on Plio-Pleistocene-aged sedimentary rocks of the Santa Clara Formation, which consist of bedded claystone, siltstone, sandstone, and conglomerate. The Santa Clara Formation is underlain by upper Cretaceous to Upper Jurassic metamorphic rocks of the Franciscan Assemblage, which consist of metashale and metagraywacke rocks (Sorg and McLaughlin, 1975). Shear-wave velocity measurements were collected at the site using an OYO Suspension PS logging system within boreholes SC-101MR, SC-104MR, and SC-105MR, which penetrated 5 m to 10 m into the foundation rock. The results of these surveys are plotted versus depth below the top of bedrock in Figure 6-1. Based on these measurements, the average shear-wave velocity within the upper 10 m of the foundation rock is 960 m/s. Based on geologic experience at the site, it is anticipated that the Santa Clara Formation to a foundation depth of 30 m would be similar to that observed within the boreholes to a depth of 10 m. Therefore, the site V_{S30} for the ground motion evaluation was estimated to be 960 m/s. The approximate depth to $Z_{1.0}$ (depth at which V_S = 1 km/sec) was estimated to be between 5 to 30 m based on the trends of the site-specific shear-wave velocity measurements, which penetrated a maximum of 10 m into foundation rock. It is estimated that the Franciscan Assemblage rock under the dam would have a relatively high shear-wave velocity (above 2.5 km/sec) and that the top of the Franciscan Assemblage would represent the $Z_{2.5}$ (depth at which V_S= 2.5 km/sec) interface. The approximate depth to the top of the Franciscan Assemblage under the site was estimated based on geologic profiles presented in Sorg and McLaughlin (1975). Based on this information, the $Z_{2.5}$ for the site was estimated to be 500 m.

6.4 ATTENUATION RELATIONSHIPS AND EARTHQUAKE GROUND MOTIONS

Although five new generation attenuation (NGA) relationships are available, only four of them were used in the evaluation documented herein . The Idriss (2008) attenuation relationship was not considered because the value of V_{s30} for Stevens Creek Dam exceeds the upper bound V_{s30} recommended by Dr. Idriss. An arithmetic average of the four remaining NGA relationships (Abrahamson and Silva, 2008; Boore and Atkinson, 2008; Campbell and Bozorgnia, 2008 and Chiou and Youngs, 2008) was used to develop design response spectral values for the dam site. The NGA relationships are considered much more “scientifically sound” than the earlier

attenuation relationships both in terms of the quantity and quality of their ground motion database and methodologies and parameters reflected in their relationships.

In using the NGA relationships a number of parameters need to be specified. These parameters include the style of faulting, maximum magnitude, and distance to each fault listed in Table 6-1.

Other required parameters associated with the site subsurface conditions include: (1) shear-wave velocity (V_{s-30}) within the upper 30 m (100 ft) of the foundation rock (about 960 m/sec), (2) depth to V_s= 1 km/sec or 3,300 ft/sec foundation material (about 5 m to 30 m for the site), and (3) depth to V_s= 2.5 km/sec (8,200 ft/sec) foundation material beneath the dam (about 0.5 km or 1,600 ft for the site). The development of these parameters is summarized in Section 6.3.

Table 6-1 also provides estimates of the median and 84th percentile peak horizontal ground acceleration (PGA), and median and 84th percentile Arias intensity using the NGA relationships. It should be noted that the Arias intensity values were obtained from the Watson-Lamprey and Abrahamson (2006) attenuation relationships.

6.5 ACCELERATION RESPONSE SPECTRA FOR MAXIMUM CREDIBLE EARTHQUAKE

Figure 6-2 shows the 84th percentile fault parallel (FP) response spectra for the three earthquake event scenarios shown in Table 6-1. As can be seen on this figure, the Stanford-Monte Vista event controls the shaking condition at the site for the lower magnitude earthquake scenario. Larger earthquake magnitude, such as the one occurring along the San Andreas fault, controls the shaking condition at the site for periods larger than about 2-second. It should also be noted that, in evaluating the response spectra discussed above, we considered a range of value for $Z_{1.0}$ (the depth to V_s=1 km/sec) from 5 to 30 m. While in general the differences are very small, the final response spectral ordinates shown on Figure 6-2 correspond to the highest value obtained from the range of $Z_{1.0}$ considered.

Figure 6-3 shows the fault normal (FN) response spectra for the three earthquake event scenarios shown in Table 6-1. Fault rupture directivity effects used to develop the fault normal component response spectra were based on DSOD guidelines (Fraser and Howard, 2002). The forward directivity effects were estimated using the near source factor developed by Somerville et al. (1997) as modified by Abrahamson (2000). As in the case of the FP response spectra, the FN response spectra are dominated by the Stanford-Monte Vista event for periods less than about 2 seconds. The San Andreas event dominates the shaking condition at the site for periods larger than about 2 seconds.

Due to the disparity in the shaking between lower magnitude events (such as the Stanford-Monte Vista and the Berrocal events) and the larger magnitude event (such as the San Andreas event), we recommend that two response spectra be used to represent the Maximum Credible Earthquake (MCE) in the seismic evaluation of the dam. We recommend that the Stanford-Monte Vista response spectra be used for the evaluation of lower magnitude events, and that the San Andreas spectra be used for the evaluation of higher magnitude events. Figure 6-4 shows the FP and FN components of these recommended response spectra. These response spectra are also provided in tabular format in Tables 6-2A, 6-2B, 6-3A and 6-3B for the FP and FN Stanford-Monte Vista event and for the FP and FN San Andreas event, respectively.

6.6 CANDIDATE ACCELERATION TIME HISTORIES AND SPECTRALLY MATCHED TIME HISTORIES FOR STANDFORD-MONTE VISTA EVENT

Based on the recommended response spectral values shown on Figure 6-4 and listed in Tables 6-2A through 6-3B, two sets of three seed acceleration-time histories are considered for potential use in developing spectrum-compatible acceleration time histories for the seismic response and deformation analyses.

The characteristics of the three selected seed time histories for the Stanford-Monte Vista event are summarized in Table 6-4A. These seed time histories are selected from the following earthquakes: the 1995 Kobe, the 1989 Loma Prieta, and the 1994 Northridge earthquakes. The acceleration, velocity, and displacement-time histories; the Arias intensity; and the response spectra for each of the seed recordings are shown on Figures 6-5, 6-6, and 6-7, respectively. It should be noted that the selected time histories shown on these figures correspond to the FN component. Because the axis of the dam is almost sub-parallel to the San Andreas Fault and on the hanging wall of the Stanford-Monte Vista Fault (the two faults controlling the shaking condition at the site), only the FN component will be used in the seismic response and deformation analyses of the dam.

Figure 6-8 shows the adjusted MDE time history based on the Kobe – Nishi-Akashi motion in terms of acceleration, velocity, displacement and Arias intensity time histories and a comparison of the response spectral values with the MDE response spectral values. On the Arias intensity plot, the 84th percentile Arias intensity value corresponds to the postulated MDE motion using the Watson-Lamprey and Abrahamson (2007) relationship. This Arias intensity plot also shows the plus and minus one standard deviation of the computed Watson-Lamprey and Abrahamson Arias intensity value. Figures 6-9 and 6-10 show the same information for the adjusted time history based on the Loma Prieta – LGPC and the Northridge – Sylmar OVMFF records, respectively. It should be noted that the Arias intensity values of the three ground motions exceed the median Arias intensity value provided by the 84th percentile Watson-Lamprey and Abrahamson relationship.

6.7 CANDIDATE ACCELERATION TIME HISTORIES AND SPECTRALLY MATCHED TIME HISTORIES FOR SAN ANDREAS EVENT

The selection of seed time histories for the San Andreas event was carried out more systematically due to the relatively small number of high quality ground motion records from stations that are very close to ruptures of very large magnitude earthquakes. The selection process began with a preliminary screening of all 3,551 records in the PEER Ground Motion Database (PEER, 2011). The records are plotted in Figure 6-11 with magnitude on the x-axis and closest distance in kilometers on the y-axis. From this pool, only records from events with Magnitude 7.0 or greater and within 40 km of the rupture were considered. This narrowed the field to 155 strong motion records as shown in the red rectangular area on Figure 6-11.

The second step in the screening process attempted to identify records with similar spectral accelerations to the target ground motion for the Fault Normal component of the San Andreas at key periods of interest. The first parameter of interest was peak ground acceleration (PGA) and all records with at least half the PGA of the target ground motion (0.35g) were flagged for

consideration. The second parameter of interest was the fundamental period of the dam, estimated as $T = 2.6*H/Vs$, with H equal to the height of the embankment and Vs equal to the average shear wave velocity of the embankment. Using this relationship, the fundamental period of the dam was estimated to be 0.26 seconds and the average spectral acceleration of the target spectrum between $0.8T$ and $1.2T$ was determined to be 1.5 g. All of the remaining records with at least half of this average spectral acceleration around the period of interest were included for consideration. These records are shown graphically in Figure 6-12 with average spectral acceleration in the fundamental period range on the x-axis and PGA on the y-axis. This second level of screening resulted in 30 records of interest as shown in the red rectangular area on Figure 6-12. An exception was made to include the Denali TAPS Pump Station #10 record which did not meet either criteria with regards to the spectral acceleration characteristics but is a record of a strike-slip event with magnitude 7.9 recorded 3.8 km from the rupture which is the closest event with respect to magnitude and distance to that postulated for the Stevens Creek Dam.

The final level of screening was based on the significant duration and Arias intensity of the seed time histories. Significant duration $D_{5\text{-}95}$, defined as the time in seconds between the 5th and 95th percentile Arias intensity, of the San Andreas event was estimated using three procedures; Kempton and Stewart (2006) procedure with no directivity effects, Kempton and Stewart with directivity effects and Bommer et.al. (2009). Using the methods, the estimated $D_{5\text{-}95}$ for the M7.9 San Andreas earthquake ranged from 16 to 29 seconds. The arias intensity of the 84th percentile ground motions of the San Andreas was estimated to be 5.95 m/s using Watson-Lamprey (2008). To compare these to the 31 records that were screened, the Arias intensity and significant duration were calculated for each record. The results of this exercise are shown on Figure 6-13 with Arias intensity plotted on the x-axis and significant duration plotted on the y-axis. As shown on Figure 6-13, eight records with similar Arias intensity and significant duration as well as the Denali TAPS record were chosen for a final candidate selection. The two horizontal components for each record were rotated to fault normal and the resulting time histories and spectral accelerations were plotted for comparison. Figure 6-14 shows the fault normal spectral acceleration of each of the final nine records as compared to the target San Andreas spectrum. Based on visual analysis of these records three time histories for spectral matching were selected as follows: the 1990 Manjil earthquake, Abbar record; the 1999 Chi-Chi earthquake, TCU065 record; and the 1992 Landers earthquake, Lucerne record. The acceleration, velocity, and displacement-time histories; the Arias intensity; and the response spectra for each of the seed recordings are shown on Figures 6-15, 6-16, and 6-17, respectively.

Figure 6-18 shows the adjusted MDE time history based on the Manjil – Abbar motion in terms of acceleration, velocity, displacement and Arias intensity time histories and a comparison of the response spectral values with the MDE response spectral values. On the Arias intensity plot, the 84th percentile Arias intensity value corresponds to the postulated MDE motion using the Watson-Lamprey and Abrahamson (2007) relationship. This Arias intensity plot also shows the plus and minus one standard deviation of the computed Watson-Lamprey and Abrahamson Arias intensity value. Figure 6-18 also shows the range of duration estimates using the approaches detailed above, along with the actual duration of the adjusted time history. Figures 6-19 and 6-20 show the same information for the adjusted time history based on the Chi Chi – TCU065 and the Landers – Lucerne records, respectively. It should be noted that the Arias intensity values of the

three ground motions exceed the median Arias intensity value provided by the 84th percentile Watson-Lamprey and Abrahamson relationship.

The key findings from this site characterization study are as follows:

1. There is little difference in the physical and index properties and shear strength of the upstream "impervious" and downstream "pervious" embankments. However, the significance of these original embankment designations is that alluvium was removed beneath the upstream "impervious" embankment but left in place beneath the downstream "pervious" embankment. In accordance with the District's preference to fade out the misnomer associated with these designations, this report refers to the embankment zones as upstream embankment and downstream embankment.
2. The upstream and downstream embankments are generally classified as clayey sand with gravel. The clay matrix was found to control the behavior of these materials and they were determined to be non-liquefiable and to have a relatively high undrained shear strength.
3. The upstream buttress constructed in 1985-1986 was generally founded on Santa Clara Formation bedrock after removal of the alluvium.
4. The downstream buttress constructed in 1985-1986 was not founded on bedrock, but on alluvium left in place in the foundation, overlain by fill material which appears to have been placed downstream of the toe of the original embankment during original dam construction.
5. The alluvium left in place beneath the downstream embankment is functioning as a very effective drainage blanket. The groundwater levels in the alluvium at the maximum dam section are low and the saturated thickness of the alluvium typically varies from 1 foot near the crest to 6 feet near the toe. The saturated thickness of the alluvium is not controlled by the elevation of the water in the reservoir but by groundwater levels in the toe area that vary with precipitation and recharge from releases through the reservoir outlet works into Stevens Creek downstream of the dam.
6. The strength of the alluvium left in place is positively influenced by the low piezometric levels and correspondingly high values of effective confining stresses in the alluvium.
7. Characterization of the liquefaction potential and post liquefaction residual shear strength for the alluvium is based on estimates of $(N_1)_{60}$, corrected standard penetration test (SPT) blow counts. The average gravel content of the alluvium is 35% and the presence of gravel within the alluvium may influence the results of SPTs and estimates of $(N_1)_{60}$ made using Cone Penetrometer Tests (CPTs).
8. After several discussions with DSOD regarding the data for the alluvium obtained at the site, DSOD concluded that the effects of gravel on the penetration resistance within the alluvium may be significant and therefore it was agreed to use $(N_1)_{60}$ values estimated using BPT test results interpreted using the method proposed by Harder (1997). However, our evaluation of the data indicates that the mean $(N_1)_{60}$ values from BPT data interpreted using the Harder method may be extremely conservative and that $(N_1)_{60}$ values estimated from other field testing methods using 16th percentile values (corresponding to mean value minus one standard deviation) should be used as a benchmark in our seismic safety evaluation.
9. The mean $(N_1)_{60}$ values from BPT data interpreted using the Harder method based on test results from borings at the toe of the dam and one boring on the lower access road is 20

blows/foot. This will be used as the DSOD-approved mean $(N_1)_{60}$ value for the purposes of our seismic deformation analyses.

10. The 16th percentile $(N_1)_{60}$ values estimated from SPT data, BPT data interpreted using the Sy and Campanella method, and CPT measurements (corresponding to mean value minus one standard deviation) range from 25 to 31 blows/foot. In order to understand the sensitivity of estimated seismic deformations to the uncertainty in $(N_1)_{60}$ values, we recommend using an $(N_1)_{60}$ value of 25 blows/ft as a benchmark value for calculating and comparing seismic deformations.
11. Acceleration response spectra were developed for 84th percentile ground motions associated with the Stanford-Monte Vista Fault and the San Andreas Fault. Three seed time histories were chosen for each of these events and spectrally-matched time histories were developed for use in the non-linear seismic deformation analyses.

Abrahamson, N.A., 2000, “Effects of rupture directivity on probabilistic seismic hazard analysis,” Proc. 6th International Conference on Seismic Zonation, Palm Springs.

Abrahamson, N.A., and Silva, W.J., 2008 (February), “Summary of the Abrahamson & Silva NGA Ground Relations,” *Earthquake Spectra*, Vol. 24, No. 1, pp. 67-98. EERI.

AMEC, 2009 (January), Technical Memorandum No. 3, Seismotectonic and Ground Motion Study, Seismic Stability Evaluation of DIP Phase 1 Dams.

Andrus, D.R. and Stoke, K.H., II, 2000 (November), "Liquefaction Resistance of Soils from Shear-Wave Velocity", ASCE, Journal of Geotechnical and Geoenvironmental Engineering, Vol. 126., No. 1, pp 1015-1025.

Bommer J.J., Stafford P.J., Alarcon J.E., 2009. “Empirical Equations for the Prediction of the Significant, Bracketed, and Uniform Duration of Earthquake Ground Motion”, Bulletin Seismological Society of America, v. 99, pp 3217-3233.

Boore, D. M. and Atkinson, G.M., 2008 (February), “Ground-Motion Prediction Equations for the Average Horizontal Component of PGA, PGV, and 5%-Damped PSA at Spectral Period between 0.01s and 10.0 s,” Earthquake Spectra, Vol. 24, No. 1, pp. 99-138. EERI.

Brabb, E.E., Graymer, R.W., and Jones, D.L., 2000, Geologic Map and Map Database of the Palo Alto 30x60 Quadrangle, California, U.S. Geological Survey Miscellaneous Field Studies Map MF-2332.

Bryant, W.A., compiler, 2000, Fault no. 56, Monte Vista-Shannon fault zone, in Quaternary fault and fold database of the United States: U.S. Geological Survey website, http://earthquakes.usgs.gov/regional/qfaults.

California Department of Water Resources, Division of Safety of Dams (DSOD), 1981 (June), Phase 1 Inspection Report for Stevens Creek Dam.

California Department of Water Resources, Division of Safety of Dams (DSOD),1935-1936, Inspection Memoranda by G.F. Engle on Construction of Stevens Creek Dam (on file at DSOD).

California Department of Water Resources, Division of Safety of Dams (DSOD), 1985-1986, Inspection of Dam Construction Reports for Stevens Creek Dam Modifications, with Memoranda of Geologic Inspection (on file at DSOD).

California Department of Water Resources, Division of Safety of Dams (DSOD), 2010 (June), DSOD Comments on DM-2 and Interim DM-4, Guadalupe, Almaden, and Calero Dams, dated June 10, 2010.

Campbell, K.W., and Bozorgnia, Y. , 2008 (February), “NGA Ground Motion Model for the geometric Mean Horizontal Component of PGA, PGV, PGD and 5% Damped Linear Elastic Response Spectra for Periods Ranging from 0.01 to 10 s,” Earthquake Spectra, Vol. 24, No. 1, pp. 139-172. EERI.

Chiou, B.S.J. and Youngs, 2008 (February), “An NGA Model for the Average Horizontal Component of Peak Ground Motion and Response Spectra,” Earthquake Spectra, Vol. 24, No. 1, pp. 173-216. EERI.

Darendeli, M.B. and Stokoe, K.H., 2001, Development of a new family of normalized modulus reduction and material damping curves, Geotech. Engrg. Rpt. GD01-1, University of Texas, Austin, Texas.

Fraser, W.A., and Howard, J.K., 2002 (October), "Guideline for Use of the Consequence-Hazard Matrix and Selection of Ground Motion Parameters," The Resource Agency, Dept. of Water Resources, Div. of Safety of Dams.

Goble, G.G., Frank Rausche, and G.E. Likins, Jr., 1980 (June), The analysis of pile driving – A state-of-the-art, International Seminar on The Application of Stress-Wave Theory on Piles, Stockholm.

Harder, L.F., Jr. and Seed, H.B., 1986, Determination of Penetration Resistance for Coarse-Grained Soils Using the Becker Hammer Drill, Report No. UBC/EERC-86/06, Earthquake Engineering Research Center, University of California at Berkeley.

Harder, L. F., Jr., 1997, Application of the Becker Penetration Test for Evaluating the Liquefaction Potential of Gravelly Soils. Proc., NCEER Workshop on Evaluation of Liquefaction Resistance of Soils, National Center for Engineering Research, Buffalo, 129–148.

Idriss, I.M., 2008 (February), "An NGA Empirical Model for Estimating the Average Horizontal Spectral Values Generated by Shallow Crustal Earthquakes," Earthquake Spectra, Vol. 24, No. 1, pp. 217-242. EERI.

Idriss, I.M. and Boulanger, R.W., 2008. Soil Liquefaction During Earthquakes. Earthquake Engineering Research Institute, MNO-12.

Jeffries, M. G. and Davies, M. P., 1993. Estimation of SPT N values from the CPT, ASTM.

Kempton, J.J. and Stewart, J.P., 2006. "Prediction Equations for Significant Duration of Earthquake Ground Motions Considering Site and Near-Source Effects", Earthquake Spectra, 22(4), pp 985-1013.

Marliave, C., 1936, Geologic Report on Stevens Creek Dam – Situated on Stevens Creek in Santa Clara County (post-construction report on geologic conditions with as-built geologic section along cutoff trench; from DSOD archives).

McLaughlin, R., and Clark, J., 2004, Stratigraphy and Structure Across the San Andreas Fault Zone in the Loma Prieta Region and Deformation During The Earthquake, in Wells, R., editor, 2004, The Loma Prieta, California, Earthquake of October 17, 1989 - Geologic Setting and Crustal Structure, USGS Professional Paper 1550E.

McLaughlin, R.J., Clark, J.C., Brabb, E.E., and Helley, E.J., 2001, Geologic Maps and Structure Sections of the Southwestern Santa Clara Valley and Southern Santa Cruz Mountains, Santa Clara and Santa Cruz Counties, California, Sheet 1: Los Gatos Quadrangle.

Mitchell, J. K., 1976, Fundamentals of Soil Behavior, John Wiley & Sons Inc.

Nelson, J.L, 2010a (January), Foundation Analysis Report on Chesbro No.72-11, Lenihan No.72-8, Stevens Creek No. 72-7, and Uvas No. 72-12 Dams (SSE-2 Dams.

Nelson, J.L, 2010b (April), 2010 Surveillance Report, March 2009 through March 2010, Stevens Creek Dam No.72-7.

Pacific Earthquake Engineering Research Center (PEER), 2011 (May), "PEER Ground Motion Database.". University of California at Berkeley, 2010. Web Version. 20 May 2011. http://peer.berkeley.edu/peer_ground_motion_database/site.

Pile Dynamics, Inc., 2006, CAPWAP® 2006, Cleveland, Ohio, www.pile.com.

Robertson, P. K., 1990. Soil Classification Using the Cone Penetration Test: Canadian Geotechnical Journal, v. 27, 151–158.

Robertson, P.K. and Wride, C.E., 1998, Evaluating Cyclic Liquefaction Potential Using the Cone Penetrometer Test, Canadian Geotechnical Journal, Vol. 35, No. 3, pp. 442-459.

Robertson, P.K., 2009, Interpretation of Cone Penetrometer Tests – a unified approach, Canadian Geotechnical Journal, Volume 46, Number 11, 1 November 2009, pp. 1337-1355.

Robertson, P. K., 2010. Evaluation of Flow Liquefaction and Liquefied Strength Using the Cone Penetration Test: Journal of Geotechnical and Geoenvironmental Engineering, v. 136, 842–853.

Santa Clara Valley Water Conservation District, 1934, Contracts, Proposals, Specifications, Maps – Contract No. 3 for Construction of Stevens Creek Dam and Spillway.

Santa Clara Valley Water District (SCVWD), 1976, Stevens Creek Reservoir Landslide Investigation.

Santa Clara Valley Water District (SCVWD), 1985, Specifications and Contract Documents for the Stevens Creek Dam Modifications.

Santa Clara Valley Water District (SCVWD), 2005, Special Seepage Investigation, Stevens Creek Dam.

Santa Clara Valley Water District (SCVWD), 2010c (June), Black and white aerial photo sets (1969, 1983, 1985(2), 1986, and 2002), on-file at SCVWD.

Santa Clara Valley Water District (SCVWD), 2010d (June), As-constructed foundation topography beneath Stevens Creek Dam, GIS data shape file.

Santa Clara Valley Water District (SCVWD), 2010e (June), Original pre-construction topography beneath Stevens Creek Dam GIS data shape file.

Shannon & Wilson, Inc. (S&W), 1976 (December), Piezometer Installation, Stevens Creek Dam.

Seed, R. B. et al, 2003, “Recent Advances in Soil Liquefaction Engineering: A Unified and Consistent Framework”, Report No. EERC 2003-06, Earthquake Engineering Research Center, College of Engineering, University of California, Berkeley.

Seed, R. B., 2010. Technical Review and Comments: 2008 EERI Monograph, Soil Liquefaction During Earthquakes. Geotechnical Report No. UCB/GT – 2010/01, University of California at Berkeley.

Sommerville, P.G., N.F. Smith, R.W. Graves, and N.A. Abrahamson, 1997, Modifications of empirical strong ground motion attenuation relations to include the amplitude and duration effects of rupture directivity, Seismological Research Letters 68, 199-222.

Sorg, D.H. and R. J. McLaughlin, 1975, "Geologic Map of the Sargent – Berrocal fault zone between Los Gatos and Los Altos Hills, Santa Clara County, California," Miscellaneous Field Studies Map MF-643.

Spudich, P., editor, 1996, "The Loma-Prieta, California, Earthquake of October 17, 1989 – Main Shock Characteristics", USGS Professional Paper 1550A.

Sy, A. and Campanella, R.G., 1994, Becker and Standard Penetration Tests (BPT-SPT) Correlations with Consideration of Casing Friction: Canadian Geotechnical Journal, v. 31, 343–356.

Terra / GeoPentech, a Joint Venture, 2010 (November), Seismic Stability Evaluations of Chesbro, Lenihan, Stevens Creek, and Uvas Dams, Phase A: Stevens Creek and Lenihan Dams, Site Investigations and Laboratory Testing at Stevens Creek Dam, Work Plan, prepared for Santa Clara Valley Water District.

Terra / GeoPentech, a Joint Venture, 2011 (January), Seismic Stability Evaluations of Chesbro, Lenihan, Stevens Creek, and Uvas Dams, Phase A: Stevens Creek and Lenihan Dams, Site Investigations and Laboratory Testing at Stevens Creek Dam, Addendum to Work Plan, prepared for Santa Clara Valley Water District.

Terra / GeoPentech, a Joint Venture, 2012 (February), Seismic Stability Evaluations of Chesbro, Lenihan, Stevens Creek, and Uvas Dams, Phase A: Stevens Creek and Lenihan Dams, Stevens Creek Dam, Site Investigations and Laboratory Testing Data Report (Report No. SC-1), prepared for Santa Clara Valley Water District.

Tolman, C.F., 1934 (October), Geology of the Murphy Dam site on Stevens Creek.

URS Corporation, 2010 (October), Design Memorandum No. 4, Task 3 – Site Specific Design Earthquake Motions, Seismic Stability Evaluation of Almaden, Calero, and Guadalupe Dams.

U.S. Geological Survey website, 2011, Rupture Length and Slip – The Northern California Earthquake April 18, 1906: http://earthquake.usgs.gov/regional/nca/virtualtour/earthquake.php.

Volpe, R.L. and Associates (RLVA), 1990, Investigation of SCVWD Dams Affected by Loma Prieta Earthquake of October 17, 1989, Report to Santa Clara Valley Water District.

Vucetic, M. and Dobry, R., 1991, Effect of Soil Plasticity on Cyclic Response, Journal of Geotechnical Engineering Division, ASCE, Vol. 117, No. 1, pp.89-107.

W.A. Wahler and Associates, 1978 (December), Seismic Safety Evaluation, Stevens Creek Dam.

Wahler Associates, 1982 (October), Report on Preliminary Remedial Design Investigation of Stevens Creek Dam.

Wahler Associates, 1984 (August), Remedial Design Report, Stevens Creek Dam.

Wahler Associates, 1986a, As-Built Drawings, Stevens Creek Dam Modifications (on file at SCVWD).

Wahler Associates, 1986b, Summary of Field Density Tests, Stevens Creek Dam Modifications (on file at DSOD).

Watson-Lamprey, J. and Abrahamson, N.A., 2006 (February), "Selection of Ground Motion Times Series and Limits on Scaling," Soil Dynamics and Earthquake Engineering, vol. 26, pp. 477-482.

Wells, R., editor, 2004, The Loma Prieta, California, Earthquake of October 17, 1989 - Geologic Setting and Crustal Structure, USGS Professional Paper 1550E.

Wills, C., Weldon, R., and Bryant, W., 2008, Appendix A: California Fault Parameters for the National Seismic Hazard Maps and Working Group on California Earthquake Probabilities 2007, USGS Open File Report 2007-1437A.

Woodward-Clyde Consultants (WCC), 1976a (January), Part 1 - Geology and Seismicity - Seismic Stability Assessment of Four Dams, Santa Clara Valley Water District.

Woodward-Clyde Consultants (WCC), 1976b (June), Part II – Field Investigations and Engineering Analyses - Seismic Stability Assessment of Four Dams, Santa Clara Valley Water District.

TABLES

TABLE 2-1

AERIAL PHOTOGRAPHS REVIEWED

Photo Type	Date	Scale	Source
Black and White Stereo	11/4/1969	~1:12,000	SCVWD
Black and White Stereo	3/31/1983	~1:16,000	SCVWD
Black and White Stereo	6/19/1985	1:4,800	SCVWD
Black and White Stereo	11/20/1985	1:4,800	SCVWD
Black and White Stereo	1/10/1986	1:4,800	SCVWD
Black and White Stereo	11/5/2002	1:12,000	SCVWD

TABLE 4-1

DAM FOUNDATION ELEVATION DATA

Boring[1]	Elevation (Feet)		Inferred Thickness (Feet) and Type[2] of Foundation Soils above QT_{sc}
	Dam Foundation	Top of Santa Clara Formation (QTsc)	
WCC-1	485	474	11 Qoa
WCC-2	485	475	10 Qoa
WCC-3	471	471	0
WCC-4	434	N.D.[3]	?
WCC-5	432	417	15 Qya
WCC-6	434	423[1]	11 Qya
S&W B-1	431	421	10 Qya
S&W B-2	N.E.[5] (below 448)	N.E. (below 448)	?
S&W B-3	N.E. (below 433.5)	N.E. (below 433.5)	?
WA SC-1	522.2	518.5[4]	3.7 Qc, Qoa
WA SC-2	N.E. (below 440)	N.E. (below 440)	?
WA T-1	N.E. (below 436)	N.E. (below 436)	?
WA T-2	463 (ground elevation on lower left abutment D/S of dam)	452.5	10.5 Qc?[4]
WA T-3	502 (ground elevation at D/S toe original embankment, right side)	N.E. below 493	4+[6] Qoa
WA T-4	431 (ground elevation at D/S toe original embankment, channel area)	N.E. (below 421)	10+ Qya
WA SC-3	N.D.	N.E. (below 428)	?
WA SC-4	N.D.	below 418?	?
WA SC-5	431	N.E. (below 428.5)	2.5+ Qya
WA SC-6	427	N.E. (below 423)	4+ Qya
WA SC-7	429	N.E. (below 425.5)	3.5+ Qya

Boring[1]	Elevation (Feet)		Inferred Thickness (Feet) and Type[2] of Foundation Soils above QT_{sc}
	Dam Foundation	Top of Santa Clara Formation (QTsc)	
WA SC-8	N.D.	below 426?	?
WA SC-9	433.5	N.E. (below 432.5)	1+ Qya
WA SC-10	436	423	13 Qya
WA SC-11	435	428?	7? Qya
WA SC-12	N.D.	N.E. (below 430)	?
SC-101S	432	421	11 Qya
SC-101MR	432	423	9 Qya
CPT-1 (at SC-101)	432	420?	~12 Qya
SC-102S	430.5	419.5	11 Qya
SC-102BPT	431	420	11 Qya
SC-103S	431.2	417.2	14 Qya
SC-103BPT	430.6	416.6	14 Qya
SC-104S	~427.4 - 426.4	412.9	13.5-14.5 Qya
SC-104MR	424.8	413.4	11.4 Qya
SC-104BPT	425.4	413.9	11.5 Qya
CPT-3 (at SC-104)	425.5	414.5	11 Qya
SC-105S	500.4	496.9	3.5 Qc, Qoa
SC-105MR	504.1	500.6	3.5 Qc, Qoa
CPT-2 (at SC-105)	500.4	596.4	4 Qc, Qoa
SC-106BPT	429.8	418.3	11.5 Qya
SC-107BPT	430.4	415.4	15 Qya
SC-108BPT	427.0	416.5	10.5 Qya
SC-109BPT	427.1	420.1	7 Qya
SC-110BPT	426.1	411.1	15 Qya

Notes:

[1] WCC - Woodward Clyde Consultants borings, 1975. S&W - Shannon & Wilson, Inc. borings, 1976. WA - Wahler Associates borings and trenches, 1978 – 1984 (T- indicates trench); Wahler elevation data corrected to reflect currently accepted nominal original dam crest elevation of 545 feet. Wahler boring designations "DH-" removed to simplify naming convention. Recent SC-100 series exploration by TGP includes sonic (designated S), mud rotary (MR), and Becker rig (BPT) borings; Cone Penetrometer Tests designated CPT.

[2] Foundation Soil Units: Qc – Colluvium (inc. residual soil); Qya – Younger Channel Alluvium; Qoa – Older Terrace Alluvium.

[3] N.D. – Not determined as per re-interpretation of previous consultant's boring log (e.g., original logged contact depths inconsistent w/ pre-construction or as-built data and/or subsurface data from other nearby exploration).

[4] Re-interpretation of previous consultant's logged contact depth and/or geologic unit based on pre-construction or as-built data and/or subsurface data from other nearby exploration.

[5] N.E. - Not encountered

[6] Pre-construction topography shows original ground surface at ~El. 497, i.e. 5 ft. lower than as indicated on WA T-3 log (upper portion T-3 possibly in fill rather than terrace alluvium as originally logged by WA).

TABLE 4-2

SUMMARY OF TOTAL HEADS MEASURED IN CASAGRANDE AND OPEN STANDPIPE PIEZOMETERS AT DOWNSTREAM TOE

Date	Reservoir Water Elevation (Feet)	Total Head at Piezometers (Feet)		
		SC-106BPT	SC-104S	SC-107BPT
11/18/10	525.94	-	418.16	-
11/26/10	525.14	-	418.49	-
11/28/10	525.14	-	418.42	-
12/07/10	524.84	-	418.67	-
12/10/10	524.84	-	418.63	-
12/16/10	524.54	-	418.53	-
12/30/10	534.74	-	420.91	-
01/11/11	535.00	-	420.79	-
01/15/11	535.24	-	420.71	-
01/24/11	534.74	-	419.96	-
02/10/11	534.54	-	419.49	-
02/18/11	536.94	-	421.22	-
02/21/11	534.54	-	423.98	-
02/22/11	534.24	-	423.86	-
02/23/11	533.94	424.03	423.68	-
02/24/11	533.94	423.82	423.49	422.91
03/15/11	536.04	423.24	421.94	420.96
04/20/11	538.04	422.04	422.14	421.46
05/24/11	537.54	420.04	419.94	419.56

TABLE 4-3

SUMMARY OF TOTAL HEADS MEASURED

AT PIEZOMETERS INSTALLED IN SC-102BPT AND SC-102S

Date	Reservoir Water Elevation (Feet)	Total Head at Piezometers (Feet)				
		VW-1[1]	VW-2[1]	VW-3[1]	VW-4[1]	SC-102S[2]
		El. 482.65	El. 461.65	El. 440.65	El. 429.65	El. 419.73
11/28/10	525.14	-	-	-	-	420.10
12/07/10	524.84	-	-	-	-	420.09
12/10/10	524.84	-	-	-	-	419.99
12/16/10	524.54	-	-	-	-	419.79
12/30/10	534.74	-	-	-	-	420.59
01/11/11	535.00	-	-	-	-	420.69
01/15/11	535.24	-	-	-	-	421.25
01/24/11	534.74	-	-	-	-	420.76
02/10/11	534.54	-	-	-	-	420.34
02/18/11	536.94	484.46	473.18	455.69	447.76	420.64
02/21/11	534.54	484.69	473.25	452.92	444.30	423.47
02/22/11	534.24	484.83	473.29	452.21	443.29	423.69
02/23/11	533.94	485.01	473.37	451.79	442.46	423.74
02/24/11	533.94	485.16	473.41	451.74	442.11	423.65
03/15/11	536.04	485.72	473.67	451.20	437.81	-
04/29/11	537.94	486.47	474.09	450.87	435.76	-
06/02/11	537.74	486.55	474.32	450.84	435.41	-

Notes:

(1) Vibrating wire piezometer installed in boring SC-102BPT.

(2) Casagrande piezometer installed in boring SC-102S.

TABLE 5-1

INDEX PROPERTIES OF EMBANKMENT AND FOUNDATION MATERIALS[1]

Idealized Material Description	Generalized USCS Classification	In-Situ Conditions[2]			Gradation[2]				Atterberg Limits[2]	
		Dry Unit Weight, γ_d (pcf)	Moisture Content, W_c (%)	Compaction (%)[3]	Gravel (%)	Sand (%)	Fines (%)	Clay Fraction, -2μ (%)	Liquid Limit LL	Plasticity Index PI
Upstream Embankment	GC-SC-CL	123.2 (111.7 to 137.5)	12.8 (9.5 to 18.0)	96 (87 to 100)	27 (13 to 57)	44 (36 to 52)	29 (4 to 44)	12 (4 to 15)	29 (15 to 31)	12 (4 to 15)
Downstream Embankment	SC-GC-GM-SM	122.6 (109.7 to 138.5)	12.1 (7.9 to 19.1)	96 (86 to 100)	31 (10 to 63)	43 (12 to 61)	26 (12 to 51)	16 (10 to 23)	29 (23 to 37)	12 (4 to 19)
Buttresses	SC-SM-GC	129.3 (114.7 to 141.7)	7.8 (2.2 to 28.8)	97 (84 to 100)	31 (8 to 65)	43 (24 to 62)	26 (5 to 56)	13 (5 to 22)	29 (NP to 35)	12 (NP to 18)
Younger Alluvium	GP-SM-GC-SC	112.0 (94.5 to 128.2)	11.0 (3.4 to 23.1)	-	35 (12 to 75)	48 (21 to 88)	17 (4 to 39)	-	21 (NP to 28)	5 (NP to 11)
Older Alluvium	GC-GP-SM-SC	128.7 (123.0 to 133.7)	8.9 (2.8 to 16.6)	-	32 (21 to 60)	45 (36 to 60)	23 (4 to 48)	-	27 (20 to 33)	11 (4 to 15)

Notes:

(1) Data in this table are averages with minimum and maximum values in parenthesis, where available. The limited data available on Filter/Drain are not presented.

(2) In-situ conditions, gradation and limits are summarized based on laboratory testing of samples performed by S&W(1976), WCC (1977), Wahler (1978, 1982, and 1984), and TGP (2011b).

(3) Per D1557 modified, 20,000 ft-lbs.

TABLE 5-2

ENGINEERING PROPERTIES OF EMBANKMENT AND FOUNDATION MATERIALS

Zone	Moist Unit Weight (pcf)	Effective Friction Angle [1]	Undrained Strength Parameter [2]	Residual Strength Parameter [3]	Dynamic Properties [4]		
	γ_t	ϕ'	S_u/σ_{vc}'	S_R/σ_{vc}'	V_s	G/G_{max}	Damping
Upstream Embankment	139	37°	(2-1)	-	(4-1)	Fig 5-12	Fig 5-12
Downstream Embankment	137	37°	(2-1)	-	(4-1)	Fig 5-12	Fig 5-12
Buttresses	140	37°	-	-	(4-2)	Fig 5-12	Fig 5-12
Younger Alluvium	125	-	-	$(N_1)_{60}$ based[3-1]	1850 fps	Fig 5-32	Fig 5-32

Notes:

[1] Effective Friction Angle, ϕ' (with no cohesion)

[2] Undrained Strength Parameter, S_u/σ_{vc}' (undrained shear strength ratio)

[2-1] $S_u = 930 + 0.53 * \sigma_{vc}'$, in psf

[3] Residual Strength Parameter, S_R/σ_{vc}' (residual shear strength ratio)

[3-1] Residual shear strength ratio to be evaluated based on $(N_1)_{60}$ correlations during analyses

[4] Dynamic Properties, V_s (shear wave velocity), G/G_{max} (shear modulus) and Damping Ratio

[4-1] $V_s = \exp(0.23 \cdot \ln(\sigma_{vc}') + 5.3$

[4-2] $V_s = \exp(0.15 \cdot \ln(\sigma_{vc}') + 6.2$

TABLE 6-1

SUMMARY OF SEIMSIC SOURCES

Fault	Fault Parameters							Distance (km)			Average PGA		Arias Intensity (cm/sec)	
	Type	M_{max}	HW	Dip	Rup. Length	DWR	DTR	R_{map}	R_{JB}	R_{rup}	Median	84th Perc	Median	84th Perc
Berrocal	RV	6.8	No	60	28	13.9	12	1.1	1.1	1.1	0.49	0.84	1.59	3.93
Stanford-Monte Vista	RV	6.9	Yes	55	38	10.5	8.6	1.6	0.0	1.3	0.68	1.17	2.82	7.01
San Andreas	SS	7.9	-	-	470	-	-	3.8	3.8	3.8	0.42	0.71	2.31	5.60

Notes:

Fault Type: RV=Reverse; SS=Strike Slip

HW: Yes=On Hanging Wall; No=Not on Hanging Wall

DWR=Downdip Width of Rupture

DTR = Depth to Bottom of Rupture

R_{map} = Map Distance

R_{JB} = Boore-Joyner Distance

R_{rup} = Fault Rupture Distance

Arias Intensity computed using Watson-Lamprey and Abrahamson relationship (2006).

TABLE 6-2A

RECOMMENDED FAULT PARALLEL SPECTRAL ORDINATES FOR STANFORD-MONTE VISTA EVENT

Spectral Damping=5%

No.	Period (s)	Frequency (Hz)	Sa (g)	Sv (cm/s)	Sv (in/s)	Sd (cm)	Sd (in)
1	0.01	100.00	1.170	1.827	0.719	0.003	0.001
2	0.02	50.00	1.200	3.748	1.476	0.012	0.005
3	0.03	33.33	1.336	6.261	2.465	0.030	0.012
4	0.05	20.00	1.666	13.015	5.124	0.104	0.041
5	0.075	13.33	2.101	24.618	9.692	0.294	0.116
6	0.10	10.00	2.469	38.573	15.186	0.614	0.242
7	0.15	6.67	2.841	66.573	26.210	1.589	0.626
8	0.20	5.00	2.796	87.346	34.388	2.780	1.095
9	0.30	3.33	2.281	106.871	42.075	5.103	2.009
10	0.40	2.50	1.925	120.283	47.356	7.657	3.015
11	0.50	2.00	1.597	124.713	49.100	9.924	3.907
12	0.75	1.33	1.081	126.689	49.878	15.122	5.954
13	1.00	1.00	0.807	126.041	49.622	20.060	7.898
14	1.50	0.67	0.493	115.489	45.468	27.571	10.855
15	2.00	0.50	0.323	100.876	39.715	32.110	12.642
16	3.00	0.33	0.167	78.399	30.866	37.433	14.737
17	4.00	0.25	0.106	66.168	26.050	42.124	16.584
18	5.00	0.20	0.079	61.857	24.353	49.224	19.380

Zero-Period Acceleration (PGA) = 1.17g

Notes:

Sa = Pseudo-Absolute Spectral Acceleration.

Sv = Pseudo-Relative Spectral Velocity.

Sd = Relative Spectral Displacement.

Significant figures in above table are provided for computation purposes only and do not necessarily reflect accuracies to those significant figures.

TABLE 6-2B

RECOMMENDED FAULT NORMAL SPECTRAL ORDINATES FOR STANFORD-MONTE VISTA EVENT

Spectral Damping=5%

No.	Period (s)	Frequency (Hz)	Sa (g)	Sv (cm/s)	Sv (in/s)	Sd (cm)	Sd (in)
1	0.01	100.00	1.170	1.827	0.719	0.003	0.001
2	0.02	50.00	1.200	3.748	1.476	0.012	0.005
3	0.03	33.33	1.336	6.261	2.465	0.030	0.012
4	0.05	20.00	1.666	13.015	5.124	0.104	0.041
5	0.075	13.33	2.101	24.618	9.692	0.294	0.116
6	0.10	10.00	2.469	38.573	15.186	0.614	0.242
7	0.15	6.67	2.841	66.573	26.210	1.589	0.626
8	0.20	5.00	2.796	87.346	34.388	2.780	1.095
9	0.30	3.33	2.281	106.871	42.075	5.103	2.009
10	0.40	2.50	1.925	120.283	47.356	7.657	3.015
11	0.50	2.00	1.597	124.713	49.100	9.924	3.907
12	0.75	1.33	1.198	140.353	55.257	16.753	6.596
13	1.00	1.00	0.993	155.120	61.071	24.688	9.720
14	1.50	0.67	0.720	168.715	66.423	40.278	15.857
15	2.00	0.50	0.535	167.283	65.860	53.248	20.964
16	3.00	0.33	0.353	165.527	65.168	79.033	31.115
17	4.00	0.25	0.266	166.173	65.423	105.789	41.649
18	5.00	0.20	0.213	166.183	65.426	132.244	52.065

Zero-Period Acceleration (PGA) = 1.17g

Notes:

Sa = Pseudo-Absolute Spectral Acceleration.

Sv = Pseudo-Relative Spectral Velocity.

Sd = Relative Spectral Displacement.

Significant figures in above table are provided for computation purposes only and do not necessarily reflect accuracies to those significant figures.

TABLE 6-3A

RECOMMENDED FAULT PARALLEL SPECTRAL ORDINATES FOR SAN ANDREAS EVENT

Spectral Damping=5%

No.	Period (s)	Frequency (Hz)	Sa (g)	Sv (cm/s)	Sv (in/s)	Sd (cm)	Sd (in)
1	0.01	100.00	0.712	1.112	0.438	0.002	0.001
2	0.02	50.00	0.729	2.278	0.897	0.007	0.003
3	0.03	33.33	0.801	3.754	1.478	0.018	0.007
4	0.05	20.00	0.983	7.681	3.024	0.061	0.024
5	0.075	13.33	1.255	14.700	5.788	0.175	0.069
6	0.10	10.00	1.468	22.923	9.025	0.365	0.144
7	0.15	6.67	1.702	39.869	15.697	0.952	0.375
8	0.20	5.00	1.676	52.344	20.608	1.666	0.656
9	0.30	3.33	1.425	66.777	26.290	3.188	1.255
10	0.40	2.50	1.218	76.090	29.957	4.844	1.907
11	0.50	2.00	1.043	81.452	32.068	6.482	2.552
12	0.75	1.33	0.774	90.676	35.699	10.824	4.261
13	1.00	1.00	0.620	96.799	38.110	15.406	6.065
14	1.50	0.67	0.446	104.594	41.179	24.970	9.831
15	2.00	0.50	0.335	104.688	41.216	33.323	13.119
16	3.00	0.33	0.227	106.281	41.843	50.745	19.979
17	4.00	0.25	0.165	103.094	40.588	65.632	25.839
18	5.00	0.20	0.133	103.797	40.865	82.599	32.519

Zero-Period Acceleration (PGA) = 0.71g

Notes:

Sa = Pseudo-Absolute Spectral Acceleration.

Sv = Pseudo-Relative Spectral Velocity.

Sd = Relative Spectral Displacement.

Significant figures in above table are provided for computation purposes only and do not necessarily reflect accuracies to those significant figures.

TABLE 6-3B

RECOMMENDED FAULT NORMAL SPECTRAL ORDINATES FOR SAN ANDREAS EVENT

Spectral Damping=5%

No.	Period (s)	Frequency (Hz)	Sa (g)	Sv (cm/s)	Sv (in/s)	Sd (cm)	Sd (in)
1	0.01	100.00	0.712	1.112	0.438	0.002	0.001
2	0.02	50.00	0.729	2.278	0.897	0.007	0.003
3	0.03	33.33	0.801	3.754	1.478	0.018	0.007
4	0.05	20.00	0.983	7.681	3.024	0.061	0.024
5	0.075	13.33	1.255	14.700	5.788	0.175	0.069
6	0.10	10.00	1.468	22.923	9.025	0.365	0.144
7	0.15	6.67	1.702	39.869	15.697	0.952	0.375
8	0.20	5.00	1.676	52.344	20.608	1.666	0.656
9	0.30	3.33	1.425	66.777	26.290	3.188	1.255
10	0.40	2.50	1.218	76.090	29.957	4.844	1.907
11	0.50	2.00	1.043	81.452	32.068	6.482	2.552
12	0.75	1.33	0.847	99.280	39.087	11.851	4.666
13	1.00	1.00	0.748	116.875	46.014	18.601	7.323
14	1.50	0.67	0.651	152.486	60.034	36.403	14.332
15	2.00	0.50	0.564	176.073	69.320	56.046	22.065
16	3.00	0.33	0.488	228.630	90.012	109.163	42.977
17	4.00	0.25	0.424	265.154	104.391	168.802	66.458
18	5.00	0.20	0.373	291.277	114.676	231.791	91.256

Zero-Period Acceleration (PGA) = 0.71g

Notes:

Sa = Pseudo-Absolute Spectral Acceleration.

Sv = Pseudo-Relative Spectral Velocity.

Sd = Relative Spectral Displacement.

Significant figures in above table are provided for computation purposes only and do not necessarily reflect accuracies to those significant figures.

TABLE 6-4A
CHARACTERISTICS OF SELECTED EARTHQUAKE RECORDS
FOR STANFORD-MONTE VISTA EVENT

No.	Earthquake Event	Recording Station	Style of Faulting [1]	Magnitude (Mw)	Closest Distance (km)	NEHRP Site Class/Vs_{30}	Highest Usable Period (sec)	Event Date
1	Kobe	Nishi-Akashi	SS	6.9	7.1	C/609	8	1/16/1995
2	Loma Prieta	LGPC	RV/OBL	6.9	3.9	C/478	8	10/18/1989
3	Northridge	Sylmar-Olive View Med. FF	RV	6.7	5.3	C/440	8.3	1/17/1994

TABLE 6-4B
CHARACTERISTICS OF SELECTED EARTHQUAKE RECORDS
FOR SAN ANDREAS EVENT

No.	Earthquake Event	Recording Station	Style of Faulting [1]	Magnitude (Mw)	Closest Distance (km)	NEHRP Site Class/Vs_{30}	Highest Usable Period (sec)	Event Date
1	Manjil	Abbar	SS	7.4	12.6	C/724	7.7	11/03/1990
2	Chi-Chi	TCU065	RV/OBL	7.6	0.7	D/305	13.3	9/20/1999
3	Landers	Lucerne	SS	7.3	2.2	C/684	10.0	6/28/1992

[1] SS = Strike-Slip
OBL = Oblique
RV = Reverse or Thrust

FIGURES

Note: Base map printed from USGS 1:24,000 scale topographic maps by TOPO! ® © 2003 National Geographic.

TERRA / GeoPentech
a Joint Venture

REGIONAL SITE LOCATION MAP
STEVENS CREEK DAM
SEISMIC STABILITY EVALUATIONS (SSE2)

Figure
2-1

N

TRENCH LOCATED 50 FEET NORTH OF LOCATION SHOWN

WA T-2

OUTLET STRUCTURE

WA T-4

ORIGINAL TOE

WA T-1

B-9

B-8

S&W B-3

B-7

BUTTRESS TOE

WA T-3

B-6

S&W B-1

B-3, B-4, & B-5

WCC-2

WCC-5

NEW CREST

11+00

10+00

9+00

8+00

7+00

6+00

5+00

4+00

3+00

2+00

WA SC-3

B-1 & B-2

S&W B-2

WCC-1

WA SC-12

WCC-4

WA SC-5

WA SC-4

WA SC-2

ORIGINAL CREST

WA SC-7

WA SC-6

WCC-3

WCC-6

WA SC-8

WA SC-10

WA SC-9

WA SC-11

WA SC-1

ORIGINAL TOE

CENTERLINE OUTLET CONDUIT

INLET STRUCTURE

BUTTRESS TOE

LEGEND

- Existing Boring into Santa Clara Formation
- Existing Boring Terminated above Santa Clara Formation
- Existing Boring Terminated in Embankment
- Existing Piezometer

Note:
Wahler borings at inlet structure not shown

APPROXIMATE SCALE (ft)

50 0 50 100 200

NORTHING, FEET

1,935,500
1,935,400
1,935,300
1,935,200
1,935,100
1,935,000
1,934,900
1,934,800
1,934,700

EASTING, FEET

6,102,400 6,102,500 6,102,600 6,102,700 6,102,800 6,102,900 6,103,000 6,103,100 6,103,200 6,103,300 6,103,400 6,103,500 6,103,600 6,103,700

TERRA / GeoPentech
a Joint Venture

PLAN OF PREVIOUS INVESTIGATIONS
STEVENS CREEK DAM
SEISMIC STABILITY EVALUATIONS (SSE2)

Figure 2-2

Rev. 4 06/08/2011 SSE2-R-2SC

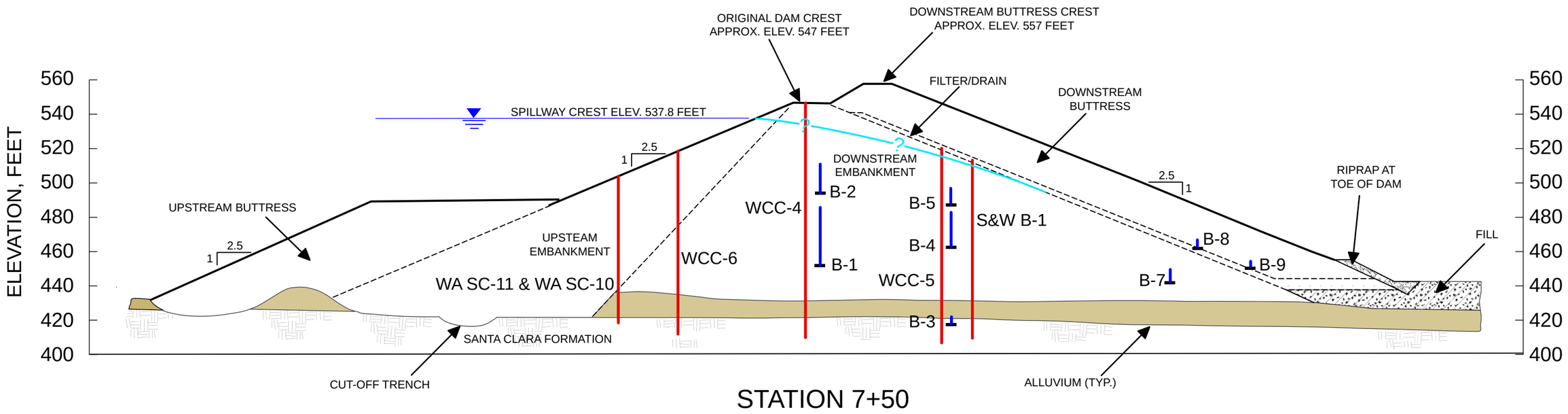

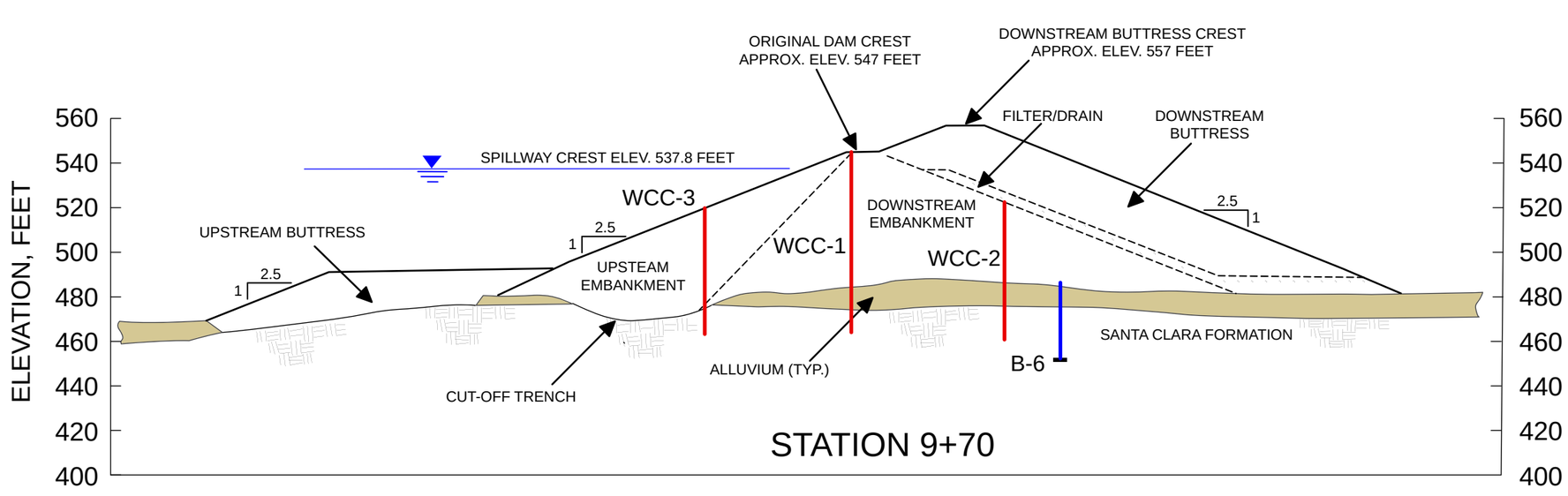

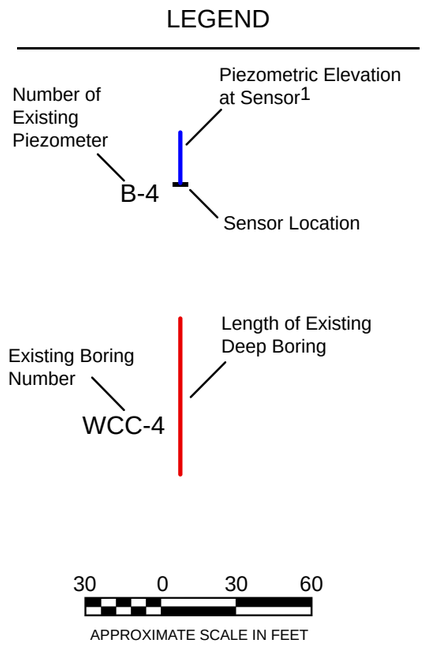

Notes:

1. Piezometric Elevations from Figure 3 of 2010 Surveillance Report.
2. Elevations of top and bottom of alluvium at Station 7+50 updated based on new borings.
3. Top flow line (phreatic surface) estimated and approximates that used by Wahler Associates (1984).

TERRA / GeoPentech a Joint Venture	CROSS-SECTIONS WITH PREVIOUS INVESTIGATIONS - STEVENS CREEK DAM SEISMIC STABILITY EVALUATIONS (SSE2)	Figure 2-3

Rev. 3 06/08/2011 SSE2-R-2SC

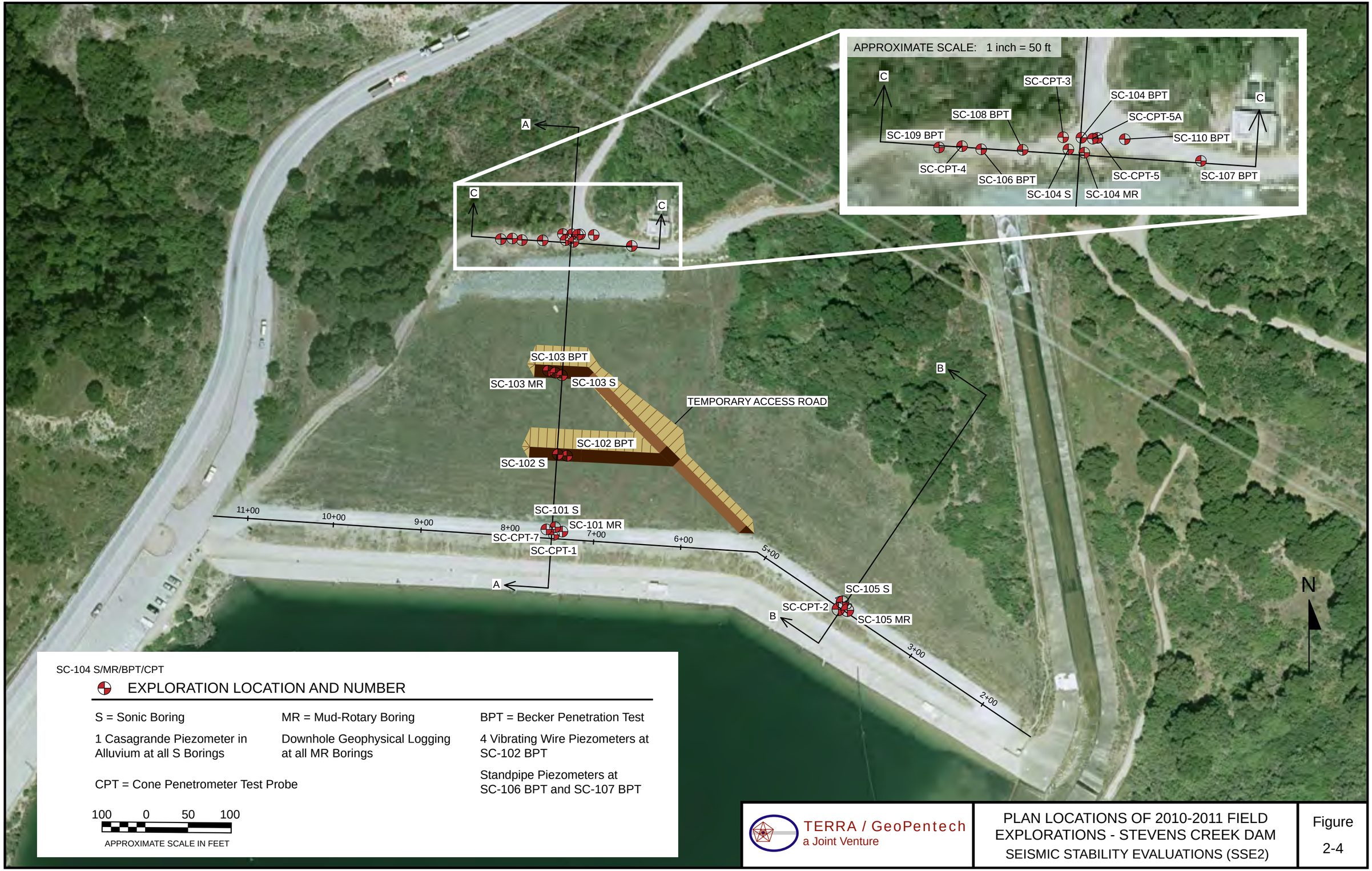

Rev. 2 11/28/2011 SSE2-R-2SC

TERRA / GeoPentech
a Joint Venture

PLAN LOCATIONS OF 2010-2011 FIELD EXPLORATIONS - STEVENS CREEK DAM
SEISMIC STABILITY EVALUATIONS (SSE2)

Figure 2-4

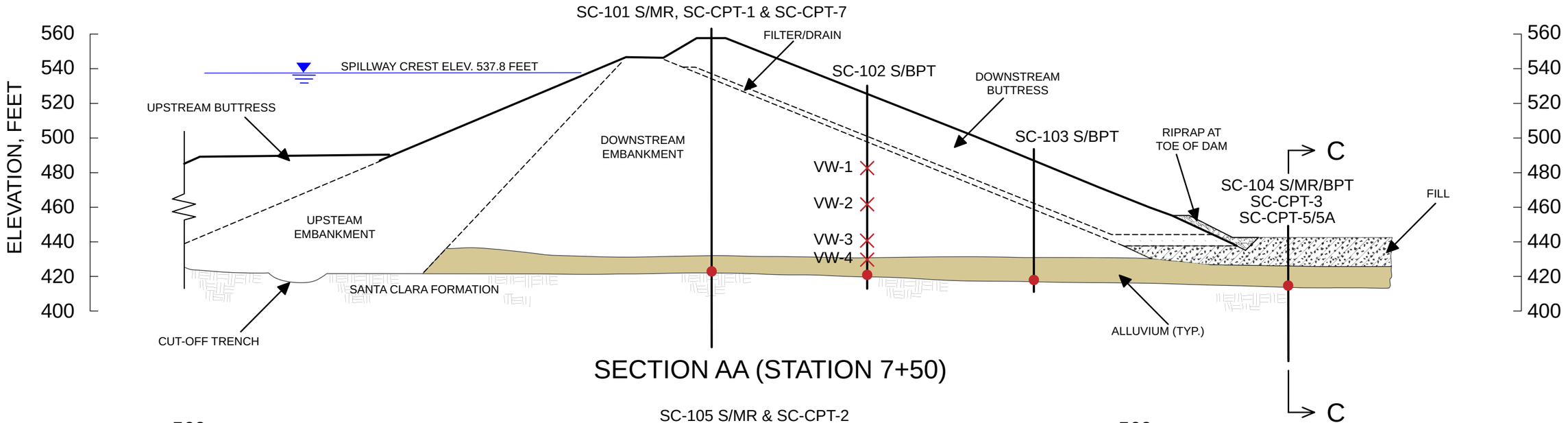

SECTION AA (STATION 7+50)

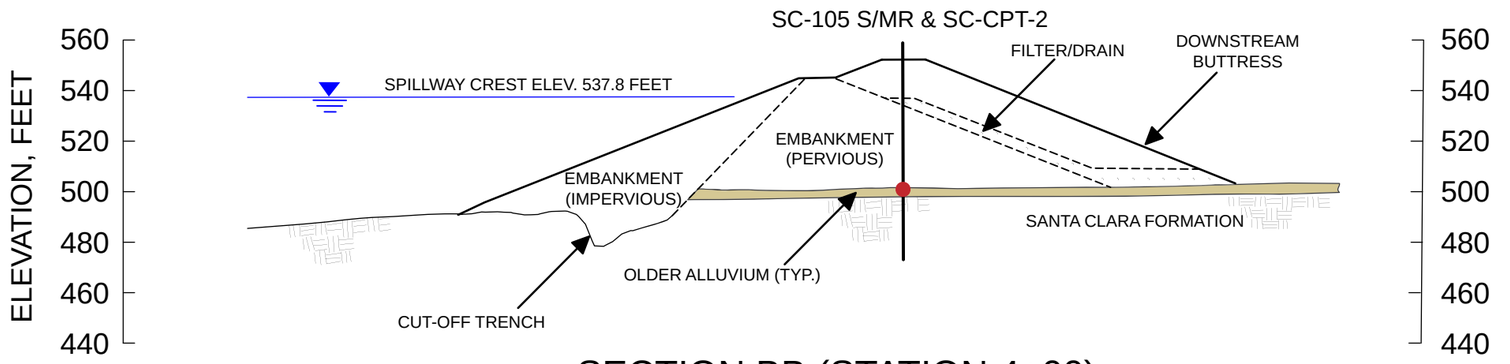

SECTION BB (STATION 4+00)

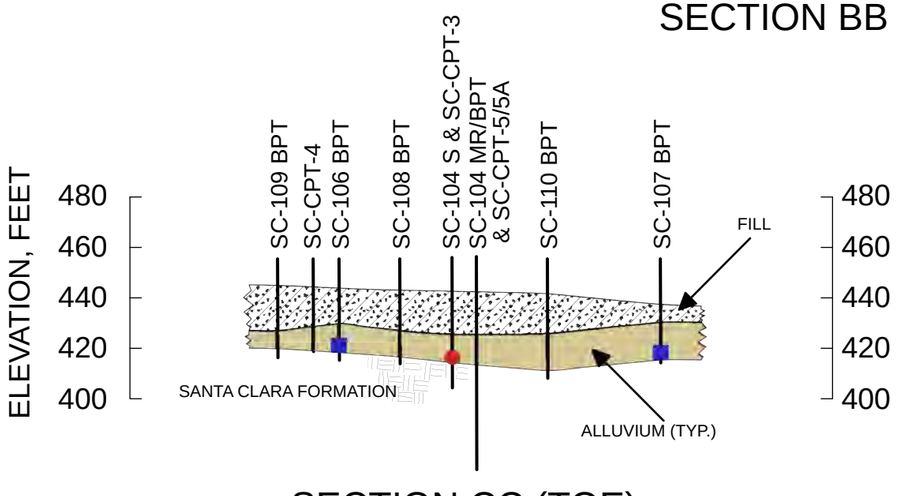

SECTION CC (TOE)

LEGEND

SC-102 S/BPT

Maximum Depth of New Boring

New Casagrande Piezometer

New Vibrating Wire Piezometer

SC-106 BPT

Maximum Depth of New Boring

New Standpipe Piezometer

30 0 30 60

APPROXIMATE SCALE IN FEET

Notes:

1. Elevations of top and bottom of alluvium updated based on new borings.

Rev. 2 01/24/2012 SSE2-R-2SC

TERRA / GeoPentech
a Joint Venture

SECTIONS SHOWING LOCATIONS OF 2010-2011 FIELD EXPLORATIONS - STEVENS CREEK DAM
SEISMIC STABILITY EVALUATIONS (SSE2)

Figure 2-5

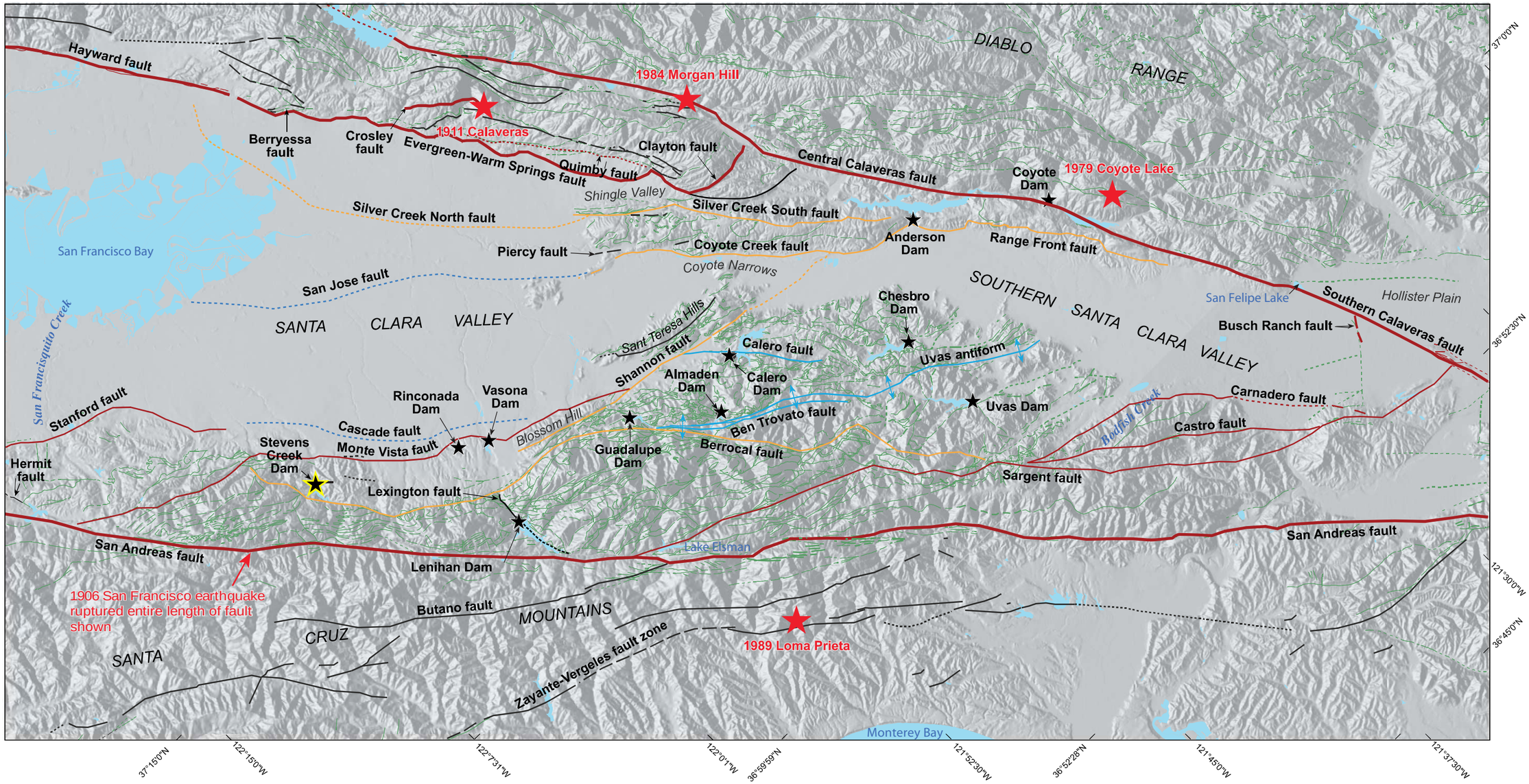

Explanation

- Active fault; dotted where concealed.
- Conditionally Active fault; dotted where concealed
- Other faults; dotted where concealed
- Jennings (1992) detailed faults
- Inactive Faults; dashed where inferred, dotted where concealed
- SCVWD Dams
- Historically significant earthquake

N

0 4 8 Miles

0 4 8 Kilometers

MAP EXCERPTED FROM AMEC (2009)

TERRA / GeoPentech
a Joint Venture

REGIONAL FAULT MAP
STEVENS CREEK DAM
SEISMIC STABILITY EVALUATIONS (SSE2)

Figure 3-1

Rev. 1 04/18/2012 SSE2-R-2SC

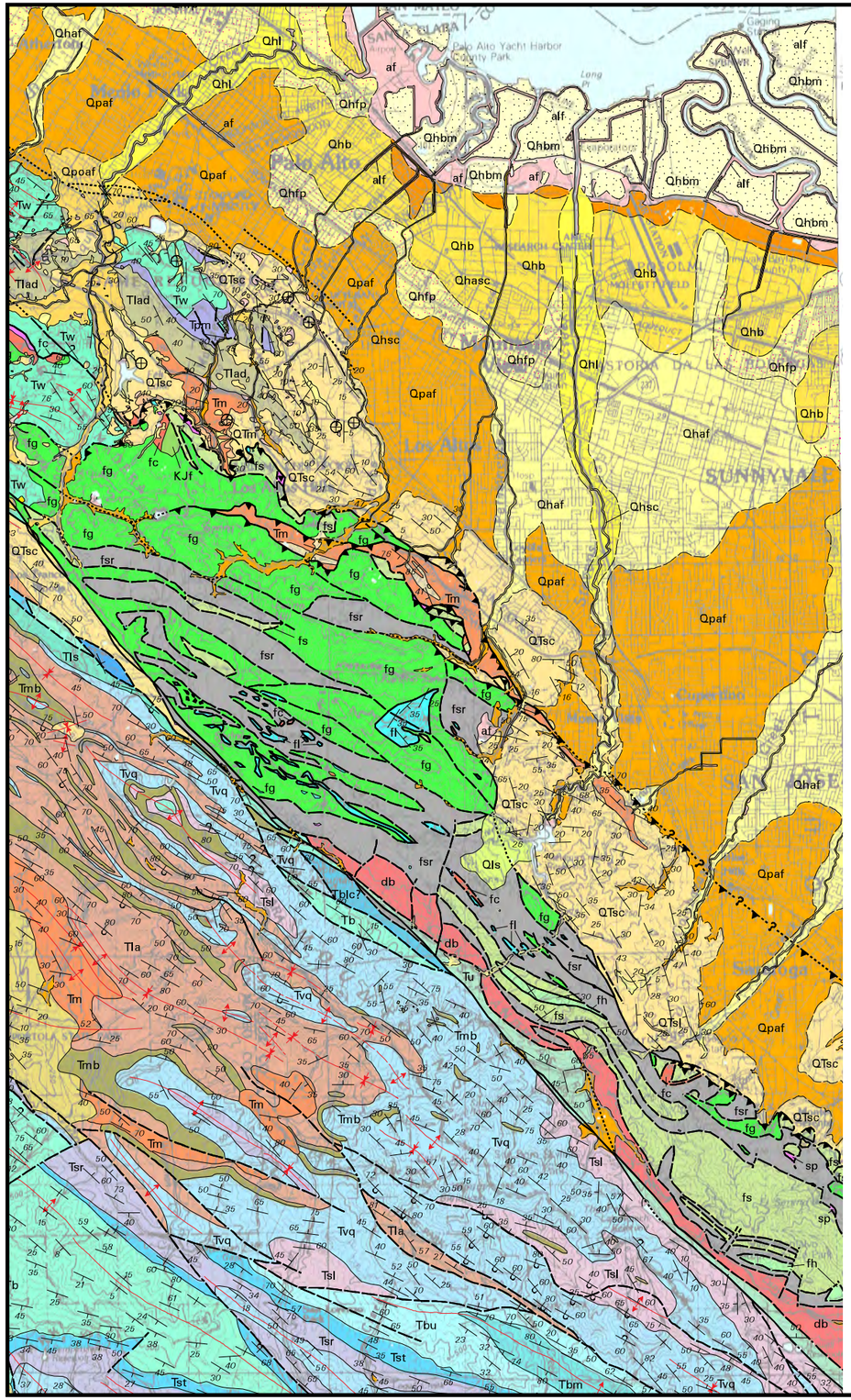

EXPLANATION

MAP UNITS

Tb	Butano Sandstone (middle and lower Eocene)
Tbu	Upper sandstone member
Tbm	Middle sandstone member
Tbl	Lower conglomerate and sandstone member
Tblc	Conglomerate
KJf	Franciscan Complex, undivided (Cretaceous and Jurrasic)
fs	Sandstone
fg	Greenstone
fc	Chert
fl	Limestone
fm	Metamorphic rocks
fh	Argillite
fsr	Sheared rock (melange)
Tmb	Mindego Basalt and related volcanic rocks (Miocene and/or Oligocene)
Tvq	Vaqueros Sandstone (lower Miocene and Oligocene)
Tsl	San Lorenzo Formation (Oligocene and upper and middle Eocene)
Tsr	RIces Mudstone Member (Oligocene and upper Eocene)
Tu	Unnamed sedimentary rocks (Eocene?)
Tw	Whiskey Hill Formation (middle and lower Eocene)
db	Diabase and gabbro (Jurrasic?)
af	Artificial fill (Historic)
Qhbm	Bay mud (Holocene)
Qhb	Basin deposits (Holocene)
Qhl	Natural levee deposits (Holocene)
Qhaf	Alluvial fan and fluvial deposits (Holocene)
Qpaf	Alluvial fan and fluvial deposits (Pleistocene)
QTsc	Santa Clara Formation (lower Pleistocene and upper Pliocene)
Tlad	Ladera Sandstone (upper(?) and middle Miocene)
Tm	Monterey Formation (middle Miocene)
Tpm	Page Mill Basalt (middle Miocene)
Tla	Lambert Shale (lower Miocene and Oligocene)

MAP SYMBOLS

Contact--Depositional or intrusive contact, dashed where approximately located, dotted where concealed

Fault--Dashed where approximately located, small dashes where inferred, dotted where concealed, queried where location is uncertain.

Reverse or thrust fault--Dashed where approximately located, dotted where concealed

Anticline--Shows fold axis, dotted where concealed

Syncline

Strike and dip of bedding

Overturned bedding

Horizontal bedding

Vertical bedding

Strike and dip of foliation

Vertical foliation

16.5°
TRUE NORTH
MAGNETIC NORTH
APPROXIMATE MEAN DECLINATION, 1983

SCALE 1:100000

1 .5 0 1 2 3 4 5 6 7 MILE

1 .5 0 1 2 3 4 5 6 7 KILOMETER

0 1 2 3 4 5 6 7 8 9 10 11 12 13 14 15 THOUSAND FEET

CONTOUR INTERVAL 50 METERS

CALIFORNIA
MAP LOCATION

FROM:
E.E. BRABB, R.W. GRAMER, AND D.L. JONES - 2000

TERRA / GeoPentech
a Joint Venture

LOCAL REGION GEOLOGIC MAP
STEVENS CREEK DAM
SEISMIC STABILITY EVALUATIONS (SSE2)

Figure 3-2

Rev. 1 06/09/2011 SSE2-R-2SC

N

1,935,800
1,935,700
1,935,600
1,935,500
1,935,400
1,935,300
1,935,200
1,935,100
1,935,000
1,934,900
1,934,800
1,934,700
1,934,600

6,102,00 6,102,100 6,102,200 6,102,300 6,102,400 6,102,500 6,102,600 6,102,700 6,102,800 6,102,900 6,103,000 6,103,100 6,103,200 6,103,300 6,103,400 6,103,500 6,103,600 6,103,700 6,103,800

Fill
QTsc
Qoa?
Qya
Qoa
Qc and/or Fill (over Qoa or QTsc)
Fill (over Qya)
OUTLET STRUCTURE
OUTLET AND STRUCTURE FOUNDED ON YOUNG ALLUVIUM
Old slide as per Vantine (1972) now heavily overgrown
Qc (over QTsc or Qoa)
Toe Drain
Qc (over QTsc)
Old slide (evident on 1955 airphoto)
Qc/QTsc/Qoa?
Qc (over Qoa)
Qc/QTsc?
QTsc?
Qc (over Qoa)?
Qc (overQTsc)
base Qoa as per Vantine (1972)
CENTERLINE OUTLET CONDUIT
INLET STRUCTURE
Qc/QTsc?

EXPLANATION

CONTOUR INTERVAL: (5')

- LOCATION OF MAPPED OUTCROP
- STRIKE & DIP OF BEDDING
- CONTACT, DASHED WHERE APPROXIMATE, DOTTED WHERE CONCEALED, QUERIED WHERE UNCERTAIN
- LANDSLIDE
- DAM OUTLINE

FILL	Over Qya
Fill or Qc -	Over Qoa
Fill or Qc -	Over Qtsc
Qya	YOUNG ALLUVIUM
Qoa	OLDER ALLUVIUM
QTsc	SANTA CLARA FORMATION

NOTES:

1: LOCATION OF INLET/OUTLET STRUCTURE PROVIDED BY SCVWD

2: LIMITS OF UPSTREAM PORTION OF EMBANKMENT AS PER 1937 AS-BUILT PLAN, 1985 WAHLER MODIFICATIONS EMBANKMENT PLAN (NO 1986 AS-BUILT PLAN AVAILABLE), AND 1986 WAHLER AS-BUILT SECTIONS FOR UPSTREAM BUTTRESS

3: GEOLOGY OF UNITS UNDERLYING EMBANKMENT ESTIMATED FROM 1937 AS-BUILT DRAWINGS, PREVIOUS EXPLORATION (1975-1984), WAHLER 1986 AS-BUILT SECTIONS OF UPSTREAM BUTRESS, AND DSOD CONSTRUCTION INSPECTION RECORDS FROM 1935-36 AND 1985-86.

4: DAMSITE GEOLOGIC MAPPING BY TGP PERFORMED IN JULY 2010

5: MAP INCORPORATES GEOLOGIC MAPPING BY VANTINE 1972, WHERE NOTED, FOR DISTRICT LANDSLIDE STUDY (SCVWD, 1976)

Rev. 2 04/20/2011 SSE2-R-2SC

TERRA / GeoPentech
a Joint Venture

GEOLOGIC MAP
STEVENS CREEK DAM
SEISMIC STABILITY EVALUATIONS (SSE2)

Figure
4-1

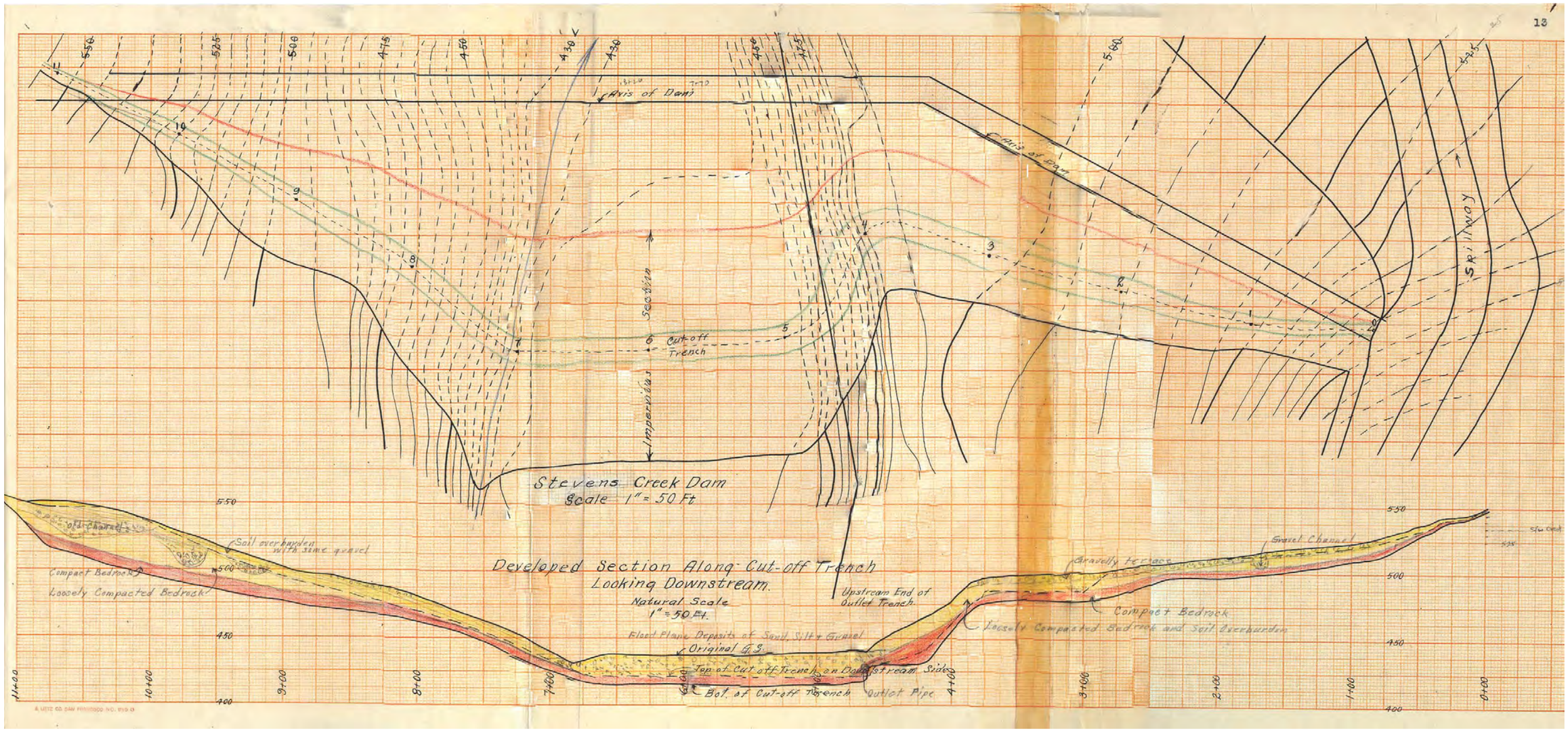

MAP PREPARED BY MARLIAVE (1936)

TERRA / GeoPentech a Joint Venture	AS-BUILT GEOLOGIC SECTION ALONG CUTOFF TRENCH - STEVENS CREEK DAM SEISMIC STABILITY EVALUATIONS (SSE2)	Figure 4-2

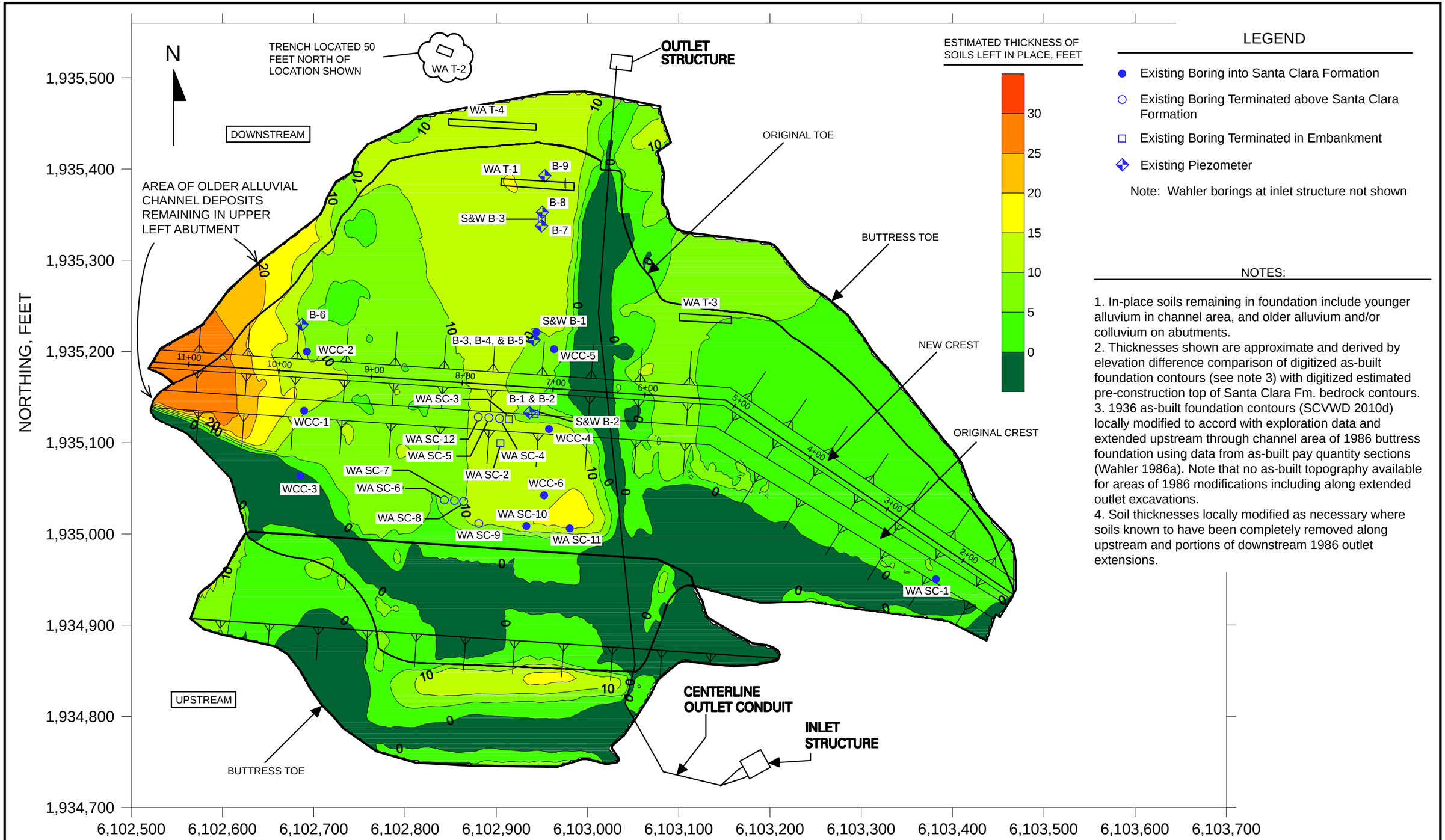

LEGEND

- Existing Boring into Santa Clara Formation
- Existing Boring Terminated above Santa Clara Formation
- Existing Boring Terminated in Embankment
- Existing Piezometer

Note: Wahler borings at inlet structure not shown

NOTES:

1. In-place soils remaining in foundation include younger alluvium in channel area, and older alluvium and/or colluvium on abutments.
2. Thicknesses shown are approximate and derived by elevation difference comparison of digitized as-built foundation contours (see note 3) with digitized estimated pre-construction top of Santa Clara Fm. bedrock contours.
3. 1936 as-built foundation contours (SCVWD 2010d) locally modified to accord with exploration data and extended upstream through channel area of 1986 buttress foundation using data from as-built pay quantity sections (Wahler 1986a). Note that no as-built topography available for areas of 1986 modifications including along extended outlet excavations.
4. Soil thicknesses locally modified as necessary where soils known to have been completely removed along upstream and portions of downstream 1986 outlet extensions.

TERRA / GeoPentech
a Joint Venture

ESTIMATED THICKNESS OF SOILS LEFT IN PLACE - STEVENS CREEK DAM
SEISMIC STABILITY EVALUATIONS (SSE2)

Figure 4-3

Rev. 4 04/14/2011 SSE2-R-2SC

Photo 1 - Silty sand layer in younger alluvium

SC-101 MR ~126-127.2 ft (left/upper 0.7 ft of sampler)

Photo 2 - Basal younger alluvium
(silty-clayey sand with gravel)

SC-104 MR (contact with underlying Santa Clara Formation siltstone at 28.4 ft)

TERRA / GeoPentech a Joint Venture	PHOTOS OF YOUNGER ALLUVIUM (1 of 3) STEVENS CREEK DAM SEISMIC STABILITY EVALUATIONS (SSE2)	Figure 4-4A

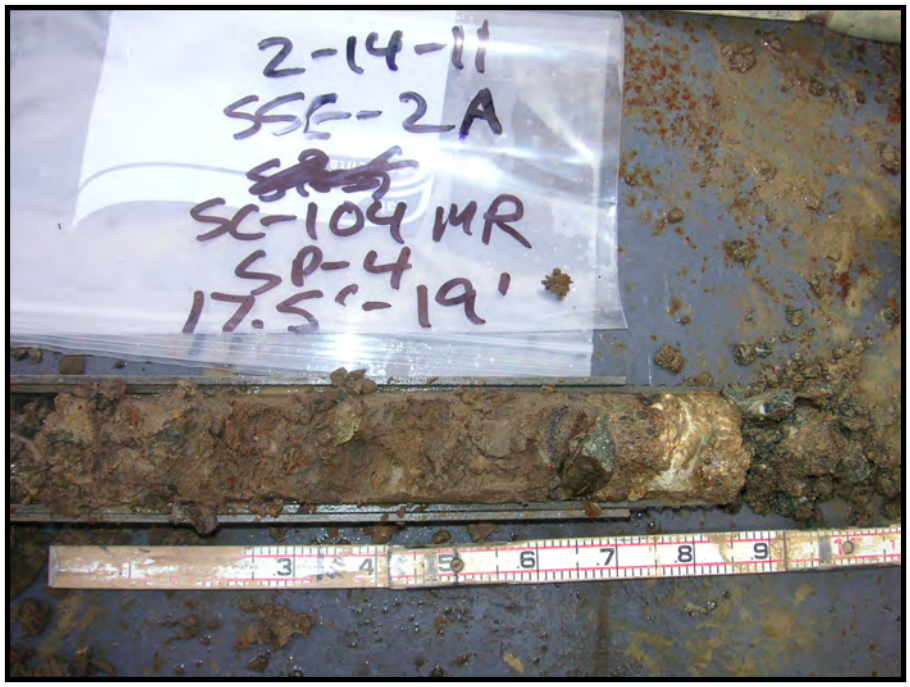

Photo 3 - Layer of clayey sand with gravel in uppermost younger alluvium

SC-104 MR ~17-18.2 ft (left/upper 0.7 ft of sampler)

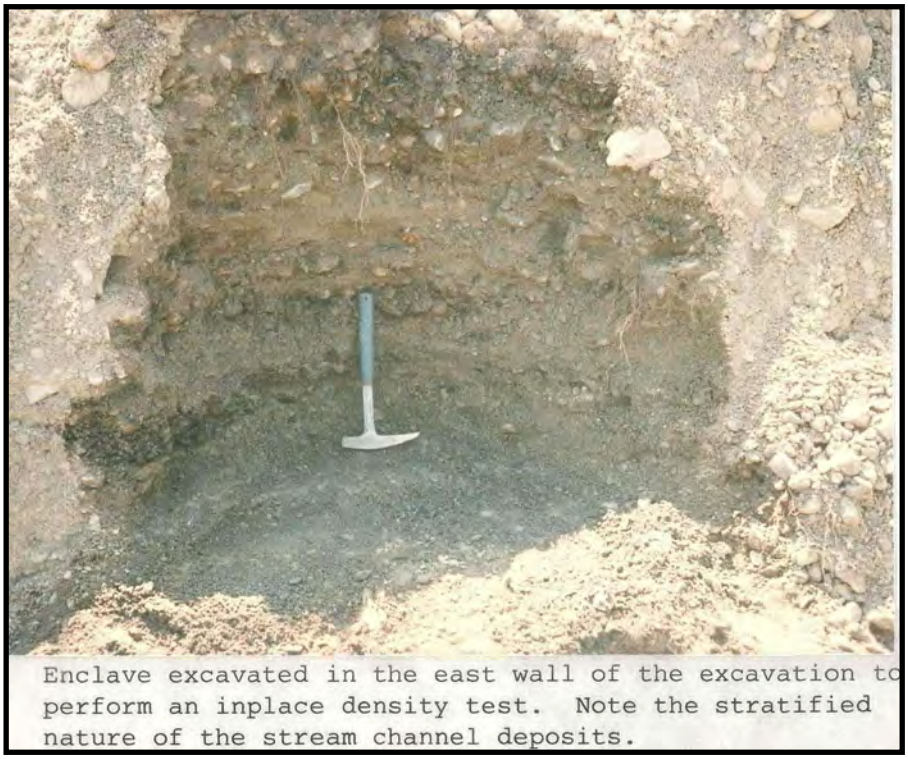

Photo 4 - Younger alluvium exposed in excavation for outlet modifications (DSOD / L.Y. Dudley, June 1985)

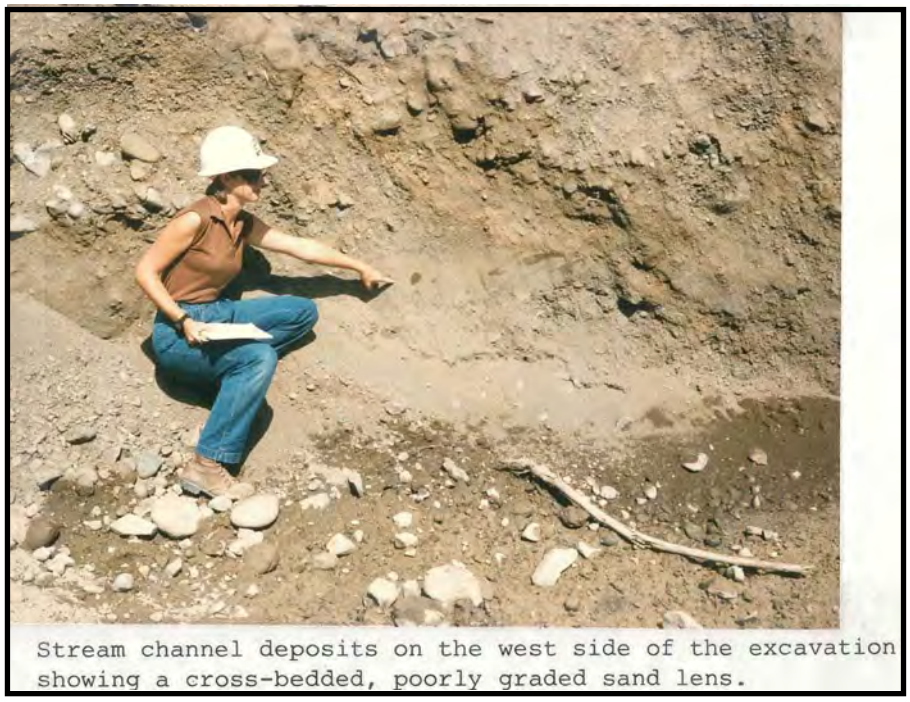

Stream channel deposits on the west side of the excavation showing a cross-bedded, poorly graded sand lens.

Photo 5 - Younger alluvium exposed in excavation for outlet modifications (DSOD / L.Y. Dudley, June 1985)

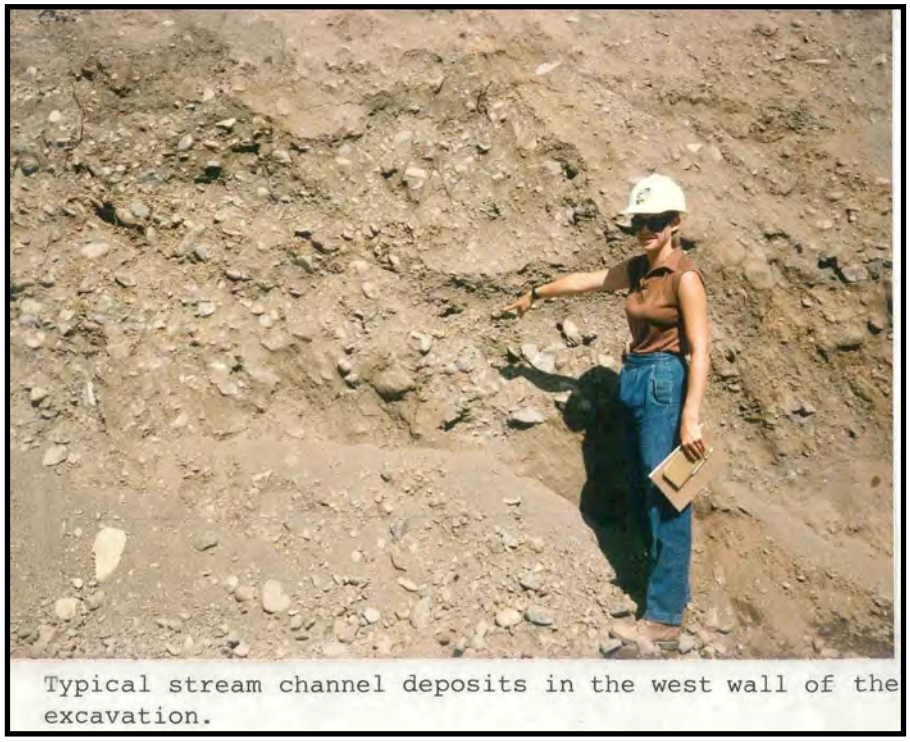

Typical stream channel deposits in the west wall of the excavation.

Photo 6 - Younger alluvium exposed in excavation for outlet modifications (DSOD / L.Y. Dudley, June 1985)

Photo 7 - Gravelly sand terrace alluvium exposed along left bank of reservoir near high water line (immediately north of boat ramp)

Photo 8 - Santa Clara Formation conglomerate (clayey sand with gravel) exposed along Stevens Canyon Road cut on left side of reservoir (300 ft upstream from left end of dam)

F.3/77

W.A. WAHLER & ASSOCIATES
PALO ALTO • NEWPORT BEACH • CALIF.

STEVENS CREEK DAM

FIELD TRENCH LOG

PROJECT NO. SCV-192B

DATE DECEMBER 1978

TRENCH NO. 4

Sheet 1 of 1

LOCATION: Downstream of dam near toe, 295,029N; 1,541,595E at SE end of trench.

NOTES: Excavated to 10' with dozer, excavated to final depth with backhoe

UNITS NO.	DESCRIPTION
	FILL
①	GRAVELLY CLAYEY SAND (SC); brown to reddish brown, low plasticity, very stiff, moist.
	ALLUVIUM
②	INTERBEDDED SILTY GRAVEL AND SILTY SAND (GM, SM); greenish gray, subrounded gravel to cobble sandstone fragments, average diameter 1–2", maximum 12", and medium to coarse grained sand, locally clayey. Coarser near upper surface.
③	SAND (SP-SM); interbeds of brown and greenish gray fine sand with some clayey sand (SC), loose to medium dense, moist.
④	SANDY GRAVEL (GP-GM); grayish brown to reddish brown, rounded gravel and cobble to 14–18" diameter, loose to medium dense, moist. Wood and other debris common. Water encountered at elevation 420'.

NO.	
[1]	FIELD DENSITY TEST
[2]	FIELD DENSITY TEST
[3]	FIELD DENSITY TEST
B-1	SAMPLE LOCATION
B-2	SAMPLE LOCATION
B-3	SAMPLE LOCATION
B-4	SAMPLE LOCATION

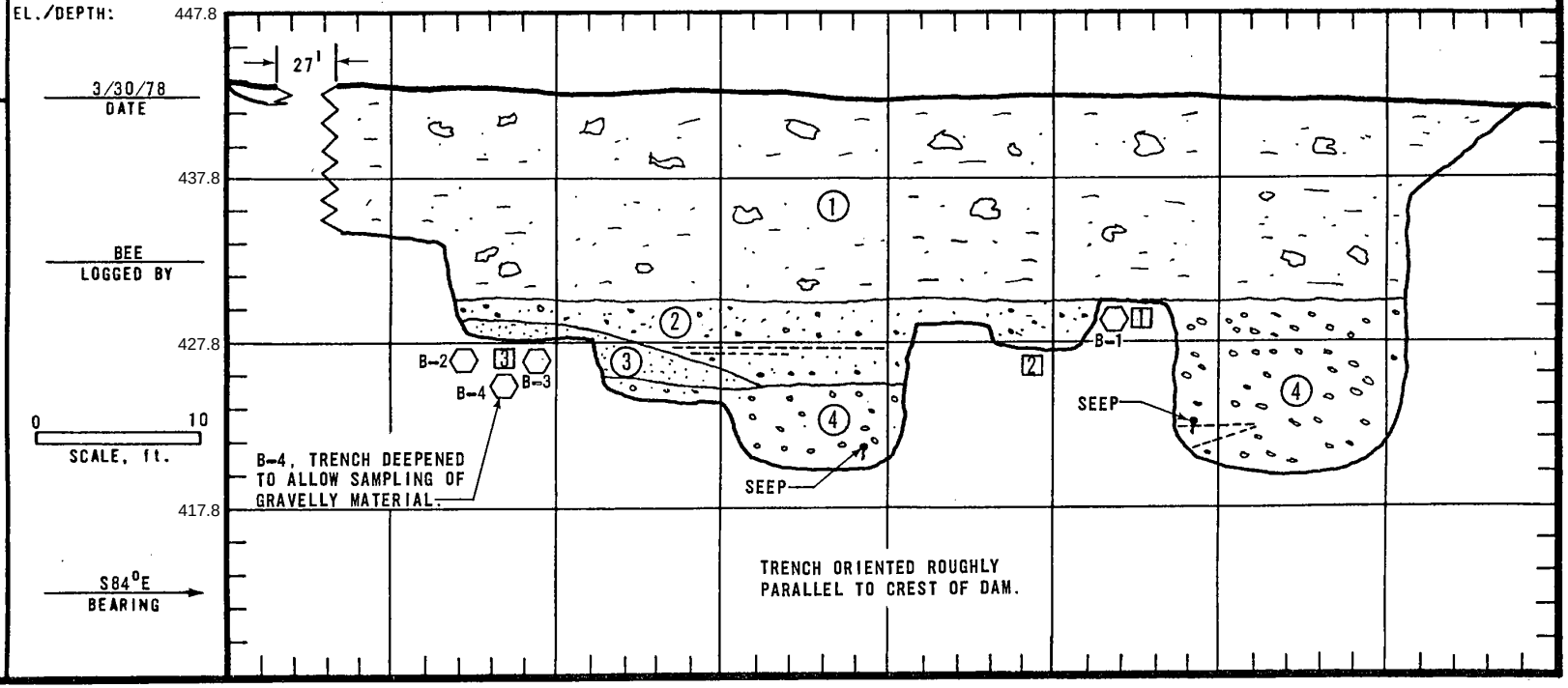

NOTE: 2.8 FEET WAS ADDED TO THE ELEVATIONS SHOWN ON LOG TO CONVERT FROM NGVD1929 TO NAVD88

TERRA / GeoPentech
a Joint Venture

LOG OF TEST TRENCH T-4
STEVENS CREEK DAM
SEISMIC STABILITY EVALUATIONS (SSE2)

Figure 4-5

Rev. 0 04/20/2011 SSE2-R-2SC

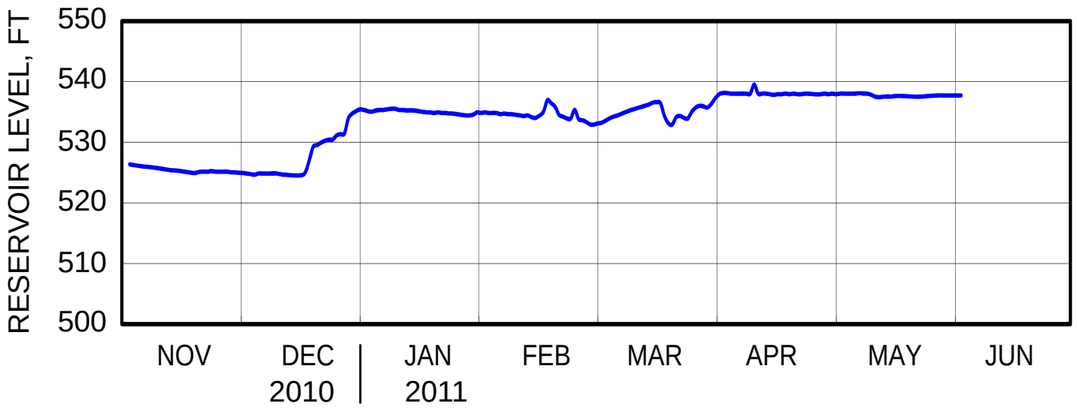

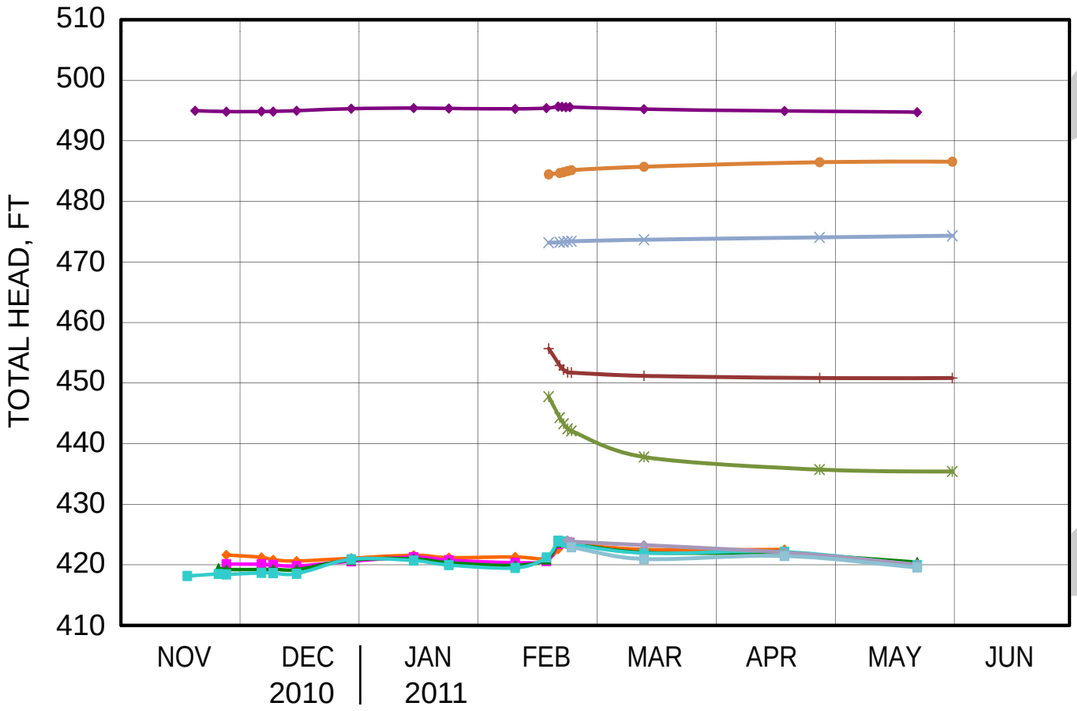

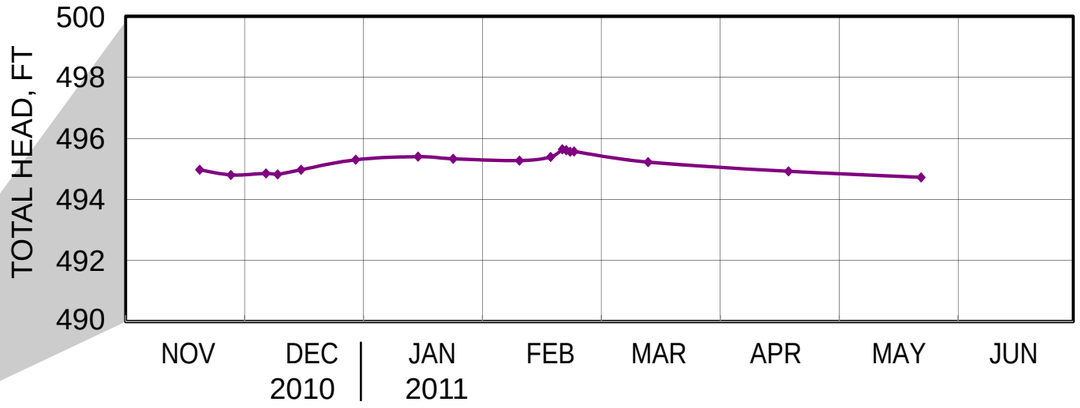

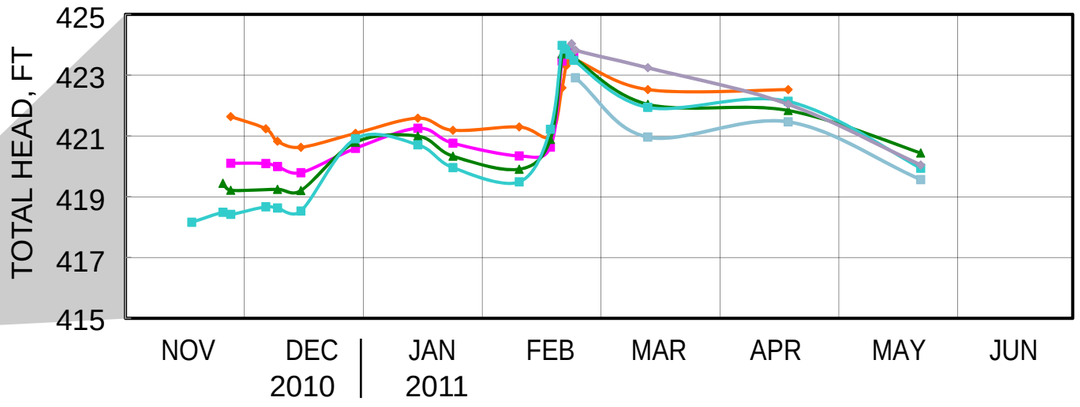

LEGEND

Reservoir Level	SC-104S	VW-1
SC-101S	SC-105S	VW-2
SC-102S	SC-106BPT	VW-3
SC-103S	SC-107BPT	VW-4

Rev. 2 04/13/2012 SSE2-R-2SC

TERRA / GeoPentech
a Joint Venture

NEW PIEZOMETERS - TOTAL HEAD VS. TIME
STEVENS CREEK DAM
SEISMIC STABILITY EVALUATIONS (SSE2)

Figure
4-6

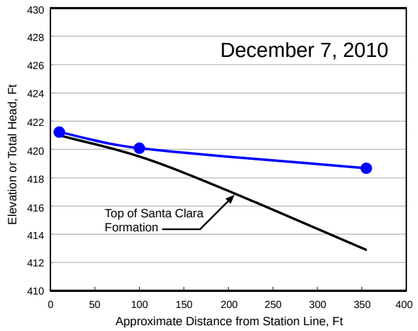

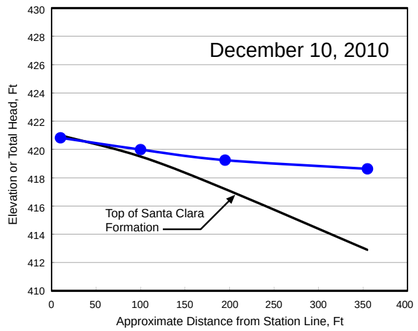

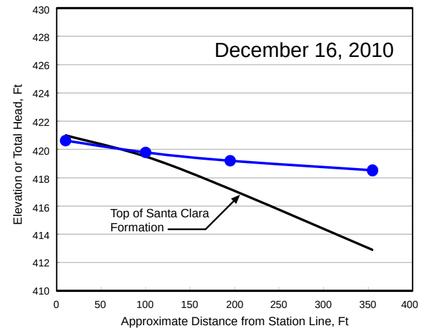

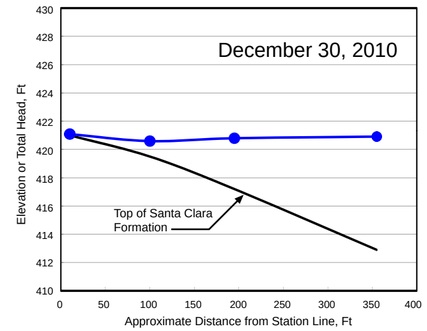

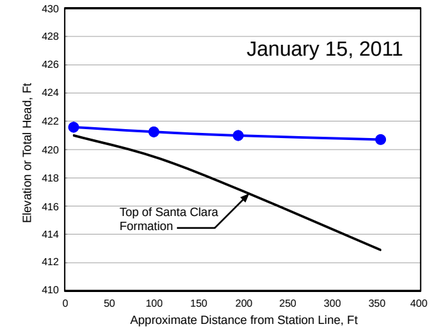

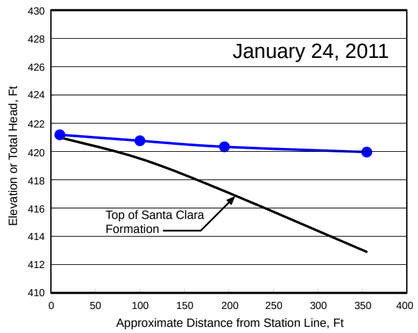

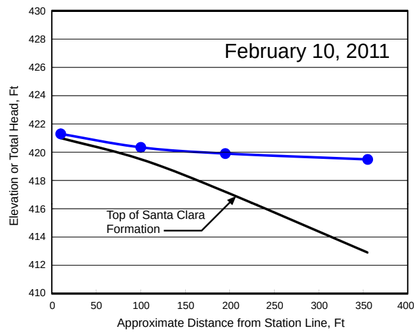

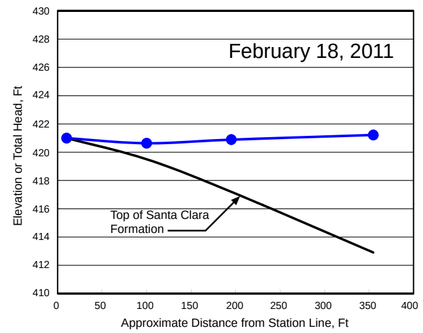

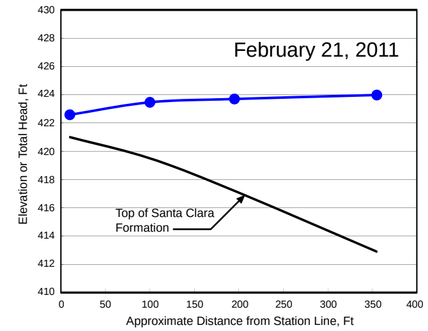

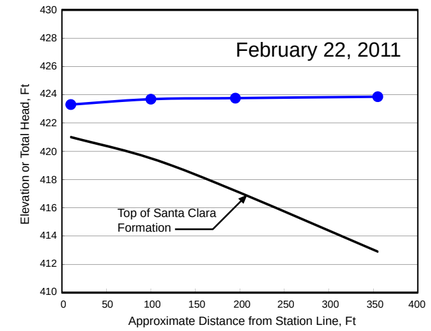

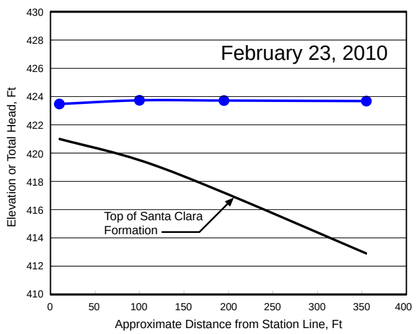

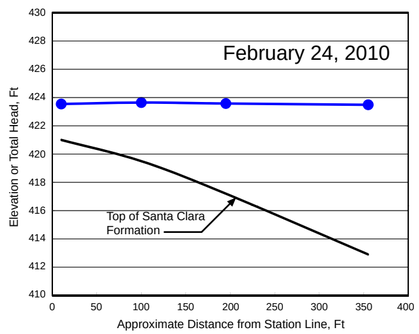

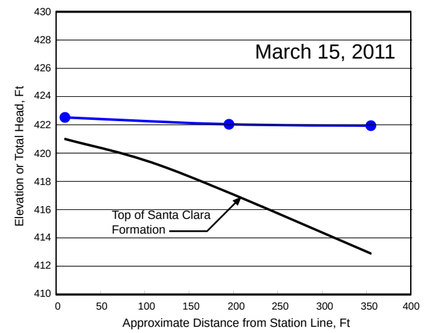

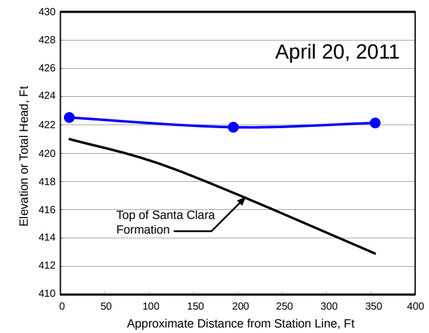

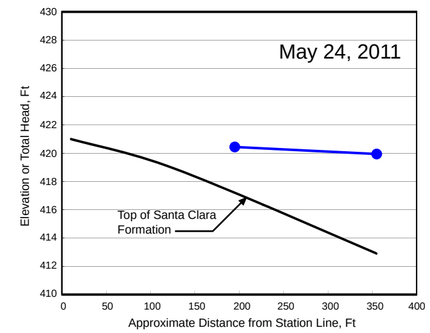

Rev. 1 06/03/2011 SSE2-R-2SC

TERRA / GeoPentech
a Joint Venture

CASAGRANDE PIEZOMETERS - TOTAL HEAD VS. DISTANCE - STEVENS CREEK DAM
SEISMIC STABILITY EVALUATIONS (SSE2)

Figure
4-7

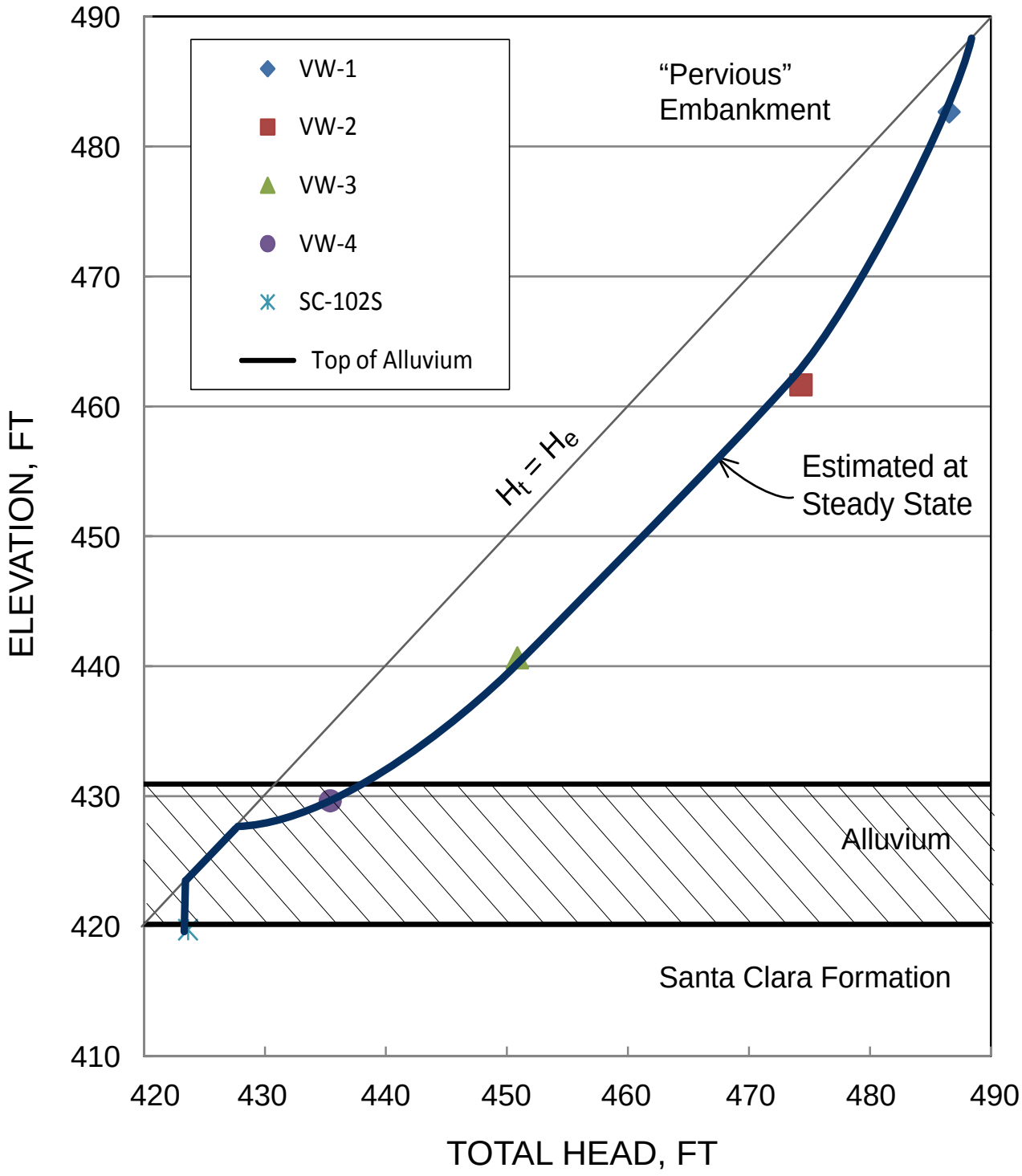

Notes:

1. Piezometer readings recorded on June 2, 2011
2. H_t = Total Head and H_e = Elevation Head

TERRA / GeoPentech a Joint Venture	VIBRATING WIRE PIEZOMETERS - TOTAL HEAD VS. ELEVATION - STEVENS CREEK DAM SEISMIC STABILITY EVALUATIONS (SSE2)	Figure 4-8

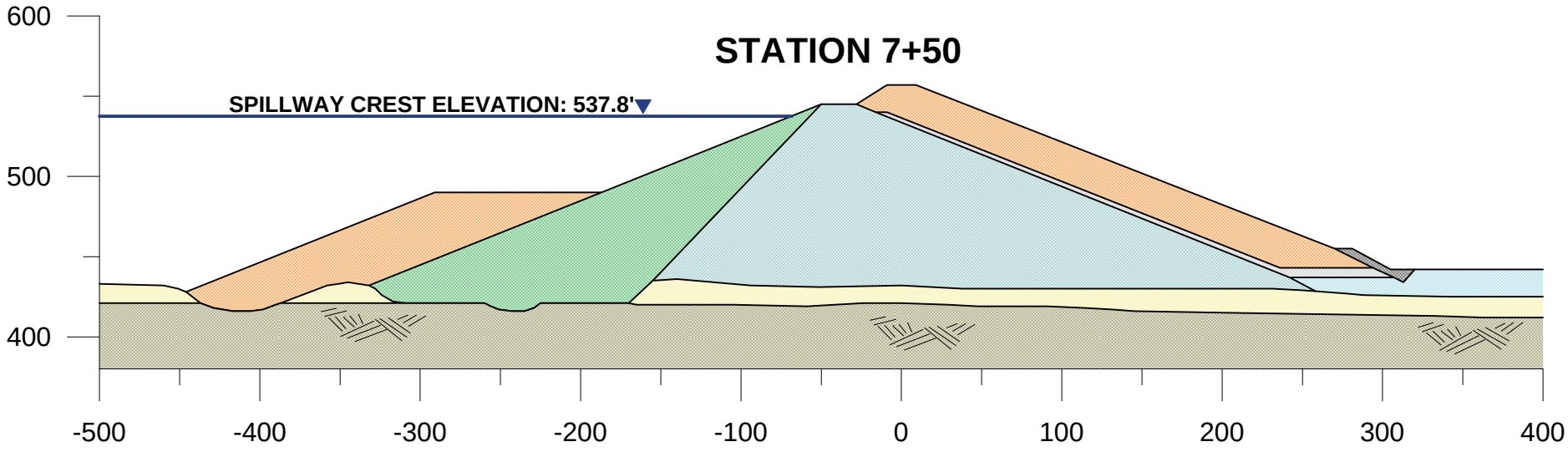

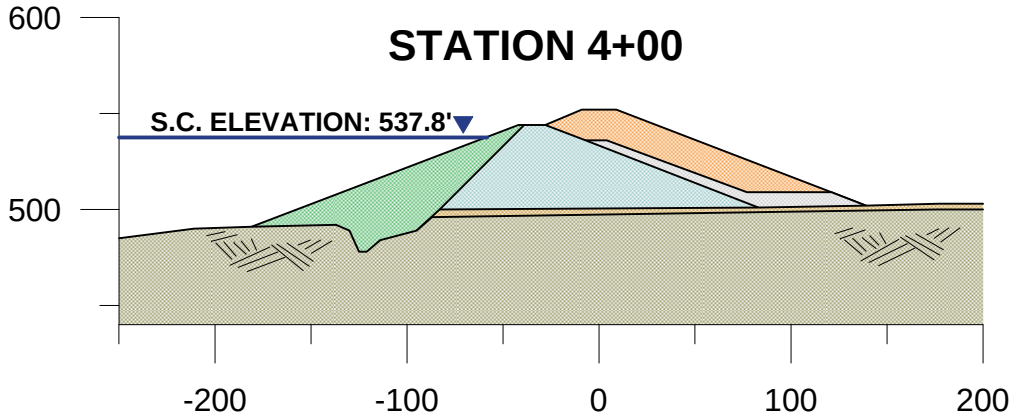

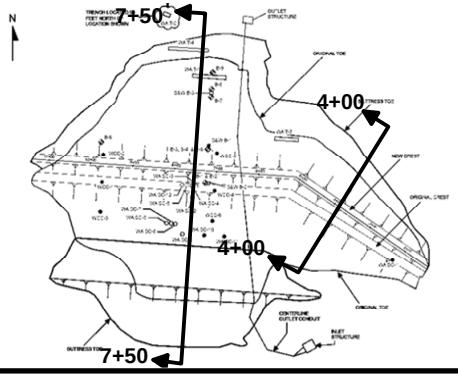

LEGEND

- ORIGINAL EMBANKMENT - UPSTREAM
- ORIGINAL EMBANKMENT - DOWNSTREAM
- UPSTREAM AND DOWNSTREAM BUTTRESSES
- FILTER/DRAIN MATERIAL
- RIP RAP AT DOWNSTREAM TOE
- FILL AT DOWNSTREAM TOE
- YOUNGER ALLUVIUM (Qya)
- OLDER ALLUVIUM (Qoa)
- BEDROCK - SANTA CLARA FORMATION

TERRA / GeoPentech
a Joint Venture

CROSS SECTIONS SHOWING DAM ZONING
STEVENS CREEK DAM
SEISMIC STABILITY EVALUATIONS (SSE2)

Figure
5-1

Rev. 1 06/09/2011 SSE2-R-2SC

Old Embankment Samples

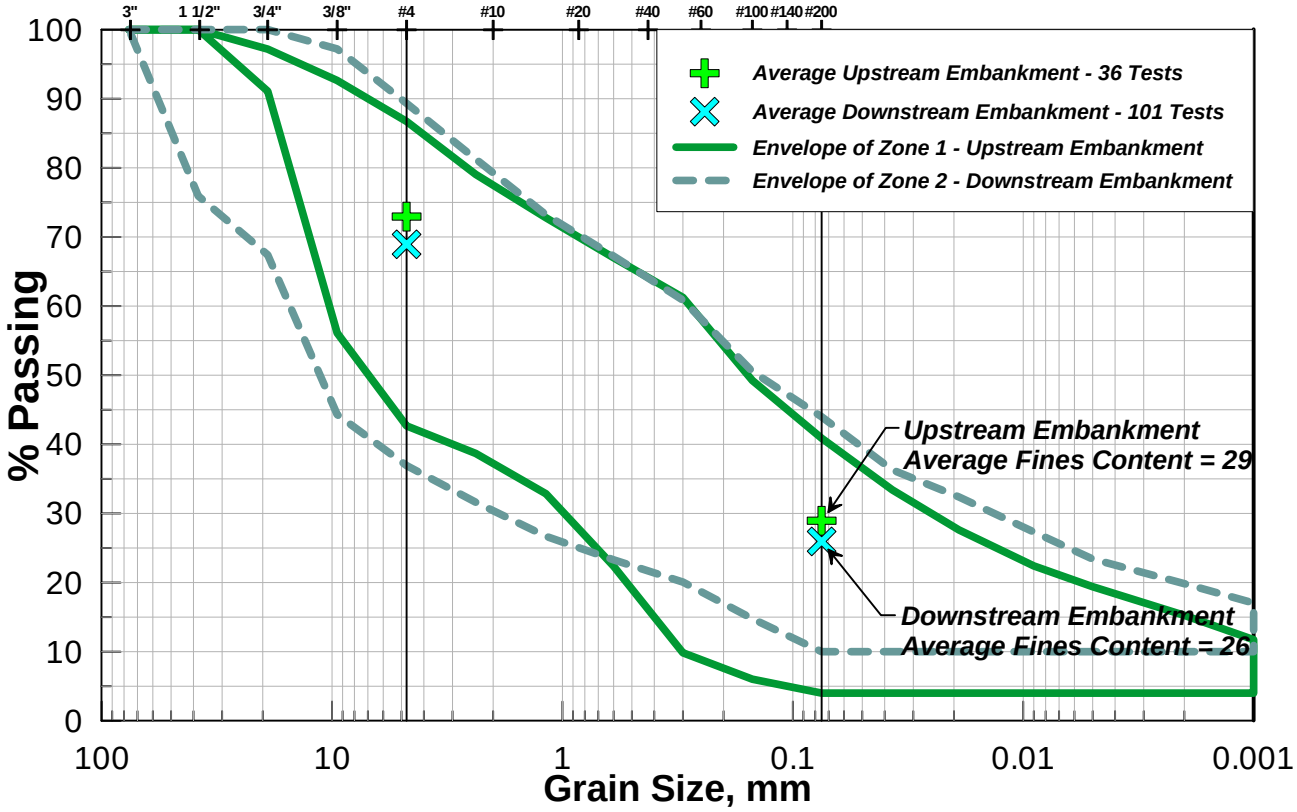

New Buttress Samples

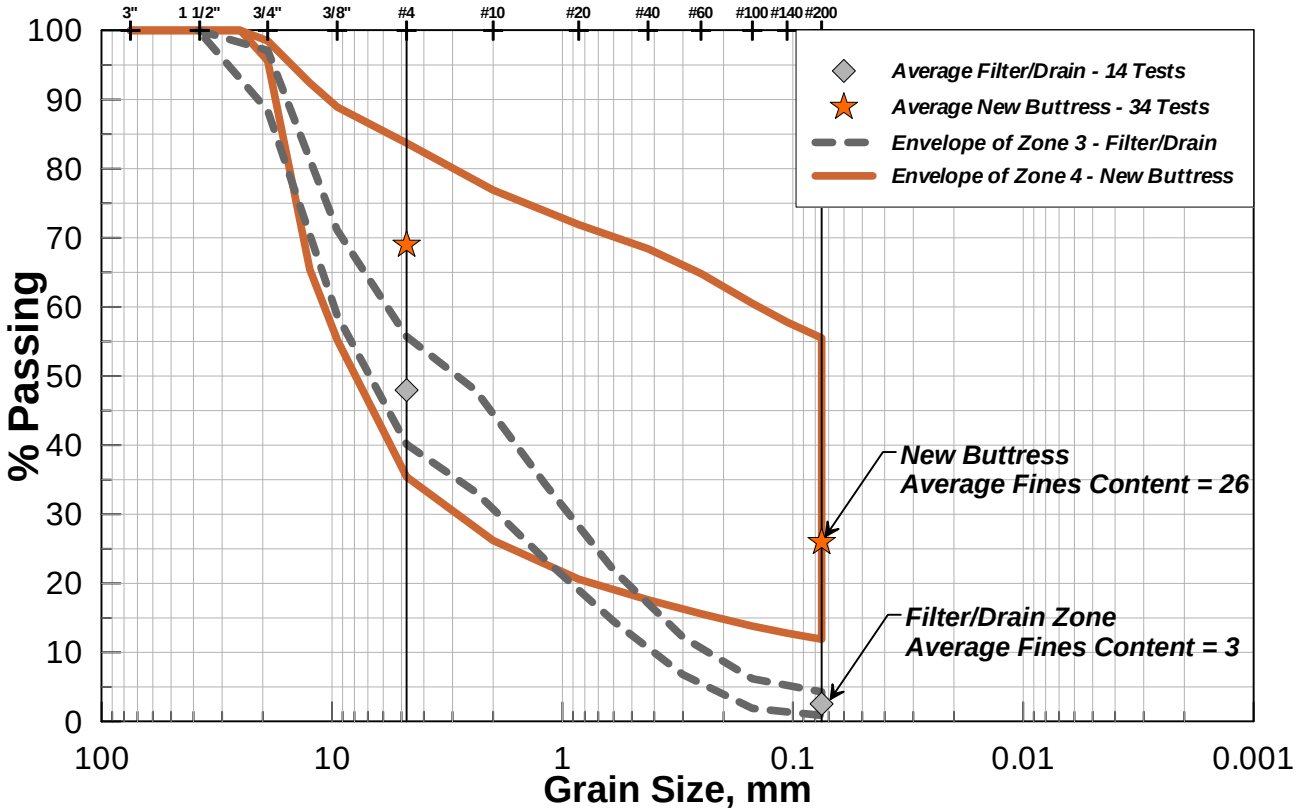

TERRA / GeoPentech a Joint Venture	GRADATION RANGES - EMBANKMENT STEVENS CREEK DAM SEISMIC STABILITY EVALUATIONS (SSE2)	Figure 5-2

Rev. 1 06/09/2011 SSE2-R-2SC

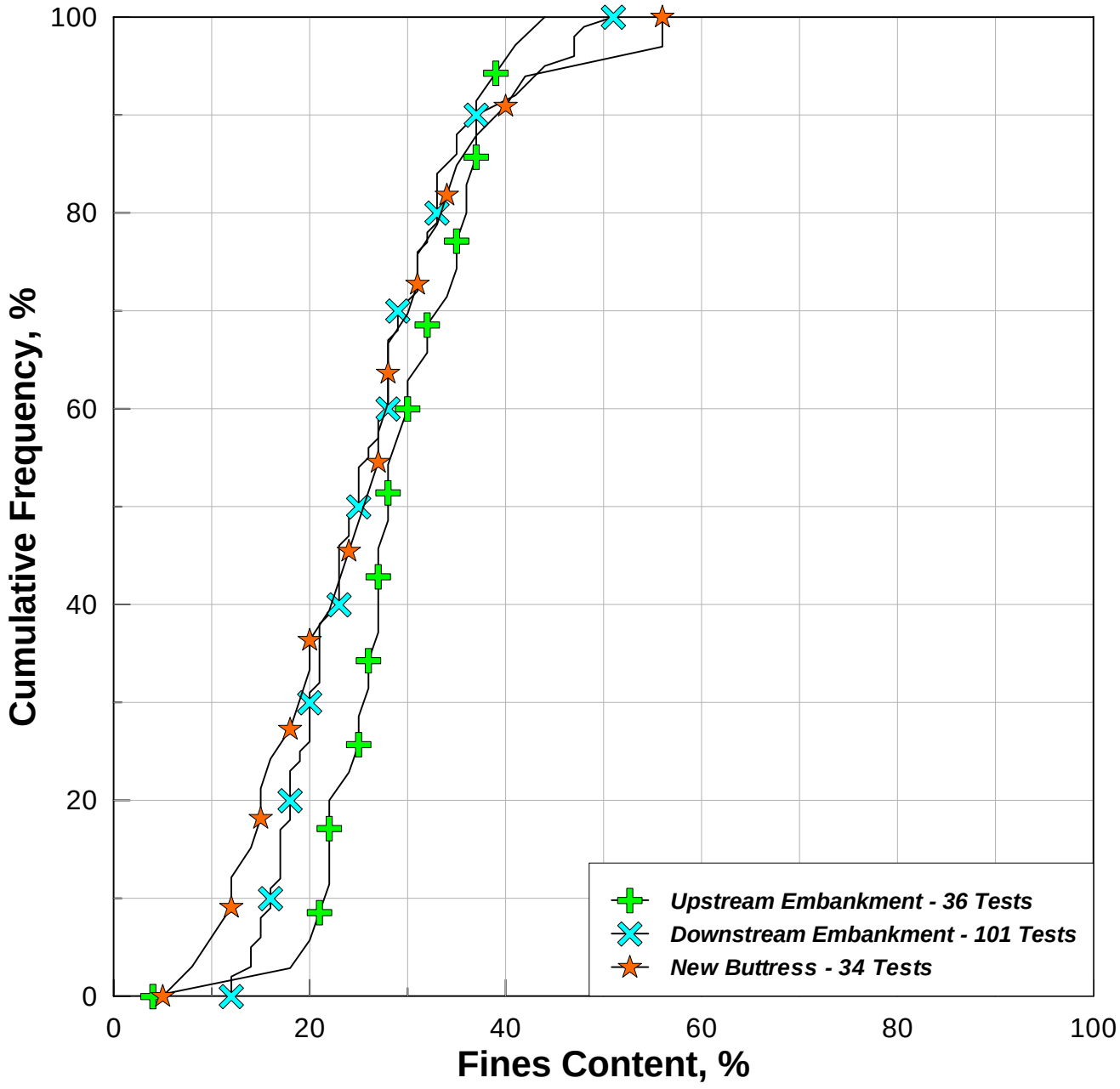

Note: Symbols on distribution lines indicate data set, total number of tests is indicated in legend.

TERRA / GeoPentech a Joint Venture	FINES CONTENT - EMBANKMENT STEVENS CREEK DAM SEISMIC STABILITY EVALUATIONS (SSE2)	Figure 5-3

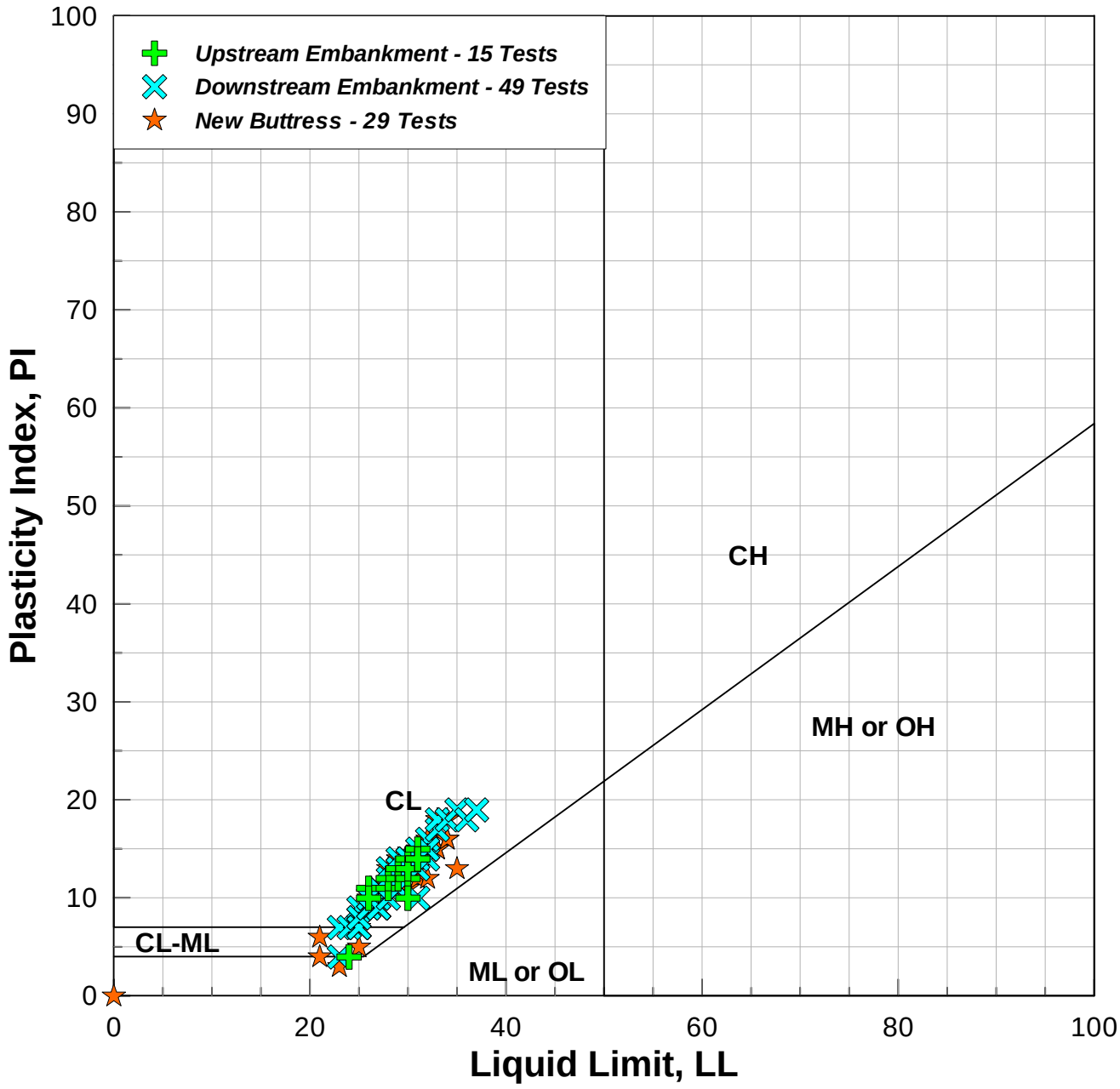

SUMMARY OF ATTERBERG LIMITS TEST RESULTS

Material	Material Description	No. Tests	Range of LL	Average LL	Range of PI	Average PI
Upstream Embankment	GC-SC-CL	15	15 to 31	29	4 to 15	12
Downstream Embankment	SC-GC-GM-SM	49	23 to 37	29	4 to 19	12
New Buttresses	SC-SM-GC	29	21 to 35	29	3 to 18	12

29

TERRA / GeoPentech
a Joint Venture

PLASTICITY CHART - EMBANKMENT
STEVENS CREEK DAM
SEISMIC STABILITY EVALUATIONS (SSE2)

Figure
5-4

Rev. 1 06/09/2011 SSE2-R-2SC

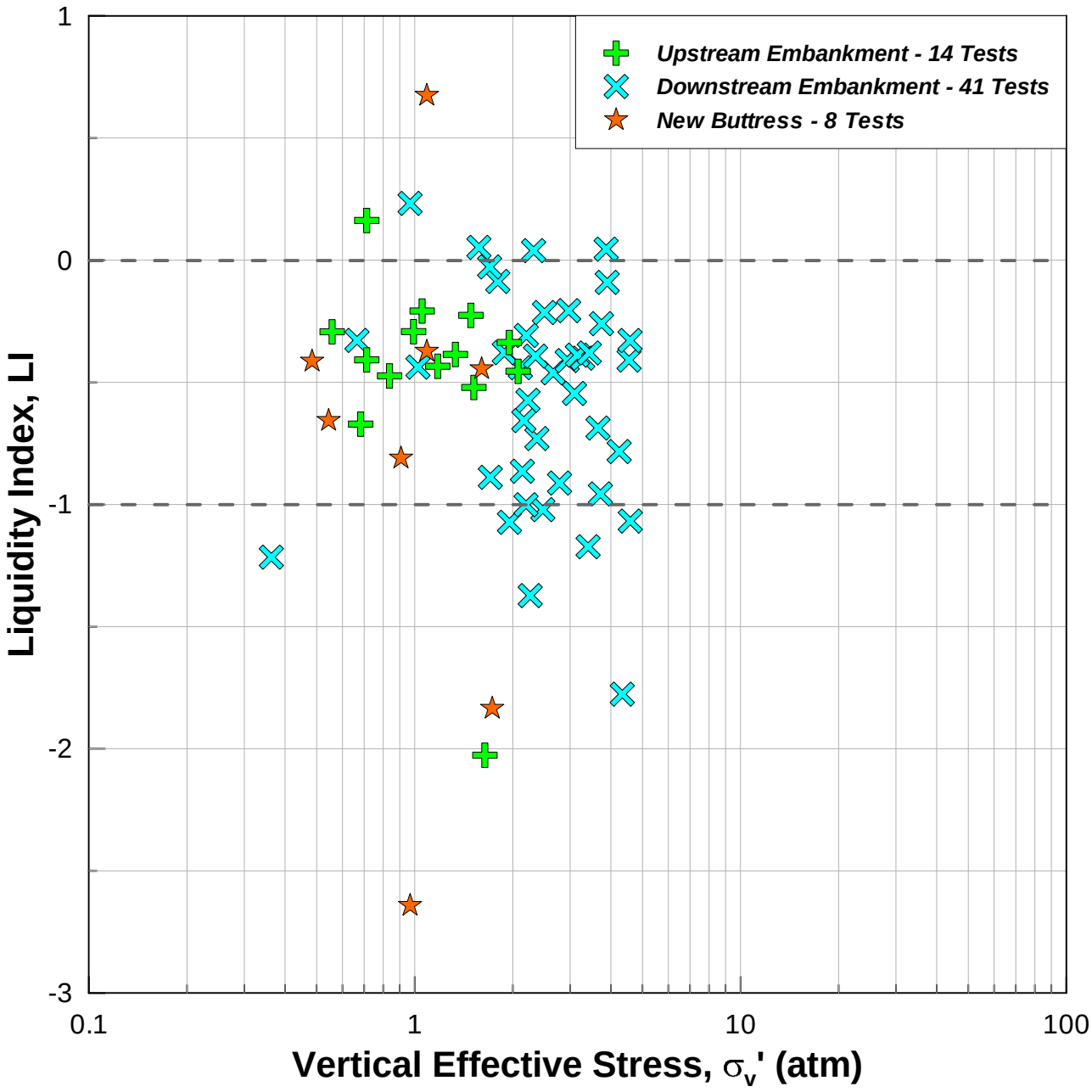

SUMMARY OF LIQUIDITY INDEX TEST RESULTS

Material	Material Description	No. Tests	Range of LI	Average LI
Upstream Embankment	GC-SC-CL	14	-2.0 to 0.2	-0.6
Downstream Embankment	SC-GC-GM-SM	41	-1.8 to 0.2	-0.6
New Buttresses	SC-SM-GC	8	-2.6 to 0.7	-0.8

TERRA / GeoPentech
a Joint Venture

LIQUIDITY INDEX - EMBANKMENT
STEVENS CREEK DAM
SEISMIC STABILITY EVALUATIONS (SSE2)

Figure
5-5

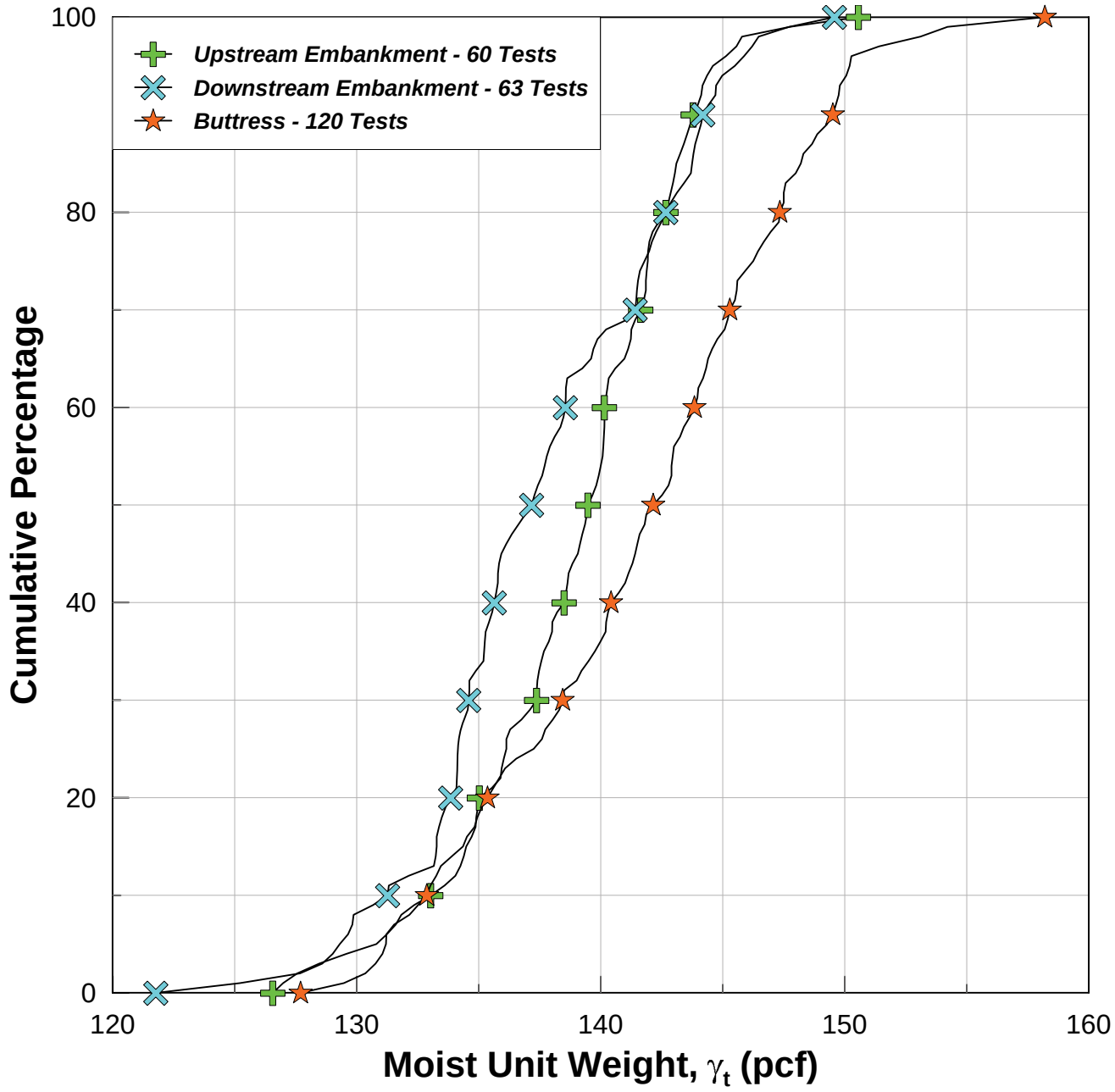

Note: Symbols on distribution lines indicate data set only, total number of tests is indicated in legend.

TERRA / GeoPentech a Joint Venture	TOTAL UNIT WEIGHT - EMBANKMENT STEVENS CREEK DAM SEISMIC STABILITY EVALUATIONS (SSE2)	Figure 5-6

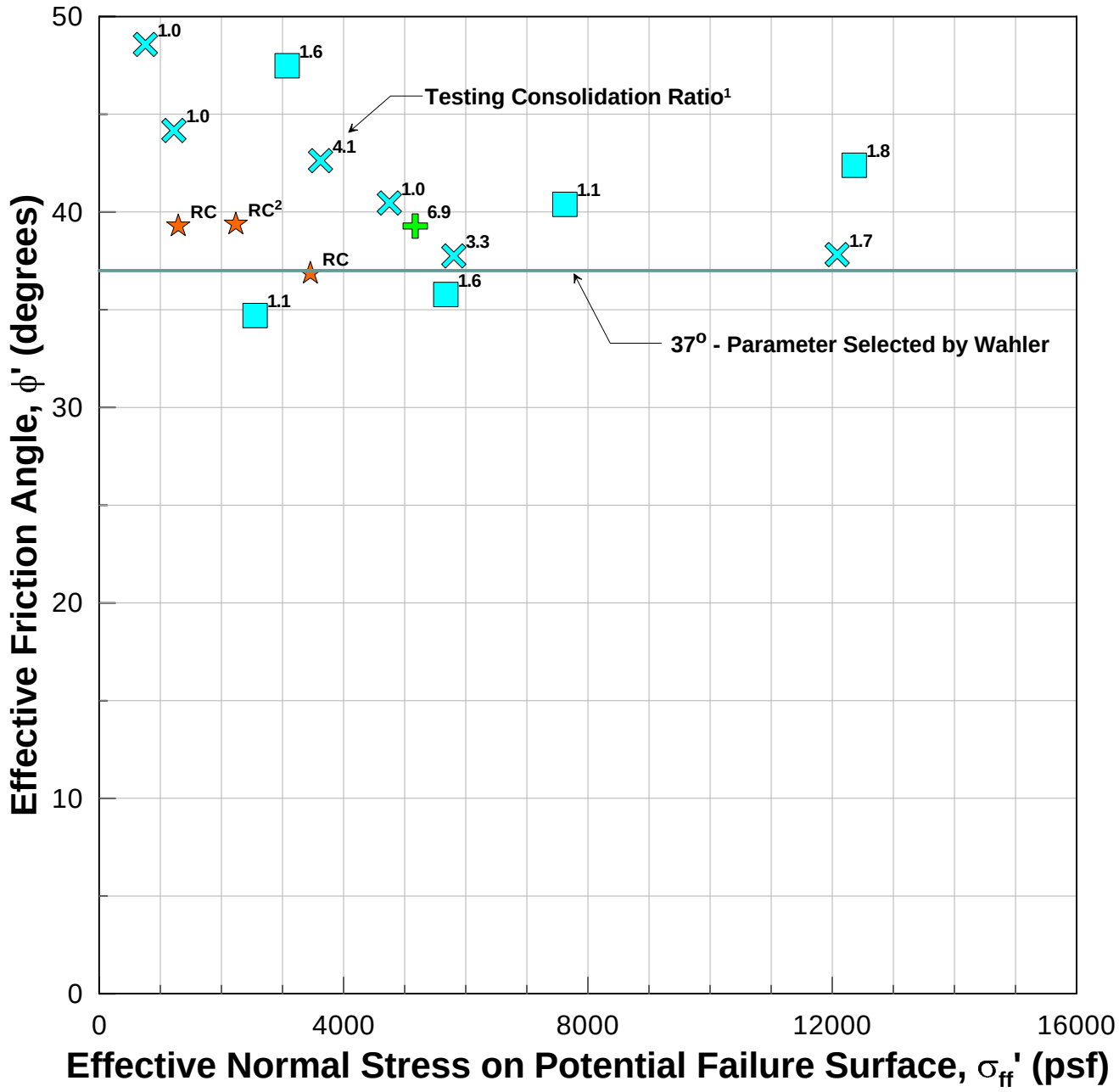

[1]Testing Consolidation Ratio = $\sigma_{vc}'_{(tested)}/\sigma_{vc}'_{(in\text{-}situ)}$

[2]RC = Recompacted Sample

TERRA / GeoPentech
a Joint Venture

EFFECTIVE STRESS STRENGTH - EMBANKMENT
STEVENS CREEK DAM
SEISMIC STABILITY EVALUATIONS (SSE2)

Figure
5-7

Rev. 1 06/09/2011 SSE2-R-2SC

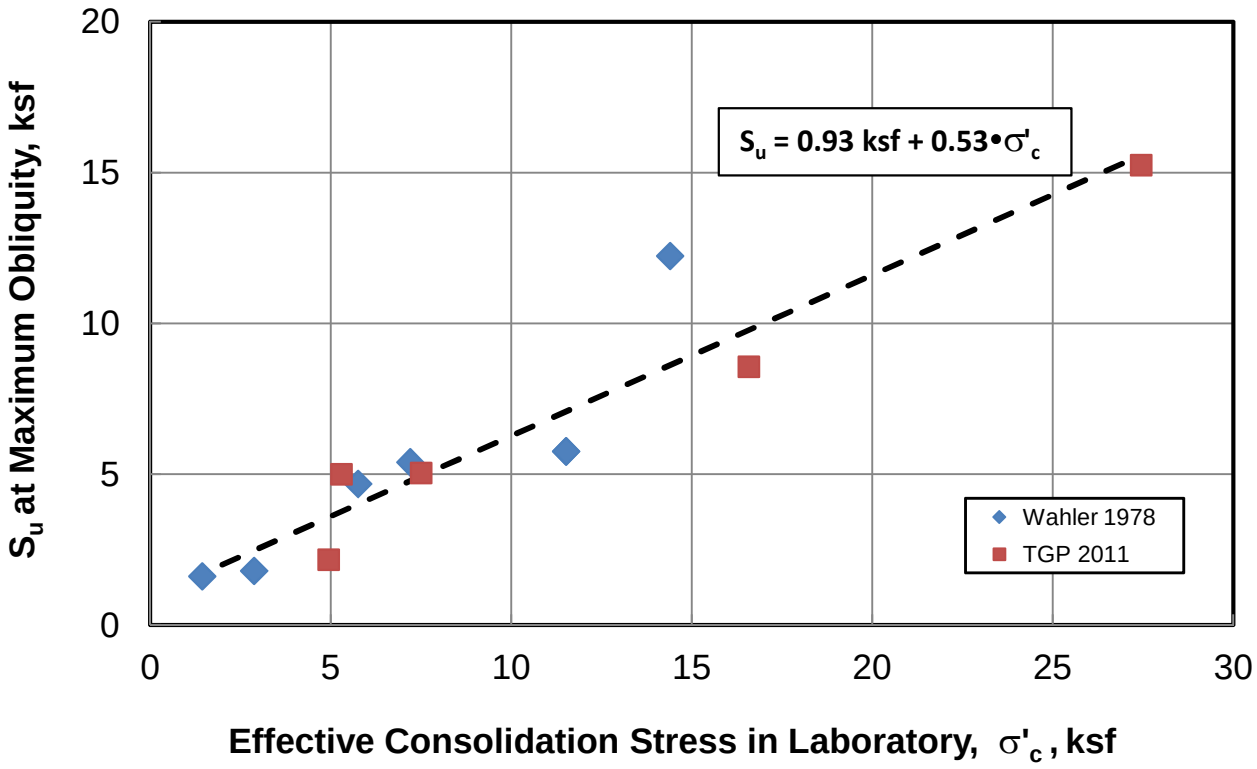

Results of Consolidated Undrained Triaxial Compression Tests

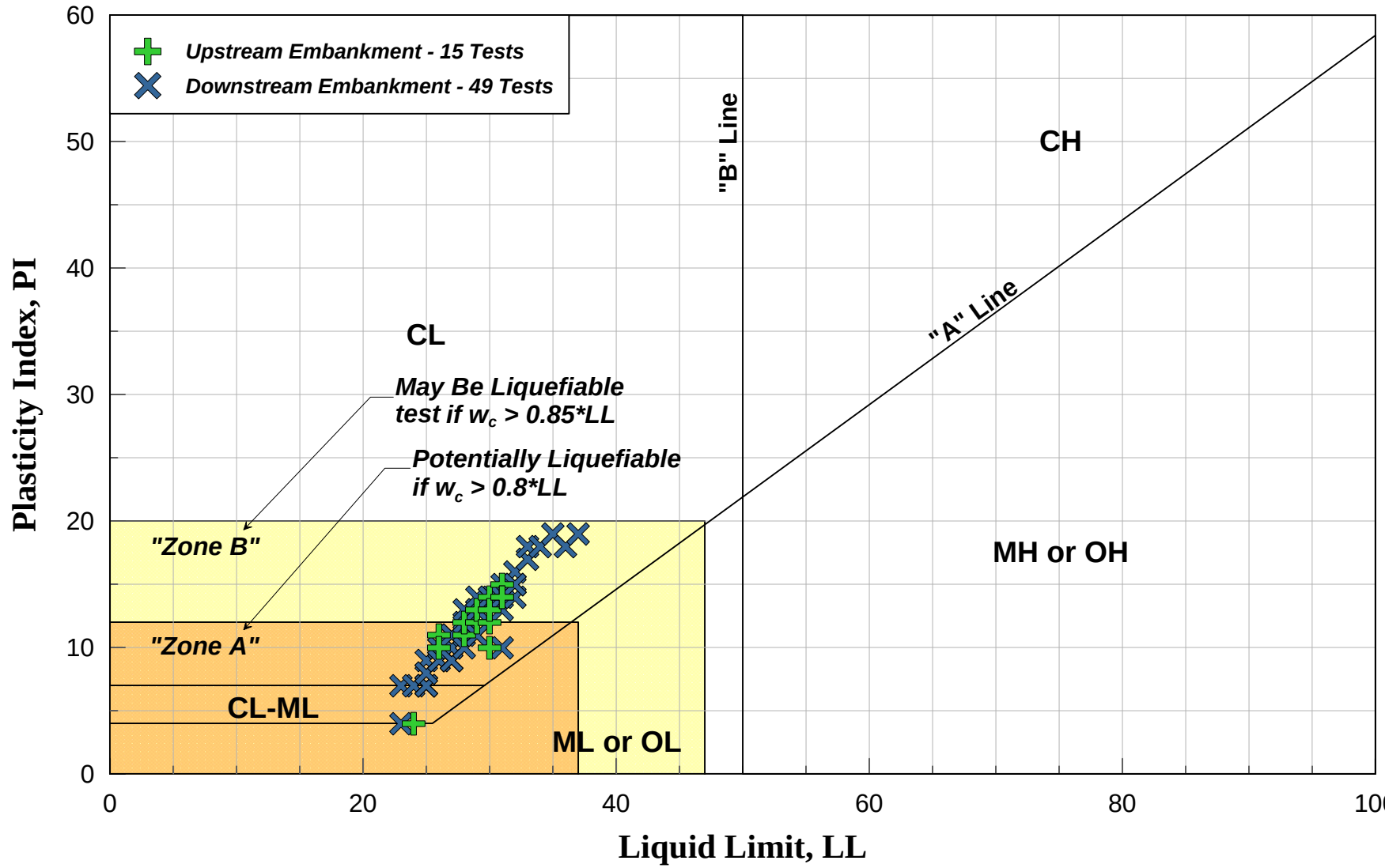

Note: 1. "Zone A" and "Zone B" from Bray, 2001 as modified by Seed et al., 2003

TERRA / GeoPentech
a Joint Venture

PLASTICITY CHART WITH LIQUEFACTION ZONES
STEVENS CREEK DAM
SEISMIC STABILITY EVALUATIONS (SSE2)

Figure
5-9

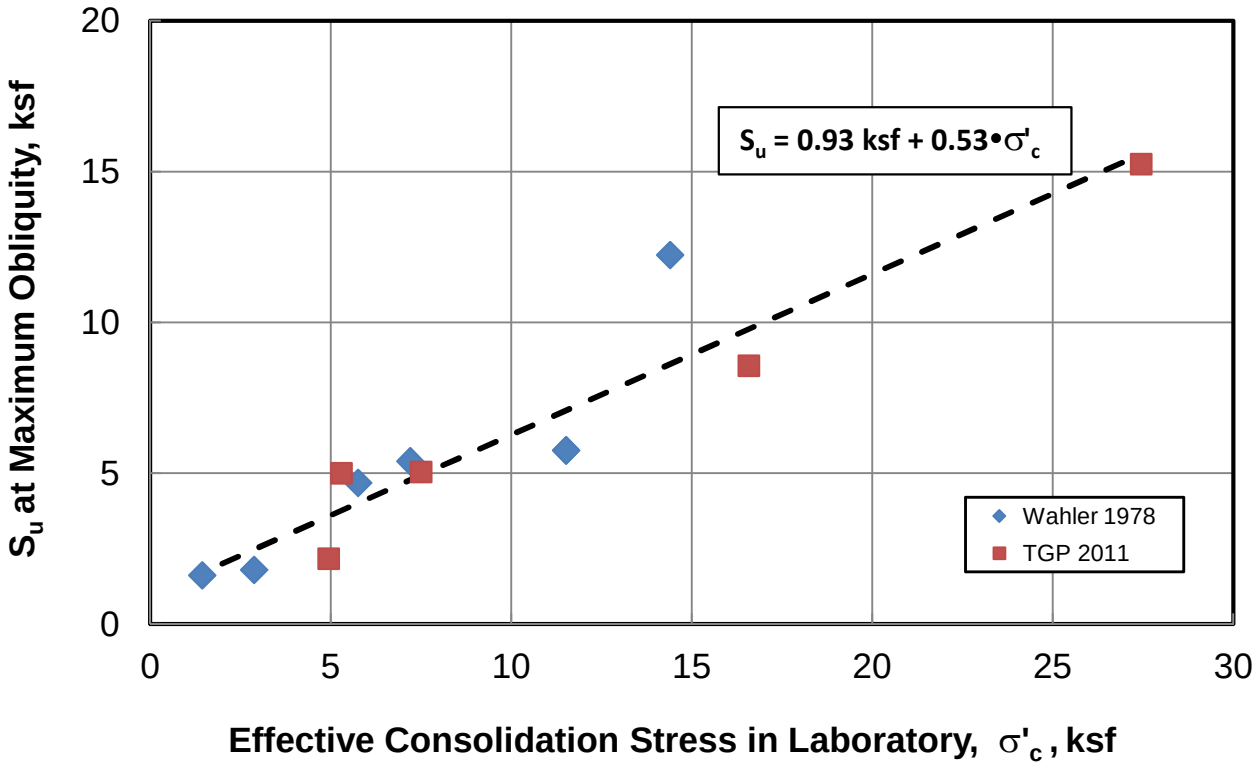

Figure 5-10A - Results of Consolidated Undrained Triaxial Compression Tests

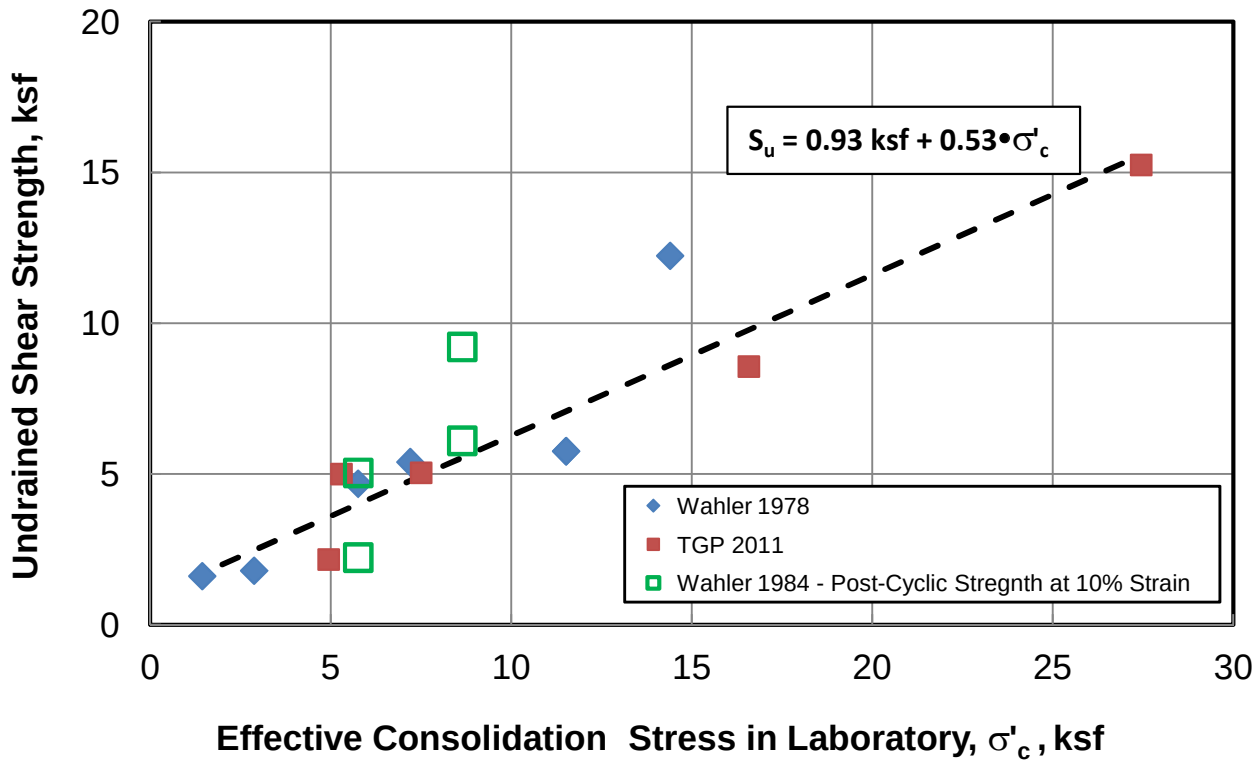

Figure 5-10B - Comparison of Post-Cyclic Strength Tests to Conventional Strengths Tests

TERRA / GeoPentech a Joint Venture	POST-CYCLIC UNDRAINED STRENGTH EMBANKMENT - STEVENS CREEK DAM SEISMIC STABILITY EVALUATIONS (SSE2)	Figure 5-10

Rev. 0 02/20/2012

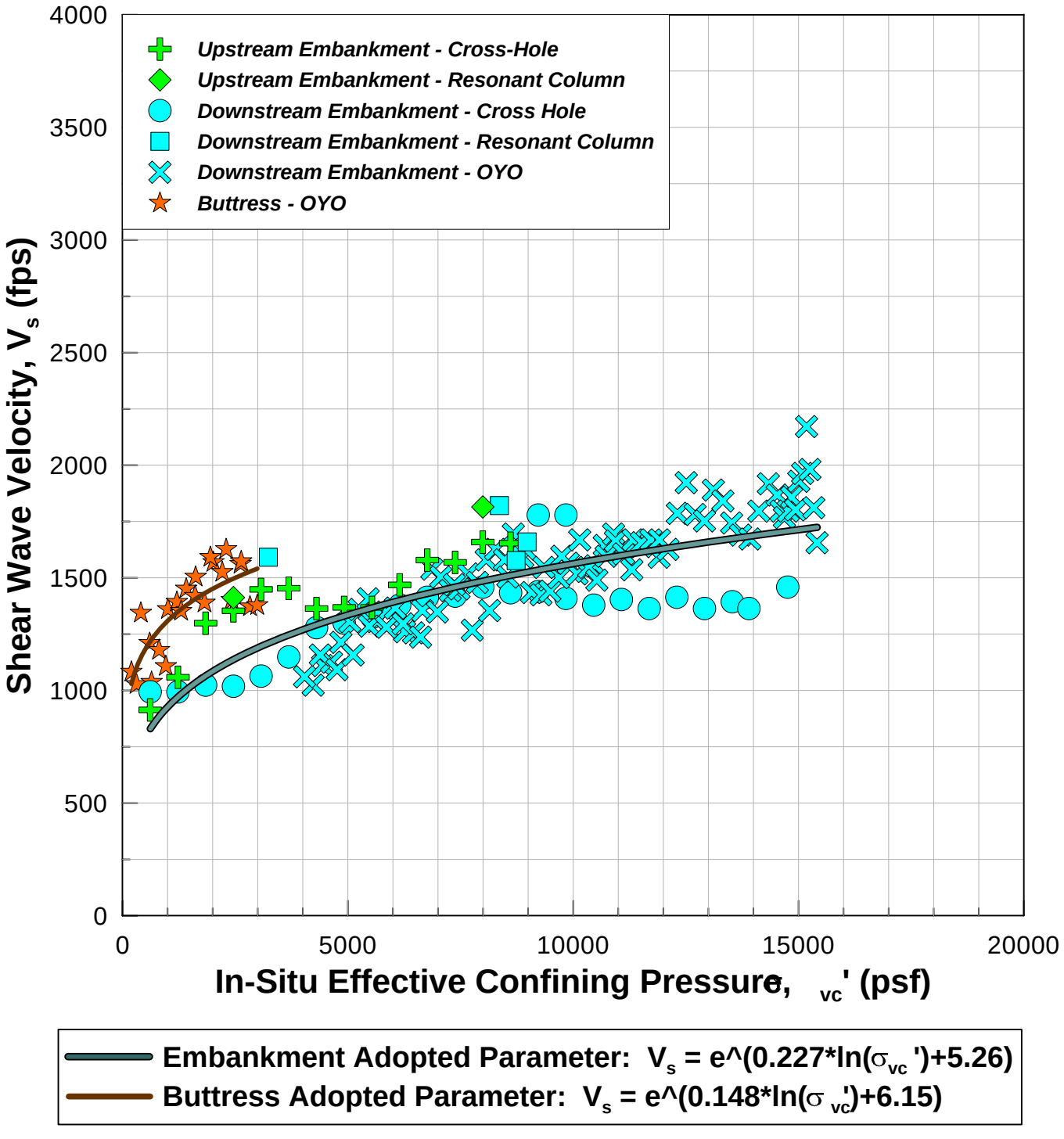

TERRA / GeoPentech
a Joint Venture

SHEAR WAVE VELOCITY - EMBANKMENT
STEVENS CREEK DAM
SEISMIC STABILITY EVALUATIONS (SSE2)

Figure
5-11

Rev. 1 06/09/2011 SSE2-R-2SC

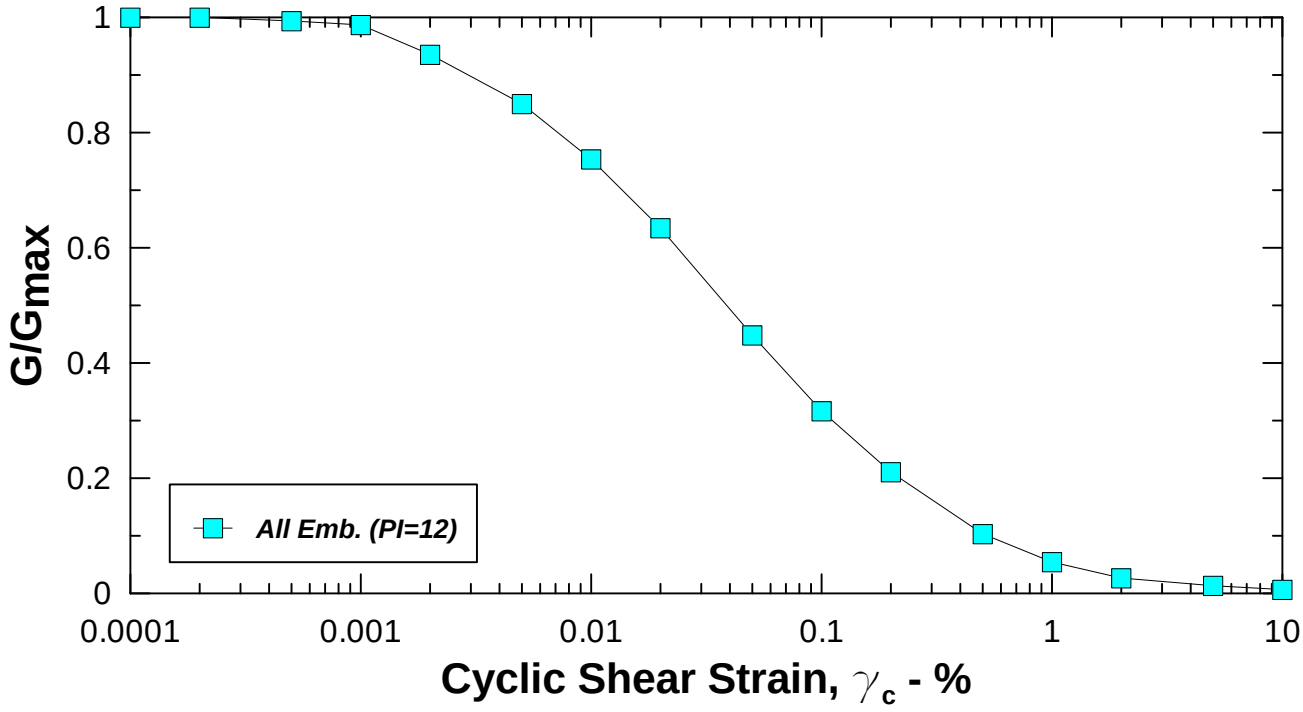

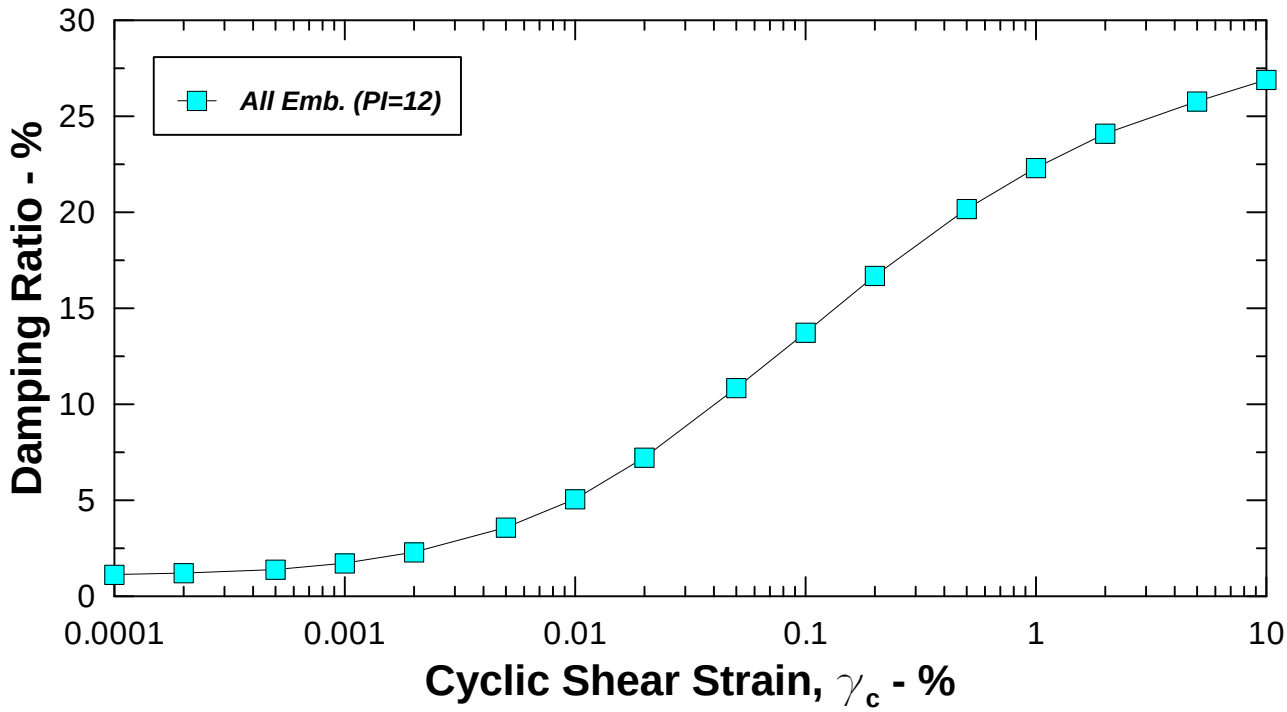

Note: Modulus reduction and damping ratio curves are based on Vucetic and Dobry, 1991

TERRA / GeoPentech
a Joint Venture

MODULUS REDUCTION & DAMPING RATIO
EMBANKMENT - STEVENS CREEK DAM
SEISMIC STABILITY EVALUATIONS (SSE2)

Figure
5-12

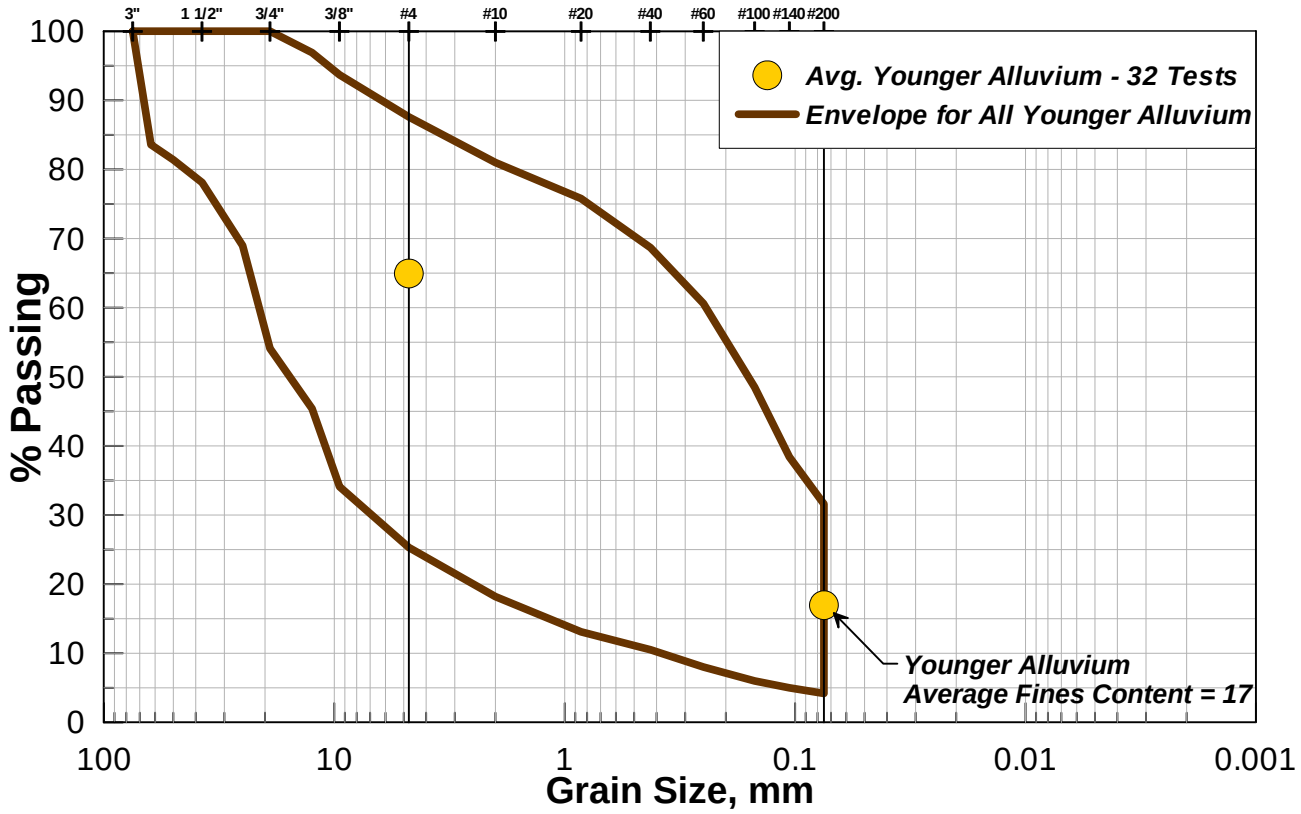

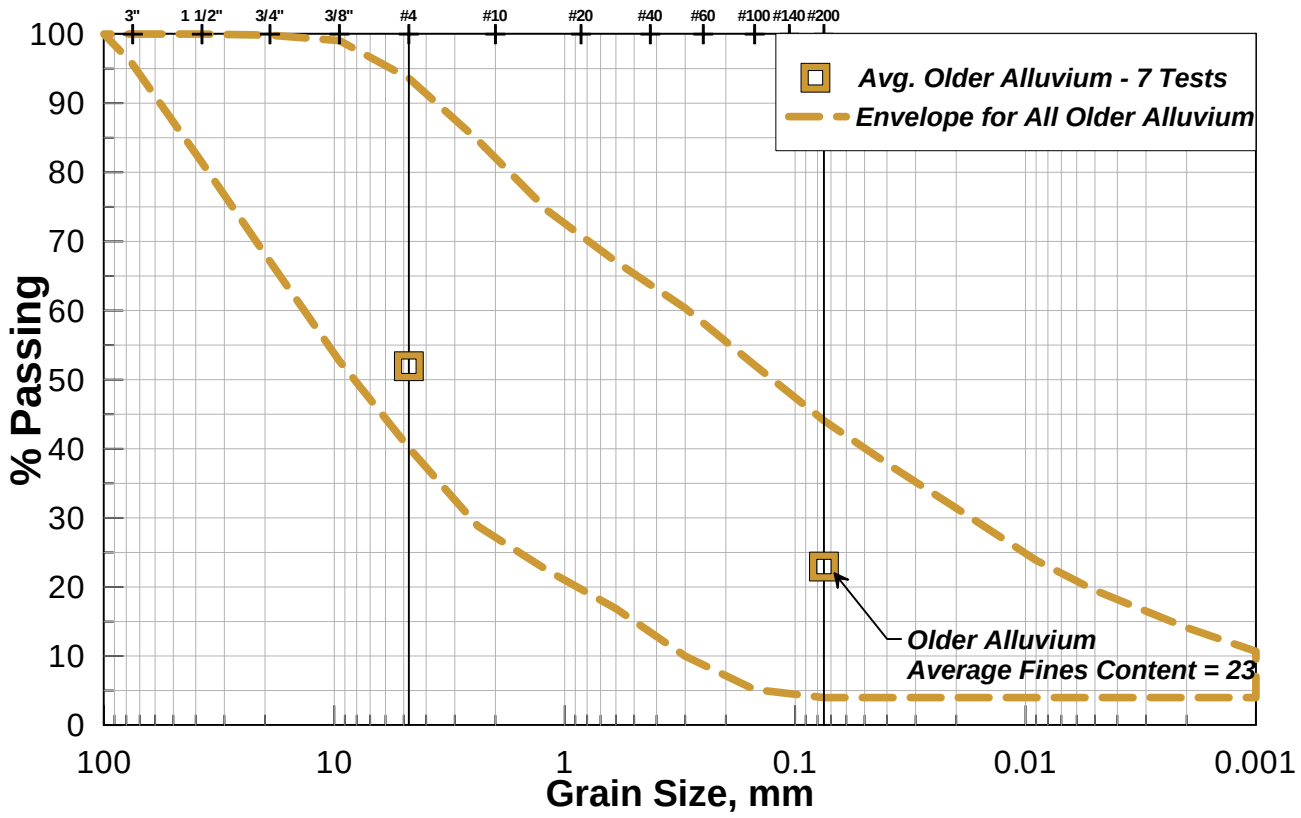

TERRA / GeoPentech
a Joint Venture

GRADATION RANGES - ALLUVIUM
STEVENS CREEK DAM
SEISMIC STABILITY EVALUATIONS (SSE2)

Figure
5-13

Rev. 0 04/20/2011 SSE2-R-2SC

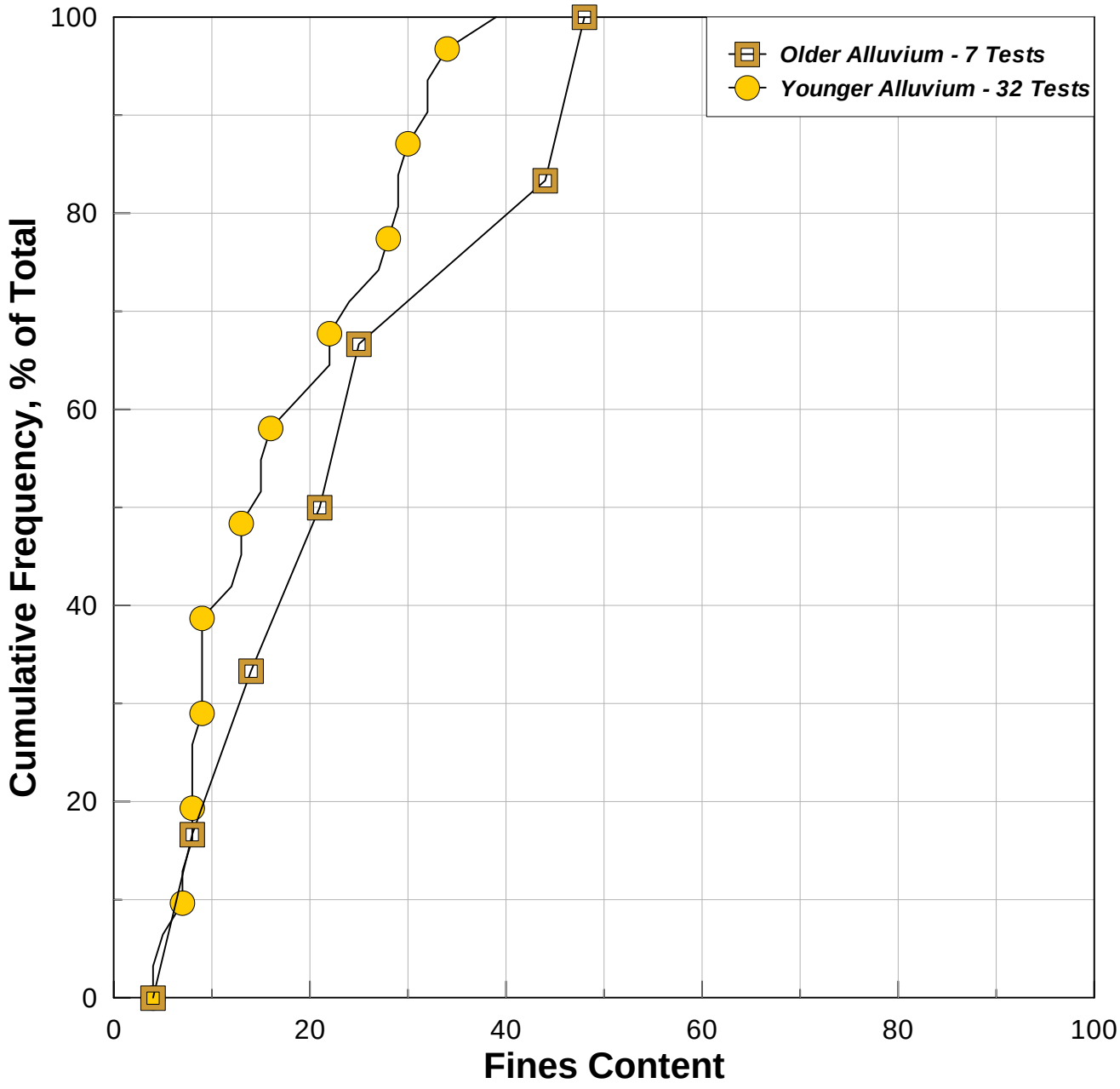

Note: Symbols on distribution lines indicate data set only, total number of tests is indicated in legend.

TERRA / GeoPentech
a Joint Venture

FINES CONTENT - ALLUVIUM
STEVENS CREEK DAM
SEISMIC STABILITY EVALUATIONS (SSE2)

Figure
5-14

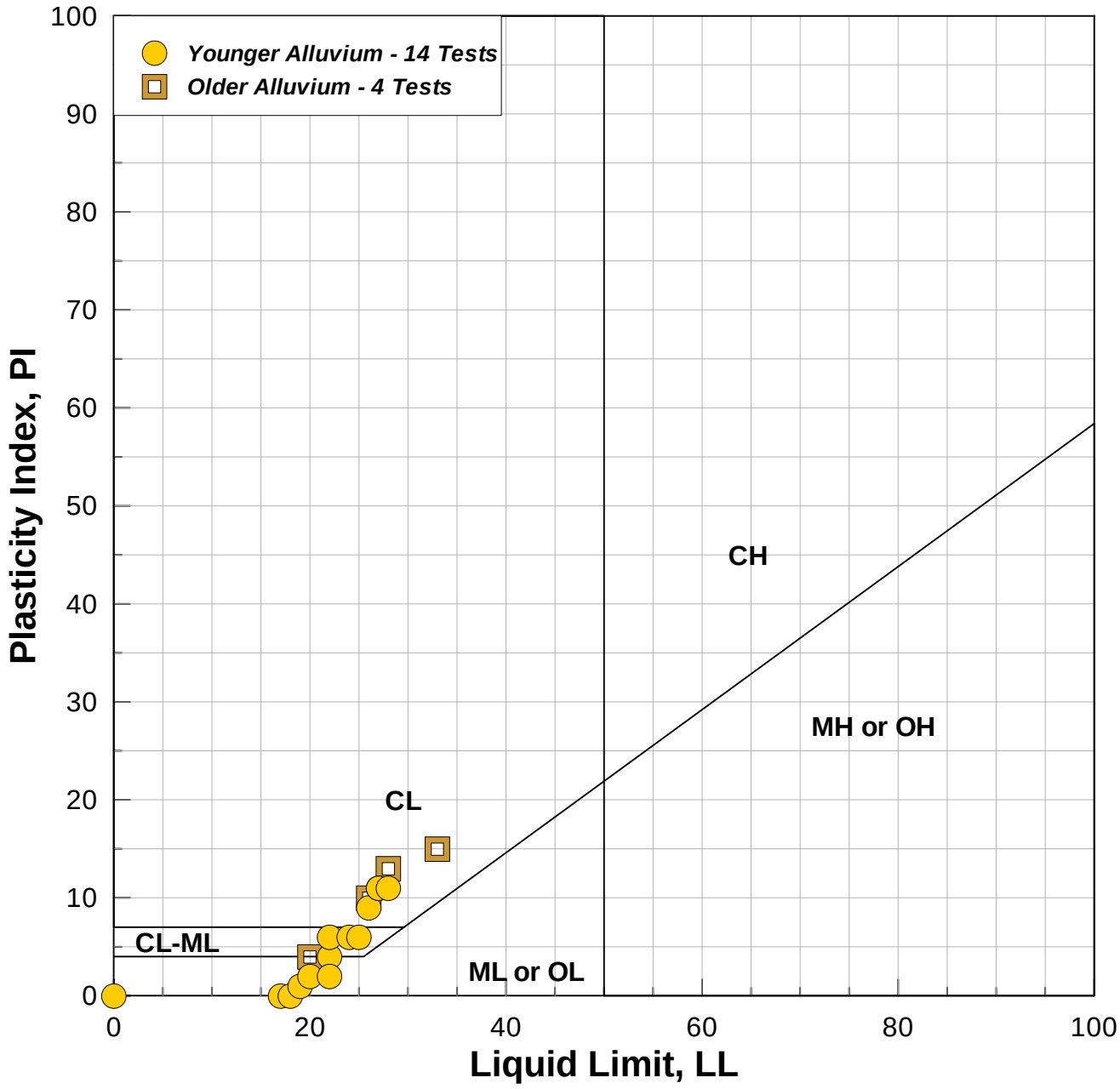

SUMMARY OF ATTERBERG LIMITS TEST RESULTS

Material	Material Description	No. Tests	Range of LL	Average LL	Range of PI	Average PI
Younger Alluvium (Qya)	GP-SM-GC-SC	14	NP to 28	21	NP to 11	5
Older Alluvium (Qoa)	GC-GP-SM-SC	4	20 to 33	27	4 to 15	11

TERRA / GeoPentech
a Joint Venture

PLASTICITY CHART - ALLUVIUM
STEVENS CREEK DAM
SEISMIC STABILITY EVALUATIONS (SSE2)

Figure
5-15

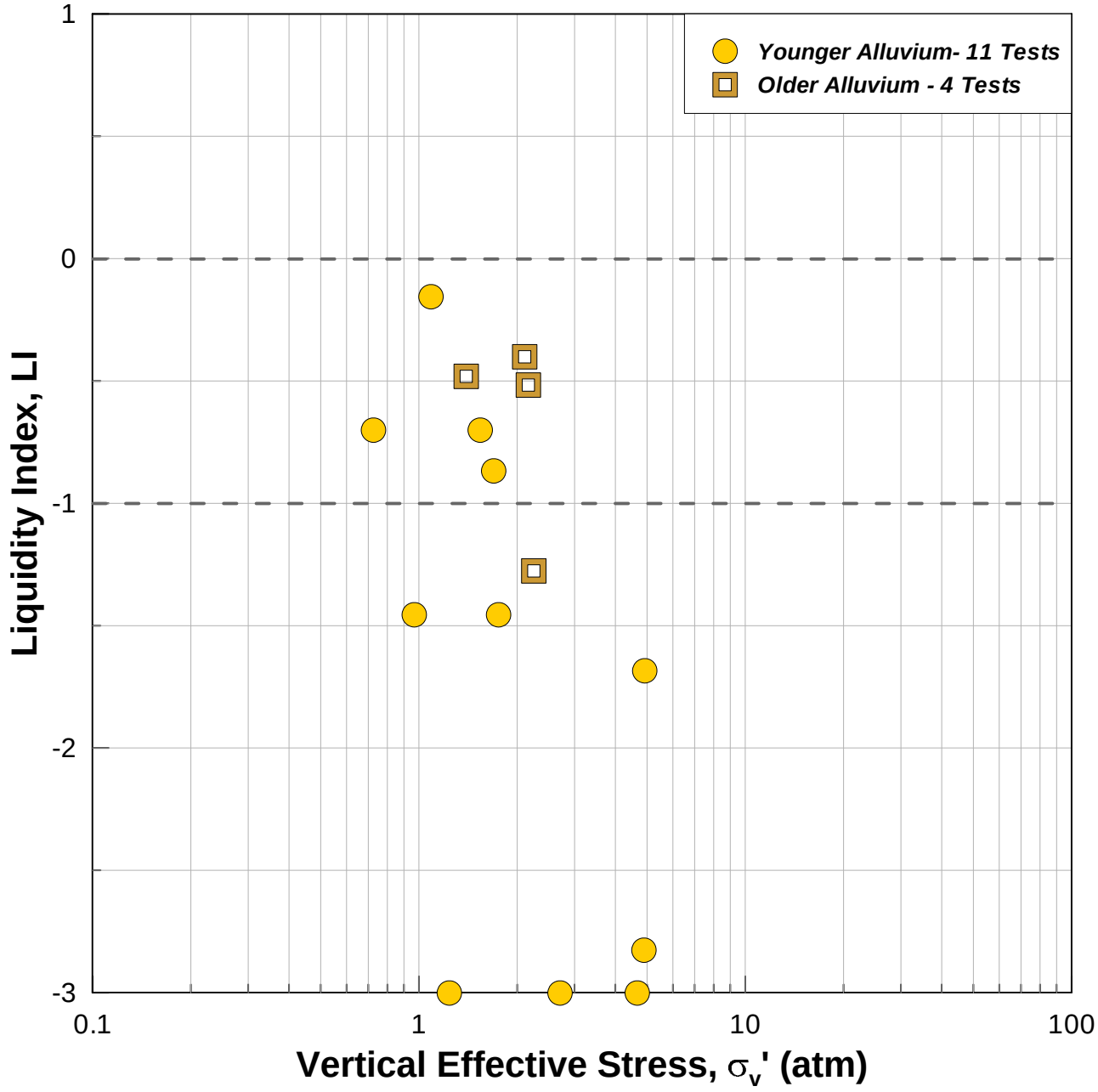

SUMMARY OF LIQUIDITY INDEX TEST RESULTS

Material	Material Description	No. Tests	Range of LI	Average LI
Younger Alluvium (Qya)	GP-SM-GC-SC	11	-5.1 to -0.2	-2.0
Older Alluvium (Qoa)	GC-GP-SM-SC	4	-1.3 to -0.4	-0.7

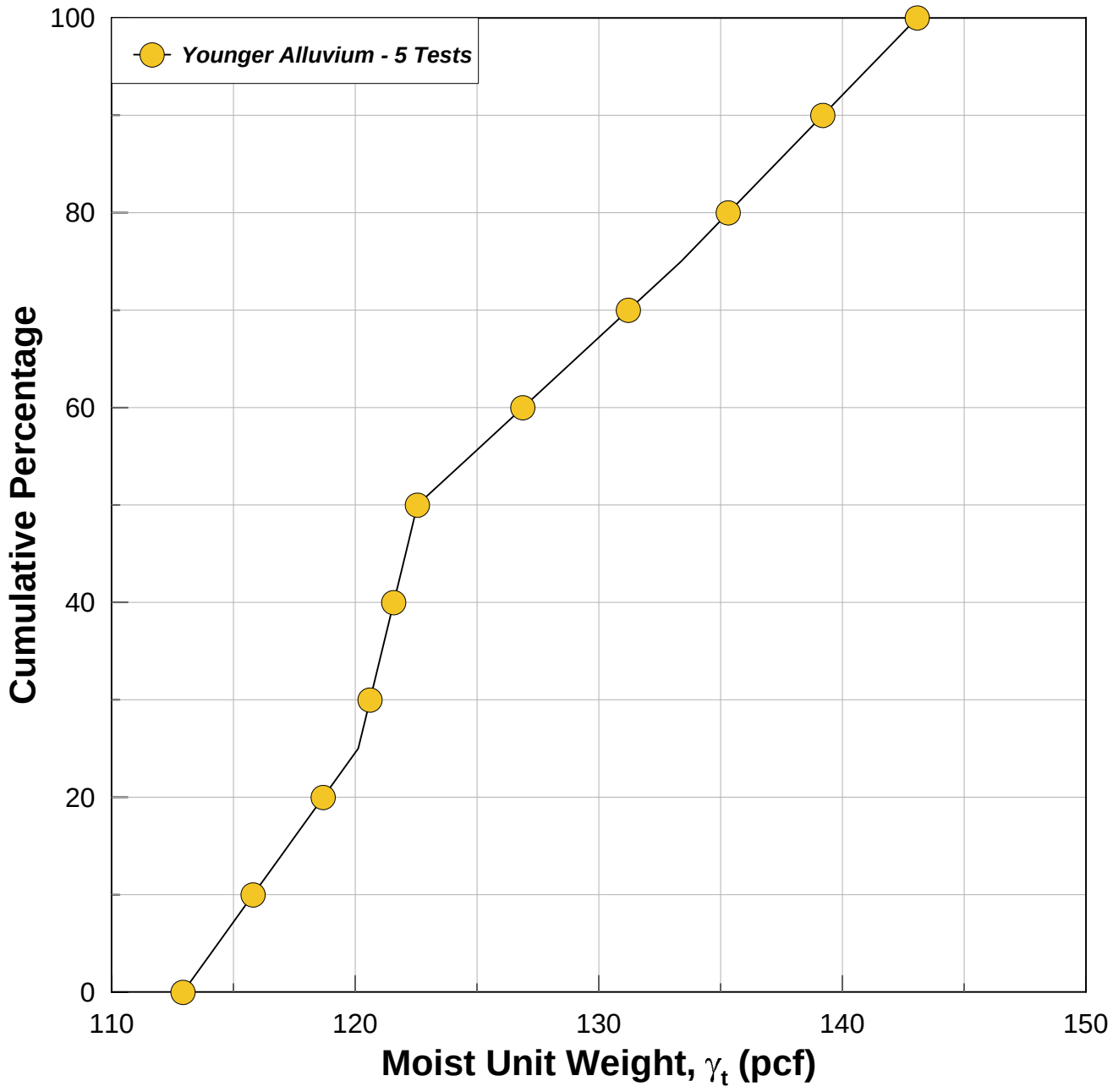

Note: Symbols on distribution lines indicate data set only, total number of tests is indicated in legend.

TERRA / GeoPentech a Joint Venture	TOTAL UNIT WEIGHT - ALLUVIUM STEVENS CREEK DAM SEISMIC STABILITY EVALUATIONS (SSE2)	Figure 5-17

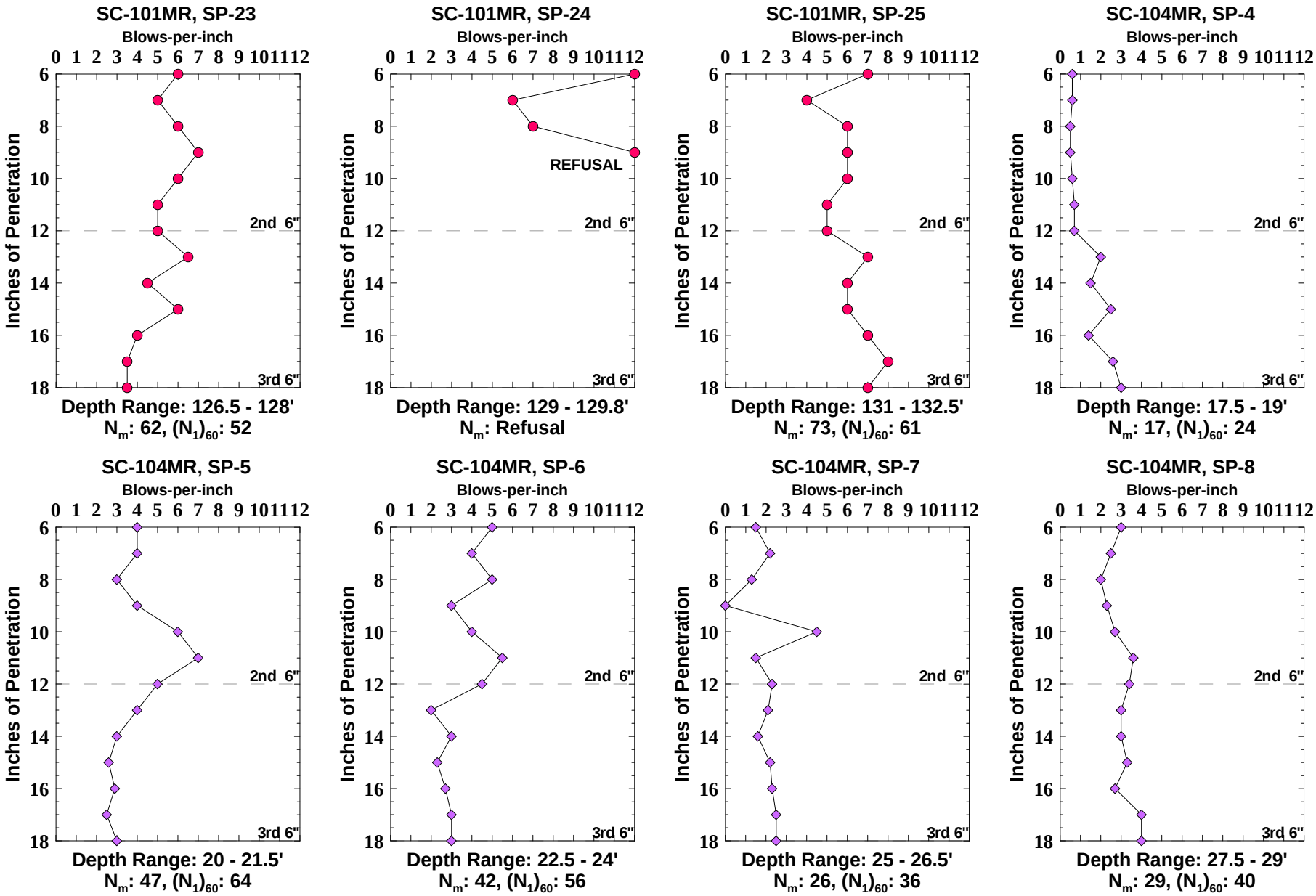

TERRA / GeoPentech
a Joint Venture

SPT BLOW-PER-INCH - ALLUVIUM
STEVENS CREEK DAM
SEISMIC STABILITY EVALUATIONS (SSE2)

Figure
5-18

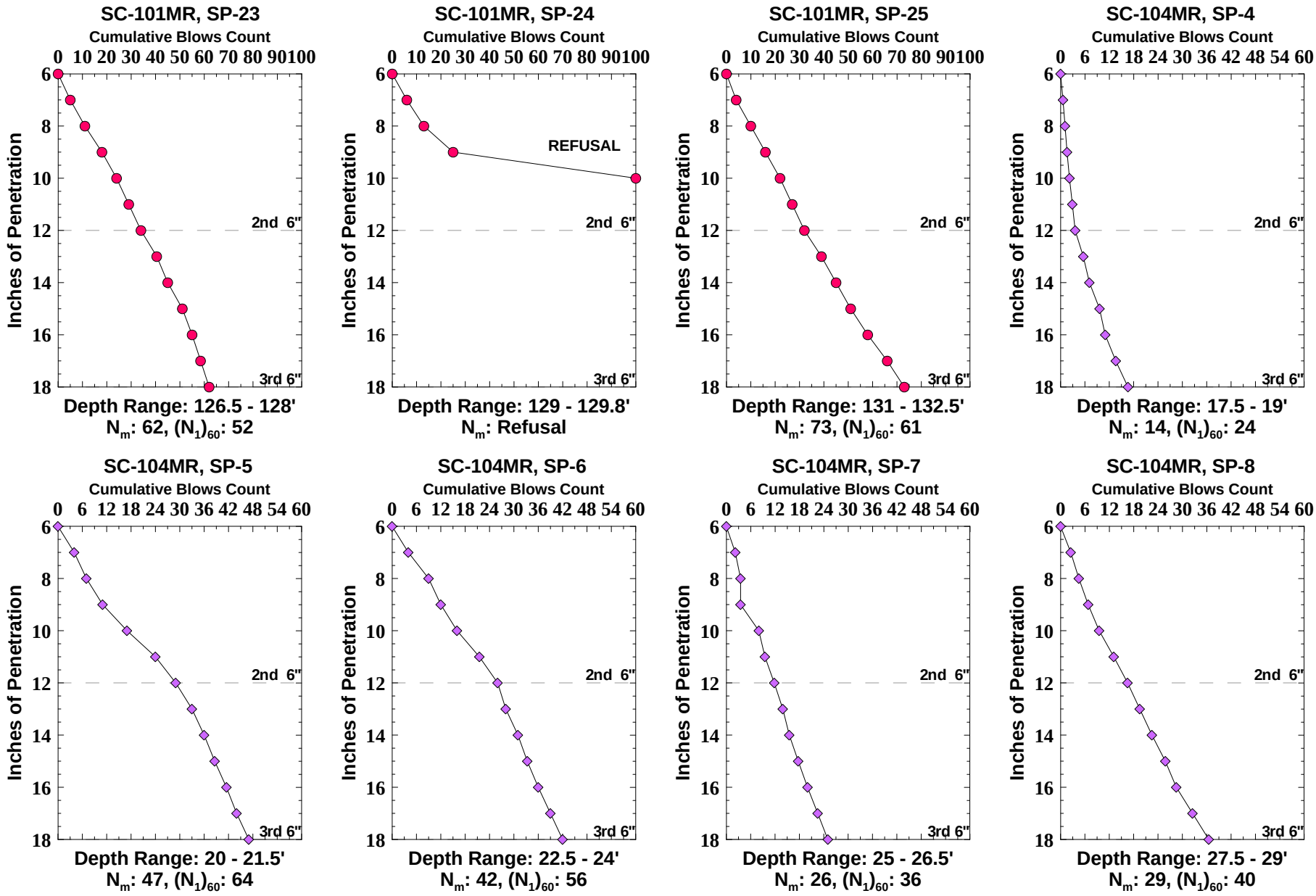

TERRA / GeoPentech
a Joint Venture

SPT CUMULATIVE BLOW COUNT - ALLUVIUM
STEVENS CREEK DAM
SEISMIC STABILITY EVALUATIONS (SSE2)

Figure
5-19

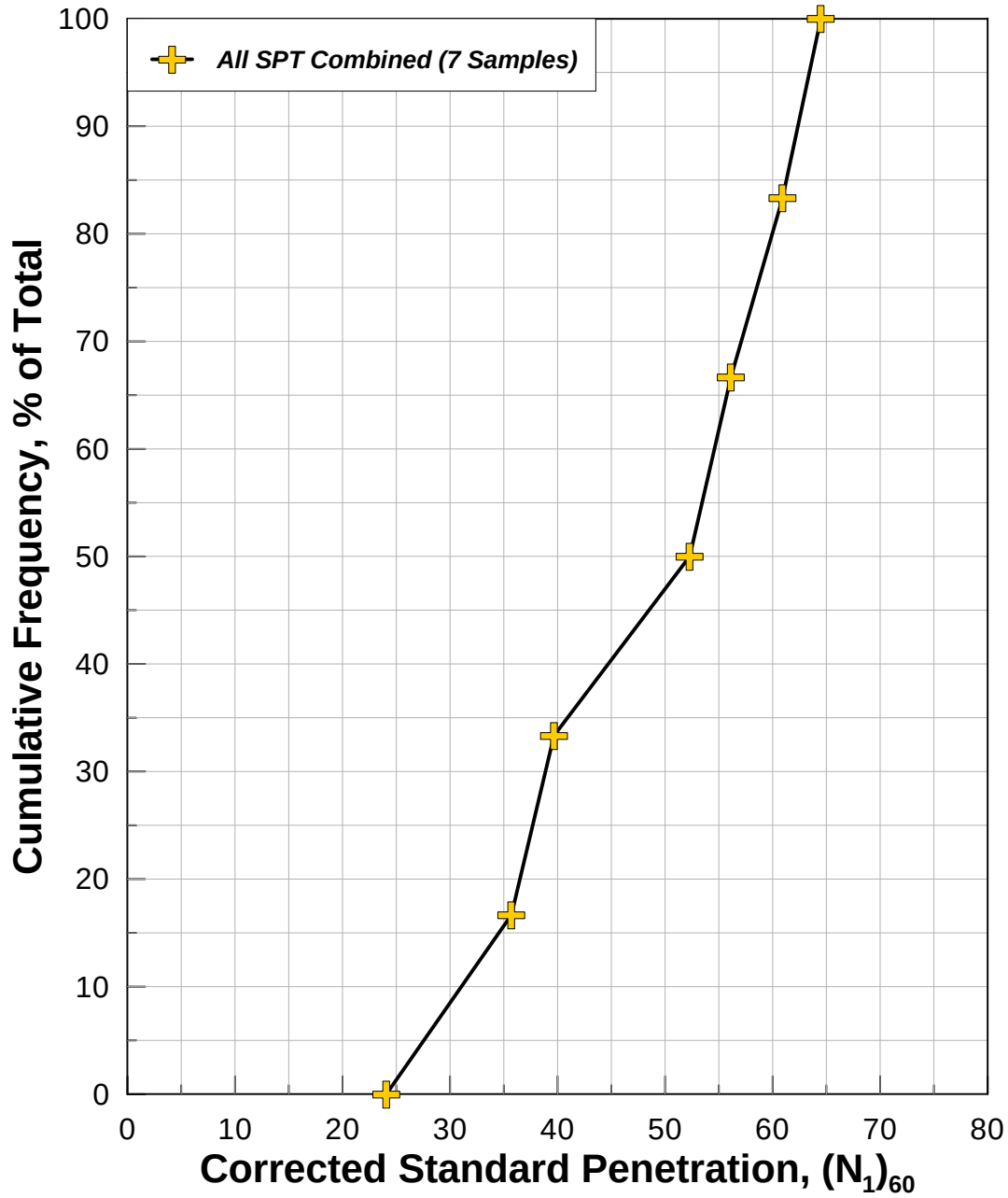

TERRA / GeoPentech
a Joint Venture

$(N_1)_{60}$ BY SPT - ALLUVIUM
STEVENS CREEK DAM
SEISMIC STABILITY EVALUATIONS (SSE2)

Figure
5-20

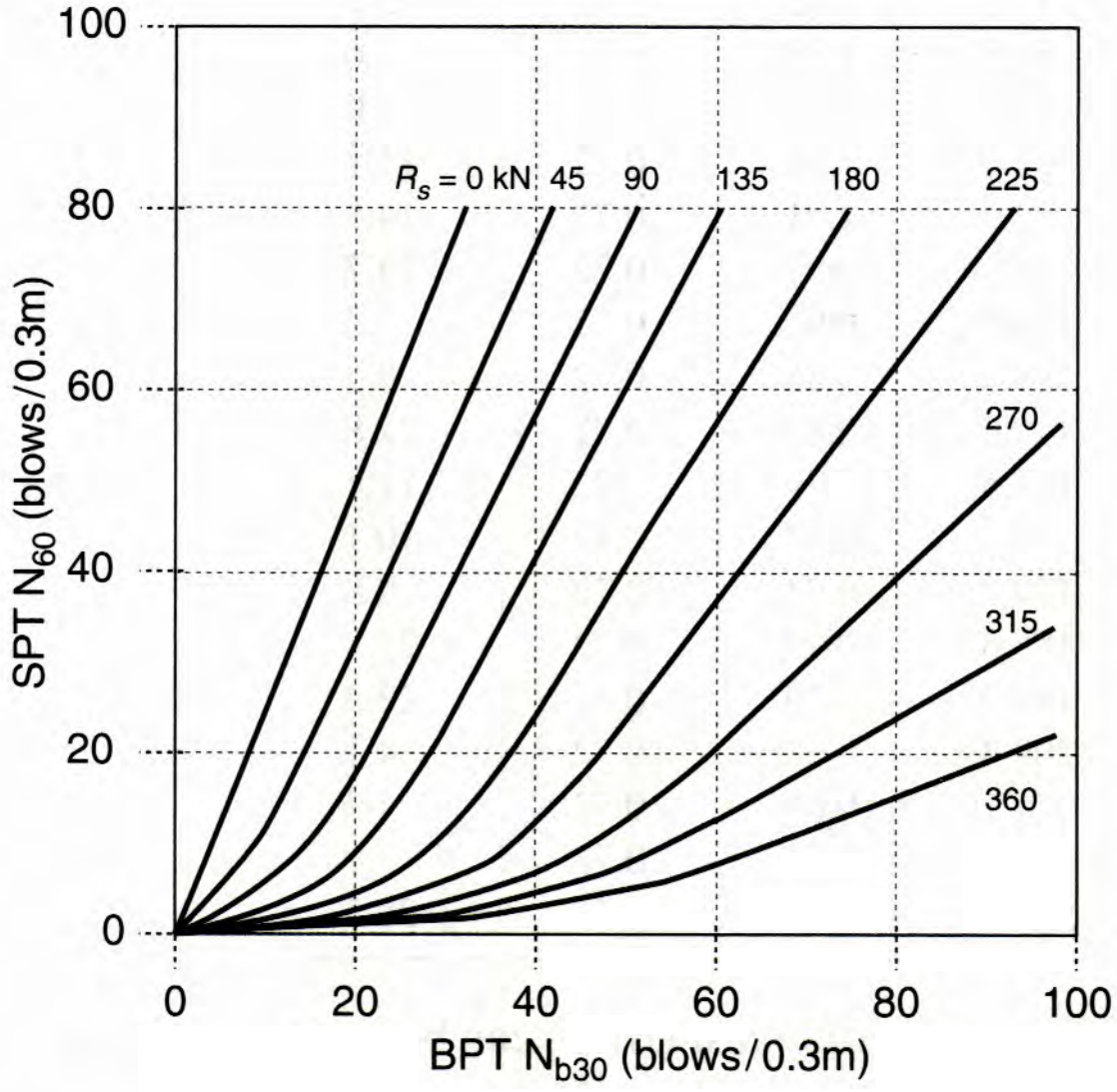

After Sy and Campanella (1984)

TERRA / GeoPentech a Joint Venture	SY AND CAMPANELLA RELATIONSHIP BETWEEN BPT AND SPT AND R_S SEISMIC STABILITY EVALUATIONS (SSE2)	Figure 5-21

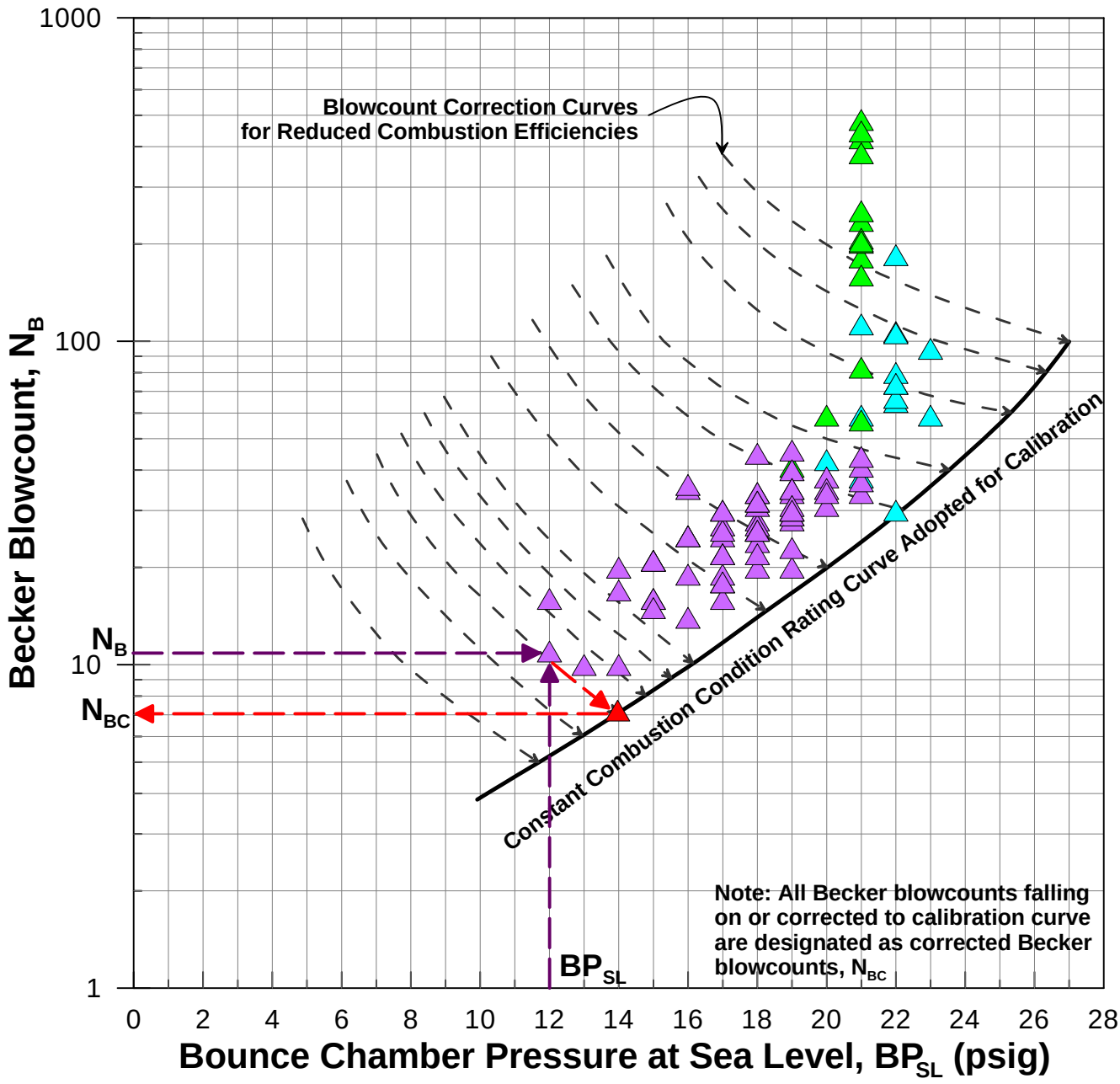

Alluvium Upper Access Road (14Tests), Avg. N_B = 272

Alluvium Lower Access Road (14Tests), Avg. N_B = 80

Alluvium at D.S. Toe (67Tests), Avg. N_B = 27

N_B

N_{BC}

Example on Actual Data Point

TERRA / GeoPentech
a Joint Venture

BPT DATA - ALLUVIUM
STEVENS CREEK DAM
SEISMIC STABILITY EVALUATIONS (SSE2)

Figure
5-22

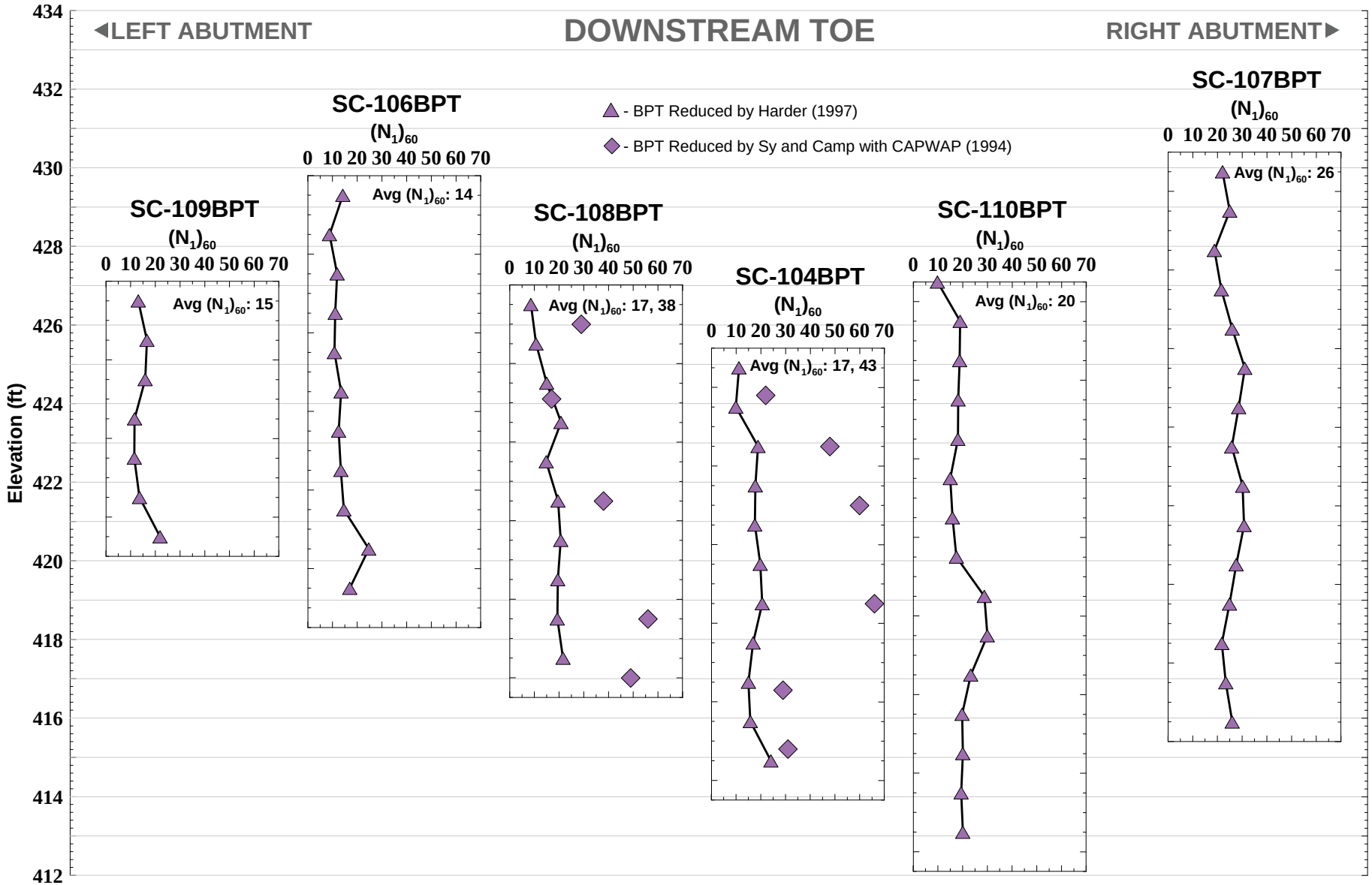

TERRA / GeoPentech
a Joint Venture

BPT DATA AT TOE - ALLUVIUM
STEVENS CREEK DAM
SEISMIC STABILITY EVALUATIONS (SSE2)

Figure
5-23

Rev. 2 04/20/2012 SSE2-R-2SC

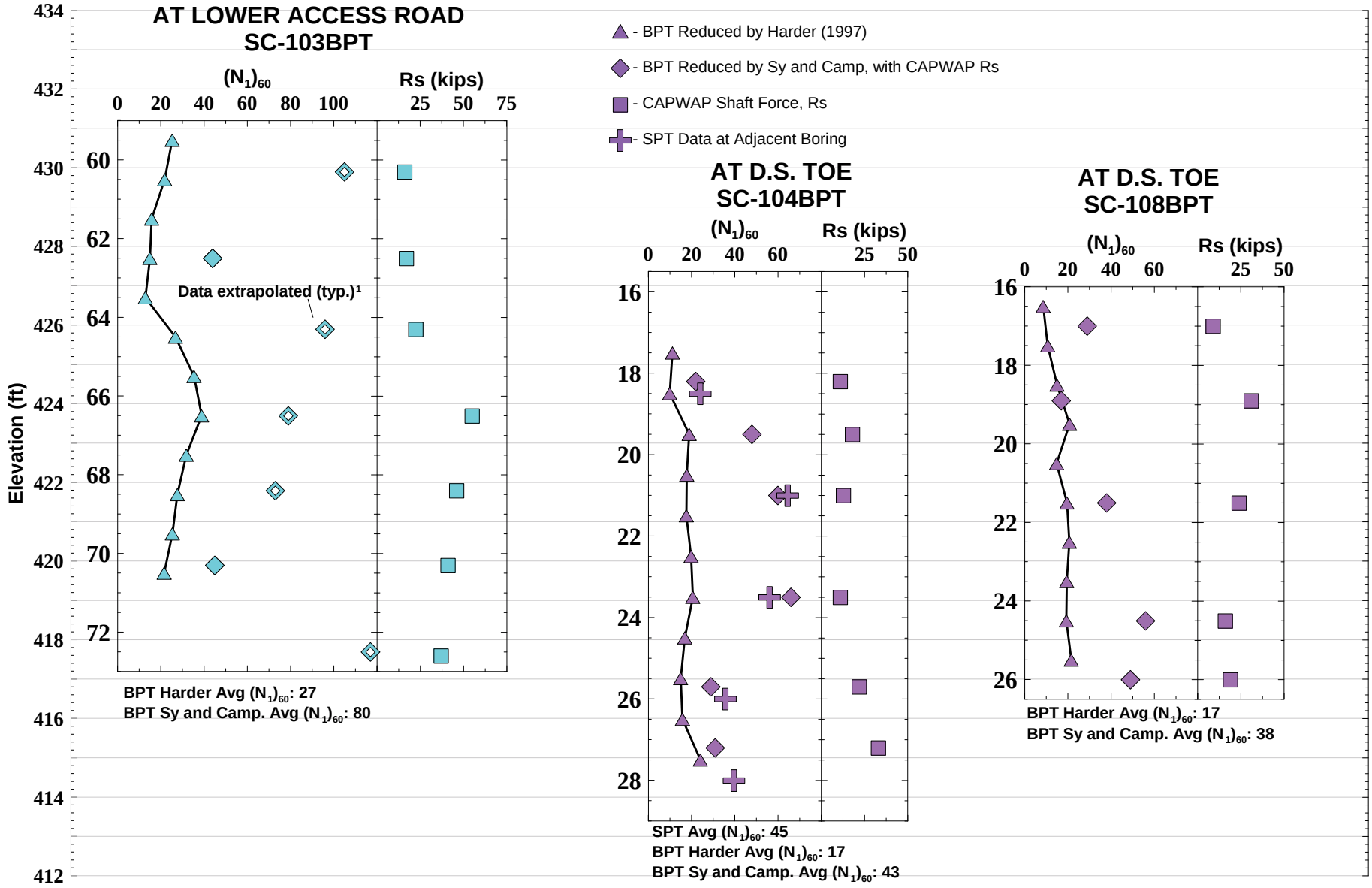

1. Data extrapolated (typ.) due to values falling beyond upper limit of Sy and Campanella curves.

TERRA / GeoPentech
a Joint Venture

$(N_1)_{60}$ PROFILES FOR BORINGS WITH PDA MEASUREMENTS - STEVENS CREEK DAM
SEISMIC STABILITY EVALUATIONS (SSE2)

Figure 5-24

Rev. 1 04/20/2012 SSE2-R-2SC

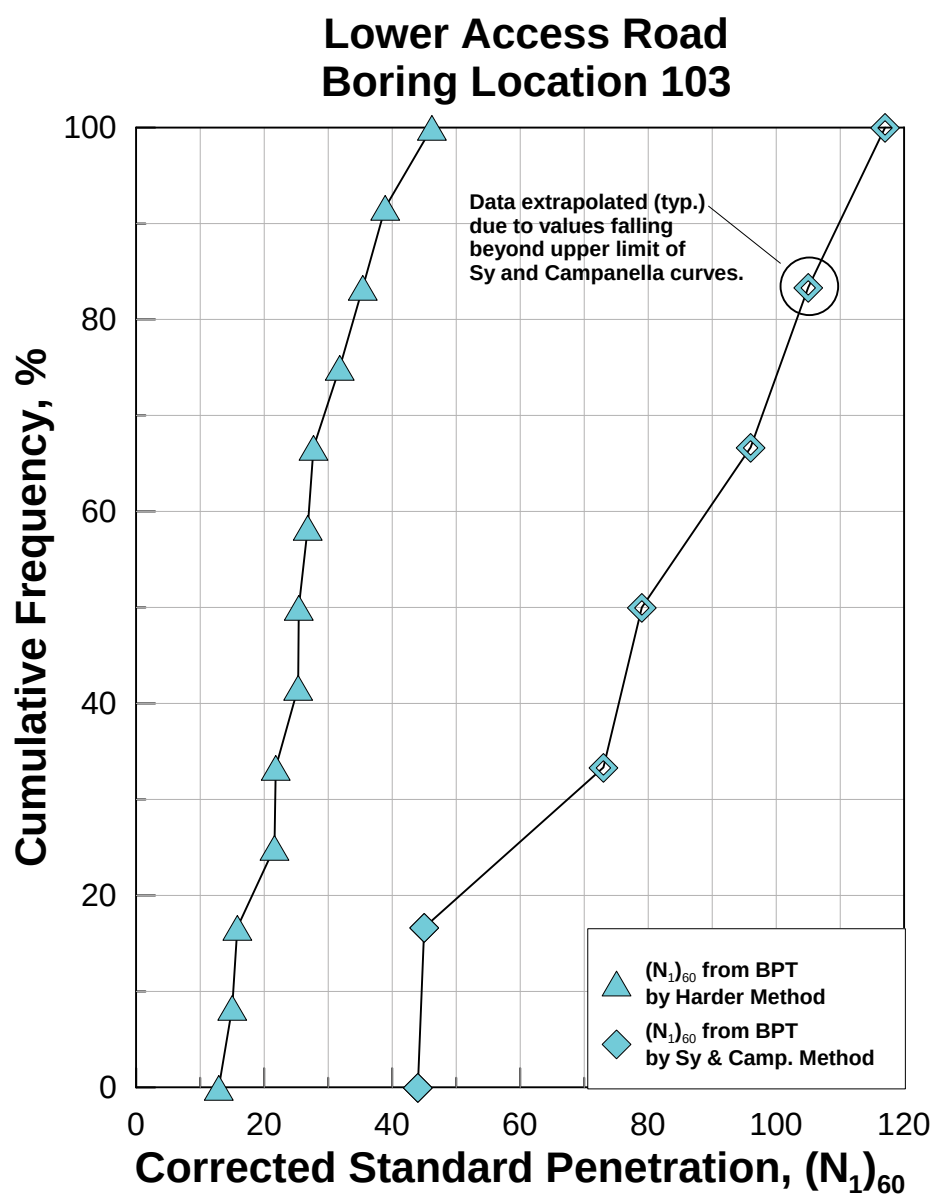

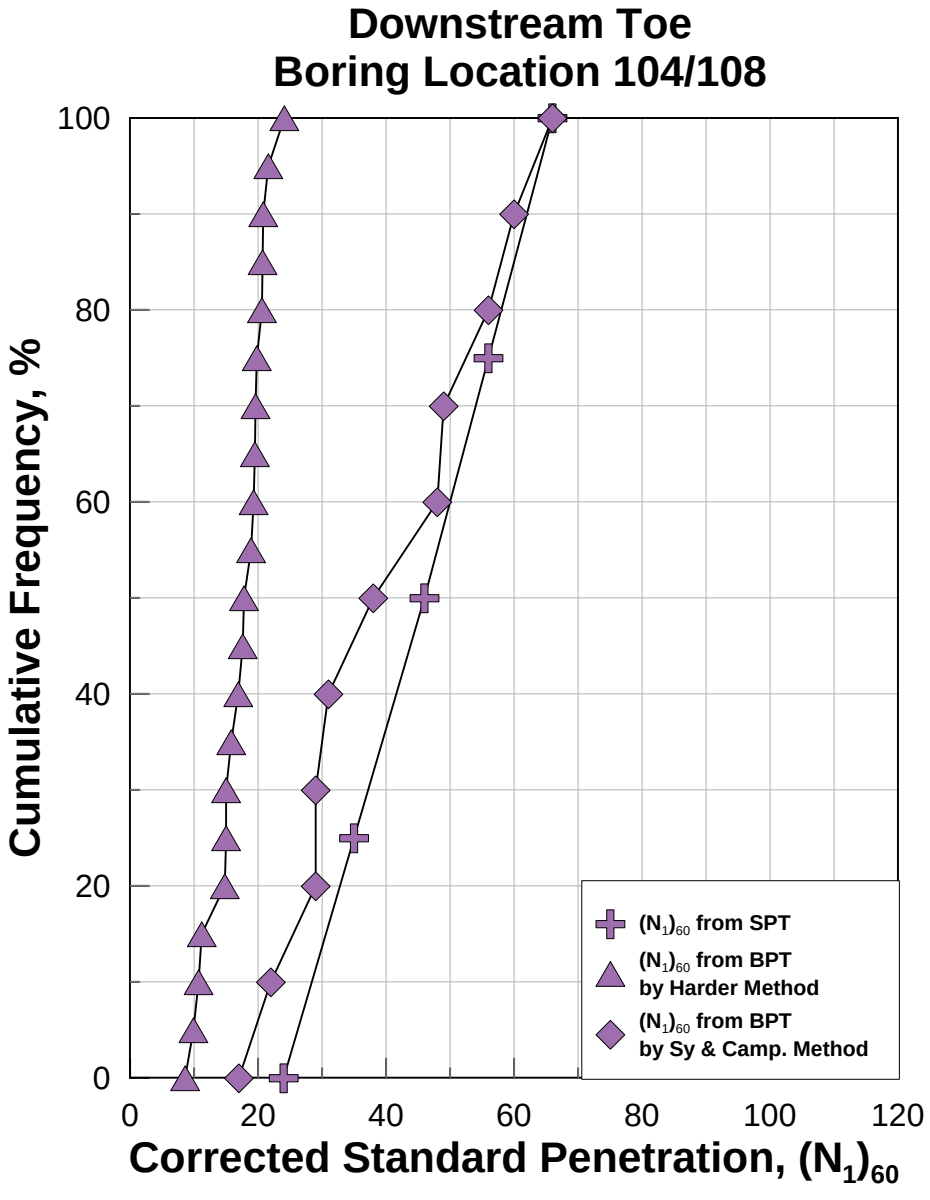

Note: Symbols on distribution lines represent total number of tests.

TERRA / GeoPentech
a Joint Venture

CUMULATIVE FREQUENCY PLOTS COMPARING $(N_1)_{60}$ FROM BPTs AND SPTs - STEVENS CREEK DAM SEISMIC STABILITY EVALUATIONS (SSE2)

Figure 5-25

Rev. 1 04/20/2012 SSE2-R-2SC

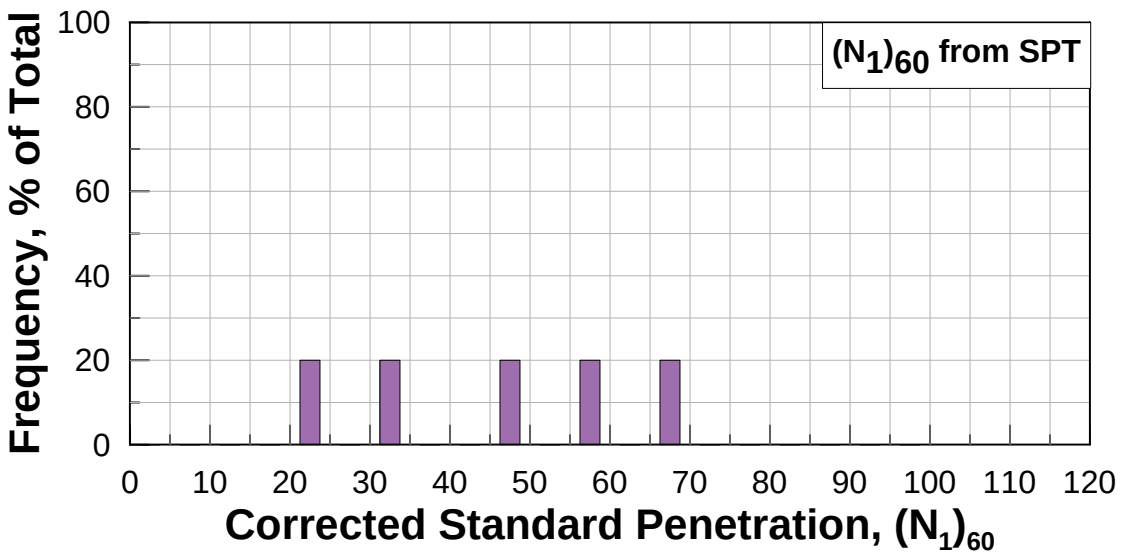

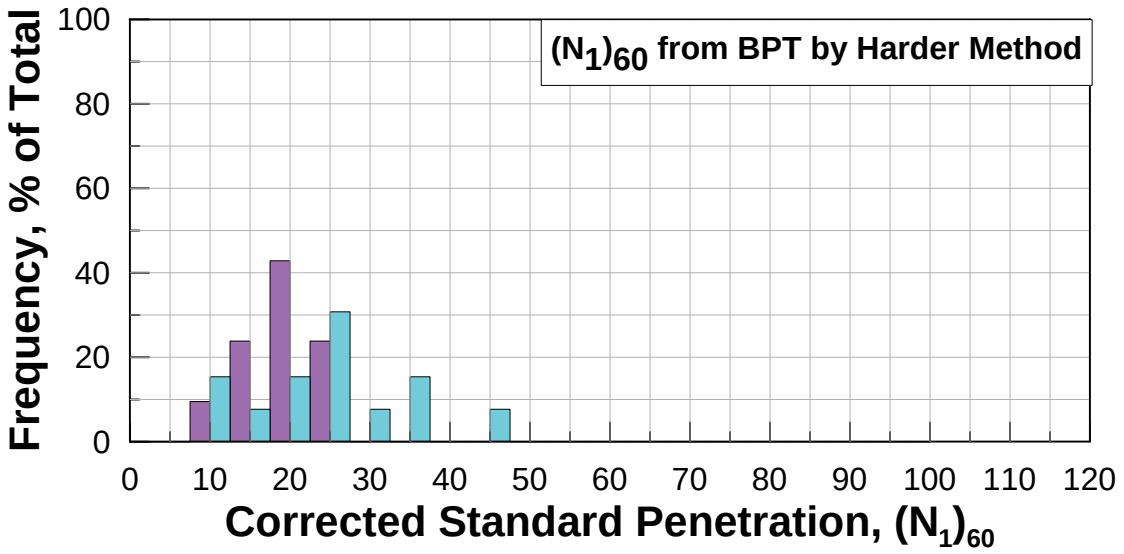

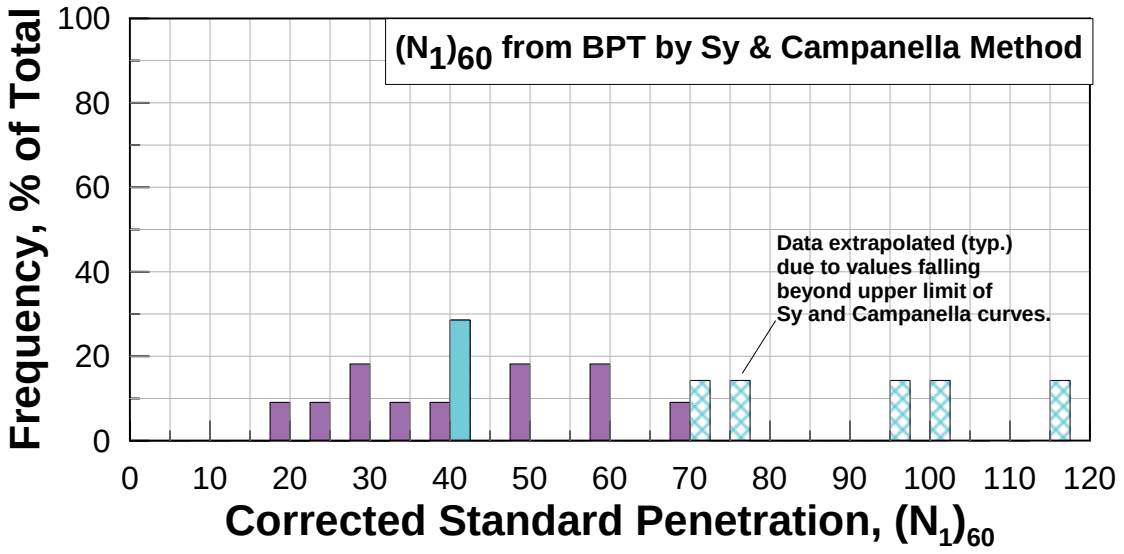

Rev. 1 04/20/2012 SSE2-R-2SC

TERRA / GeoPentech
a Joint Venture

FREQUENCY PLOTS (HISTOGRAMS) COMPARING $(N_1)_{60}$ FROM BPTs AND SPTs - STEVENS CREEK DAM SEISMIC STABILITY EVALUATIONS (SSE2)

Figure 5-26

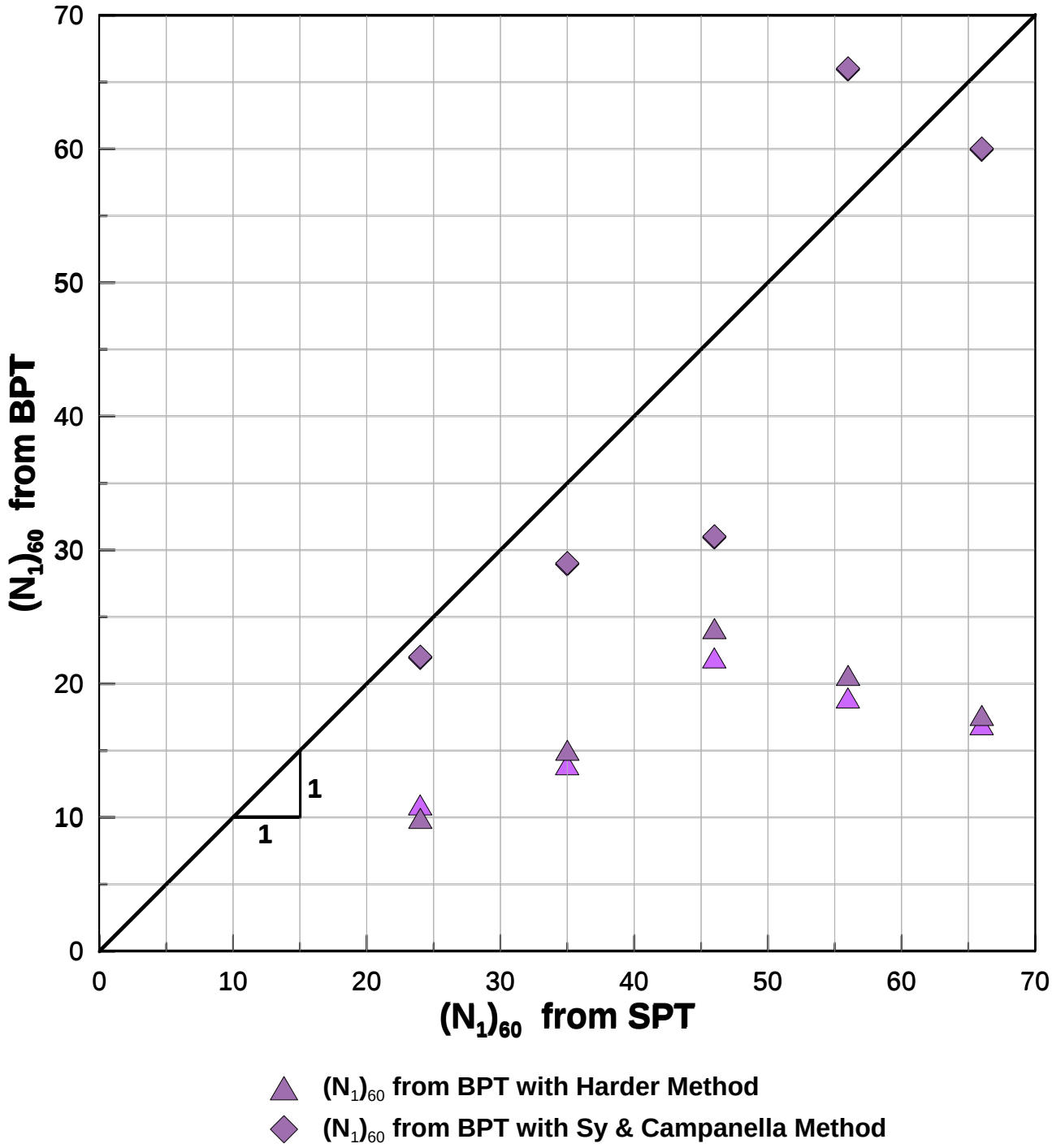

TERRA / GeoPentech
a Joint Venture

POINT BY POINT COMPARISON OF $(N_1)_{60}$ VALUES FROM BPTs AND SPTs - STEVENS CREEK DAM SEISMIC STABILITY EVALUATIONS (SSE2)

Figure 5-27

Rev. 1 04/20/2012 SSE2-R-2SC

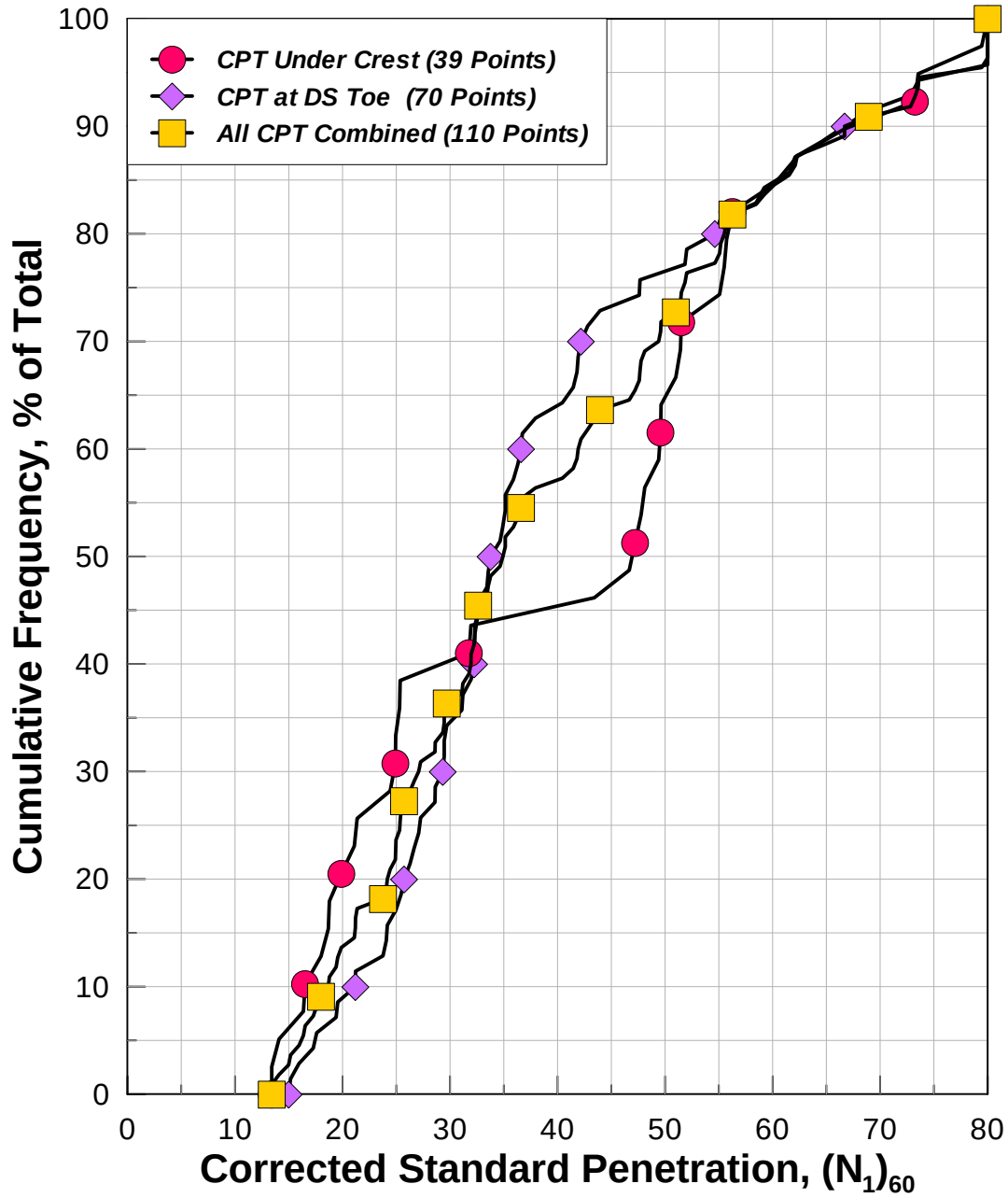

Note: Symbols on distribution lines indicate data set only, total number of tests is indicated in legend.

TERRA / GeoPentech
a Joint Venture

CPT INFERRED $(N_1)_{60}$ - ALLUVIUM
STEVENS CREEK DAM
SEISMIC STABILITY EVALUATIONS (SSE2)

Figure
5-28

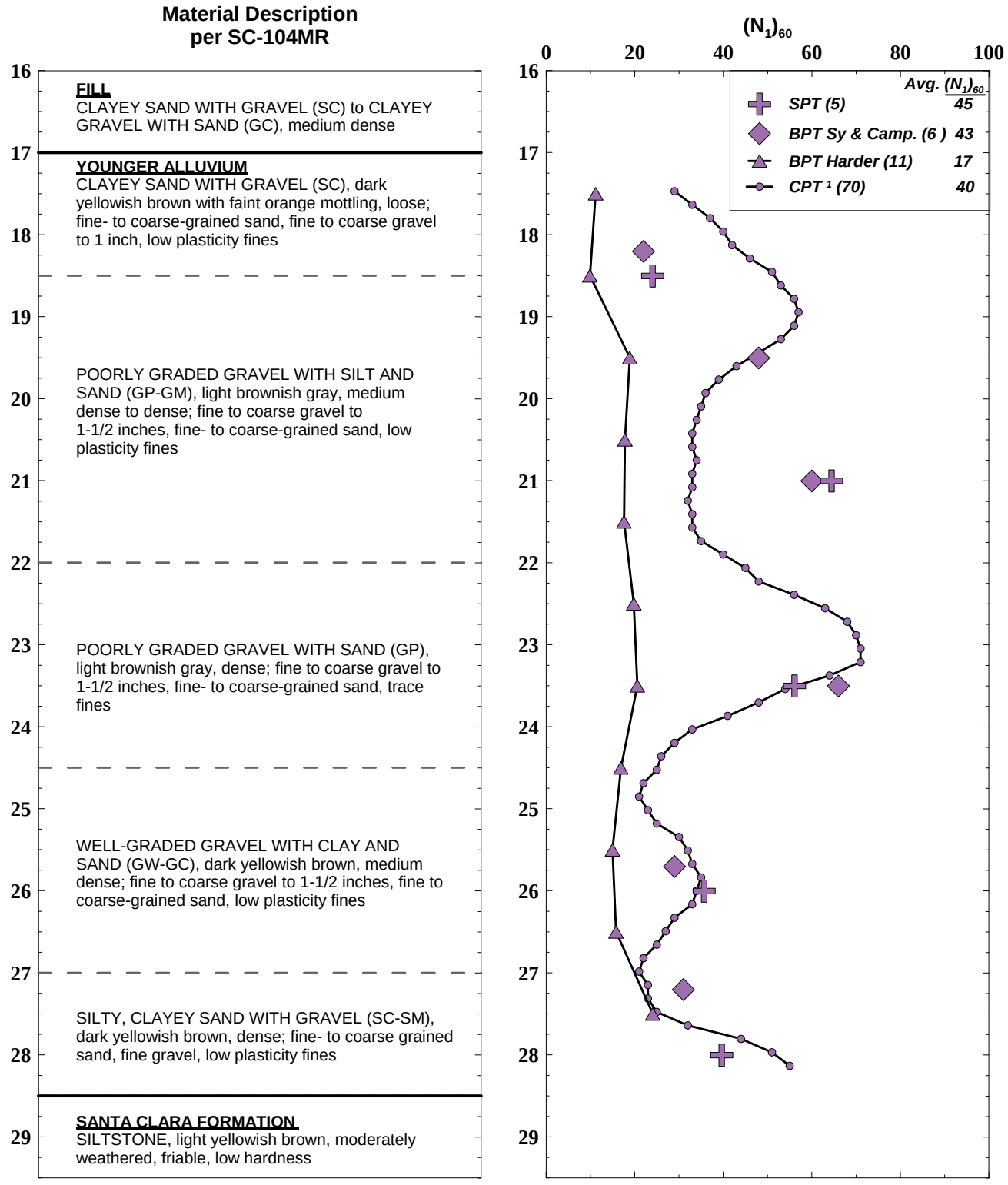

Notes:
1. CPT data has been screened for influence of gravel per consultation with Dr. Robertson, screened points are plotted in gray for comparison.
2. BPT data reduced following the procedure developed by Sy and Campanella (1994) used Rs based on results of CAPWAP Analyses.

TERRA / GeoPentech
a Joint Venture

$(N_1)_{60}$ COMPARISON AT SC-104
STEVENS CREEK DAM
SEISMIC STABILITY EVALUATIONS (SSE2)

Figure
5-29

Rev. 2 04/20/2012 SSE2-R-2SC

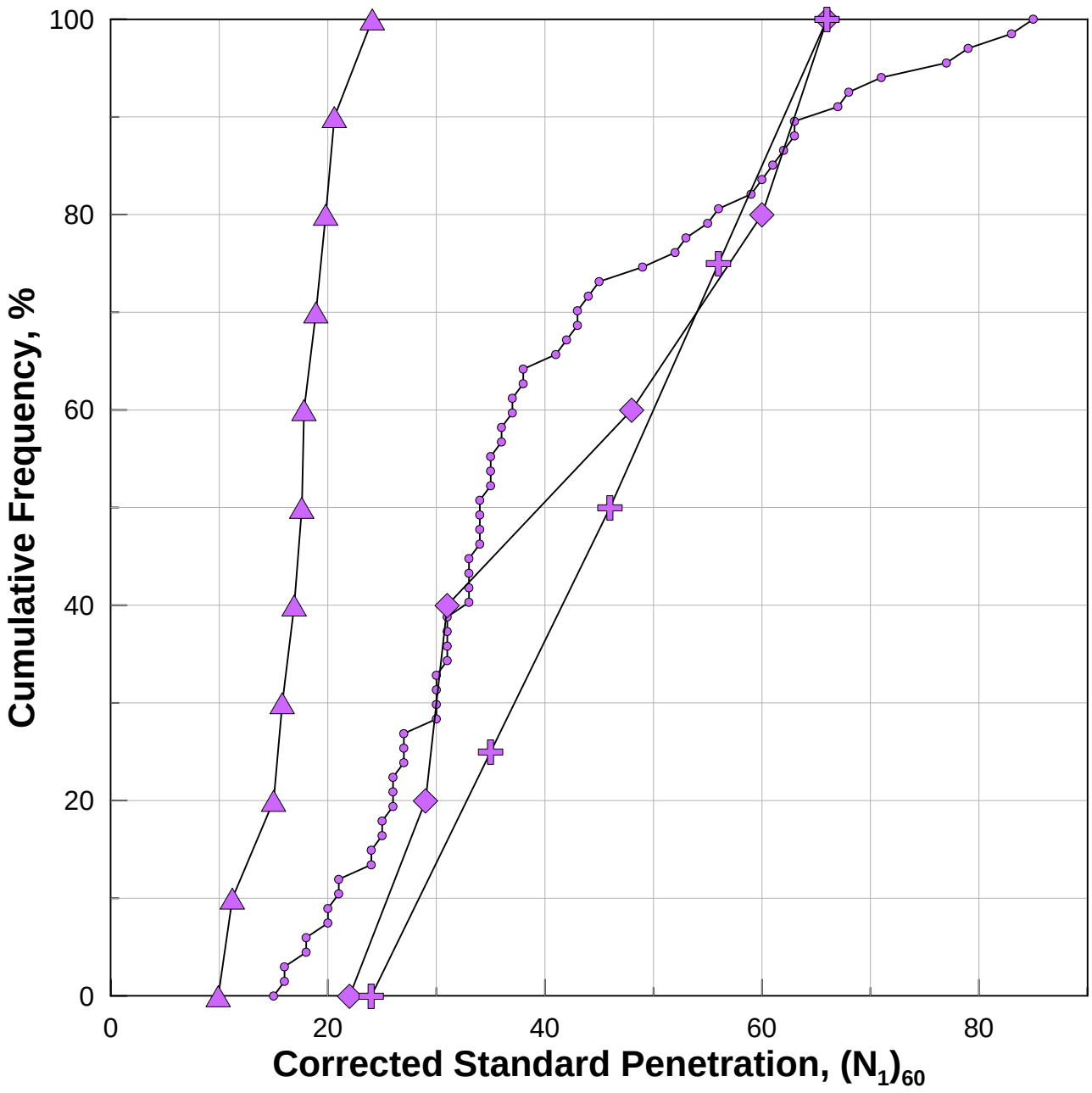

Note: Number of data points shown after data description

TERRA / GeoPentech
a Joint Venture

CUMULATIVE FREQUENCY PLOTS COMPARISON OF $(N_1)_{60}$ AT SC-104 - STEVENS CREEK DAM
SEISMIC STABILITY EVALUATIONS (SSE2)

Figure 5-30

Rev. 1 04/20/2012 SSE2-R-2SC

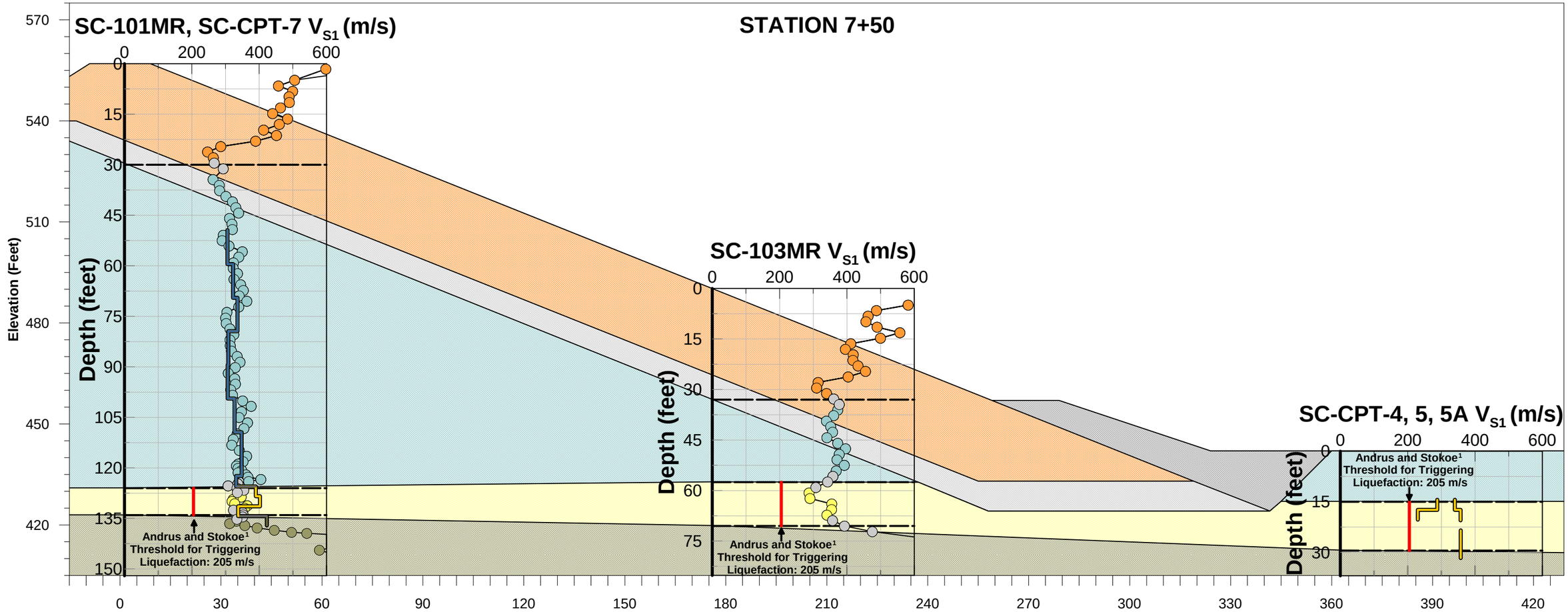

Alluvium - Normalized Shear Wave Velocity Data Summary

	Dam Crest		Downstream Slope		Downstream Toe	
	ID	Average V_{S1} (m/s)	ID	Average V_{S1} (m/s)	ID	Average V_{S1} (m/s)
OYO Measurements	SC-101MR	339	SC-103MR	325	--	--
CPT Measurments	SC-CPT-7	376	--	--	SC-CPT-4	259
					SC-CPT-5	347
					SC-CPT-5A	357
Weighted Average:		360		325		321

Oyo Measurements
- *DS Buttress*
- *DS Shell*
- *Alluvium*
- *Bedrock*
- *Overlapping Vs Measurements*

CPT Measurements
- *CPT DS Shell*
- *CPT Alluvium*
- *CPT Bedrock*
- *CPT Overlaping Vs Measurments*

LEGEND
- ORIGINAL DOWNSTREAM EMBANKMENT
- DOWNSTREAM BUTTRESS - CONSTRUCTED IN 1985
- FILTER/DRAIN MATERIAL
- RIP RAP AT DOWNSTREAM TOE
- YOUNGER ALLUVIUM (Qya)
- BEDROCK - SANTA CLARA FORMATION

Notes: 1. From Andrus, R. D., and Stokoe, K. H., 2000. Liquefaction Resistance of Soils from Shear-Wave Velocity, *J. Geotechnical and Geoenvironmental Eng.*, ASCE 126(11), 1015-1025

TERRA / GeoPentech
a Joint Venture

MAXIMUM SECTION WITH NORMALIZED V_S DATA - STEVENS CREEK DAM
SEISMIC STABILITY EVALUATIONS (SSE2)

Figure 5-31

Rev. 1 11/28/2011 SSE2-R-2SC

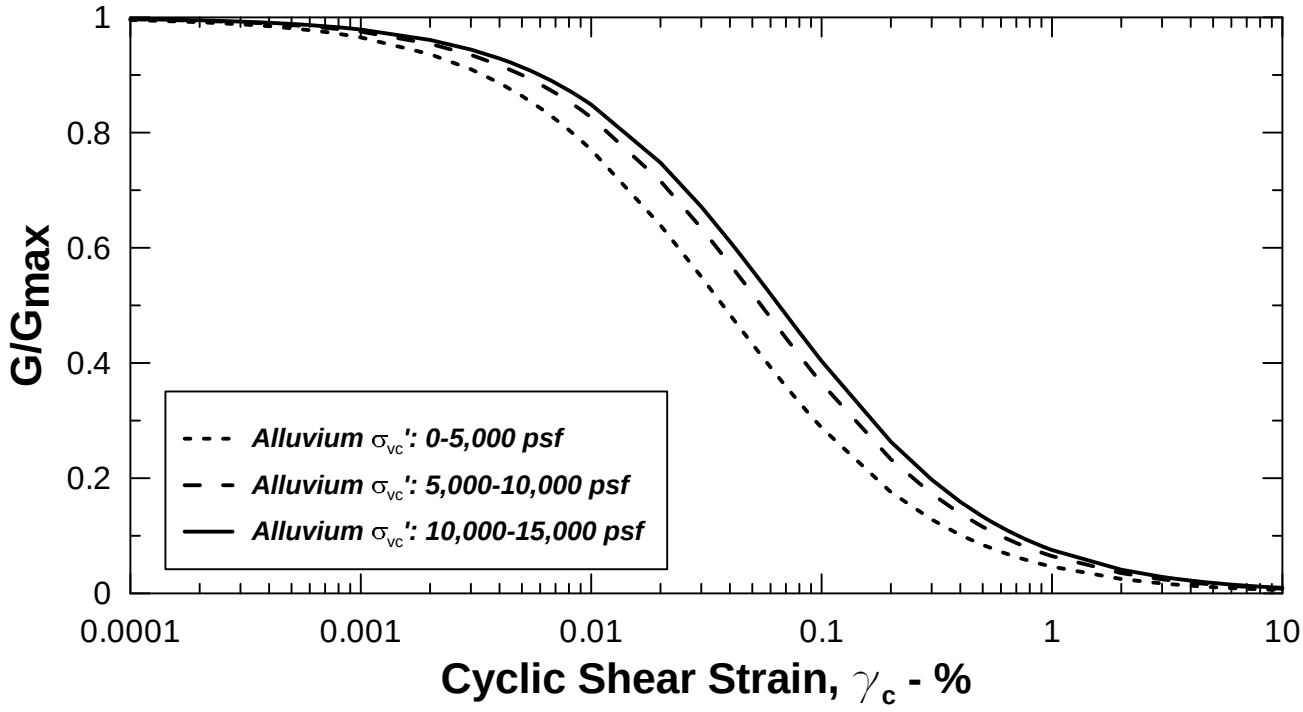

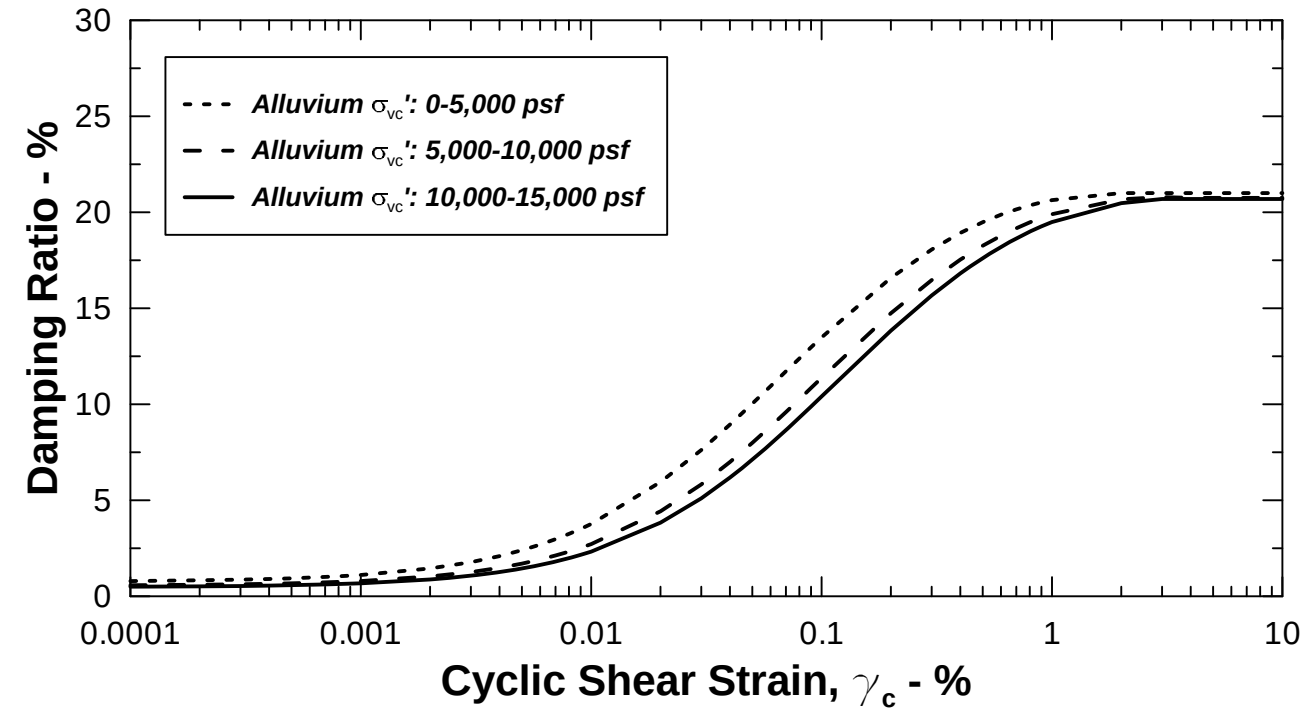

Note: Modulus reduction and damping ratio curves are based on Darendeli and Stokoe, 2001

TERRA / GeoPentech a Joint Venture	MODULUS REDUCTION & DAMPING RATIO ALLUVIUM - STEVENS CREEK DAM SEISMIC STABILITY EVALUATIONS (SSE2)	Figure 5-32

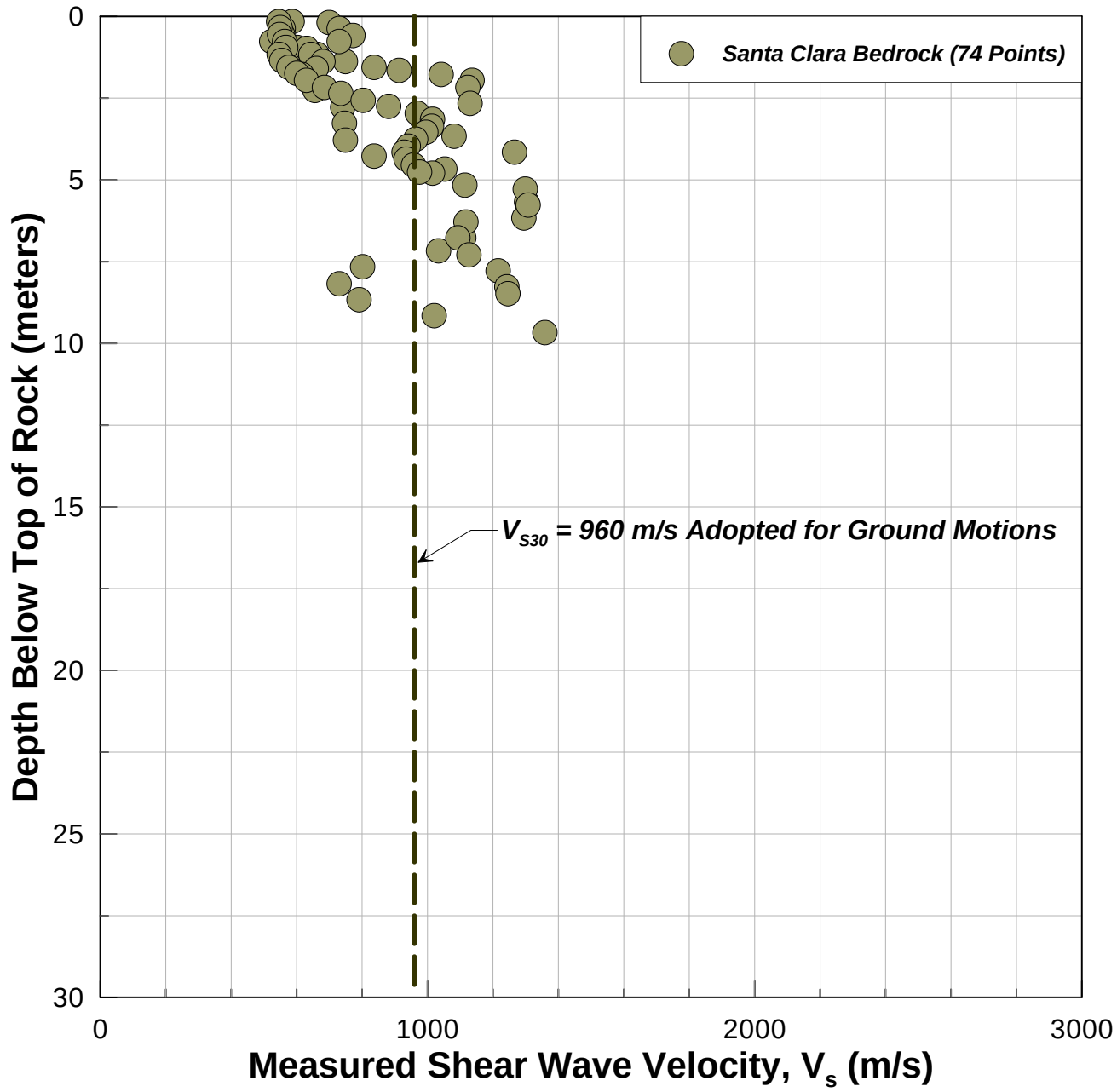

TERRA / GeoPentech
a Joint Venture

BEDROCK SHEAR WAVE VELOCITY DATA
STEVENS CREEK DAM
SEISMIC STABILITY EVALUATIONS (SSE2)

Figure
6-1

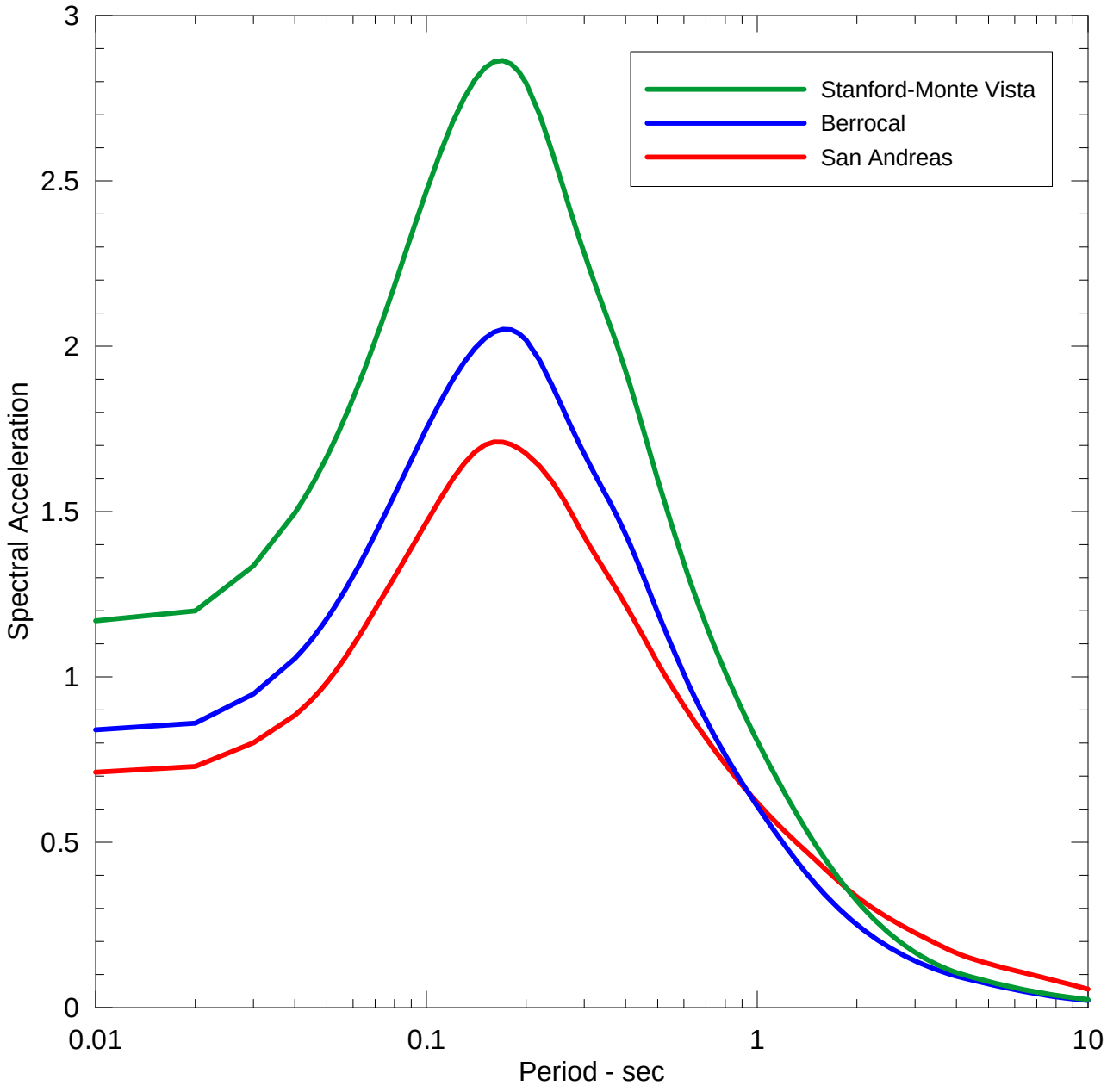

TERRA / GeoPentech
a Joint Venture

FAULT PARALLEL (FP) RESPONSE SPECTRA
STEVENS CREEK DAM
SEISMIC STABILITY EVALUATIONS (SSE2)

Figure
6-2

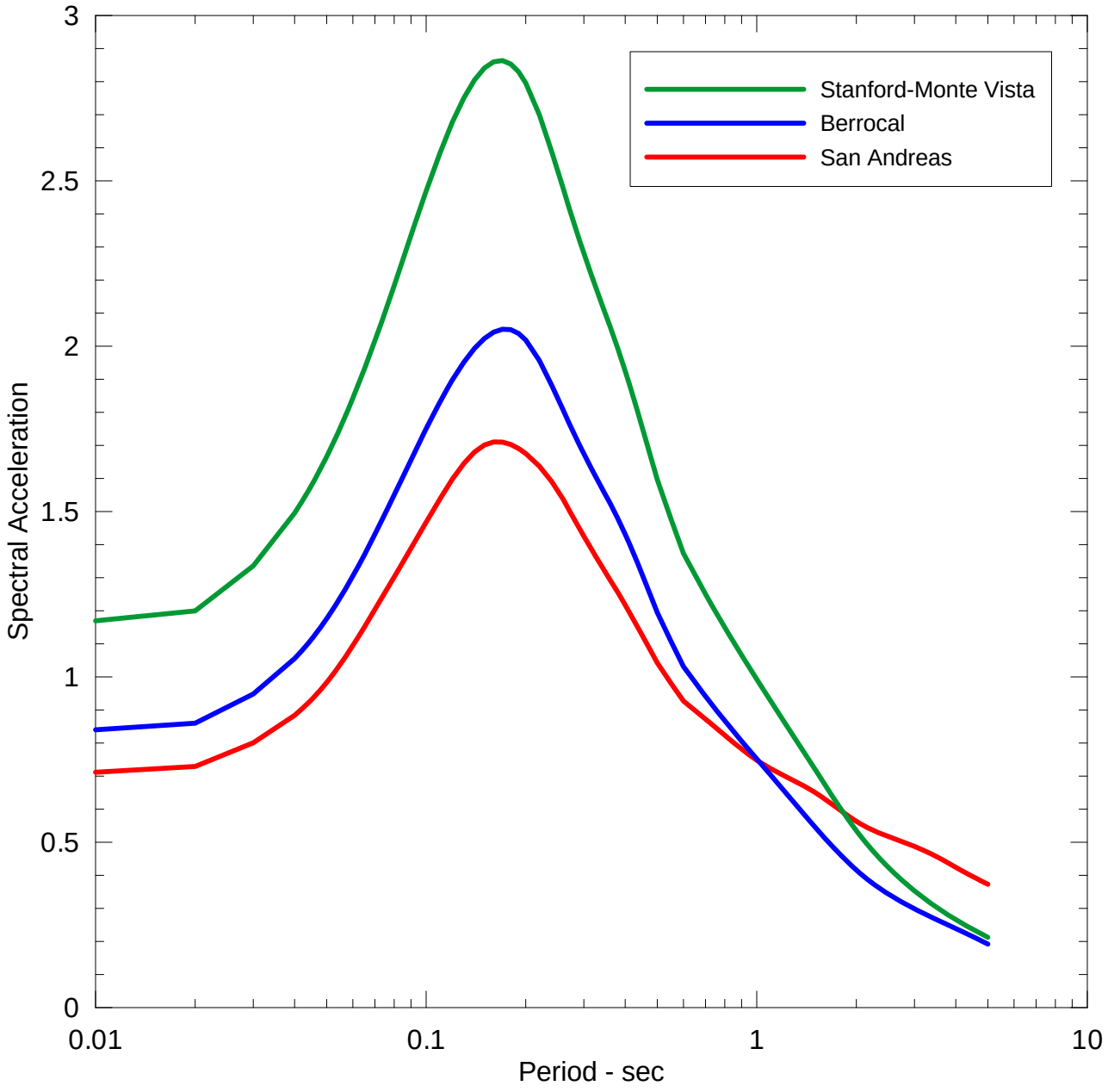

TERRA / GeoPentech
a Joint Venture

FAULT NORMAL (FN) RESPONSE SPECTRA
STEVENS CREEK DAM
SEISMIC STABILITY EVALUATIONS (SSE2)

Figure
6-3

Rev. 0 04/20/2011 SSE2-R-2SC

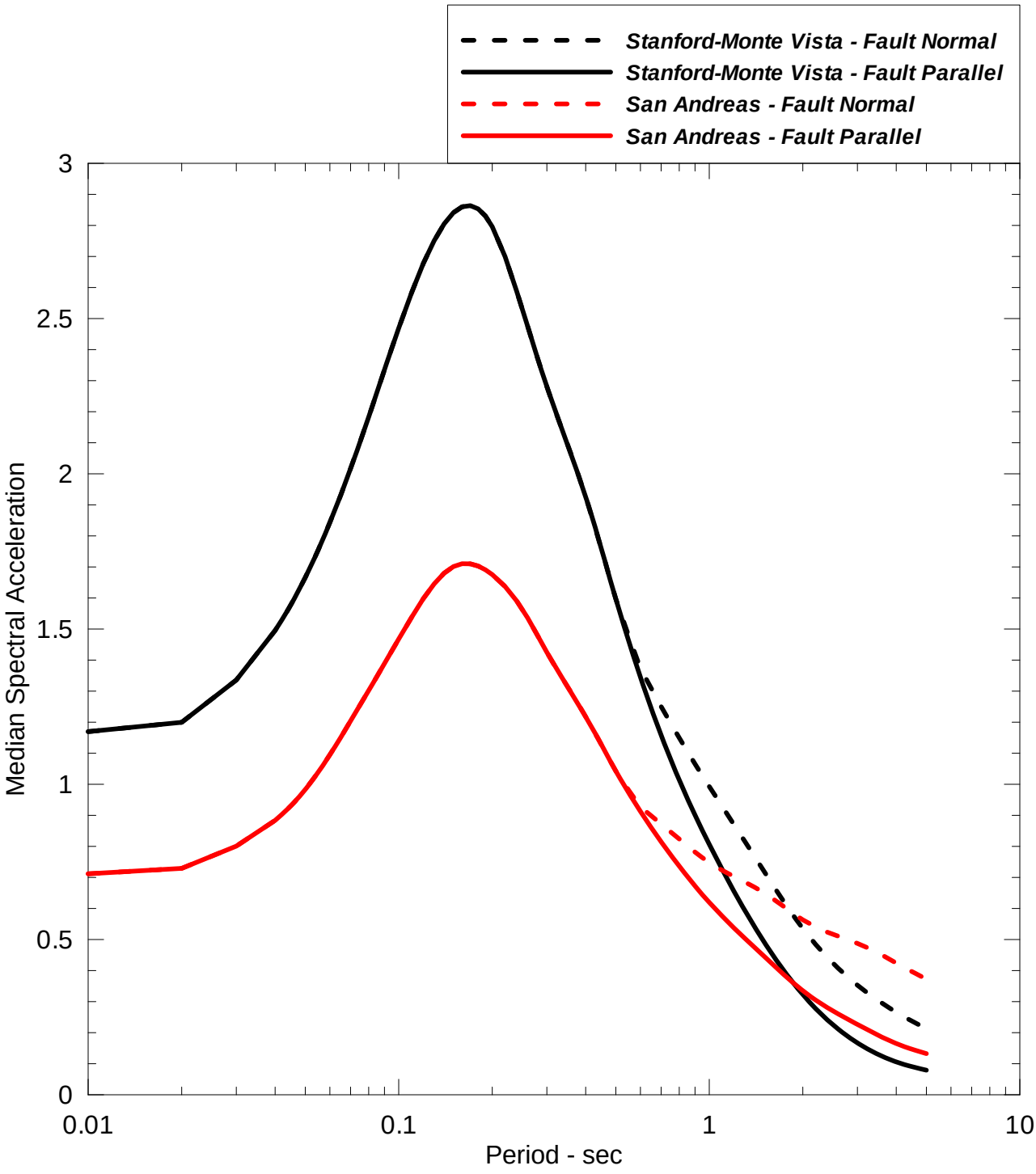

TERRA / GeoPentech
a Joint Venture

RECOMMENDED RESPONSE SPECTRA
STEVENS CREEK DAM
SEISMIC STABILITY EVALUATIONS (SSE2)

Figure
6-4

Rev. 1 06/09/2011 SSE2-R-2SC

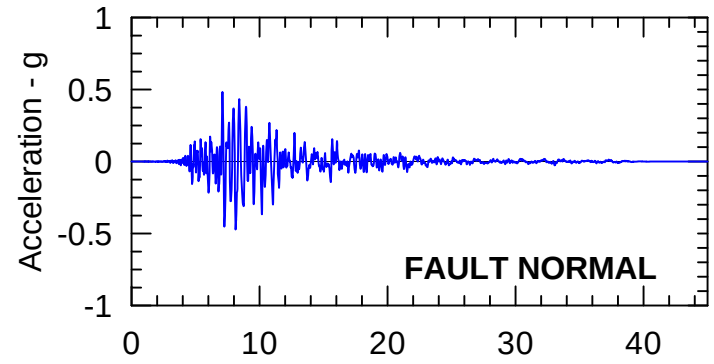

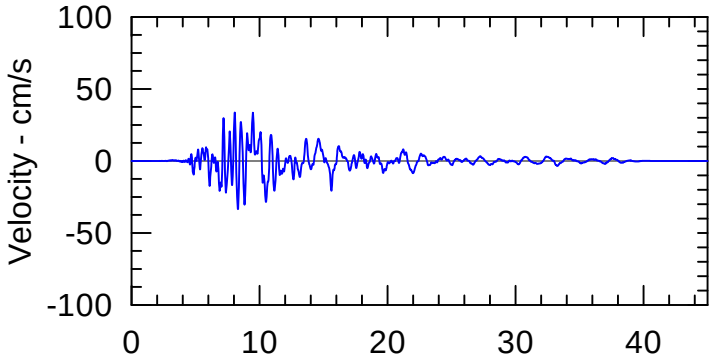

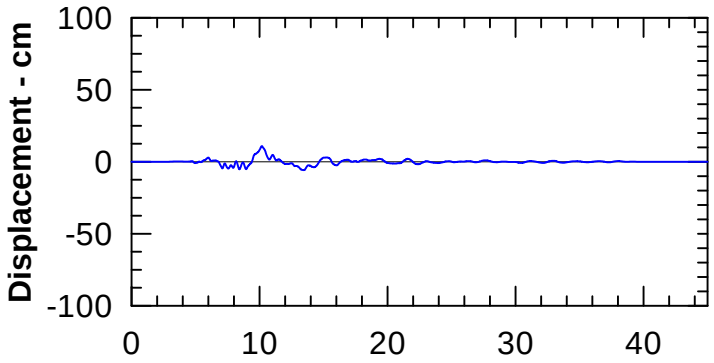

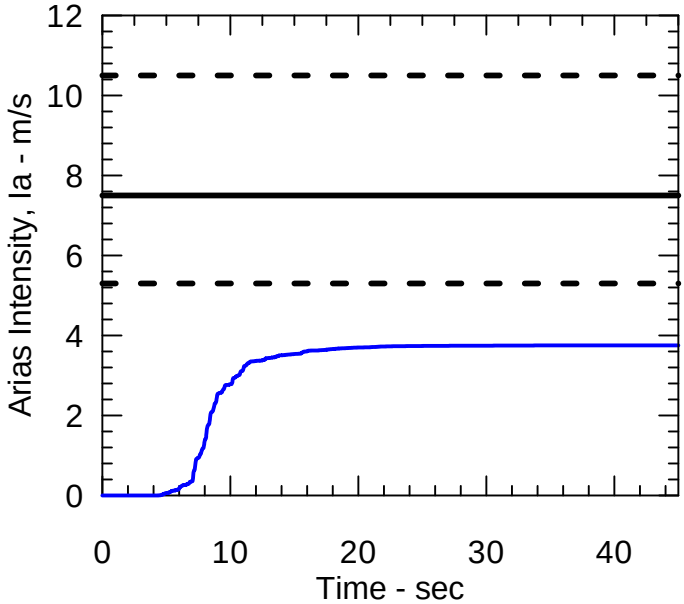

Kobe - Nishi-Akashi
Strike Slip Event
Rotated to Fault Normal

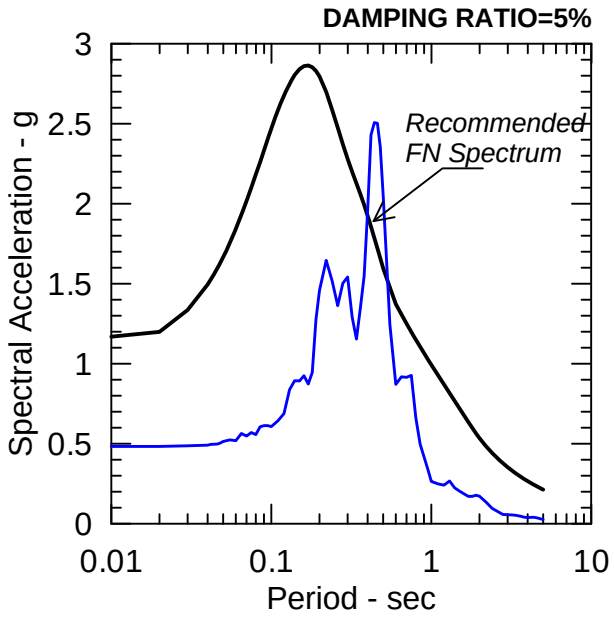

Watson-Lamprey Ia plus σ

Ia from Watson-Lamprey (2007)
@84th Percentile [7.5 m/s]

Watson-Lamprey Ia minus σ

Rev. 1 06/09/2011 SSE2-R-2SC

TERRA / GeoPentech
a Joint Venture

CHARACTERISTICS OF KOBE E/Q,
NISHI-AKASHI (FN) RECORD
SEISMIC STABILITY EVALUATIONS (SSE2)

Figure
6-5

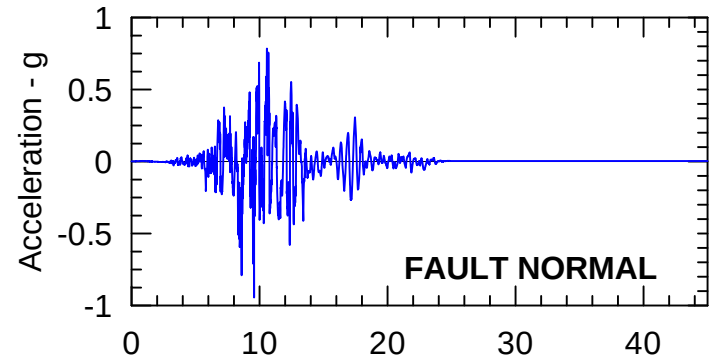

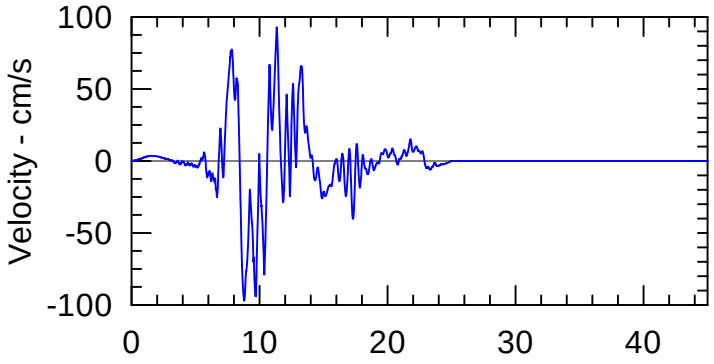

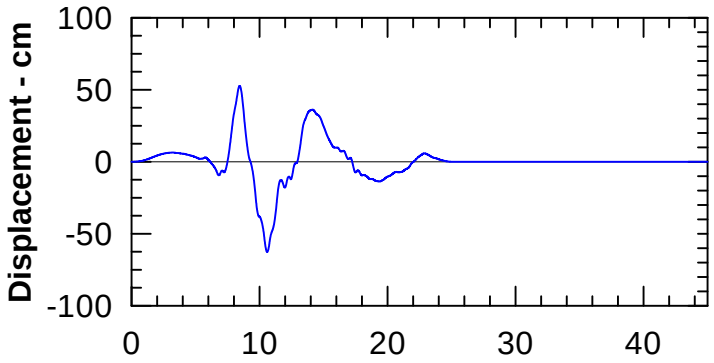

Loma Prieta - LGPC
Reverse Oblique Event
Rotated to Fault Normal

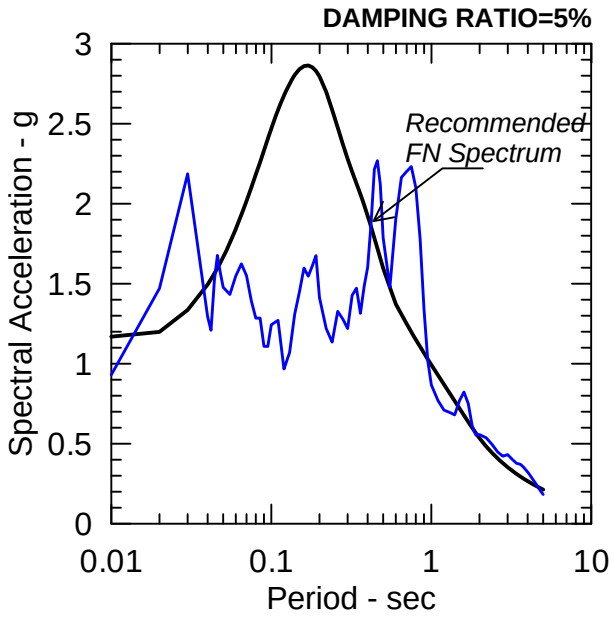

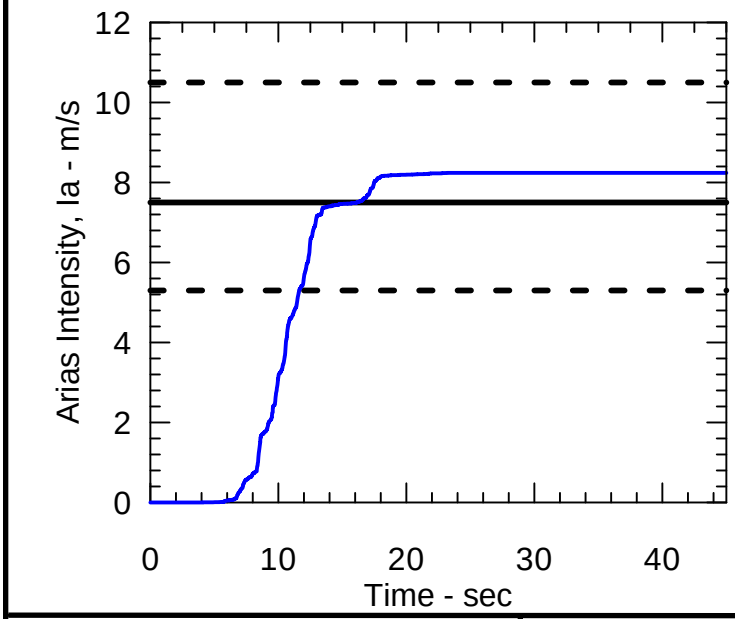

Watson-Lamprey Ia plus σ

Ia from Watson-Lamprey (2007)
@84th Percentile [7.5 m/s]

Watson-Lamprey Ia minus σ

TERRA / GeoPentech
a Joint Venture

CHARACTERISTICS OF LOMA PRIETA E/Q, LGPC (FN) RECORD
SEISMIC STABILITY EVALUATIONS (SSE2)

Figure
6-6

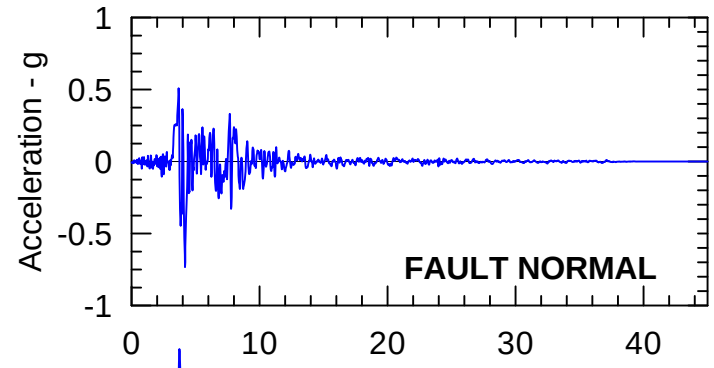

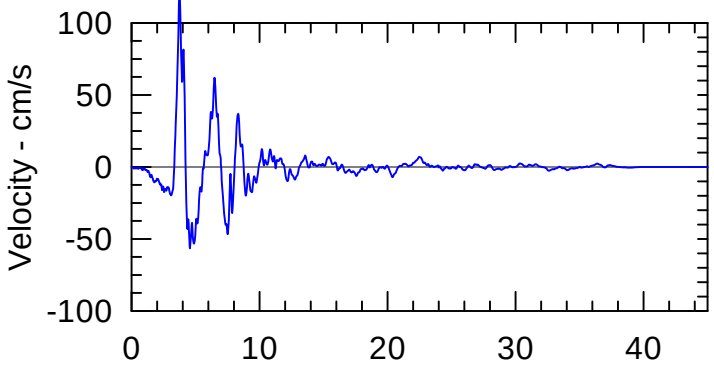

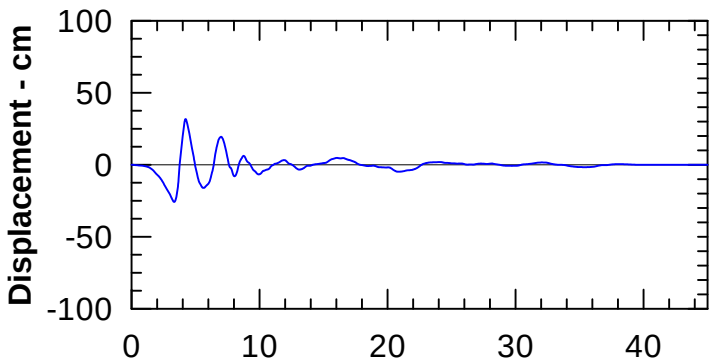

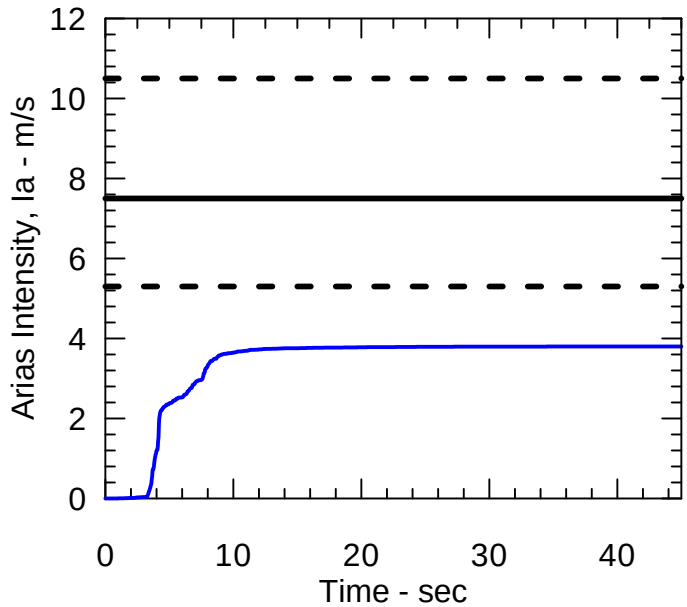

Northrigde - Sylmar
Reverse Event
Rotated to Fault Normal

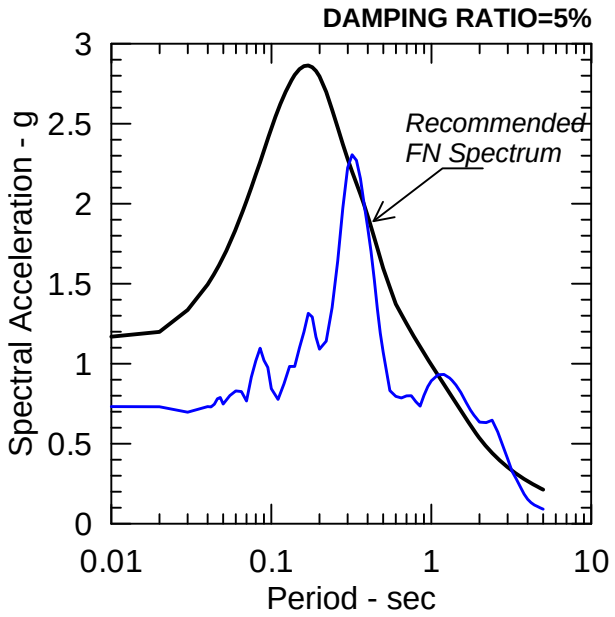

Watson-Lamprey Ia plus σ

Ia from Watson-Lamprey (2007)
@84th Percentile [7.5 m/s]

Watson-Lamprey Ia minus σ

Rev. 1 06/09/2011 SSE2-R-2SC

TERRA / GeoPentech
a Joint Venture

CHARACTERISTICS OF NORTHRIDGE E/Q,
SYLMAR COUNTY HOSP. (FN) RECORD
SEISMIC STABILITY EVALUATIONS (SSE2)

Figure
6-7

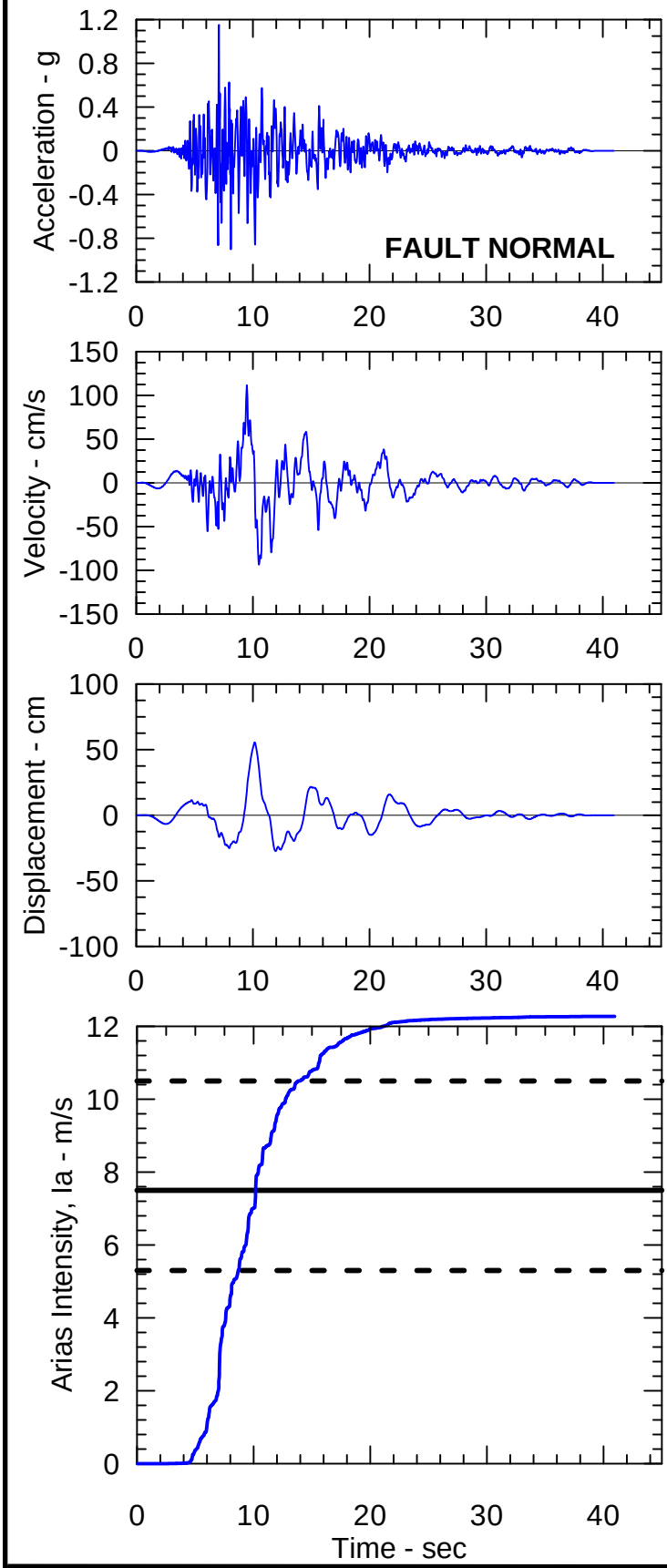

Kobe - Nishi-Akashi
Strike Slip Event
Matched to S-MV Event

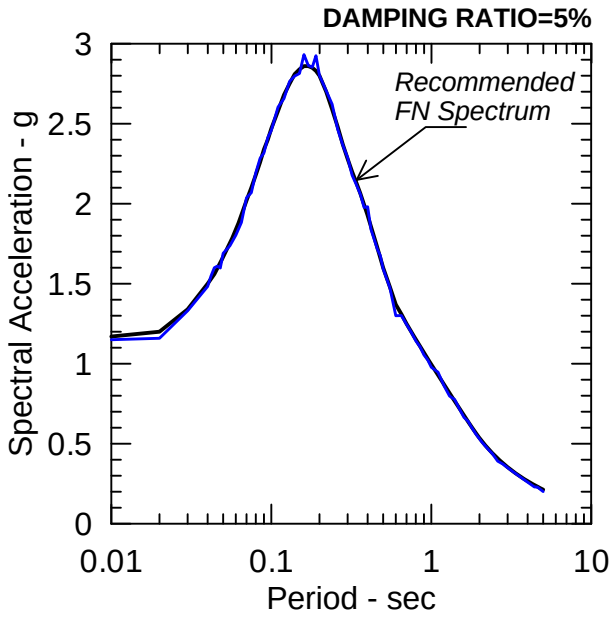

Rev. 0 06/09/2011 SSE2-R-2SC

TERRA / GeoPentech
a Joint Venture

SPECTRALLY MATCHED KOBE E/Q,
NISHI-AKASHI (FN) RECORD
SEISMIC STABILITY EVALUATIONS (SSE2)

Figure
6-8

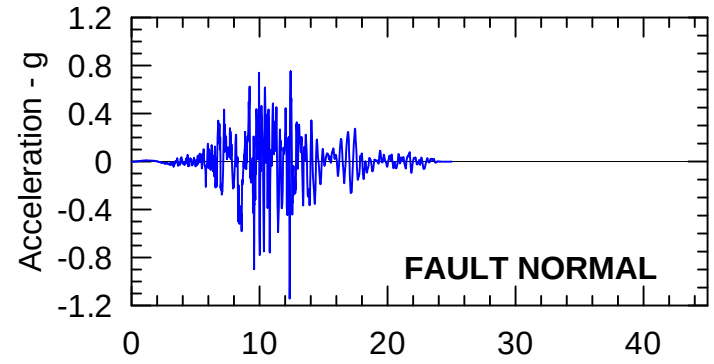

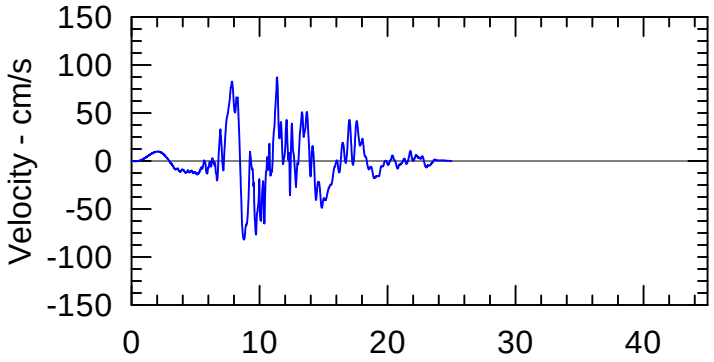

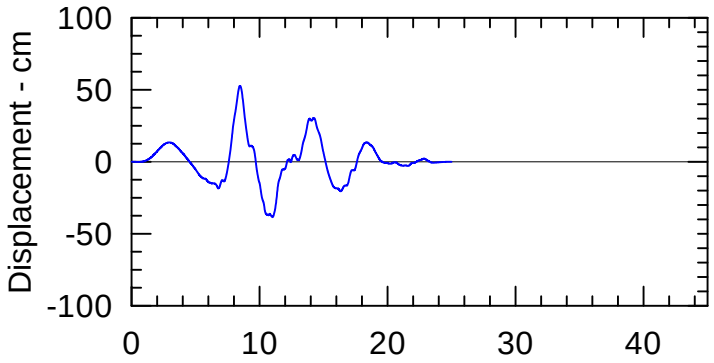

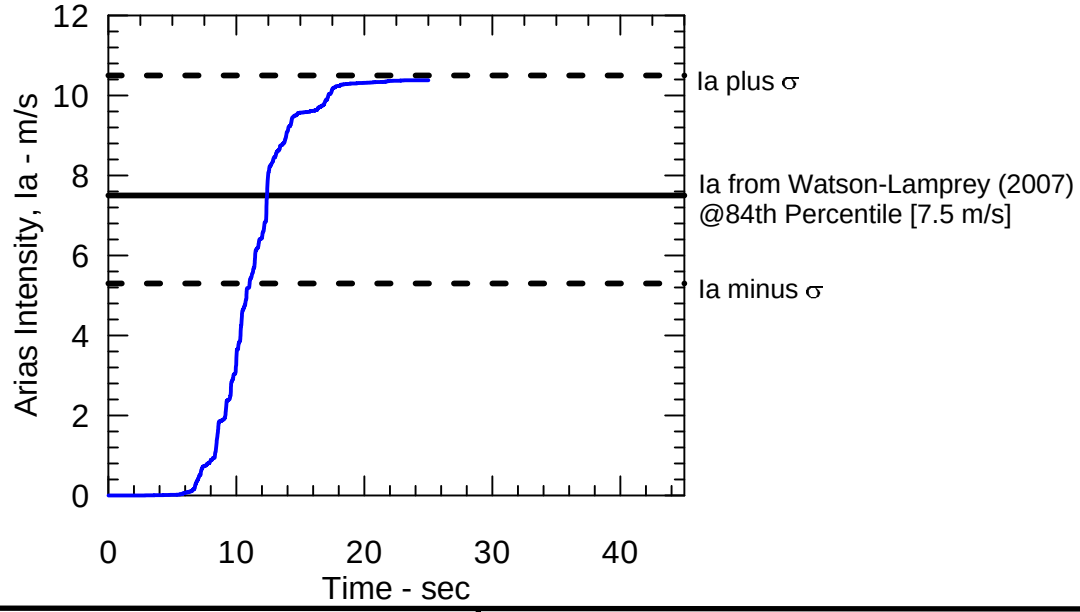

Loma Prieta - LGPC
Reverse Oblique Event
Matched to S-MV Event

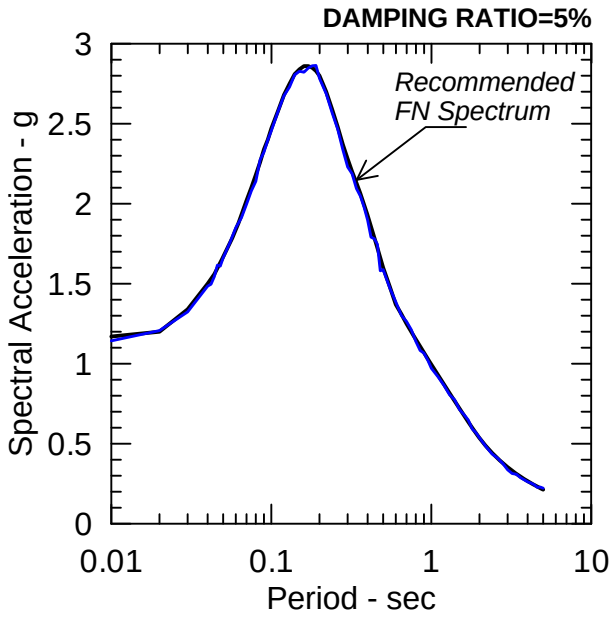

Rev. 0 06/09/2011 SSE2-R-2SC

TERRA / GeoPentech
a Joint Venture

SPECTRALLY MATCHED LOMA PRIETA E/Q, LGPC (FN) RECORD
SEISMIC STABILITY EVALUATIONS (SSE2)

Figure
6-9

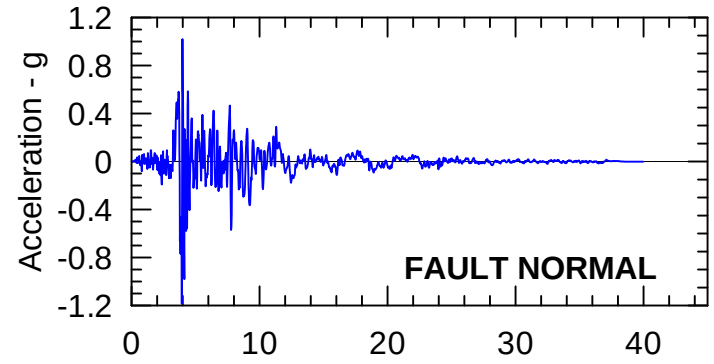

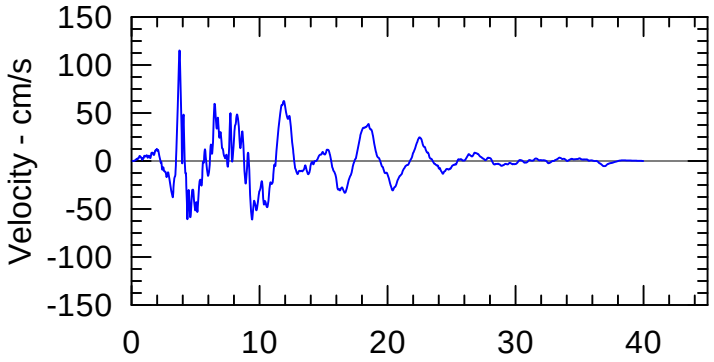

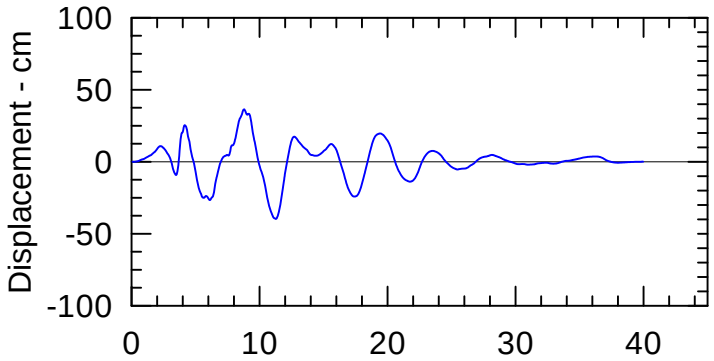

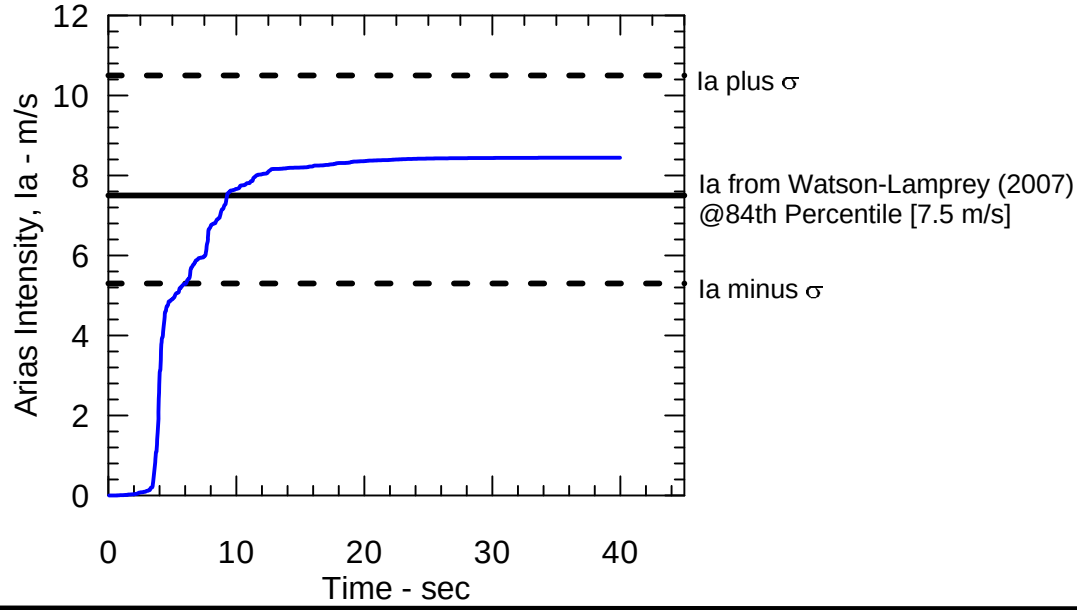

Northridge - Sylmar OVMFF
Reverse Event
Matched to S-MV Event

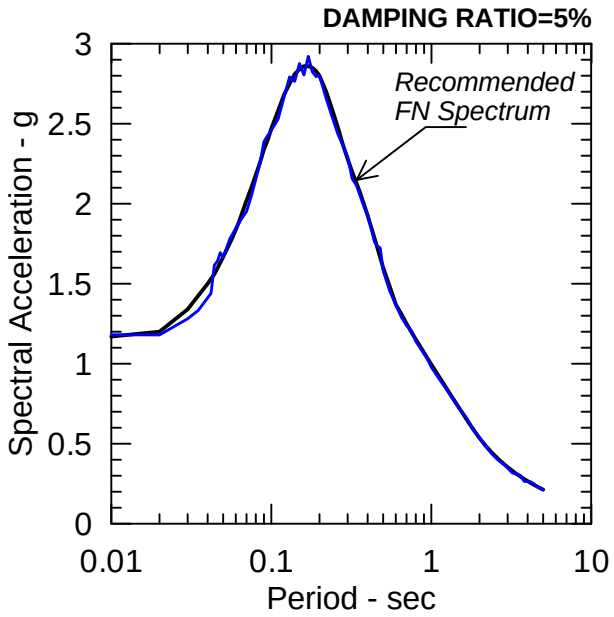

TERRA / GeoPentech
a Joint Venture

SPECTRALLY MATCHED NORTHRIDGE E/Q,
SYLMAR COUNTY HOSP. (FN) RECORD
SEISMIC STABILITY EVALUATIONS (SSE2)

Figure
6-10

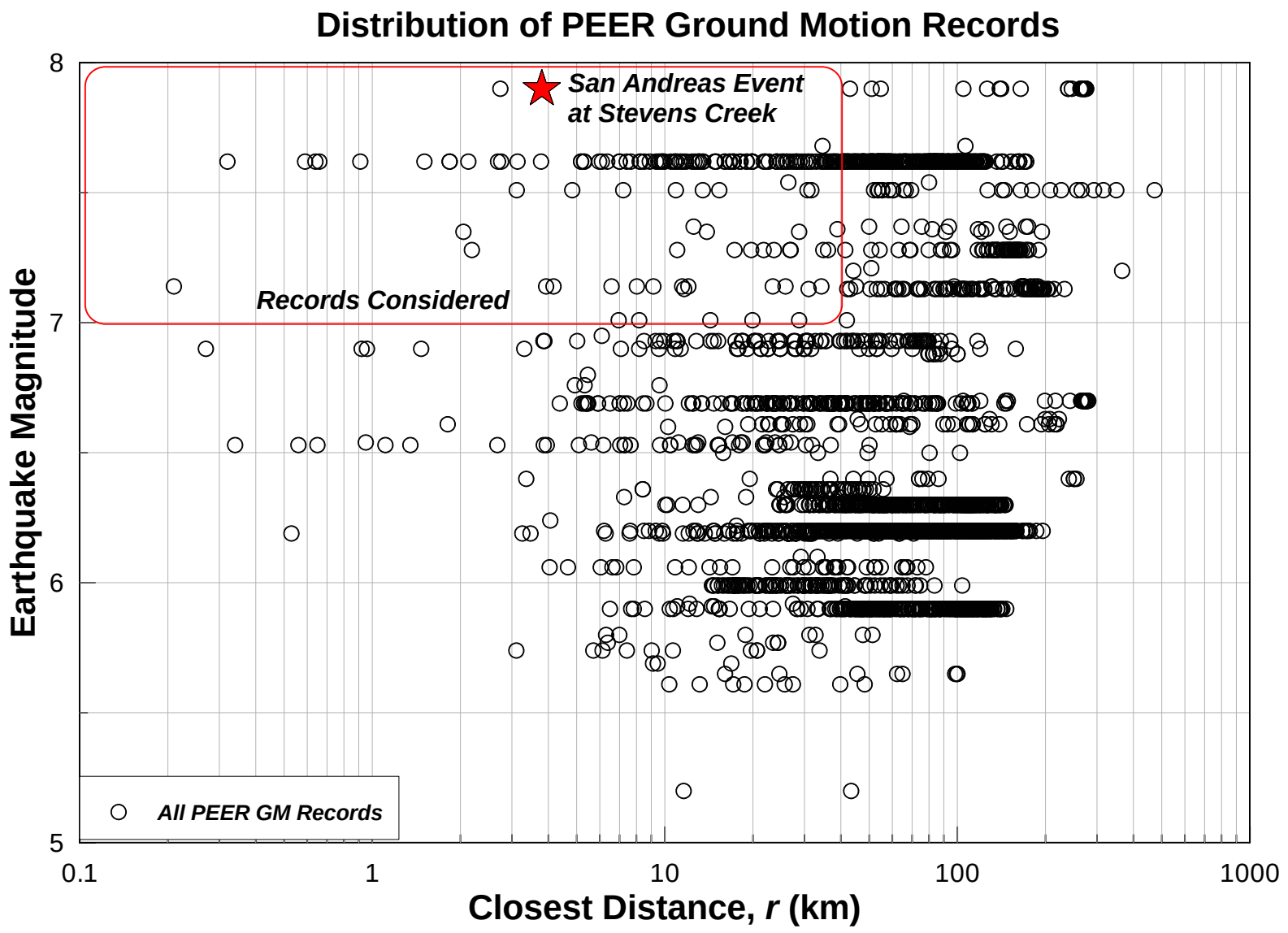

TERRA / GeoPentech
a Joint Venture

SAN ANDREAS INITITIAL CANDIDATE SCREENING - STEVENS CREEK DAM
SEISMIC STABILITY EVALUATIONS (SSE2)

Figure 6-11

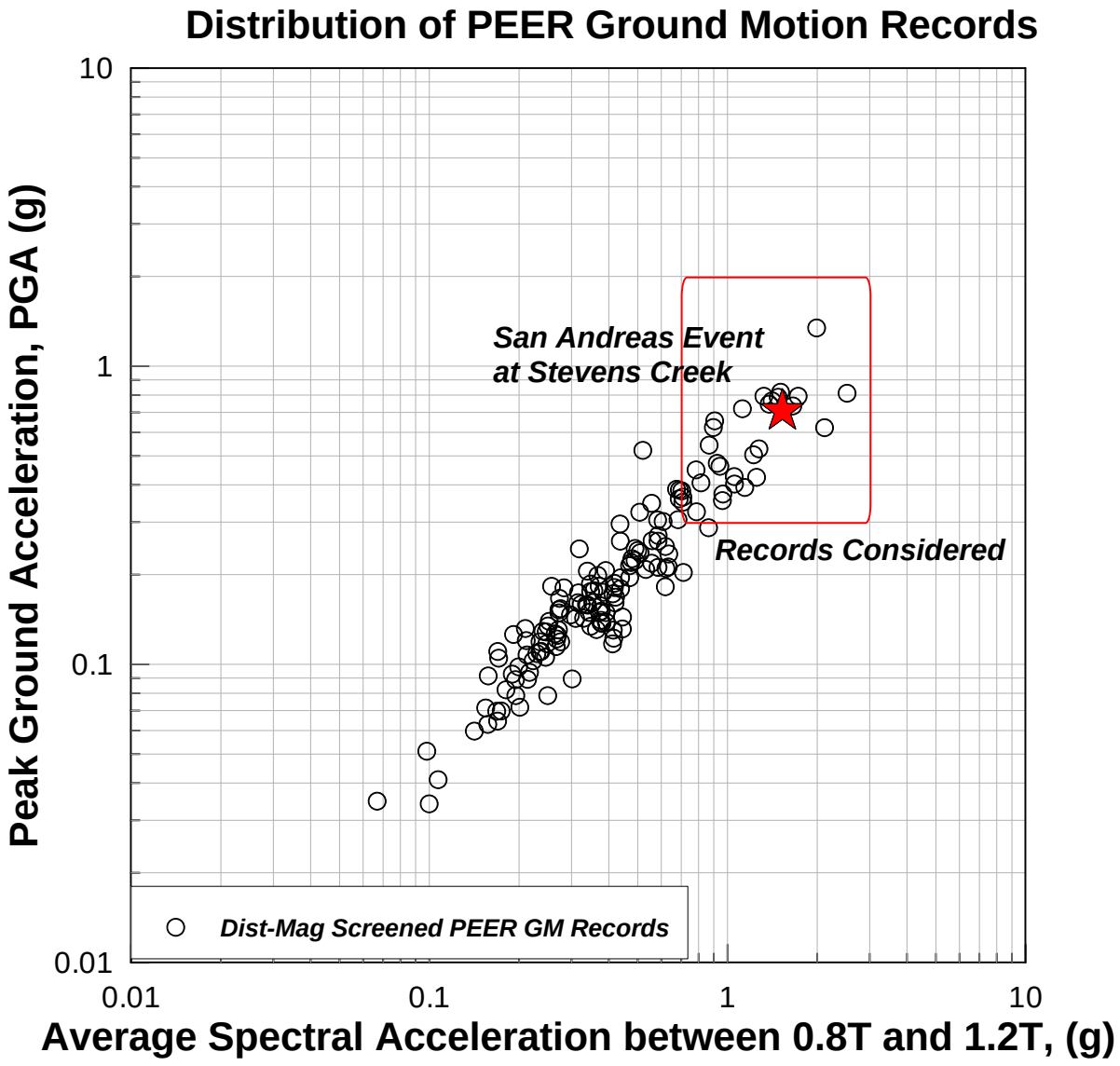

TERRA / GeoPentech
a Joint Venture

SAN ANDREAS SECONDARY CANDIDATE SCREENING - STEVENS CREEK DAM
SEISMIC STABILITY EVALUATIONS (SSE2)

Figure 6-12

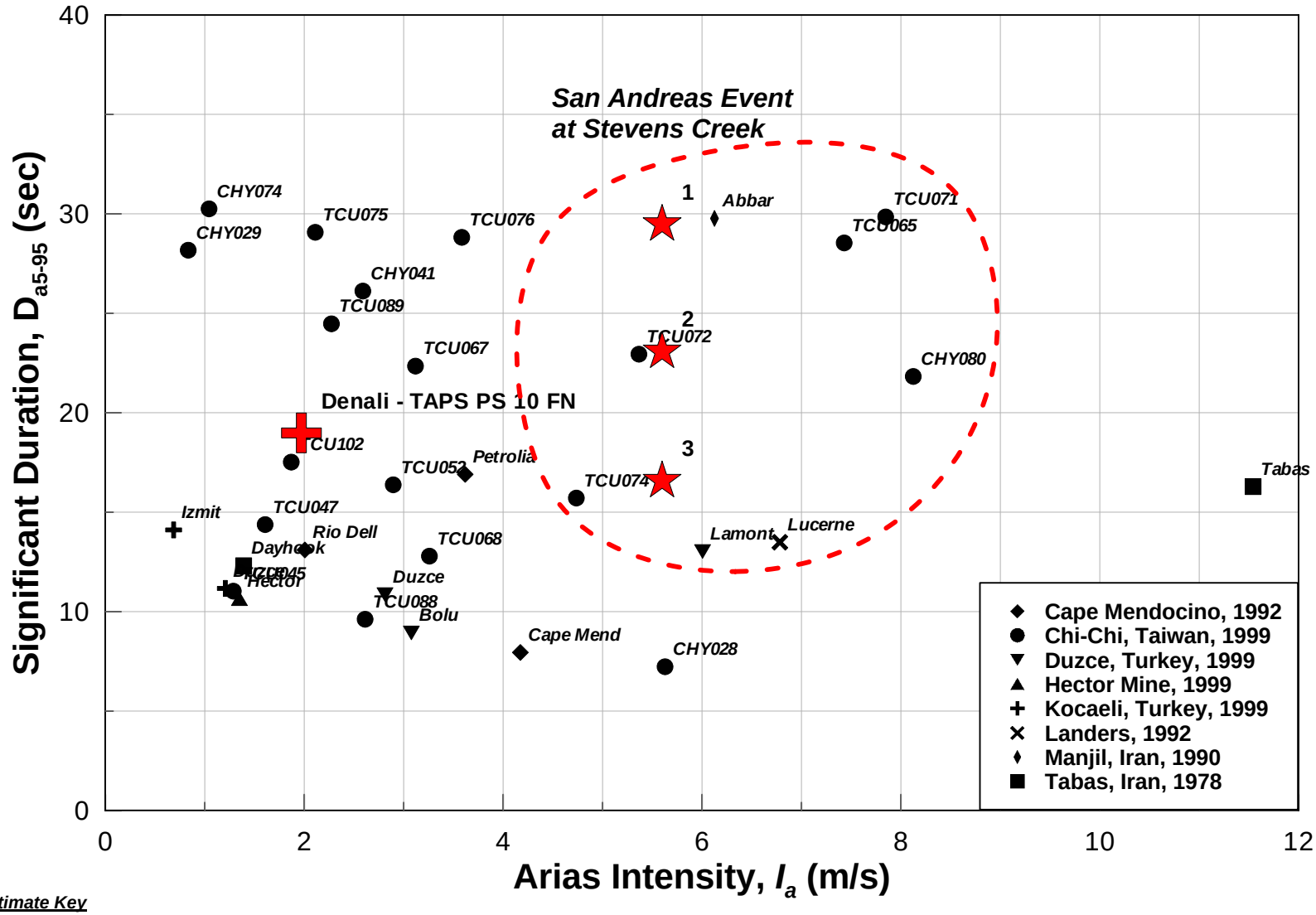

Duration Estimate Key

[1]Kempton and Stewart, 2006 wo/Directivity
[2]Kempton and Stewart, 2006 w/Directivity
[3]Bommer et. al., 2009

TERRA / GeoPentech
a Joint Venture

SAN ANDREAS FINAL CANDIDATE SCREENING - STEVENS CREEK DAM
SEISMIC STABILITY EVALUATIONS (SSE2)

Figure 6-13

Rev. 0 06/09/2011 SSE2-R-2SC

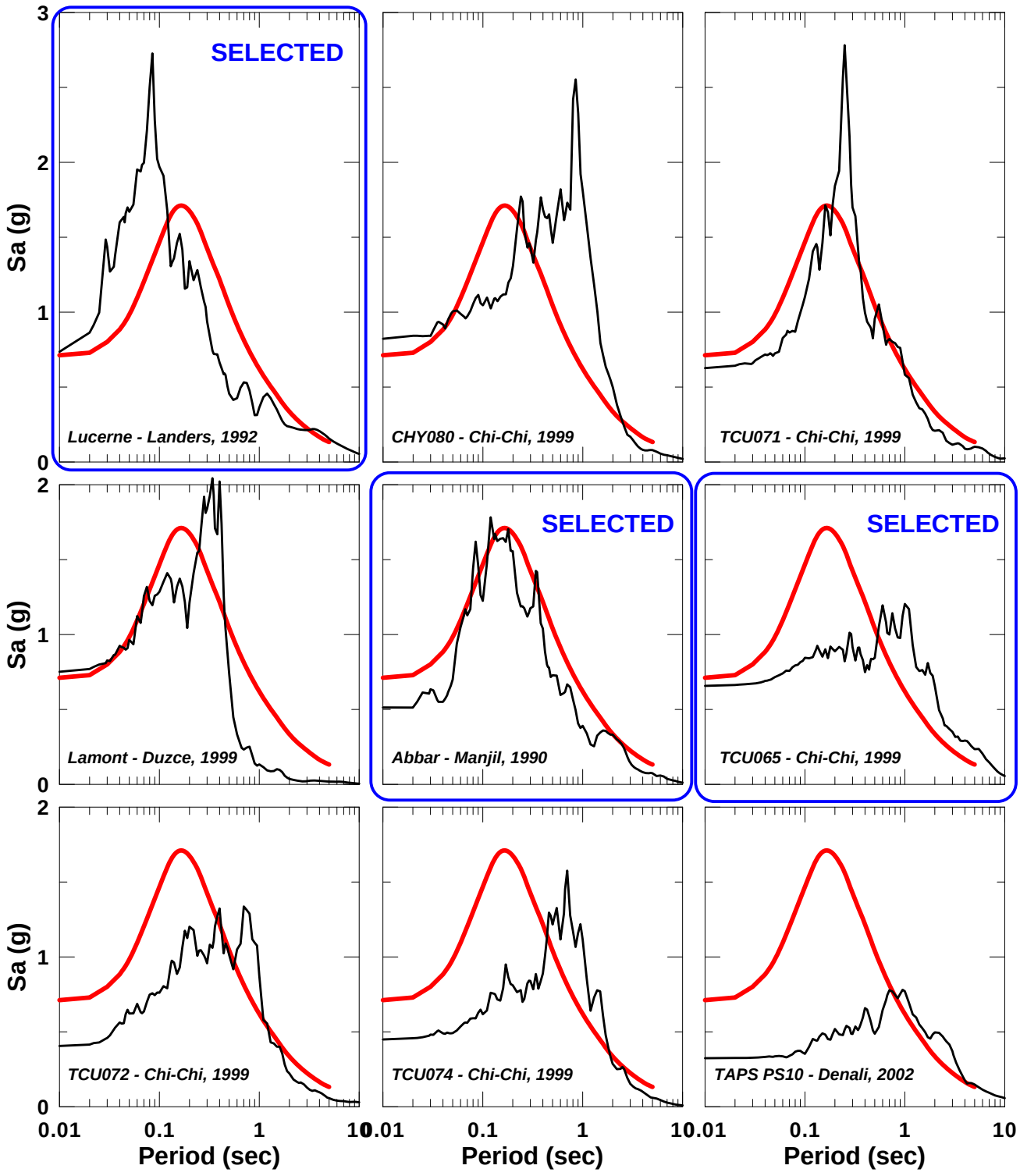

San Andreas Recommended Response Spectra vs.
Geometric Average of Acceleration Response Spectra (5% Damped)

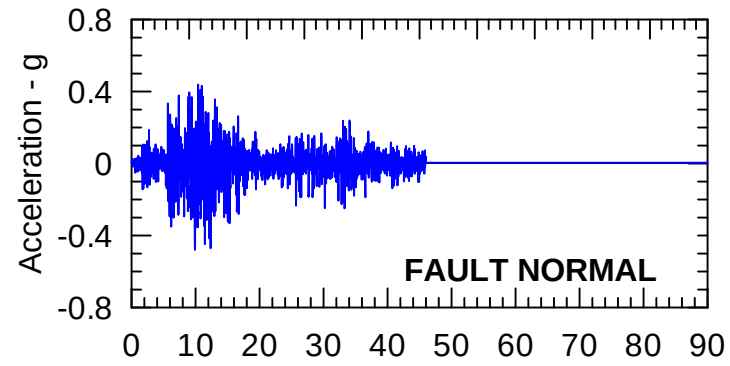

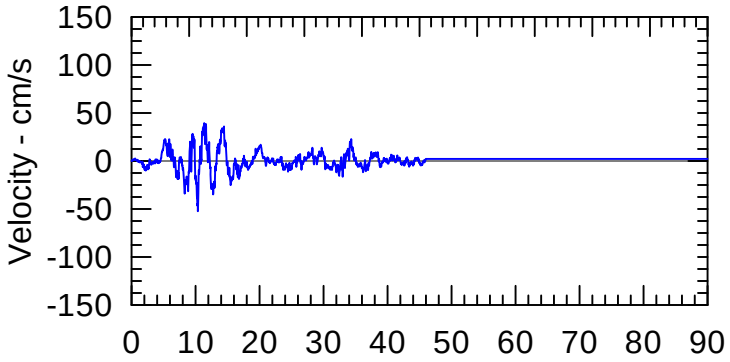

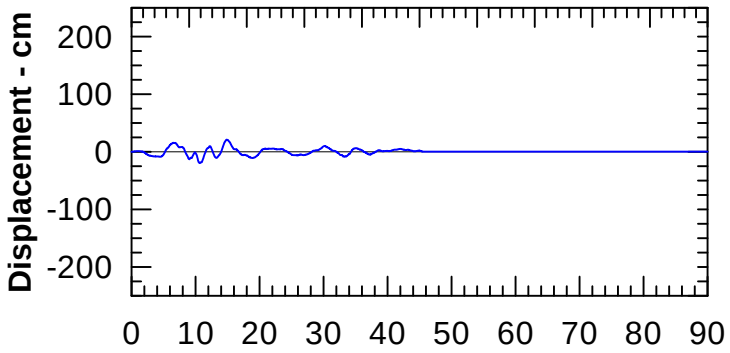

Manjil - Abbar
Strike Slip Event
Rotated to Fault Normal

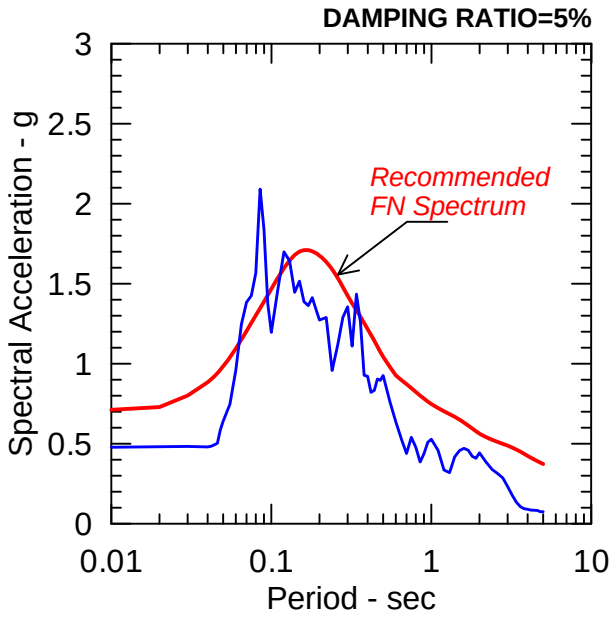

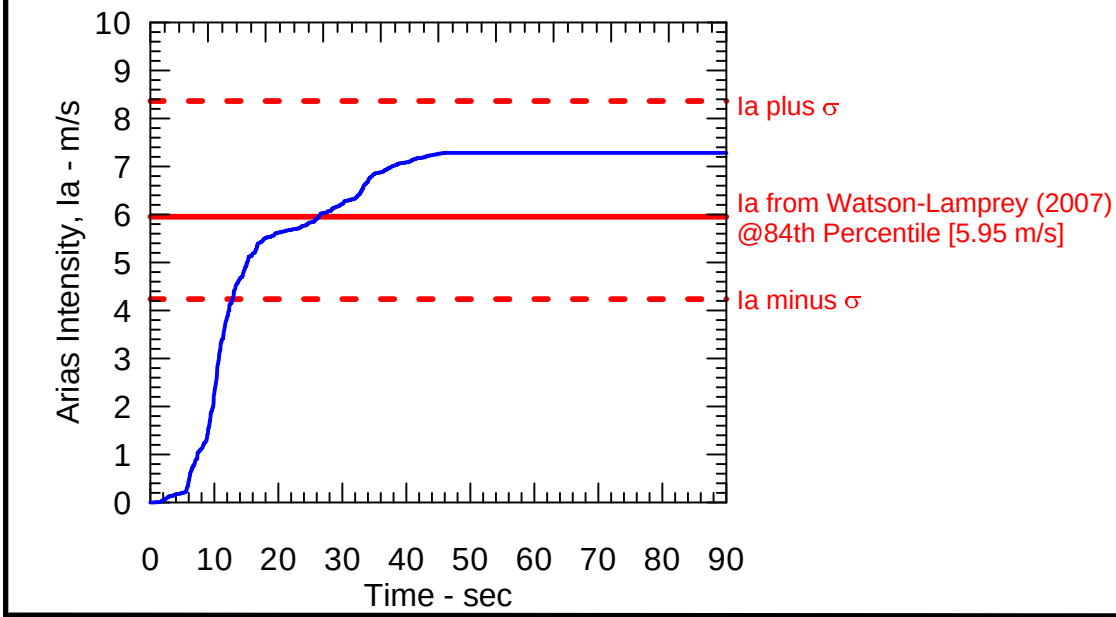

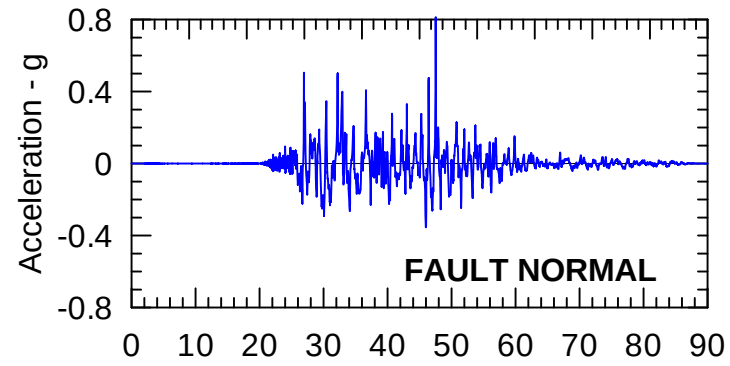

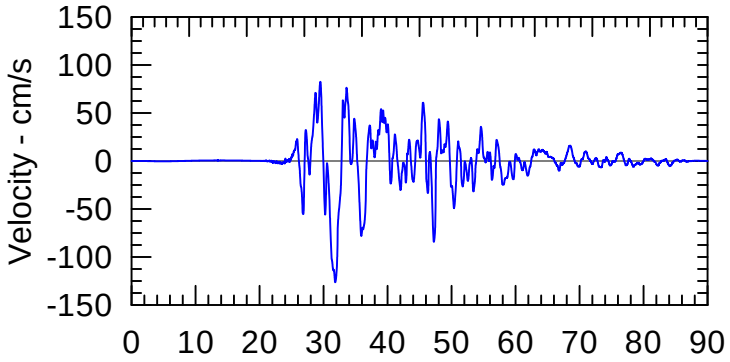

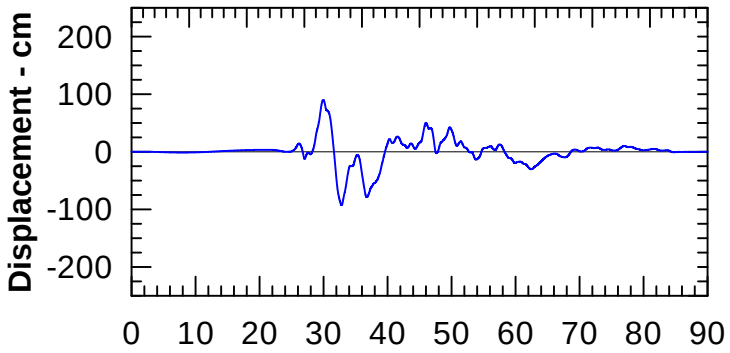

Chi Chi - TCU065
Reverse-Oblique Event
Rotated to Fault Normal

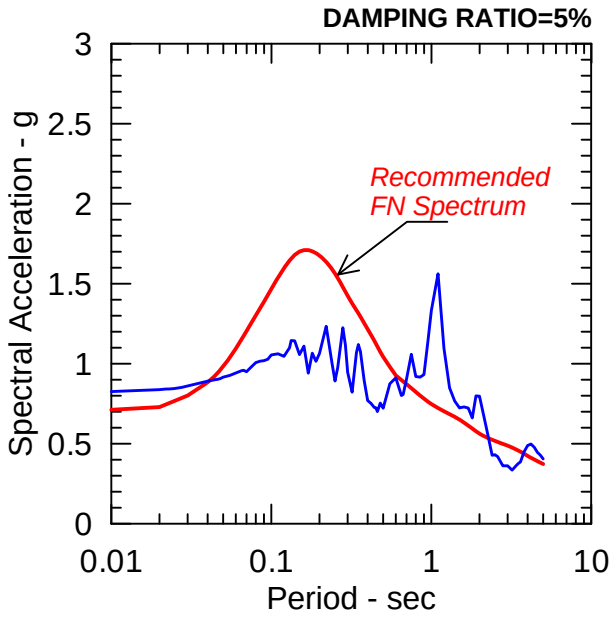

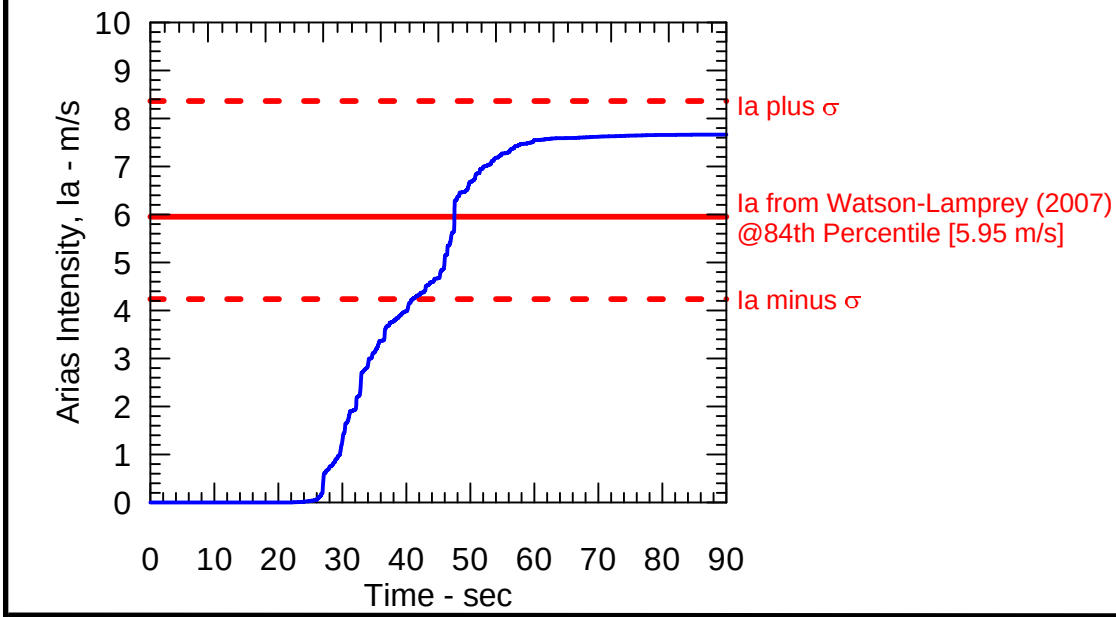

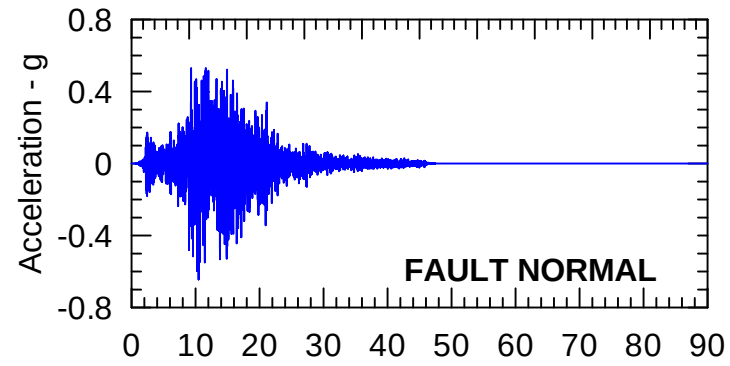

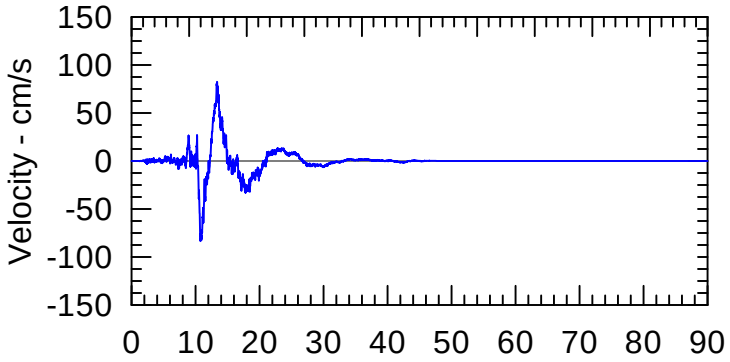

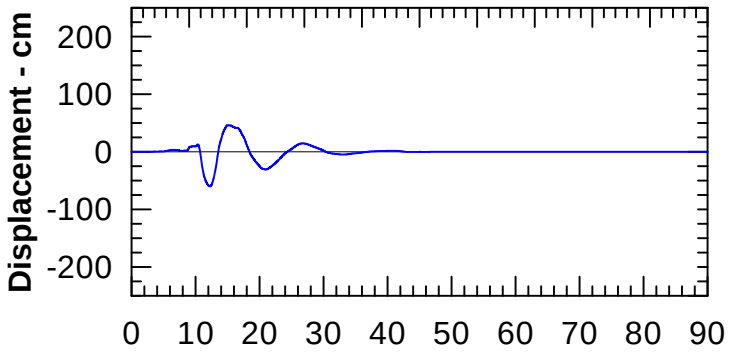

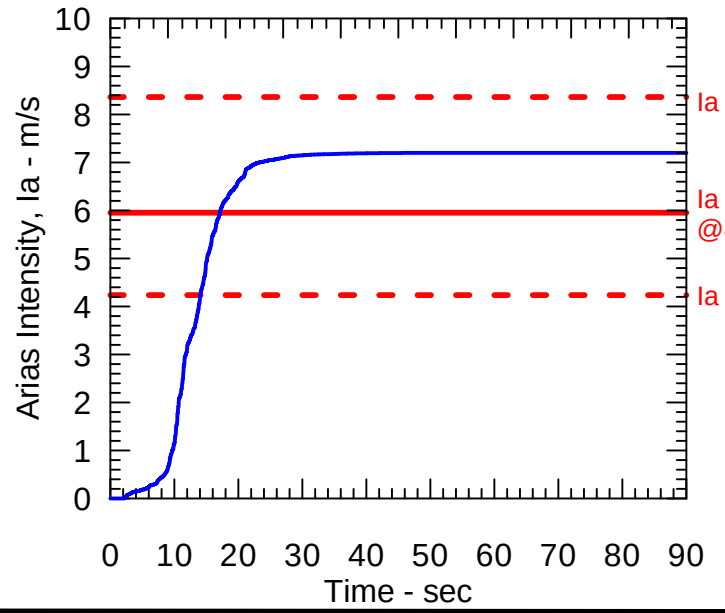

Landers - Lucerne
Strike Slip Event
Rotated to Fault Normal

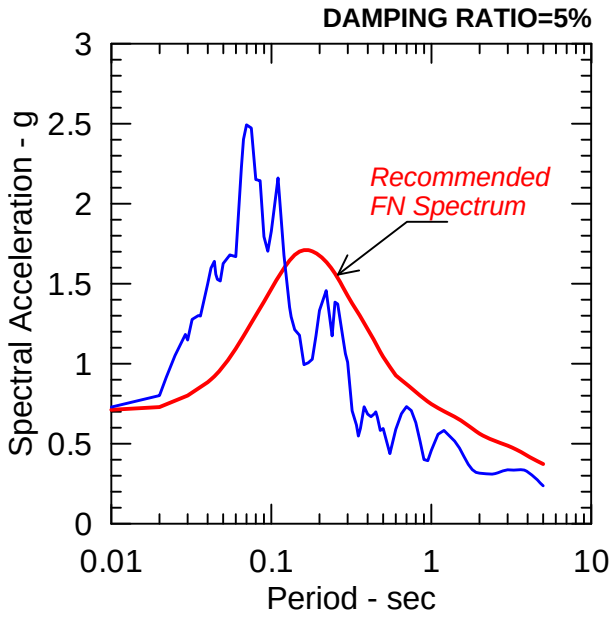

Rev. 0 06/09/2011 SSE2-R-2SC

TERRA / GeoPentech
a Joint Venture

CHARACTERISTICS OF LANDERS E/Q,
LUCERNE (FN) RECORD
SEISMIC STABILITY EVALUATIONS (SSE2)

Figure
6-17

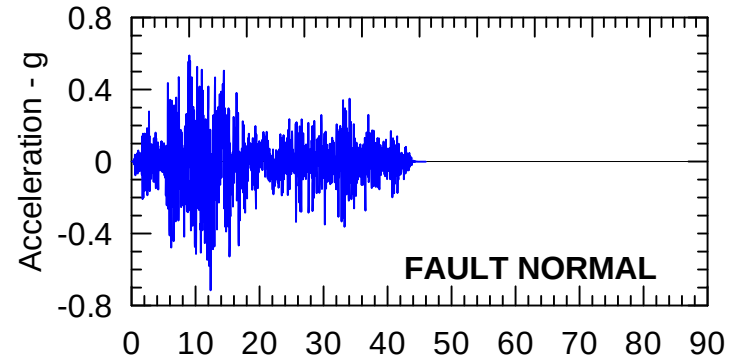

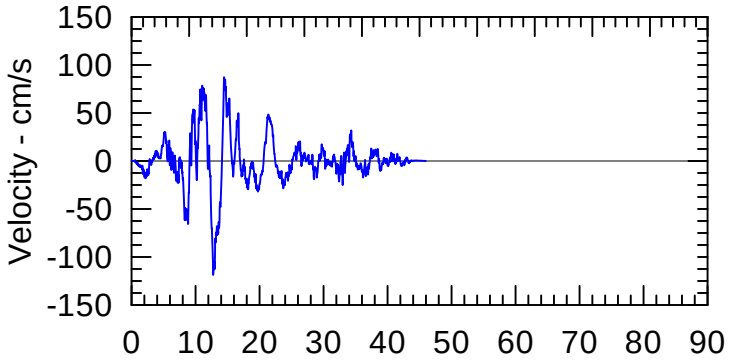

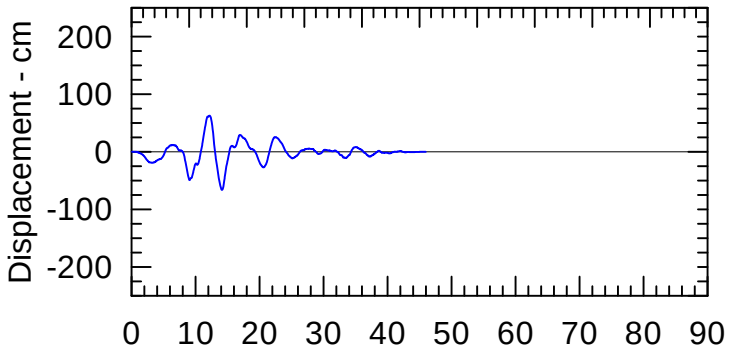

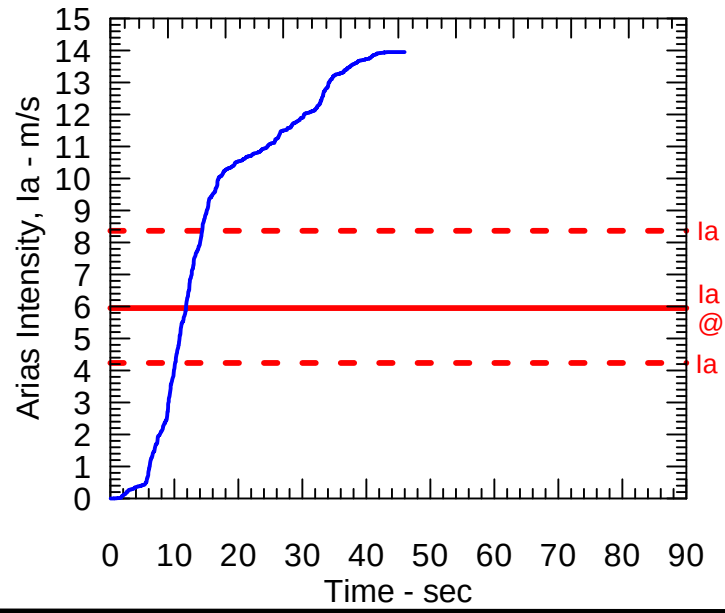

Manjil - Abbar
Strike Slip Event
Matched to San Andreas

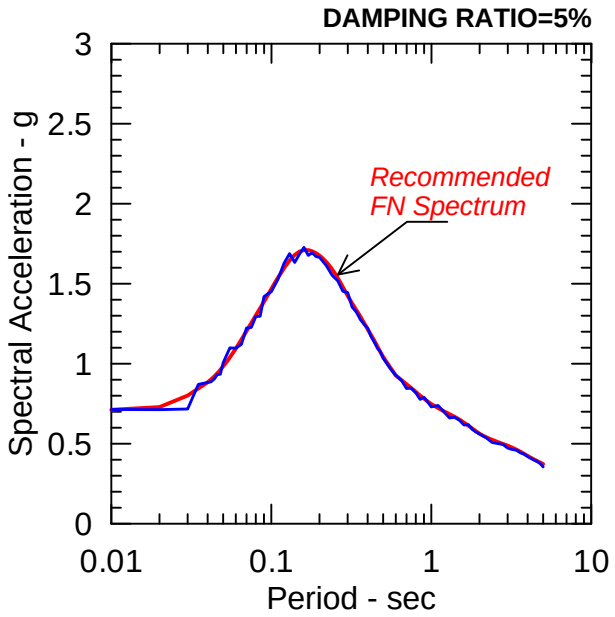

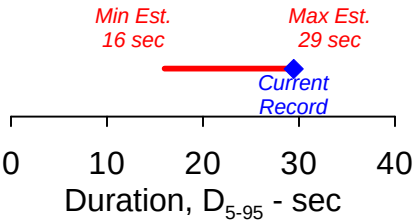

TERRA / GeoPentech a Joint Venture	SPECTRALLY MATCHED MANJIL E/Q, ABBAR (FN) RECORD SEISMIC STABILITY EVALUATIONS (SSE2)	Figure 6-18

Rev. 0 06/09/2011 SSE2-R-2SC

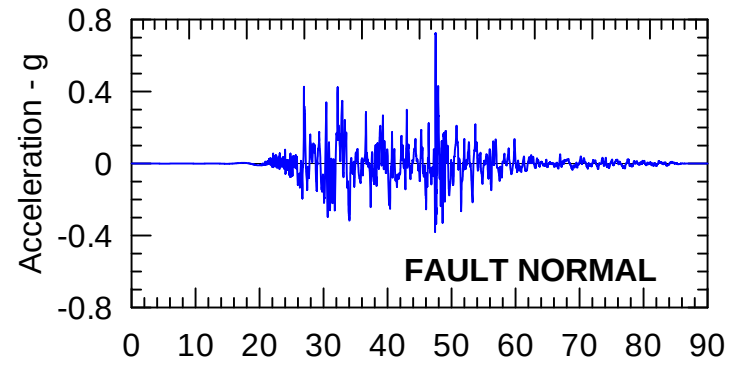

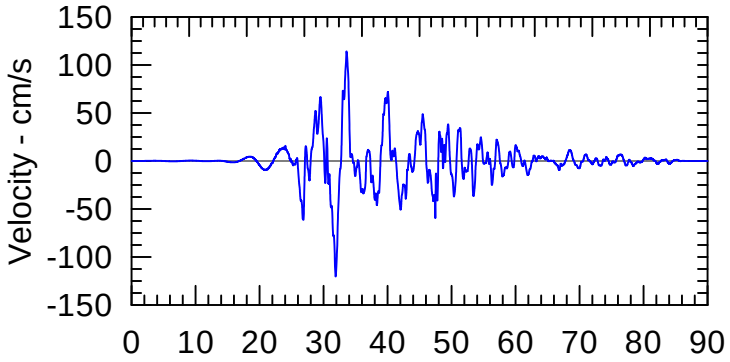

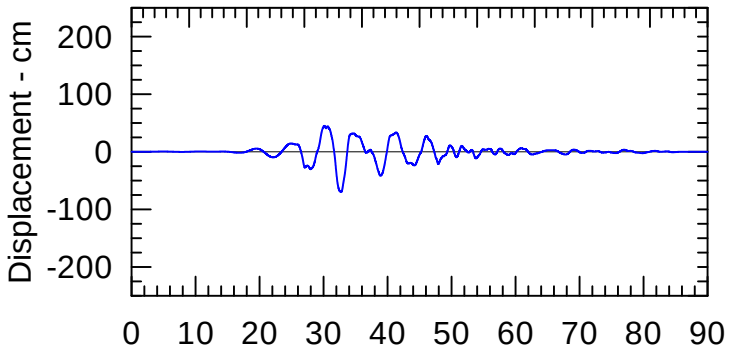

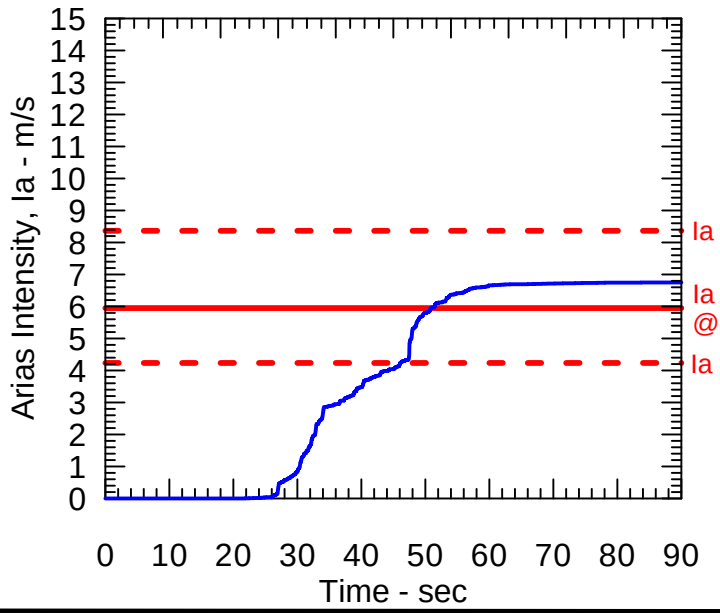

Chi Chi - TCU065 Reverse/Oblique Event Matched to San Andreas

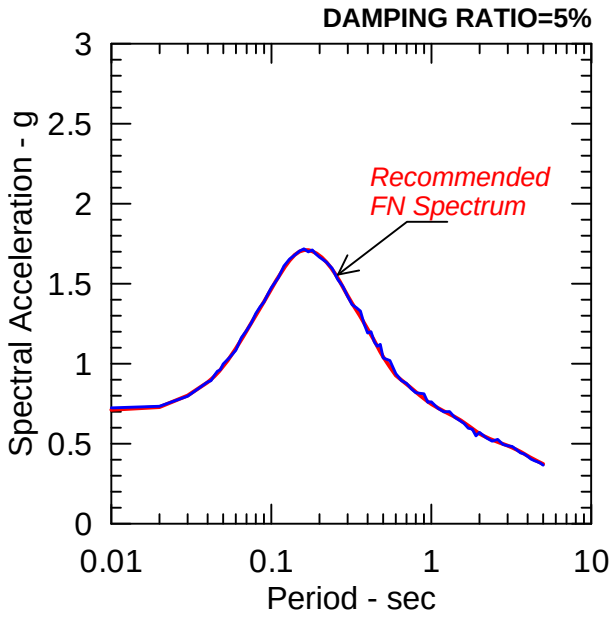

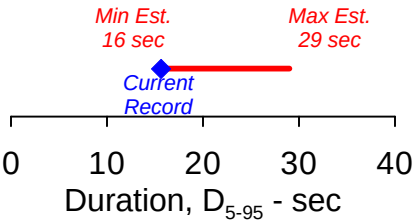

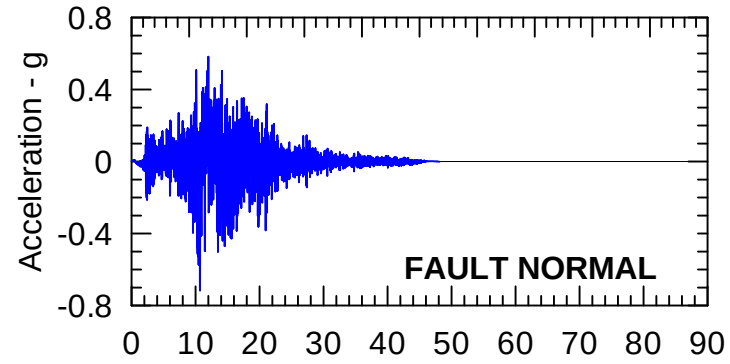

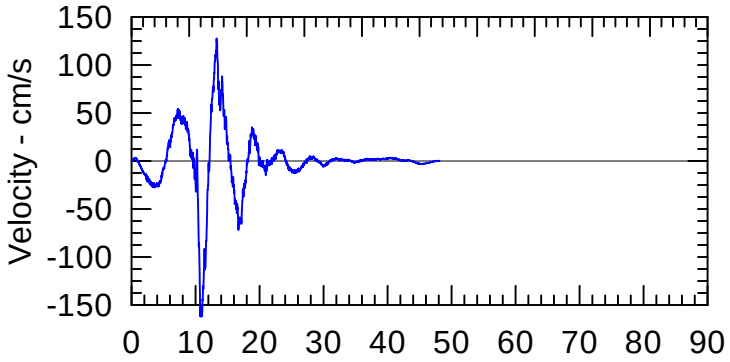

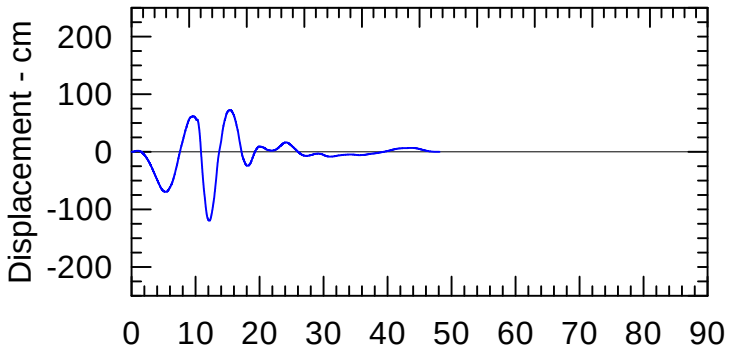

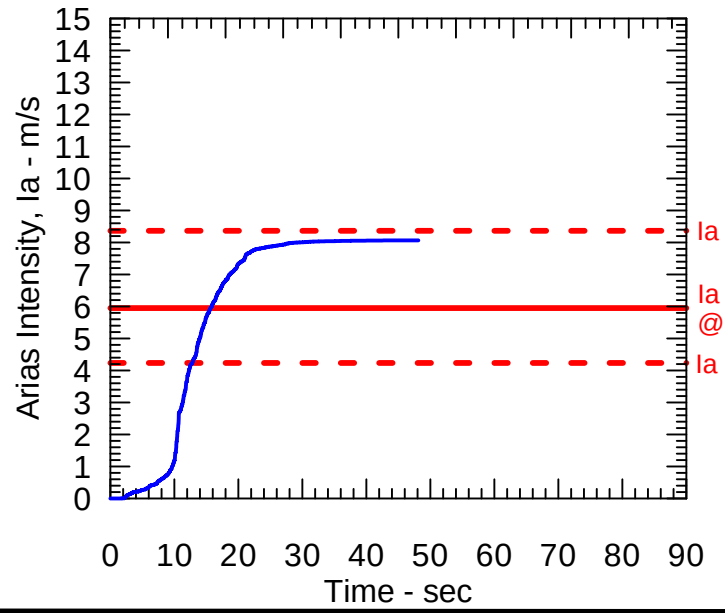

Landers - Lucerne
Strike Slip Event
Matched to San Andreas

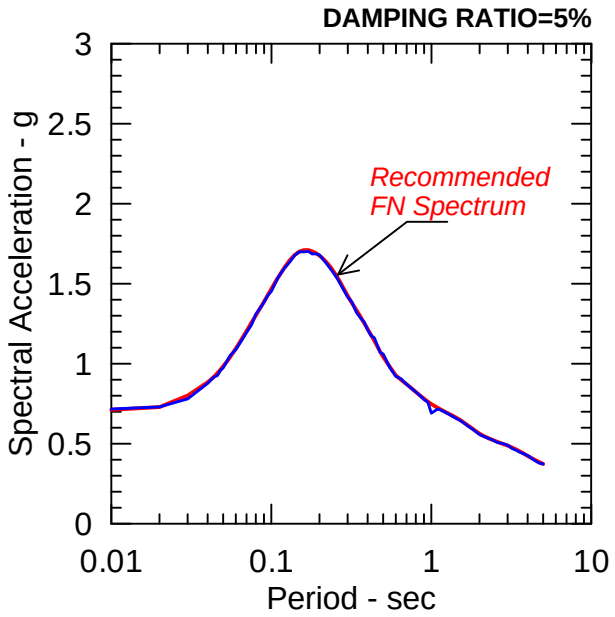

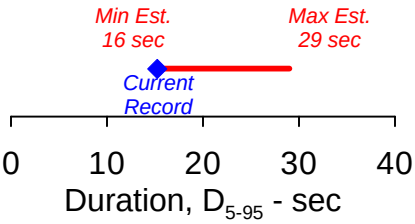

TERRA / GeoPentech a Joint Venture	SPECTRALLY MATCHED LANDERS E/Q, LUCERNE (FN) RECORD SEISMIC STABILITY EVALUATIONS (SSE2)	Figure 6-20

Rev. 0 06/09/2011 SSE2-R-2SC